

THE SYNTHESIS OF A FERROMAGNETIC POLYMER

PETER EDWARD BROUGH

A thesis submitted for the degree of

Doctor of Philosophy

ASTON UNIVERSITY

June 1999

This copy of the thesis has been supplied on condition that anyone who consults it is understood to recognise that its copyright rests with its author and that no quotation from the thesis and no information derived from it may be published without proper acknowledgement.



If you have discovered material in AURA which is unlawful e.g. breaches copyright, (either yours or that of a third party) or any other law, including but not limited to those relating to patent, trademark, confidentiality, data protection, obscenity, defamation, libel, then please read our [Takedown Policy](#) and [contact the service](#) immediately

Aston University

THE SYNTHESIS OF A FERROMAGNETIC POLYMER

PETER EDWARD BROUGH

A thesis submitted for the degree of

Doctor of Philosophy

June 1999

SUMMARY

The aim of this study was to prepare a ferromagnetic polymer using the design elements of molecular magnets. This involved the preparation of co-polyradicals of phenylacetylenes bearing nitronyl nitroxides and nitro/cyano groups. The magnetic properties of the materials were determined using a SQUID magnetometer.

A novel rhodium catalyst, $\text{Rh}(\text{NBD})(\text{NH}_3)\text{Cl}$, was prepared in order to obtain good yields of polymerisation. A wide range of substituted phenylacetylenes were first homopolymerised in order to assess the efficiency of the catalyst. Yields were generally high, between 75% and 98%, and the time of polymerisation was short (one hour). SEC analysis revealed that the Mw of the polymers were in the range of 200,000 and 250,000. The discovery that phenylboronic acid acts a co-catalyst for the polymerisation served to increase the yields by 10% to 20% but the Mw of the polymers was reduced to approximately 100,000.

Co-polyradicals were prepared in good to excellent yield using the new catalyst. The magnetic properties in the temperature range of 300K to 1.8K were investigated by SQUID, which revealed a spin glass system, antiferromagnets and possible dipolar magnets. Short-range ferromagnetic interactions between 300K and 100K were found in a co-polyradical containing nitronyl nitroxide and cyano substituted monomers. The magnetic properties were dependent upon both the type of monomers utilised and the ratio between them.

The effects of ring substituents on the terminal alkyne have been studied by carbon-13 NMR. There was no correlation however, between the chemical shift of terminal alkyne and the polymerisability of the monomer.

Key words : polymerisation; phenylacetylene; nitronyl nitroxide; polyradical, ferromagnetic.

To my parents.

ACKNOWLEDGEMENTS

Of course, I am indebted to Dr Allan Amass for his supervision. Many thanks to Dr I. M. Hohn and Dr E. M. Colclough of DERA for their guidance and external supervision.

I am grateful to my Dad and Olivia for scrutinising this thesis.

Thanks to Dr Michael Perry for all the NMR analysis. I also acknowledge Karen for all the mass spectrometry analysis. I would also like to express my gratitude to Dr Andrew Harrison (University of Edinburgh) for all the SQUID analysis, and many helpful discussions; Professor John Walton (University of St-Andrews) for the EPR expertise.

For all the laughs and jokes a mention of Nige, Tris, Bear, and Rob is required.

Finally, I acknowledge DERA and EPSRC for the funding of this project.

CONTENTS

TITLE.....	1
DEDICATION	3
ACKNOWLEDGEMENTS	4
CONTENTS	5
LIST OF FIGURES.....	11
LIST OF SCHEMES.....	15
LIST OF TABLES.....	16
LIST OF EQUATIONS.....	17
LIST OF ABBREVIATIONS	18
CHAPTER 1 . INTRODUCTION.....	20
1.1 GENERAL INTRODUCTION	21
1.2 THEORY OF MAGNETISM	22
1.2.1 SPIN INTERACTIONS	24
1.2.1.1 <i>Orbital Interactions</i>	24
1.2.1.2 <i>Dipolar coupling</i>	26
1.2.2 CRITERIA FOR AN ORGANIC MAGNET	27
1.3 ORGANIC RADICALS AS MAGNETS.....	27
1.3.1 STABLE ORGANIC RADICALS	28
1.3.1.1 SUBSTITUTION.....	28
1.3.1.2 RESONANCE	28
1.3.1.3 STERIC HINDRANCE.....	29
1.3.1.4 NEIGHBOURING HETEROATOMS.....	30
1.3.1.4.1 NITROXIDES.....	30
1.3.1.4.2 OTHER HETERO RADICALS	31
1.3.1.4.3 NITRONYL NITROXIDES	32
1.3.2 THE FIRST ORGANIC FERROMAGNET.....	34
1.3.3 A THIOAMINYL MAGNETIC MOLECULE.....	35

1.3.4	AN ORGANIC MOLECULE POSSESSING THE HIGHEST T_c	36
1.4	SPIN CONTROL IN MOLECULAR MAGNETS	37
1.4.1	THE INFLUENCE OF SUBSTITUENT GROUPS	37
1.4.2	HYDROGEN BONDING	38
1.4.3	DIAMAGNETIC BRIDGES	40
1.5	POLYRADICALS	42
1.5.1	EARLY "FERROMAGNETIC" ORGANIC MATERIALS	42
1.5.2	POLYRADICALS BY POST-POLYMERISATION REACTIONS	42
1.5.3	POLYRADICALS FROM RADICAL MONOMERS	44
1.5.4	POLYRADICALS BY DESIGN	45
1.5.5	EARLY CONJUGATED POLYRADICALS	47
1.5.6	PROBLEMS IN CONJUGATED POLYRADICALS	48
1.5.7	FERROMAGNETIC SPIN INTERACTIONS IN POLYRADICALS	51
1.5.8	POLYRADICALS UTILISING THROUGH-SPACE SPIN INTERACTIONS	52
1.6	THE STRATEGY EMPLOYED IN THIS RESEARCH	53
CHAPTER 2.	EXPERIMENTAL	55
2.1	CHEMICALS AND SOURCES	56
2.2	SOLVENTS AND SOURCES	58
2.3	PURIFICATION OF CHEMICALS	59
2.3.1	ETHANOL	59
2.3.2	DISTILLATION OF SOLVENTS USING A HIGH VACUUM LINE	60
2.4	CHARACTERISATION TECHNIQUES	62
2.4.1	ELECTRON PARAMAGNETIC RESONANCE (EPR)	62
2.4.2	GAS CHROMATOGRAPHY (GC)	63
2.4.3	ULTRA VIOLET - VISIBLE SPECTROMETRY (UV)	63
2.4.4	INFRA RED SPECTROMETRY (IR)	63
2.4.5	MASS SPECTROMETRY (MS)	63
2.4.6	NUCLEAR MAGNETIC RESONANCE (NMR)	64
2.4.7	SIZE EXCLUSION CHROMATOGRAPHY (SEC)	64
2.4.8	SUPERCONDUCTING QUANTUM INTERFERENCE DEVICE (SQUID)	64
2.4.9	ELEMENTAL ANALYSIS (EA)	66

CHAPTER 3. SYNTHESIS AND CHARACTERISATION OF PHENYLACETYLENE MONOMERS	67
3. OBJECTIVES	68
3.1 CLASSICAL SYNTHESIS OF PHENYLACETYLENES.....	68
3.2 SYNTHESIS OF PHENYLACETYLENES USING PALLADIUM CATALYSED CROSS-COUPLING, OR SONOGASHIRA COUPLING.....	69
3.2.1 MECHANISM OF THE SONOGASHIRA COUPLING, AND ARYL HALIDE REACTIVITY.....	71
3.2.2 SUMMARY OF THE SONOGASHIRA COUPLING REACTION	73
3.3 TYPICAL SYNTHESIS OF A PHENYLACETYLENE MONOMER, 4-ETHYNYLBENZALDEHYDE	75
3.4 DERIVATIVES OF PHENYLACETYLENE MONOMERS	79
3.4.1 SYNTHESIS OF TETRAHYDRO-2 <i>H</i> -PYRAN PHENYLACETYLENE DERIVATIVES.....	79
3.4.2 SYNTHESIS OF 2,4-DINITROPHENYLHYDRAZINE DERIVATIVE	81
3.4.3 SYNTHESIS OF NITRONYL NITROXIDE MONOMERS.....	82
3.5 INTRODUCTION TO THE RESULTS	85
3.6 BY-PRODUCTS OBTAINED.....	90
3.6.1 SIDE-REACTIONS WITH THE ETHYL ESTER GROUP	90
3.6.2 TEA SALT FORMATION OF A REACTIVE BENZYL BROMIDE.....	94
3.6.3 ATTEMPTED SYNTHESIS OF 4-HYDROXYPHENYLACETYLENE	96
3.6.4 CONDENSATION REACTION OF AN <i>O</i> -FLUOROBENZALDEHYDE (PEB923B)	97
3.6.5 UNEXPECTED PRODUCT FROM AN ALKYL CHLORIDE MONOMER (PB014).....	101
3.7 RECOMMENDATIONS FOR SONOGASHIRA COUPLING	107
CHAPTER 4. POLYMERS AND POLYRADICALS.....	108
4.1 OVERVIEW	109
4.1.1 THERMAL POLYMERISATION.....	109
4.1.2 METATHESIS CATALYSTS.....	110
4.1.3 RHODIUM CATALYSTS	112
4.1.3.1 LIVING POLYMERISATION USING [Rh(NBD)(OCH ₃)] ₂	113
4.1.3.2 POLYMERISATION BY RHODIUM CATALYSTS IN WATER.....	113
4.1.4 POLYMERISATION OF PHENYLACETYLENE BEARING A STABLE NITRONYL NITROXIDE RADICAL ..	114
4.1.5 SYNTHESIS OF CO-POLYMERS BY RHODIUM CATALYSTS	115

4.2	POLYMERISATION MECHANISM OF PHENYLACETYLENE	116
4.2.1	HYDROGEN TRANSFER MECHANISM	116
4.2.2	MONOMER INSERTION MECHANISM	119
4.2.1	THE ROLE OF THE SOLVENT DURING POLYMERISATION WITH RHODIUM COMPLEXES	122
4.3	TYPES OF STRUCTURE AND PROPERTIES OF POLYPHENYLACETYLENE	123
4.3.1	<i>TRANS-TRANS</i> PPA FROM METATHESIS CATALYSTS	123
4.3.1.1	COLOURS AND SOLUBILITY	124
4.3.2	<i>CIS-TRANS</i> PPA FROM RHODIUM CATALYSTS	124
4.3.2.1	COLOURS AND SOLUBILITY	125
4.3.2.2	CHARACTERISATION.....	127
4.3.2.3	CRYSTALLISATION OF <i>CIS-TRANS</i> TO GIVE <i>CIS-CIS</i> POLYPHENYLACETYLENE.....	127
4.4	INTRODUCTION TO THE RESULTS.....	128
4.4.1	DESIGN OF A NEW CATALYST	129
4.4.2	SYNTHESIS OF NOVEL CATALYST $RH(NBD)(NH_3)Cl$ - (MCAT).....	131
4.4.3	USE OF THE NOVEL CATALYST MCAT.....	132
4.4.3.1	SOLVENTS AND CONDITIONS EMPLOYED.....	133
4.5	EXAMPLE SYNTHESIS OF POLYPHENYLACETYLENE USING MCAT (PB027)	133
4.5.1	INTERPRETATION AND COMMENTS	136
4.6	POLYMERISATION OF SOME SIMPLE DERIVATIVES OF PHENYLACETYLENE	137
4.6.1	CHARACTERISATION AND INTERPRETATION.....	140
4.6.2	LINE BROADENING IN THE 1H NMR OF POLY(4-METHOXYPHENYLACETYLENE).....	141
4.6.3	POLY 1-(4-ETHYNYLPHENYL)PYRROLE : A POLYMER EXHIBITING CHANGES OF COLOUR IN DIFFERENT SOLVENTS	142
4.7	SYNTHESIS OF POLYMERS BEARING A THP GROUP	143
4.7.1	CHARACTERISATION OF THP DERIVATIVES.....	144
4.8	SYNTHESIS OF POLYMERS BEARING A BRIDGING GROUP	145
4.9	ENHANCEMENT OF POLYMER YIELD	148
4.9.1	SYNTHESIS OF POLYPHENYLACETYLENE IN THE PRESENCE OF BBA	149
4.9.2	CHARACTERISATION AND INTERPRETATION OF PB047	149
4.9.3	SYNTHESIS OF A POLYMER BEARING A 2,4-DINITROPHENYLHYDRAZINE GROUP.....	151
4.10	INHIBITION OF POLYMERISATION.....	152

4.11	SUMMARY OF THE NOVEL CATALYST MCAT	153
4.12	THE SYNTHESIS OF CO-POLYRADICALS.....	154
4.12.1	EXAMPLE SYNTHESIS OF A COPOLYRADICAL - POLY 4NPA CO 4EPNN.....	154
4.12.1.1	CHARACTERISATION AND INTERPRETATION	156
4.12.2	IMPROVEMENT OF POLYMERISATION PROCEDURE - ELIMINATION OF METAL CONTACT.....	159
4.13	RESULTS OF CO-POLYRADICALS	160
4.13.1	PHYSICAL PROPERTIES OF THE CO-POLYRADICALS	161
4.14	A HOMOPOLYRADICAL	161
4.15	MAGNETIC CHARACTERISATION BY SQUID	162
4.15.1	THE CURIE WEISS LAW AND ITS USE.....	163
4.15.2	SYMBOLS USED IN GRAPHS	164
4.15.3	PARAMAGNETIC CO-POLYRADICALS	165
4.15.4	AN ANTIFERROMAGNET.....	167
4.15.5	ENHANCED MAGNETISATION UPON COOLING IN AN APPLIED FIELD – A “SPIN GLASS”.....	170
4.14.6	A CO-POLYRADICAL EXHIBITING FERROMAGNETIC, PARAMAGNETIC, AND ANTIFERROMAGNETIC INTERACTIONS	173
4.15.7	CO-POLYRADICALS EXHIBITING WEAK AND STRONG ANTIFERROMAGNETISM	175
4.16	SUMMARY OF MAGNETIC EFFECTS.....	181
	CHAPTER 5. CHEMICAL SHIFTS OF PHENYLACETYLENES	182
5.	CHEMICAL SHIFTS OF PHENYLACETYLENES	183
5.1	INTRODUCTION.....	183
5.1.1	TECHNIQUES OF MEASUREMENT.....	183
5.1.2	SUBSTITUENT INDUCED CHEMICAL SHIFTS	184
5.2	EXPERIMENTAL	184
5.3	RESULTS	185
5.4	DISCUSSION	187
5.4.1	ELECTRON DONATING GROUPS AT THE PARA POSITION	187
5.4.2	ELECTRON DONATING GROUPS AT THE META POSITION.....	187
5.4.3	ELECTRON WITHDRAWING GROUPS IN THE PARA POSITION	188
5.4.4	ELECTRON WITHDRAWING GROUPS IN THE META POSITION.....	189
5.4.5	COMPARISON OF PARA AND META SCS	190

5.5	POLYMERISABILITY IN RELATION TO THE NMR DATA	191
5.6	CONCLUSION	192
CHAPTER 6. CONCLUSION AND FURTHER WORK.....		193
6.1	CONCLUSION	194
6.2	FURTHER WORK.....	197
REFERENCES		199
APPENDIX		211

LIST OF FIGURES

FIGURE 1 : SPIN ALIGNMENT IN MAGNETIC MATERIALS	23
FIGURE 2 : FERROMAGNETIC SPIN EXCHANGE POMO TO NLUMO	25
FIGURE 3 : ANTIFERROMAGNETIC SPIN EXCHANGE POMO TO POMO	25
FIGURE 4 : EFFECT OF SUBSTITUTION ON STABILITY OF A RADICAL.....	28
FIGURE 5 : A RADICAL STABILISED BY RESONANCE.....	29
FIGURE 6 : PERCHLOROTRIPHENYLMETHYL, A STABLE RADICAL.....	29
FIGURE 7 : TEMPO STABLE RADICAL	30
FIGURE 8 : RESONANCE FORMS OF NITROXIDES.....	30
FIGURE 9 : HYBRID REPRESENTATION OF A NITROXIDE	30
FIGURE 10 : EXAMPLE OF TEMPO STABILITY.....	31
FIGURE 11 : VERDAZYL STABLE RADICAL	31
FIGURE 12 : THIOAMINYL STABLE RADICAL	32
FIGURE 13 : NITRONYL NITROXIDE STABLE RADICAL	32
FIGURE 14 : A NITRONYL NITROXIDE WITH REDUCED STABILITY.....	33
FIGURE 15 : RESONANCE STRUCTURES OF NITRONYL NITROXIDE	33
FIGURE 16 : NITRONYL NITROXIDE BASED FERROMAGNET (4NPNN).....	34
FIGURE 17 : A THIOAMINYL RADIAL WITH HIGH T_c	36
FIGURE 18 : A "CANTED FERROMAGNET".....	36
FIGURE 19 : HIGHEST T_c ORGANIC MAGNET	37
FIGURE 20 : FERROMAGNETIC SPIN ALIGNMENT THROUGH A NITRO GROUP.....	38
FIGURE 21 : FM INTERACTIONS USING HYDROGEN BONDING	39
FIGURE 22 : STABLE RADICAL EXHIBITING STRONG FM COUPLING VIA HYDROGEN BONDING.....	40
FIGURE 23 : BENZENEBOIRONIC ACID	41
FIGURE 24 : SPIN COUPLING THROUGH A "BRIDGE"	41
FIGURE 25 : POSSIBLE MAGNETIC SPECIES IN AN OXIDISED POLYMER.....	43
FIGURE 26 : CONJUGATION LEADING TO AFM PROPERTIES	45
FIGURE 27 : CONJUGATION LEADING TO FM COUPLING.....	45
FIGURE 28 : FM INTERACTIONS IN A CONJUGATED POLYRADICAL	46
FIGURE 29 : AFM COUPLING IN A CONJUGATED POLYRADICAL	46
FIGURE 30 : OVERVIEW OF SPIN INTERACTIONS THROUGH A CONJUGATED SYSTEM	47
FIGURE 31 : A POORLY DESIGNED "CONJUGATED" POLYRADICAL	47
FIGURE 32 : LOW MOLECULAR WEIGHT POLYRADICAL	49
FIGURE 33 : CONJUGATED POLYRADICAL EXHIBITING AFM INTERACTIONS	49
FIGURE 34 : PHENOXY RADICAL ON A POLYPHENYLACETYLENE BACKBONE	50
FIGURE 35 : POLYRADICAL WITH FERROMAGNETIC SPIN INTERACTIONS.....	52
FIGURE 36 : FERROMAGNETIC SPIN INTERACTIONS IN A CONJUGATED POLYRADICAL	52
FIGURE 37 : A LIQUID CRYSTALLINE POLYRADICAL.....	53

FIGURE 38 : APPARATUS USED TO OBTAIN DRY ETHANOL	60
FIGURE 39 : HIGH VACUUM LINE USED FOR DISTILLATION	61
FIGURE 40 : SCHEMATIC OF SQUID MAGNETOMETER	65
FIGURE 41 : TLC OF 4APA (CHCl ₃ 1 : HEXANE 1)	76
FIGURE 42 : EXAMPLE IR OF ALDEHYDIC MONOMER 4APA	77
FIGURE 43 : EXAMPLE ¹ H NMR OF ALDEHYDIC MONOMER 4APA	78
FIGURE 44 : EXAMPLE ¹³ C NMR OF ALDEHYDIC MONOMER 4APA	78
FIGURE 45 : EXAMPLE MASS SPECTRUM (APCI) OF ALDEHYDIC 4APA	79
FIGURE 46 : IR SPECTRUM OF RADICAL MONOMER 3EPNN	84
FIGURE 47 : IR SPECTRUM (ATTENUATED) OF RADICAL MONOMER 3EPNN	84
FIGURE 48 : MASS SPECTRUM (APCI) OF 3EPNN	85
FIGURE 49 : EPR OF MONOMER RADICAL 3EPNN	85
FIGURE 50 : STRUCTURE OF ETHYL-4-ETHYNYLBENZOATE	90
FIGURE 51 : ¹³ C NMR OF TRANS-ESTERIFIED MONOMER 4MEPA	91
FIGURE 52 : ¹ H NMR OF TRANS-ESTERIFIED MONOMER 4MEPA	91
FIGURE 53 : STRUCTURE OF PRODUCT METHYL-4-ETHYNYLBENZOATE (4MEPA)	92
FIGURE 54 : STRUCTURE OF INTERMEDIATE ETHYL ESTER (PEB121)	92
FIGURE 55 : ¹ H NMR OF ETHYL ESTER INTERMEDIATE PEB121	93
FIGURE 56 : ¹³ C NMR OF ETHYL ESTER INTERMEDIATE PEB121	93
FIGURE 57 : STRUCTURE OF 4-ETHYNYL-2-FLUOROBENZALDEHYDE	97
FIGURE 58 : ¹ H NMR OF CONDENSATION PRODUCT PEB923B	98
FIGURE 59 : ¹³ C NMR OF CONDENSATION PRODUCT PEB923B	99
FIGURE 60 : STRUCTURE OF PRODUCT 1-(4-ETHYNYL-2-FLUOROPHENYL)BUT-1-EN-3-ONE (PEB923B)	99
FIGURE 61 : ¹ H NMR OF CYCLISED MONOMER PB014	102
FIGURE 62 : ¹³ C NMR OF CYCLISED MONOMER PB014	103
FIGURE 63 : CYCLISED PRODUCT CYCLOPROPYL-4-ETHYNYLPHENYL KETONE (PB014)	103
FIGURE 64 : ATOMIC STRUCTURE OF CYCLOPROPYL DERIVATIVE PB014	104
FIGURE 65 : STRUCTURE OF THE UNCYCLISED TRIMETHYLSILYL INTERMEDIATE PEB997	105
FIGURE 66 : ¹ H NMR OF TRIMETHYLSILYL INTERMEDIATE PEB997	105
FIGURE 67 : ¹³ C NMR OF UNCYCLISED TRIMETHYLSILYL INTERMEDIATE	106
FIGURE 68 : SCHROCK TYPE CATALYST	111
FIGURE 69 : [Rh(COD)(Cl)] ₂ CATALYST FOR POLYMERISATION OF PHENYLACETYLENE	112
FIGURE 70 : POPULAR POLYMERISATION CATALYST [Rh(NBD)Cl] ₂	113
FIGURE 71 : [Rh(NBD)OCH ₃] ₂ "LIVING" TYPE RHODIUM CATALYST	113
FIGURE 72 : Rh(COD)(NH ₃)Cl - A CATALYST TOLERANT OF NITRONYL NITROXIDE GROUPS	115
FIGURE 73 : THE MONOMER 4-(<i>N,N</i> -DIMETHYLAMINO)PHENYLACETYLENE	116
FIGURE 74 : ASSOCIATION OF PHENYLACETYLENE TO THE RHODIUM CENTRE	117
FIGURE 75 : CHANGE OF BONDING MODE OF THE MONOMER	117
FIGURE 76 : PROPAGATION - HYDROGEN TRANSFER FROM MONOMER TO POLYMER	118

FIGURE 77 : REARRANGEMENT TO GIVE POLYMER	118
FIGURE 78 : THE STRUCTURE OF TRANS-TRANS PPA FROM METATHESIS CATALYSTS	124
FIGURE 79 : THE STRUCTURE OF CIS-TRANS PPA AS OBTAINED FROM RHODIUM CATALYSTS	125
FIGURE 80 : THE CIS-CIS FORM OF POLYPHENYLACETYLENE	128
FIGURE 81 : STRUCTURE OF NOVEL CATALYST $\text{Rh}(\text{NBD})(\text{NH}_3)\text{Cl}$ - (MCAT).....	130
FIGURE 82 : ^1H NMR SPECTRUM OF POLYMERISATION CATALYST $\text{Rh}(\text{NBD})(\text{NH}_3)\text{Cl}$ - (MCAT).....	132
FIGURE 83 : ^1H NMR OF POLYPHENYLACETYLENE OBTAINED USING MCAT - (PB027).....	135
FIGURE 84 : ^{13}C NMR OF POLYPHENYLACETYLENE OBTAINED USING MCAT - (PB027).....	135
FIGURE 85 : SEC ANALYSIS OF POLYPHENYLACETYLENE - PB027.....	136
FIGURE 86 : ^1H NMR OF POLYPHENYLACETYLENE BEARING A CYCLOPROPYL-KETONE GROUP (PB024).....	141
FIGURE 87 : EXAMPLE OF LINE BROADENING IN THE ^1H NMR OF 4-(METHOXY)PHENYLACETYLENE – PB033	142
FIGURE 88 : COLOUR CHANGES OF POLY 1-(4-ETHYNYLPHENYL)PYRROLE (PB057)	143
FIGURE 89 : ^1H NMR OF A POLYMER BEARING A THP GROUP - (PB038)	145
FIGURE 90 : "POISONING" EFFECT OF THE CYANO GROUP.....	147
FIGURE 91 : ^1H NMR OF POLY(4-FLUOROPHENYLACETYLENE)	148
FIGURE 92 : ^1H NMR OF PPA USING BBA CO-CATALYST (PB047)	150
FIGURE 93 : POSSIBLE MECHANISM FOR THE "POISONING" EFFECT OF AMINE GROUPS.....	153
FIGURE 94 : IR OF CO-POLYRADICAL PEB965.....	157
FIGURE 95 : IR SIGNATURE PEAKS OF NITRONYL NITROXIDE RADICAL (PEB965).....	157
FIGURE 96 : SOLUTION STATE EPR OF PEB965	158
FIGURE 97 : SOLID STATE EPR OF PEB965	158
FIGURE 98 : POLYMERISATION APPARATUS FOR MINIMUM METAL CONTACT.....	159
FIGURE 99 : TYPICAL SQUID PLOT SHOWING PARAMAGNETISM	166
FIGURE 100 : SQUID PLOT SHOWING WEAK ANTIFERROMAGNETIC INTERACTIONS (PB066)	167
FIGURE 101 : SQUID PLOT OF ANTIFERROMAGNET PEB963	168
FIGURE 102 : SQUID PLOT SHOWING ANTIFERROMAGNETIC INTERACTIONS	168
FIGURE 103 : PROPAGATION OF AFM COUPLING.....	169
FIGURE 104 : AFM SPIN COUPLING THROUGH A "BRIDGING" CYANO GROUP.....	170
FIGURE 105 : SQUID OF PEB965 OBTAINED UNDER FC AND ZFC CONDITIONS.....	171
FIGURE 106 : A MANGANESE BRIDGING GROUP	172
FIGURE 107 : REPRESENTATION OF A "SPIN GLASS".....	172
FIGURE 108 : POSSIBLE COUPLING IN SPIN GLASS PEB965	173
FIGURE 109 : SQUID SHOWING FERRO, PARA, AND ANTIFERROMAGNETIC INTERACTIONS	175
FIGURE 110 : UNUSUAL FC AND ZFC MAGNETIC PROPERTIES (PB064).....	176
FIGURE 111 : SPIN INTERACTIONS 300K TO 2K (PB064)	177
FIGURE 112 : AFM SPIN INTERACTIONS (PB064).....	177
FIGURE 113 : UNUSUAL MAGNETIC BEHAVIOUR IN PB028	178
FIGURE 114 : FORMATION OF A "BUBBLE" PHASE	179

FIGURE 115 : CHANGE OF MAGNETIC PHASE IN PB064.....	180
FIGURE 116 : ATTENUATED ^{13}C PENDANT NMR SPECTRUM OF 4NPA IN CDCl_3	185
FIGURE 117 : KEY TO NMR DATA.....	185
FIGURE 118 : SCHEMATIC OF π -POLARISATION	189

LIST OF SCHEMES

SCHEME 1 : CREATION OF A POLYRADICAL BY MODIFICATION OF A POLYMER.....	43
SCHEME 2 : POLYMERISATION OF A MONOMER BEARING A STABLE RADICAL	44
SCHEME 3 : DEHYDROHALOGENATION OF CINAMMIC ACID TO GIVE PHENYLACETYLENE	68
SCHEME 4 : SYNTHESIS OF PHENYLACETYLENES USING DE-HALOGENATION	69
SCHEME 5 : THE STEPHENS CASTRO COUPLING REACTION.....	69
SCHEME 6 : SYNTHESIS OF PHENYLACETYLENES USING THE SONOGASHIRA REACTION	70
SCHEME 7 : LOSS OF ACETYLENIC HYDROGEN BY TRIETHYLAMINE.....	71
SCHEME 8 : FORMATION OF THE ACTIVE PALLADIUM(0) CATALYST	71
SCHEME 9 : OXIDATIVE ADDITION OF THE ARYL HALIDE TO THE PALLADIUM(0) CATALYST	72
SCHEME 10 : SUBSTITUTION OF HALOGEN FOR ACETYLIDE.....	72
SCHEME 11 : REDUCTIVE ELIMINATION TO GIVE THE COUPLED PRODUCT.....	73
SCHEME 12 : THE SYNTHESIS OF A PHENYLACETYLENE DERIVATIVE, 4-ETHYNYLBENZALDEHYDE (4APA)....	75
SCHEME 13 : SYNTHESIS OF A THP DERIVATIVE 2-(3-ETHYNYLPHENOXY)TETRAHYDRO-2 <i>H</i> -PYRAN (PB018)	80
SCHEME 14 : SYNTHESIS OF A 2,4DNP DERIVATIVE OF 3APA	81
SCHEME 15 : SYNTHESIS OF A NITRONYL NITROXIDE MONOMER, 3-ETHYNYLPHENYLNITRONYLNITROXIDE....	82
SCHEME 16 : POSSIBLE TRANS-ESTERIFICATION OF ESTERS DURING DEPROTECTION IN METHANOL.....	94
SCHEME 17 : ATTEMPTED SYNTHESIS OF A PHENYLACTYLENE MONOMER BEARING A BENZYL BROMIDE GROUP	95
SCHEME 18 : TEA SALT FORMATION OF A BENZYL BROMIDE COMPOUND.....	95
SCHEME 19 : ATTEMPTED PREPARATION OF 4-HYDROXYPHENYLACETYLENE.....	96
SCHEME 20 : CONDENSATION OF 4-ETHYNYL-2-FLUOROBENZALDEHYDE WITH ACETONE.....	100
SCHEME 21 : ATTEMPTED SYNTHESIS OF AN ALKYL CHLORIDE FUNCTIONALISED MONOMER	101
SCHEME 22 : NEIGHBOURING-GROUP MECHANISM FOR THE INTRAMOLECULAR CYCLISATION OF PB014.....	107
SCHEME 23 : POLYMERISATION OF <i>o</i> -CF ₃ PHENYLACETYLENE BY WCL ₆ -Ph ₄ Sn	110
SCHEME 24 : POLYMERISATION OF PPA IN WATER USING A RHODIUM COMPLEX	114
SCHEME 25 : ASSOCIATION OF PHENYLACETYLENE WITH RHODIUM(I) CENTRE	119
SCHEME 26 : OXIDATIVE ADDITION OF PHENYLACETYLENE TO GIVE A RHODIUM(III) CENTRE	120
SCHEME 27 : PROPAGATION – ASSOCIATION OF ANOTHER MOLECULE OF PHENYLACETYLENE	120
SCHEME 28 : INSERTION OF COORDINATED PHENYLACETYLENE	121
SCHEME 29 : REDUCTIVE ELIMINATION – TO GIVE PPA AND REFORM THE RHODIUM(I) CENTRE.....	121
SCHEME 30 : RHODIUM COMPLEX WITH TRIETHYLAMINE.....	122
SCHEME 31 : RHODIUM COMPLEX WITH ALCOHOL	123
SCHEME 32 : SYNTHESIS OF NOVEL CATALYST FOR THE POLYMERISATION OF PHENYLACETYLENES, Rh(NBD)(NH ₃)Cl -(MCAT)	131
SCHEME 33 : SYNTHESIS OF A POLYPHENYLACETYLENE (PB027)	133
SCHEME 34 : SYNTHESIS OF A COPOLYRADICAL PEB965	155

LIST OF TABLES

TABLE 1 : FERROMAGNETIC MOLECULES CONTAINING A NITRONYL NITROXIDE	35
TABLE 2 : SUMMARY OF PHENYLACETYLENE MONOMERS	86
TABLE 3 : PHENYLACETYLENE MONOMERS SYNTHESISED POSSESSING A BRIDGING GROUP	89
TABLE 4 : SOLUBLE DERIVATIVES OF POLYPHENYLACETYLENE	126
TABLE 5 : INSOLUBLE DERIVATIVES OF POLYPHENYLACETYLENE	126
TABLE 6 : RESULTS USING $[\text{Rh}(\text{NBD})(\text{OCH}_3)_2]$	129
TABLE 7 : RESULTS OF THE POLYMERISATION OF SOME SIMPLE DERIVATIVES OF PHENYLACETYLENE	138
TABLE 9 : SUMMARY OF POLYMERS CONTAINING A THP GROUP	144
TABLE 10 : SUMMARY OF POLYMERS CONTAINING BRIDGING GROUPS	146
TABLE 12 : SUMMARY OF POLYMERS SYNTHESISED USING THE BBA/MCAT SYSTEM	152
TABLE 13 : SUMMARY OF COPOLYRADICALS USING 4EPNN	160
TABLE 14 : SUMMARY OF COPOLYRADICALS USING 3EPNN	161
TABLE 15 : RESULT OF THE SYNTHESIS OF A HOMOPOLYRADICAL	162
TABLE 16 : ^{13}C NMR SHIFTS OF THE TERMINAL ACETYLENIC CARBON C2, AND THE NON-TERMINAL C1 (δ IN PPM RELATIVE TO TMS), OF SUBSTITUTED PHENYLACETYLENES.	186

LIST OF EQUATIONS

EQUATION 1 : RELATIONSHIP OF MAGNETISATION TO SUSCEPTIBILITY	163
EQUATION 2 : THE CURIE EXPRESSION	163
EQUATION 3 : DEFINITION OF THE CURIE CONSTANT	163
EQUATION 4 : THE CURIE WEISS LAW	164
EQUATION 5 : DEFINITION OF EFFECTIVE SPIN MOMENT	164

LIST OF ABBREVIATIONS

2,4DNP	2,4-dinitrophenylhydrazine
APCI	Atmospheric Pressure Chemical Ionization
AFM	Antiferromagnetic
BBA	Benzeneboronic Acid
COD	1,5-cyclooctadiene
DCM	Dichloromethane
DERA	Defence and Evaluation Research Agency
DHP	3,4-dihydro-2 <i>H</i> -pyran
DMAP	4-dimethylaminopyridine
DMF	N,N-dimethylformamide
DMSO	Dimethylsulfoxide
EA	Elemental Analysis
EI	Electron Impact
EPR	Electron Paramagnetic Resonance
FC	Field Cooled
FID	Free Induction Decay
FM	Ferromagnetic
GC	Gas Chromatography
HPLC	High Performance Liquid Chromatography
IR	Infra Red
KBr	Potassium bromide
Mn	Number average molecular weight (of polymer)
Mp	Melting point
MS	Mass Spectrometry
Mw	Weight average molecular weight (of polymer)
NBD	2,5-norbornadiene, or bicyclo[2.2.1]hepta-2,5-diene
NG	Neighbouring Group
NHOMO	Next Highest Occupied Molecular Orbital
NLUMO	Next Lowest Unoccupied Molecular Orbital
NMR	Nuclear Magnetic Resonance
PA	Phenylacetylene
Pd	Polydispersity (of polymer)

PENDANT	Polarisation Enhancement that is Nurtured during Attached Nucleus Testing
PM`	Paramagnetic
POMO	Partially Occupied Molecular Orbital
PPA	Polyphenylacetylene
PTS	Pyridium <i>p</i> -toluenesulfonate
RBF	Round Bottom Flask
RMM	Relative Molecular Mass
RT	Room temperature
ROMP	Ring Opening Metathesis Polymerisation
SCS	Substituent-induced Chemical Shift
SEC	Size Exclusion Chromatography
SQUID	Superconducting Quantum Universal Interference Device
T _c	Curie Temperature
TEMPO	2,2,6,6-tetramethyl-1-piperidinyloxy, free radical
THF	Tetrahydrofuran
TLC	Thin Layer Chromatography
UV	Ultra Violet - Visible
ZFC	Zero-field Cooled

CHAPTER 1.
INTRODUCTION

CHAPTER 1. INTRODUCTION

1.1 General introduction

Imagine a material that is transparent, soluble in organic solvents, mouldable, 30% lighter than conventional materials, and is magnetic. Such a material would have considerably more application than conventional magnetic materials, such as metals (cobalt, nickel, and iron), metal oxides (lodestone – Fe_3O_4), and alloys¹, which are heavy, non-transparent, insoluble, and costly to process. With a large diversity of applications ranging from the mundane (fridge stickers) to the high technology of a synchrotron, the commercial value of such a light weight magnetic material would be high. These properties can be envisaged in a magnetic polymer.

A magnetic polymer based purely on organic atoms is theoretically possible, but has eluded all research groups around the world up to the present time. However, with the recent discovery of two organic molecules that possess magnetic properties, a polymeric magnet may still be a viable proposition. This report studies a novel approach to the design of a magnetic polymer.

In this chapter the origins of magnetic behaviour and how this can be applied to an organic species are detailed, followed by a review of known organic molecular magnets, an overview of polyradicals and their properties, and finally the strategy that encompasses the project.

In order to attempt the synthesis of organic materials that have magnetic properties it is necessary to review how magnetism actually arises.

1.2 Theory of magnetism

The definition of a magnet can be regarded as the attractive (or repulsive) behaviour of a material in a magnetic field. In order to explain how magnetism occurs^{2,3,4,5} it is necessary to consider the nature of electrons and their spin about the nucleus of an atom. Every electron has a quantum mechanical property called “spin” which has associated with it a magnetic moment. When a magnetic field is applied the spin can either align with the field, “spin-up” (↑) or oppose the magnetic field, “spin-down” (↓). Atoms have regions of space around them, called orbitals, in which electrons can reside. Each orbital can accommodate two electrons and these are filled in the most energetically favourable way. This is where one electron is spin-up (↑) and the other is spin-down (↓) such that the spins cancel (↑↓) and therefore there is no net magnetic moment. If an atom possesses an odd number of electrons then spins cannot cancel (the electrons which cannot cancel are called “unpaired” electrons) and hence there is a net magnetic moment associated with the species.

There are four main classes of magnetic behaviour, paramagnetism, ferromagnetism, antiferromagnetism, and ferrimagnetism. The type of behaviour is dependent upon how a spin interacts and aligns with its neighbours, as shown in Figure 1.

Classical magnetic materials, e.g. iron and nickel, are ferromagnetic in which each atom has several unpaired electrons that reside in different non-bonding *d* orbitals. These orbitals are all of similar energy, which leads to parallel alignment of the electrons, giving the atom a large magnetic moment. Furthermore, if the distance between electrons on neighbouring atoms is sufficiently close then they will “cooperatively” align with one another. This alignment occurs in small regions of the material, known as “domains”. If all the domains throughout the bulk of the material align in the same direction, then a strong magnet is formed (ferromagnet).

Using the same scenario but where adjacent spins align opposing each other, i.e. spins cancel, then there is no net magnetic moment, and this is called an antiferromagnet. The elements manganese and chromium are examples of antiferromagnets.

A ferrimagnet (strong magnet) occurs when there are different magnetic moments on adjacent species that align antiferromagnetically, but still possess net magnetic moment. Lodestone (Fe_3O_4) is an example of a ferrimagnet.

If adjacent spins are too far apart, or if the cooperative forces are very weak, then there is no interaction between them. In these materials the spins are not ordered, but are randomly orientated throughout the bulk. This type of material is called a paramagnet (weak magnet).

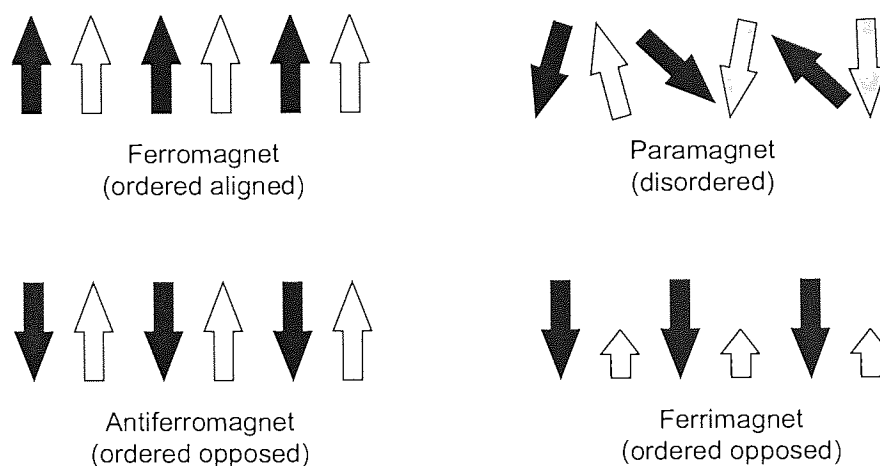


Figure 1 : Spin alignment in magnetic materials

In ferromagnets, antiferromagnets, and ferrimagnets there are forces between adjacent spins that create the alignment, which are characteristic of the species and are independent of temperature. Thermal energies force the spins towards disorder, and therefore loss of magnetic properties. When the thermal energies exceed the forces between neighbouring spins then alignment is lost and the material becomes paramagnetic. The paramagnetic-ferromagnetic transition occurs at a critical temperature, termed the Curie temperature (T_c), and paramagnetic-antiferromagnetic transitions occur at the Néel temperature (T_n).

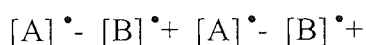
1.2.1 Spin interactions

There are two main pathways for spins to interact with one another^{6,7}:-

- 1) exchange coupling (via orbitals)
- 2) dipolar coupling (through-space)

1.2.1.1 Orbital Interactions

There are many mechanisms of exchange interaction, which depend upon how the molecular orbitals are populated in the spin containing species. It is unnecessary to consider all of these exchange mechanisms, but an overview of the one that has recently been invoked to account for the ferromagnetic interactions in an organic molecule⁸ is now described. Orbital interactions between the partially occupied molecular orbital (POMO) and the next lowest unoccupied molecular orbital (NLUMO) on an adjacent molecular species determine the exchange interaction. This theory relies on the sharing of an electron between a spin site and its neighbour by charge-transfer. A typical material can be envisaged by the structure:-



where A = donor and B = acceptor. If an electron is excited from the POMO of A to the NLUMO of B then ferromagnetic exchange takes place, as shown in Figure 2.

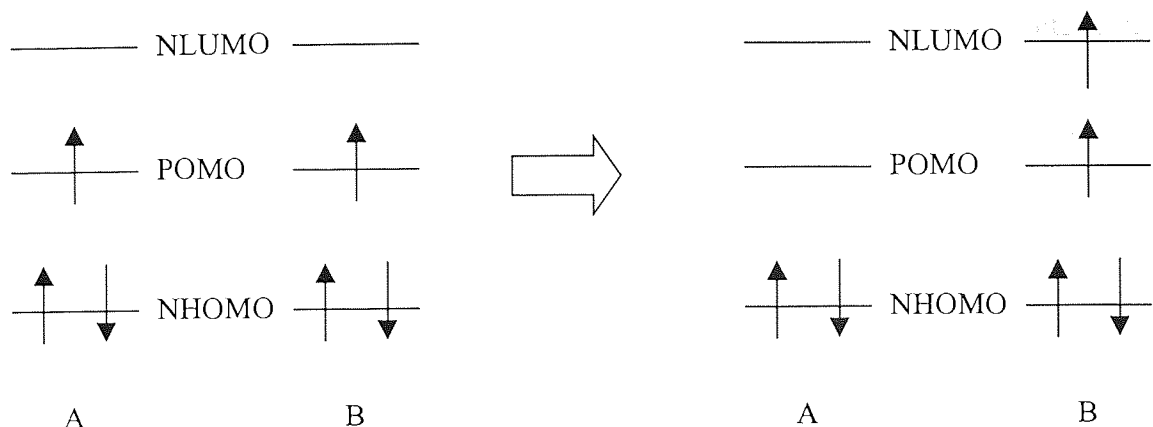


Figure 2 : Ferromagnetic spin exchange POMO to NLUMO

Ferromagnetic exchange can also be obtained by the virtual excitation of the next highest occupied molecular orbital (NHOMO) of A to the POMO of B, in which the two electrons remaining on A align ferromagnetically.

If there is a virtual excitation of an electron from the POMO of A to the POMO of B, then antiferromagnetic exchange predominates, as shown in Figure 3. The two electrons of the virtual POMO of B have to exist anti to each other because of the Pauli principle, in which electrons occupying the same space are forbidden.

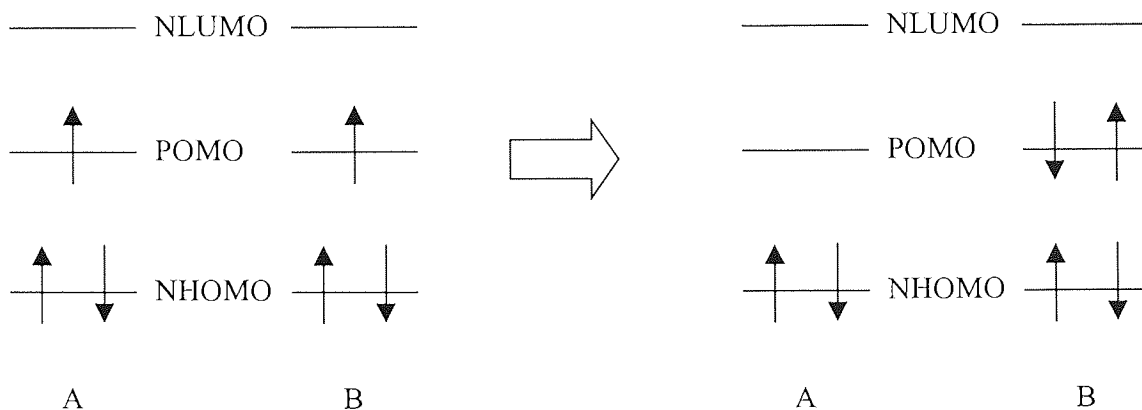


Figure 3 : Antiferromagnetic spin exchange POMO to POMO

The type of exchange interaction is determined by the overlap of molecular orbitals. If the POMOs of A and B overlap, then antiferromagnetic exchange is the result, but if this is somehow prevented then the ferromagnetic exchange is possible (POMO to NLUMO).

It is important to emphasise the fact that both donor A and acceptor B are free radicals, and that these types of spin exchange are intermolecular effects.

1.2.1.2 Dipolar coupling

Dipolar coupling does not involve the overlap of electron orbitals, but is the result of spin interactions due to the magnetic fields generated by the magnetic moment associated with each spin. This type of interaction is much weaker than that of the exchange interaction. It is theoretically possible that dipolar coupling could result in ferromagnetic spin alignment but only at low temperatures (lower than 1K).

The spin of an unpaired electron can also induce a polarisation of an electron in a neighbouring atom, “spin polarisation”. This is an intramolecular effect only, but it is sometimes important in determining magnetic properties in organic molecules. An example of spin polarisation is when an unpaired electron on a carbon-based p orbital polarises the paired spin in an orthogonal C-H σ bond so that one of the paired electrons is more in the vicinity of the C atom. There is no unpaired spin density on the hydrogen atom.

If only a few neighbouring spin sites take up alignment then the effects are said to be “short range”. When the spin alignment takes place in many neighbouring sites it is termed “long range”.

1.2.2 Criteria for an organic magnet

From this theoretical consideration some initial conclusions can be made about how magnetism may be produced in purely organic materials:-

- a) each molecule in the material must have at least one unpaired electron.
- b) there is an optimum distance between spin sites which leads to alignment
- c) spin alignment must be a property of the whole material.

If an organic material is to have magnetic properties then all of these criteria must be fulfilled. There are several strategies towards the design of synthetic magnets, the most successful being charge transfer complexes⁵. These transition metal complexes, however, are unstable to air and are notoriously difficult to synthesise⁴. Other attempts have utilised oligomeric carbenes, but these have proved to be highly unstable and are prone to synthetic defects⁹. This project, however, is primarily focused on organic materials that are stable and easily synthesised. It is necessary to consider the design features of a magnetic material without the presence of unstable carbenes/metal complexes.

1.3 Organic Radicals as Magnets

Normally, electrons in organic molecules are spin-paired, so that their spins cancel each other out. An unpaired electron is required in a molecule for it to possess a net magnetic moment. An organic molecule containing an unpaired electron (a “radical”) meets this criterion. Radicals, however, are normally transient and their lifetimes are extremely short, e.g. a methyl radical decomposes with a half-life of 10 to 15 minutes in methanol at 77K^(10 pp.186).

The short lifetime of these species is associated with their high reactivity, so once the radicals are formed they are consumed quickly. They react with their environment, e.g. solvents, oxygen in the air, and other organic radicals. Their magnetic properties will be lost if the spins in an organic magnet degrade or react with each other, so it is imperative that the radicals are stable.

1.3.1 Stable Organic Radicals

A stable radical can be defined as one that can be obtained in a pure form, stored, and handled in the laboratory with no more precaution than that taken with conventional organic compounds¹¹. The stability of a radical species is dependent upon four main factors.

1. Substitution
2. Resonance
3. Steric hindrance
4. Presence of a hetero atom

1.3.1.1 Substitution

The stability of a radical is affected weakly by the degree of substitution around it^(10 pp. 188), as shown in Figure 4. The series is a reflection of the hyperconjugation effects possible, which stabilise radical species. Although tertiary radicals are more stable than primary, they are still transient under ordinary conditions.

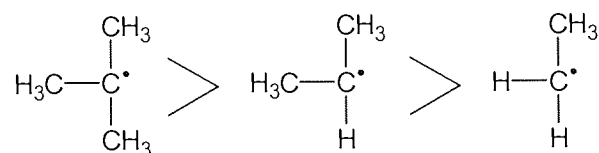


Figure 4 : Effect of substitution on stability of a radical

1.3.1.2 Resonance

Radicals can be stabilised by resonance interactions, in which the unpaired electron is delocalised over a π conjugated system^(10 pp.189-190). The radical is more stable because the average electron density on each possible site is reduced. For example, the radical depicted in Figure 5 exists in equilibrium with its dimer in solution. In the solid state, resonance interactions are insufficient for the radical to exist in the monomeric form.

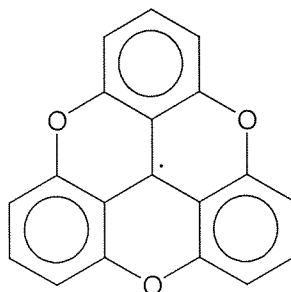


Figure 5 : A radical stabilised by resonance

1.3.1.3 Steric Hindrance

The effect of steric hindrance is one of the most important factors that govern the stability of a radical. This is exemplified by the perchlorotriphenylmethyl radical¹² (Figure 6), which is stable to oxygen, solvents (inert in boiling toluene), halogens, and remains stable at temperatures up to 300°C. In this example, the contribution from resonance delocalisation is minimal because the aryl rings are forced into a propeller arrangement about the radical centre. These fascinating properties are ascribed to the huge steric hindrance, which not only conceals the radical from the environment but also from other radical species as well.

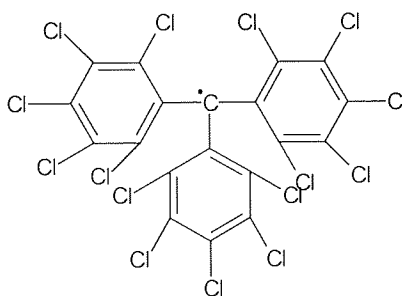


Figure 6 : Perchlorotriphenylmethyl, a stable radical

1.3.1.4 Neighbouring heteroatoms

1.3.1.4.1 Nitroxides

The stability of a radical is increased greatly by the presence of a neighbouring heteroatom, e.g. 2,2,6,6-tetramethyl-1-piperidinyloxy free radical (TEMPO)¹¹, as shown in Figure 7. Radicals containing the (N-O[•]) group are generally known as nitroxides, and this term will be used throughout this work.

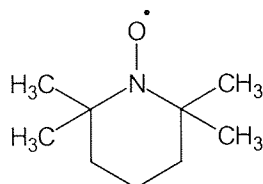


Figure 7 : TEMPO stable radical

TEMPO is sufficiently stable to exist in the monomeric form at room temperature. The adjacent methyl groups sterically shield the radical from its environment. In addition, the electronic configuration between the nitrogen and oxygen atoms enhances the stability of the radical¹³, as shown in Figure 8. This occurs via orbital overlap between the oxygen radical and a lone pair of electrons on a neighbouring hetero atom, in this case nitrogen.

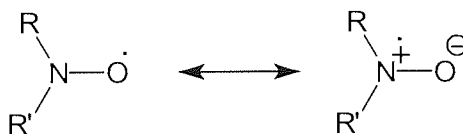


Figure 8 : Resonance forms of nitroxides

The TEMPO moiety is probably more accurately represented in Figure 9, in which there is a three electron bond between the nitrogen and oxygen.

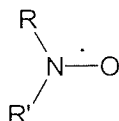


Figure 9 : Hybrid representation of a nitroxide

This electronic arrangement makes the radical very stable, because the spin density of three electrons is shared between two atoms. Standard chemical reactions can be performed on nitroxide containing molecules without degradation of the radical group. This is exemplified by the reduction of a carboxylic acid derivative of TEMPO with lithium aluminium hydride, as shown in Figure 10.

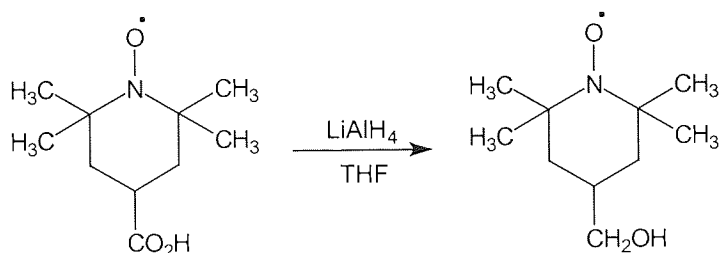


Figure 10 : Example of TEMPO stability

1.3.1.4.2 Other hetero radicals

There are many more examples of stable radicals that utilise a neighbouring hetero atom, such as verdazyl¹⁴ (Figure 11) and thioaminyls¹⁵ (Figure 12). The verdazyl group is based upon a tetrazine ring, in which the radical is delocalised over five of the six possible atoms¹⁶. Verdazyls however, are sensitive to oxygen and can be difficult to synthesise. Thioaminyls are not as stable as verdazyls and sometimes the radical can be degraded by dimerisation of two molecules, owing to a lack of steric hindrance.

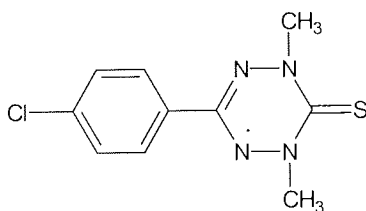


Figure 11 : Verdazyl stable radical

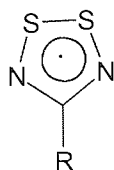


Figure 12 : Thioaminyl stable radical

1.3.1.4.3 Nitronyl nitroxides

Ullman first reported a stable radical based upon a nitroxide in conjugation with a nitrone¹⁷, as shown in Figure 13. It is generally called “nitronyl nitroxide” and this term will be used throughout this report. Much research has focussed on this stable radical because of its excellent stability and ease of synthesis. It is used throughout this research so the chemical and electronic properties will now be examined in depth.

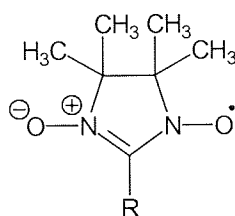


Figure 13 : Nitronyl nitroxide stable radical

When R is saturated, the radicals are generally red and are stable enough to be stored for months at 0°C. Stability is markedly increased when R is unsaturated, or aromatic, in which the radicals can be stored indefinitely at room temperature. An example of this stability is the fact that aryl nitronyl nitroxides can withstand harsh conditions, such as boiling water or alkali, without significant decomposition. These aryl derivatives are usually blue, or can sometimes be obtained as violet depending upon other substituents on the phenyl ring¹⁸.

The steric hindrance provided by the four methyl groups is of great significance for the stability of the radical. For example, it was reported that the stability of the nitronyl nitroxide group was considerably reduced upon replacement of these methyl groups by a phenyl ring¹⁹, as shown in Figure 14. It was reported to partially decompose in solvents such as acetone, diethyl ether, and benzene, in which most other nitronyl nitroxides are

stable. The radical was stable in the solid state, however, which indicates that the nitronyl nitroxide group is inherently quite stable.

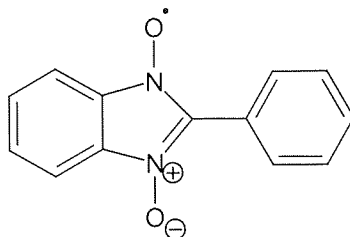


Figure 14 : A nitronyl nitroxide with reduced stability

The nitronyl nitroxide group is an excellent stable radical because it is sterically shielded, it has heteroatoms adjacent to the radical, and it is also stabilised by resonance. Theoretical models have been carried out in order to assess on which atom/atoms the unpaired electron actually resides, but the results often differ depending upon the program and parameters used²⁰. A more satisfactory spin analysis was carried out experimentally, using neutron diffraction²¹. This revealed that within each molecule the unpaired electron is shared between both sets of oxygen and nitrogen atoms, which must be attributable to resonance forms²³, as shown in Figure 15. Furthermore, the spin is evenly shared between the nitrogen and oxygen atoms of each group. The spin distribution may change if the solvent is polar, as this tends to stabilise resonance forms with increased spin density on the nitrogen atom¹⁷.

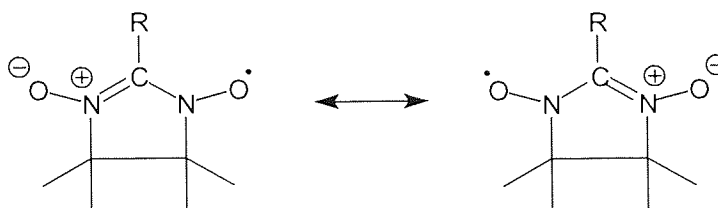


Figure 15 : Resonance structures of nitronyl nitroxide

The ring structure of the nitronyl nitroxide group exists in an almost planar conformation. However, this group is actually twisted out of plane with the phenyl ring. The dihedral angle usually varies between 30° and 50° , depending upon the other substituents on the phenyl ring. Spin delocalisation over the phenyl ring is therefore minimal. An orbital node at the central carbon of the O-N-C-N-O group also prevents delocalisation²².

This radical has been tested in applications such as non-linear optics^{18,23} and photochromism²⁴ but has found little use when compared to conventional materials. The recent discovery of a ferromagnetic, nitronyl nitroxide containing molecule has fuelled the interest in this type of stable radical.

1.3.2 The first organic ferromagnet

The first organic molecule to exhibit bulk ferromagnetism was 4-nitrophenylnitronyl nitroxide (4NPNN, as shown in Figure 16) discovered in 1989 by Awaga *et al*²⁵ and later characterised in greater depth by Tamura²⁶. 4NPNN exists in four different crystalline phases, of which only the β exhibits bulk ferromagnetism²⁷. The temperature at which bulk ferromagnetic behaviour breaks down into paramagnetism, known as the Curie temperature T_c , is 0.6K. Although this temperature seems very low it was a significant advance because bulk ferromagnetic behaviour had never been observed before in purely organic molecules. Hysteresis was observed in 4NPNN below its T_c , which confirms the bulk ferromagnetic properties of the material.

Ferromagnetic spin interactions are also present in the γ phase, but the bulk sample is paramagnetic⁸.

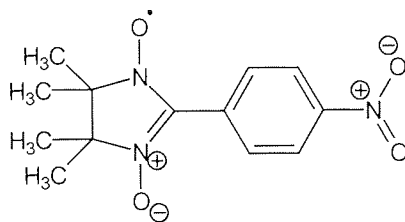
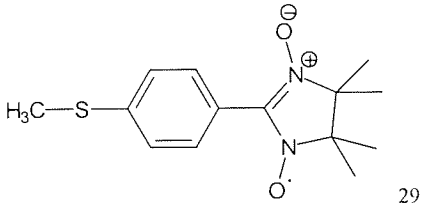
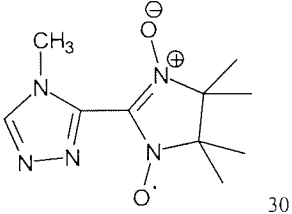
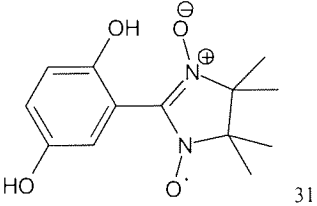
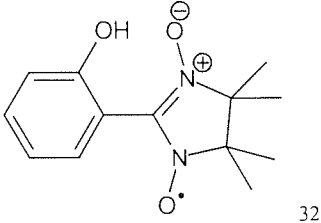


Figure 16 : Nitronyl nitroxide based ferromagnet (4NPNN)

Many other nitronyl nitroxides have been prepared and found to be ferromagnetic, although none have a higher T_c than that of 4NPNN. Nakatsuji has reported an extensive review of the magnetic properties of nitronyl nitroxides²⁸. A few examples of these molecules and their T_c 's are listed in Table 1.

Table 1 : Ferromagnetic molecules containing a nitronyl nitroxide

Structure	T_c (K)
 29	0.2
 30	0.6
 31	0.5
 32	0.45

1.3.3 A thioaminyl magnetic molecule

A molecule containing a thioaminyl group was recently reported to be magnetic at 36K³, as shown in Figure 17. The high T_c of this molecule was a step forward in the design of room temperature organic magnets. On closer examination this molecule is not a ferromagnet strictly speaking. It is an unusual type of magnet called a “canted

ferromagnet", in which the spins are aligned antiferromagnetically but they all tend to point to one side, as shown in Figure 18. It was estimated that the material is approximately one thousandth of the magnetic strength of iron.

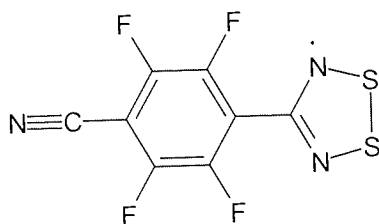


Figure 17 : A thioaminyl radical with high T_c

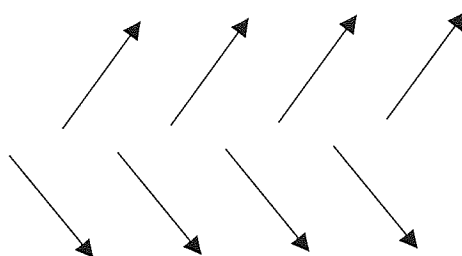
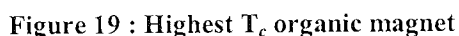


Figure 18 : A "canted ferromagnet"

1.3.4 An organic molecule possessing the highest T_c

The highest T_c (1.48K) of an organic material belongs to a nitroxide biradical, *N,N'*-dioxo-1,3,5,7-tetramethyl-2,6-diazaadamantane³³, as shown in Figure 19. This molecule is based on an adamantane molecule, and it was shown to exhibit three dimensional intramolecular and intermolecular ferromagnetism. The ferromagnetic spin coupling in this molecule was cleverly designed using topological considerations, as described by Yoshizawa³⁴. It is most likely that the spin interaction is of the dipolar type (through-space), but the T_c is relatively high for this to be the only coupling mechanism. Instead the FM behaviour is probably the result of a combination of dipolar and exchange spin interactions. Curiously, hysteresis was not detected in this material and no account was made to explain it.



The bulk magnetic effects observed in molecular magnets are the result of spin alignment in two or more dimensions. Most radicals however, do not have bulk magnetic properties. In this research, polyradicals possessing bulk FM properties are required, and as Dougherty points out, "... one cannot simply create a large number of spins, crystallise or otherwise condense them, and then hope for the best. Most solid samples of radicals will, at low temperatures, behave as antiferromagnets"⁶. It is essential therefore, to examine the factors that contribute to FM exchange and FM bulk properties in some of the known organic radicals. These design considerations can then be applied to polyradical systems.

The bulk ferromagnetic effects observed in the β phase of 4NPNN are directly related to the crystalline structure. Structural determination using X-ray techniques found that there was close contact between the radical of one molecule and that of a neighbouring molecule²⁵. Between these two radicals was a nitro group of another molecule, as shown in Figure 20. This contrasts with the simple phenylnitronylnitroxide (PNN), in which spins are too far apart for ferromagnetic coupling to take place³⁵. The difference between 4NPNN and PNN is the presence of a *para* nitro substituent. Theoretical modelling shows no spin density (from spin polarisation) on the nitro group^{20,22}. The ferromagnetic alignment, therefore, is likely to originate from spin interactions that go through the nitro group. The low Curie temperature suggests that the FM couplings originate from dipolar interactions. Compression of a crystal of 4NPNN should therefore increase the T_c of the material, as the distance between the radicals becomes shorter. However, a reduction of T_c was found when pressure was applied to 4NPNN, suggesting that the spin interactions are

the result of a mixture of exchange and dipolar couplings, or exchange coupling alone³⁶. These exchange interactions in 4NPNN are thought to be very similar to those described earlier in this report (refer to 1.2.1 Spin interactions).

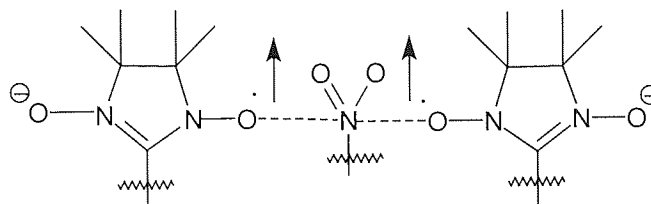


Figure 20 : Ferromagnetic spin alignment through a nitro group

Only the β phase of 4NPNN has a nitro group sandwiched between two radicals. The other phases of 4NPNN do not have this structural feature, and hence are not ferromagnetic in the bulk. Spin exchange of the nitronyl nitroxide with the phenyl ring (NO-Ar) of another molecule gives rise to ferromagnetic spin interactions in the other phases⁸. There are many examples of ferromagnetic NO-Ar spin couplings which do not result in bulk properties, such as 4-fluorophenyl nitronyl nitroxide³⁷, a quinolyl nitronyl nitroxide³⁸, a triazole nitronyl nitroxide³⁰, and a N-methylpyridinium nitronyl nitroxide³⁹.

In the molecule 4-cyanophenyl nitronyl nitroxide, both NO-Ar and spin coupling through a cyano group are thought to take place⁴⁰. This molecule does not have ferromagnetic bulk properties, only short range FM exchange interactions.

In summary, the substituents of the phenyl ring do not provide a path for the interaction of neighbouring spins, except in the case of β 4NPNN and 4-cyanophenyl nitronyl nitroxide. Instead, they influence the structure of the crystalline material by electrostatic forces. Spin interactions are related therefore to the crystal packing.

1.4.2 Hydrogen bonding⁴¹

If the crystalline packing could be controlled to make FM interactions favourable, then new organic magnets with higher T_c 's may be possible. Veciana was the first to study the influence of hydrogen bonding on the crystalline structure of nitronyl nitroxides^{42,43}. This was accomplished by the introduction of a para hydroxyl group onto phenyl nitronyl-

nitroxide, as shown in Figure 21. This compound exhibited FM interactions between the radicals, but bulk magnetic properties were absent. X-ray structure analysis showed that there was hydrogen bonding between the NO of one molecule and the OH group of a neighbouring molecule. Such hydrogen bonding between molecules gives rise to a zigzag chain. Weak hydrogen bonds form between the free NO and the CH₃ of another chain, which results in a 2D network. It is thought that FM interactions occur because of the short contact distance between radical species. As a direct consequence of the short contact distance SOMO-SOMO interactions, and hence AFM coupling, are prevented.

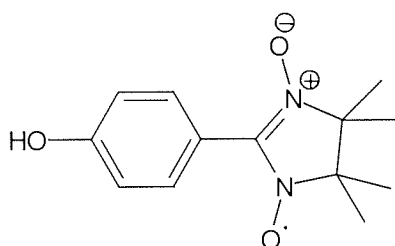


Figure 21 : FM interactions using hydrogen bonding

A study of several hydroxyl substituted nitronyl nitroxides revealed that the ortho isomer exhibited a bulk ferromagnetic interaction with a T_c of 0.45K³². The hydrogen bonding in this molecule is intramolecular, between the OH and the NO. The crystalline ordering is the result of very weak hydrogen bonding between the other NO group and the CH₃ of another molecule. It is thought that the FM interactions are the result of the 3D assembly of the crystalline state (long range order).

There are no bulk, or local ferromagnetic interactions when the hydroxyl group is in the meta position, or when there are two hydroxyl groups on the phenyl ring. Thus, the number and relative positions of the OH groups have a significant influence on the crystalline packing. The impact of the hydroxyl function on the spin polarisation in the molecule is minimal⁴¹. Thus, it is apparent that the effect of the OH group is to control the crystalline structure mainly.

The role of hydrogen bonding has been investigated by exchanging the hydrogen atoms of a ferromagnetic nitronyl nitroxide for deuteriums³¹. The main effect of this is to elongate the hydrogen bonds so that spin interaction should be decreased. If hydrogen bonds were to control the crystalline packing only then there would be a minimal impact on the spin interaction. If however, they were to play an important part in the FM interactions, then a decrease in the spin moment would be expected. This reduction of spin moment was found to occur in the deuterated molecule, which implies that hydrogen bonds are very likely to take part in the spin generation/transmission interactions.

Hydrogen bonding between a nitronyl nitroxide and a terminal alkyne has also been suggested as a possible mechanism for FM spin interactions⁴⁴. FM interactions, but no bulk behaviour, were also observed below 100K for a triazole based nitronyl nitroxide⁴⁵, as shown in Figure 22. The FM coupling was ascribed to hydrogen bonding between the N-O of one molecule and the hydrogen atom of a neighbouring triazole ring.

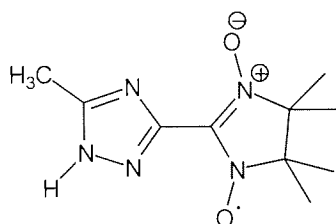


Figure 22 : Stable radical exhibiting strong FM coupling via hydrogen bonding

In summary, the hydrogen bonding can have a dual purpose. Between molecules in different planes it can lead to supramolecular assembly, and the formation of 3D interactions necessary for magnetic behaviour. The hydrogen bond can also provide a mechanism through which spin may be exchanged.

1.4.3 Diamagnetic bridges

Normally spin interactions occur via a substituent on the phenyl ring, but in 1995 it was discovered that a (1:1) complex derived from phenyl nitronyl nitroxide and phenylboronic acid (Figure 23) exhibited ferromagnetic spin interactions below 30K⁴⁶. (Phenylboronic acid is usually called benzenboronic acid; this name will be used throughout this report). A molecular chain of the type A-B-A-B was formed between the radical and the

benzeneboronic acid (BBA), in which intermolecular spin coupling via hydrogen bonds results in the ferromagnetic exchange.

At the present time, the radical/BBA complex has not been characterised completely so its ferromagnetic properties are not fully understood.

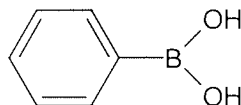


Figure 23 : Benzeneboronic acid

Phenylnitronylnitroxide exhibits paramagnetic spin interactions in the absence of benzeneboronic acid³⁵. Thus, the benzeneboronic acid provides a route through which spins can couple. Groups or molecules that facilitate spin coupling through them are known as “intermolecular spin-couplers”⁴⁷, as shown in Figure 24. This name is rather long, so in this report the term “bridge” will be synonymous with this effect.

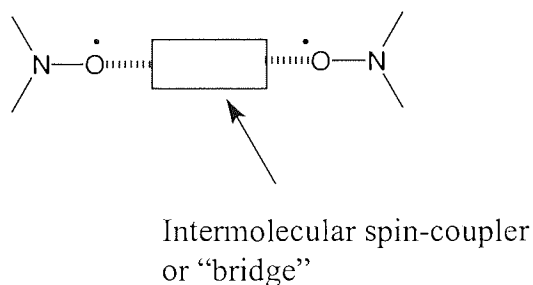


Figure 24 : Spin coupling through a "bridge"

This is the first example of spin transmission through a diamagnetic “bridge”, which is not on the same molecule as the radical. It is possible therefore, that the mixing of a simple radical species with a suitable “bridging” compound could create an organic ferromagnetic material.

1.5 Polyradicals

High spin density is required if strong ferromagnetic properties are to be obtained in organic materials. This may be achieved by creating a polymer bearing a stable radical on each repeat unit, a “polyradical”⁹. Ferromagnetic exchange may be achieved if the distance and electronic forces between radicals are favourable. Bulk ferromagnetic properties will only occur if the spin alignment occurs in at least two dimensions, and preferably three⁴. This implies that it is not sufficient for spins on the same polymer chain to be aligned ferromagnetically, but there must also be alignment between chains. Spin interactions, therefore, must be both intermolecular and intramolecular.

Two main strategies towards the development of polyradicals can be distinguished. Firstly, non-conjugated polymers bearing a pendant stable radical group. The second class of materials is those that contain pendant stable radicals which are conjugated to the polymer backbone, e.g. substituted polyacetylenes.

1.5.1 Early “ferromagnetic” organic materials

Before polyradicals were designed, it was common to pyrolyse organic materials with the aim of obtaining a magnetic material. The pyrolysis of polyacrylonitrile was a typical example of this strategy⁴⁸. Magnetic behaviour was observed in a small fraction of the material. This magnetic behaviour, however, was not the result of the magnetic regions inside the polymer, but was due to metallic impurities originating from careless experimental technique. This seems to be common throughout much of the earlier literature on magnetic polymers^{49,50}.

1.5.2 Polyradicals by post-polymerisation reactions

The most obvious way to synthesise a polyradical is to take a normal polymer and oxidise it to create the spin sites. This strategy is not widely reported in the literature, but has been shown to be very effective in the conversion of poly(*m*-anilines)⁵¹. The polymer was oxidised using several oxidising agents and magnetic characterisation showed that one of these modified polymers exhibited ferromagnetic properties in the bulk. An interesting variation on this theme is to employ a protecting group that can be removed by photochemical oxidation⁵². The problem with polyradicals obtained from post-

polymerisation modifications such as these is that the radical species are difficult to characterise. For example, in the case of the oxidised poly(*m*-aniline) it is unclear whether the spins correspond to a radical cation or to a nitroxide radical, the structures of which are shown in Figure 25.

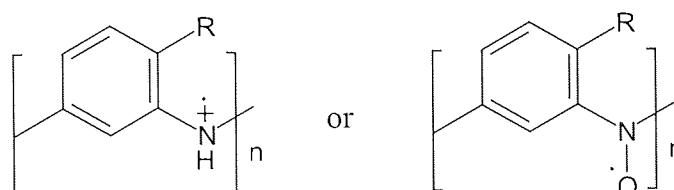
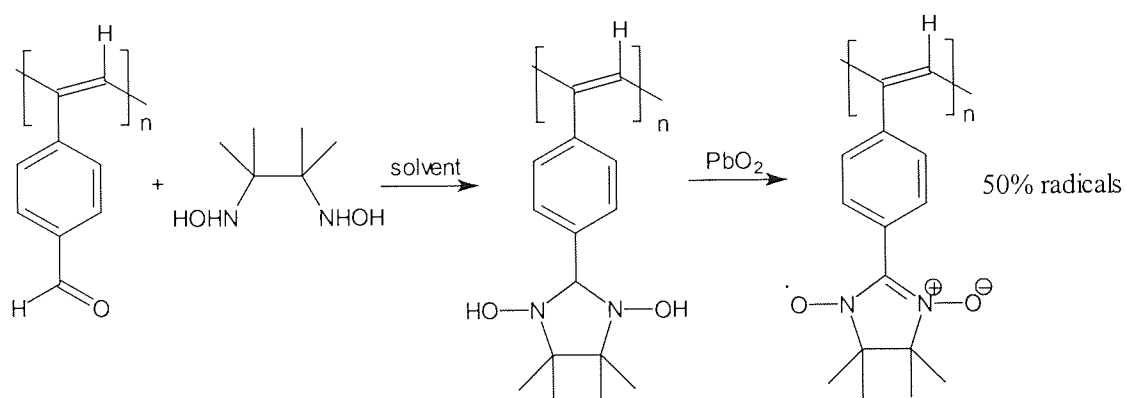


Figure 25 : Possible magnetic species in an oxidised polymer

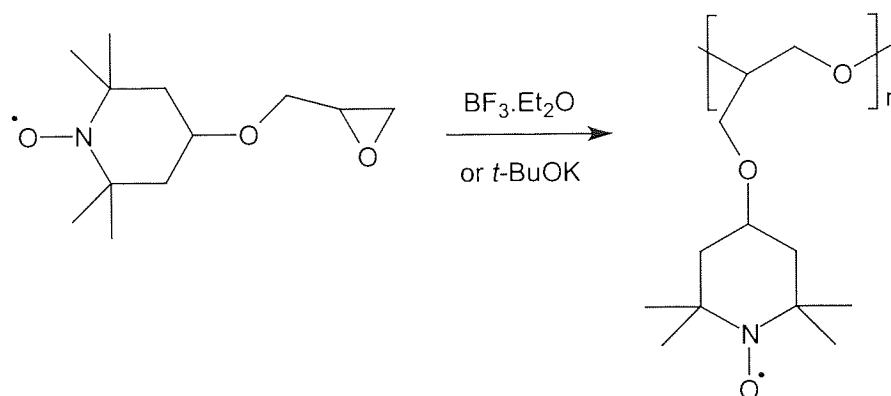
Incomplete oxidation of all the possible radical sites presents another significant problem. This is exemplified by the attempted synthesis of a polymer bearing a nitronyl nitroxide pendant group, in which a polymer possessing an aldehyde group was derivatised to the precursor of a nitronyl nitroxide⁵³, as shown in Scheme 1. Oxidation gave the nitronyl nitroxide containing polymer. On examination of the spin concentration it was found that only 50% of the possible spins had been created. This low conversion is most likely the result of the inability of the oxidant to penetrate fully the matrix of a pre-formed polymer. Hence, it is advantageous to incorporate the radicals into the monomer prior to polymerisation but this presents other problems that will be discussed later.



Scheme 1 : Creation of a polyradical by modification of a polymer

1.5.3 Polyradicals from radical monomers

The polymerisation of stable radical containing monomers would avert the problems of generating radicals by post-polymerisation reactions. An example of this type of polymerisation is that of a derivative of TEMPO bearing an epoxy group⁵⁴, as shown in Scheme 2. The yield of polyradical obtained was dependent upon the catalyst used, e.g. $\text{BF}_3 \cdot \text{Et}_2\text{O}$ gave 15% yield only, whereas *tert*-BuOK gave 92% yield. The incorporation of spin in this polyradical was 97% efficient, as measured by EPR analysis, which demonstrates the effectiveness of this synthetic strategy. The polyradical, however, was paramagnetic only.



Scheme 2 : Polymerisation of a monomer bearing a stable radical

Other examples of this strategy are the polymerisation of an isocyanide monomer containing TEMPO⁵⁵, and the polymerisation of a diacetylene based TEMPO derivative⁵⁶. The latter polyradical was found to exhibit FM interactions in 0.7% of the material only. The magnetic characterisation of this material has recently been questioned, because attempts to repeat the synthesis failed to produce any similar magnetic properties⁴⁹.

In summary, should an effective mechanism exist for the synthesis of a polymer with a high spin count it is not satisfactory just to have a large number of spins in a material. The spins must have a mechanism by which they can interact with one another if magnetic properties are to occur.

1.5.4 Polyradicals by design

To build materials with bulk magnetic properties one needs spin interactions between many radicals^{6,57}. This may be achieved in polyradicals by conjugating radicals. An overview of this theory is now given.

A radical can polarise a neighbouring bond, which leads to “spin polarisation” throughout the molecule. Consider two radicals conjugated through a para substituted phenyl ring, as shown in Figure 26. Positive spin polarisation is denoted as a star, and a negative polarisation as unstarred. If the number of starred atoms and unstarred atoms are equal, then antiferromagnetic coupling (singlet state) is predicted. Conjugated systems that operate in this way are known as “disjoint”.

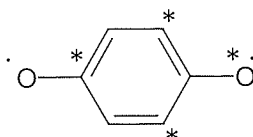


Figure 26 : Conjugation leading to AFM properties

On the other hand, if the number of starred atoms is greater than the number of unstarred atoms, then a triplet state leading to FM coupling is predicted. This is exemplified by two radicals linked through a meta substituted phenyl ring, as shown in Figure 27. Conjugated systems that lead to this scenario are known as “non-disjoint” or as “ferromagnetic coupling” units.

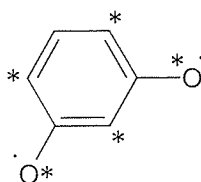


Figure 27 : Conjugation leading to FM coupling

In the case of polyradicals one needs to consider the spin polarisation of radical monomer units which are linked by a conjugated polymer backbone, as shown in Figure 28. The number of starred atoms is greater than the number of unstarred atoms, so the conditions for FM interactions are set up.

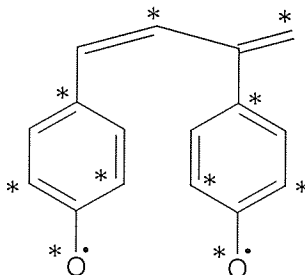


Figure 28 : FM interactions in a conjugated polyradical

Antiferromagnetic spin interactions will occur if a para substituted monomer is conjugated to a meta substituted monomer, because the number of starred and unstarred atoms are equal, as shown in Figure 29.

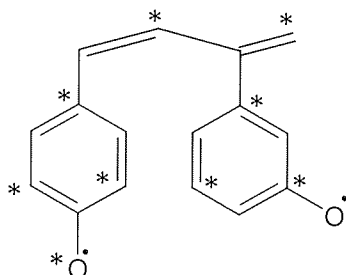


Figure 29 : AFM coupling in a conjugated polyradical

The type of radical employed is not of critical importance. It is the spin polarisation of the conjugated system that will determine the magnetic properties. Using this design philosophy, a radical can interact with another radical through a conjugated system, which favours FM coupling, as shown in Figure 30.

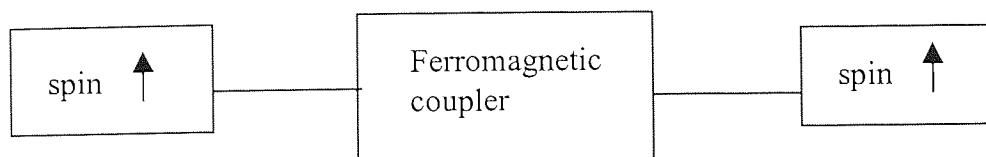


Figure 30 : Overview of spin interactions through a conjugated system

Conjugated polyradicals require careful design if ferromagnetic properties are to be realised.

1.5.5 Early conjugated polyradicals

Early attempts to synthesise conjugated polyradicals were poorly conceived because they just attached a non-conjugated radical to a conjugated polymer backbone. For example, a phenylacetylene monomer bearing two nitroxide radicals was polymerised⁵⁸ (Figure 31). Spin interactions in the polyradical were paramagnetic only.

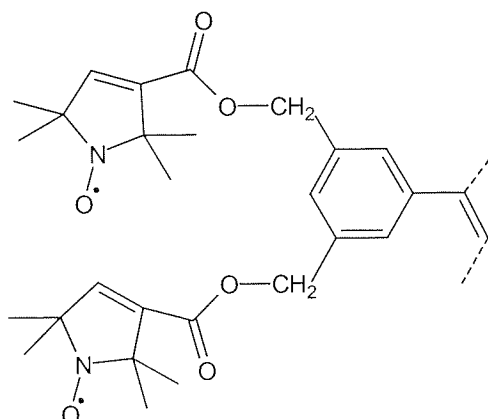


Figure 31 : A poorly designed "conjugated" polyradical

Another attempt consisted of polymerising a TEMPO based monomer bearing an isocyanide group⁵⁵. The backbone of this polyradical is not formally conjugated but is better described as "cross-conjugated"^(10 pp.33-34). The polyradical was found to be paramagnetic.

These two examples show that interactions between neighbouring spins demand conjugation between them.

1.5.6 Problems in conjugated polyradicals

The discovery of ferromagnetic interactions in a fully conjugated polyradical has led to an increasing amount of research into these types of materials. However, radicals conjugated to each other via a conjugated polymer backbone have been difficult to synthesise because of the tendency of the radicals to react with the catalyst or solvents employed during polymerisation. In some cases a few monomer units only constitute each polymer chain because the high rigidity of the backbone leads to insolubility during polymerisation.

There are problems associated with the stability of some polyradicals, which are the result of poor steric hindrance and insufficient delocalisation of the radical species. In these materials the conjugation is correct for FM coupling to occur, but if the radicals dimerise or degrade then spin interactions cannot be attained. A triphenylmethyl radical attached to a polyacetylene backbone is an example of this⁵⁹. Only 1% of the total theoretical spins were observed in this polyradical. The radicals employed in this system are stabilised by resonance, and extra stability might be given by delocalisation into the polymer backbone. However, radicals located on carbon atoms tend to be unstable without steric protection, as already described in reference to molecular magnets. It is most likely that the pendant radicals have degraded away.

The conditions employed during polymerisation can have a substantial impact on the magnetic properties of the resultant polyradical. Triethylamine was found to degrade nitroxide radicals when used as a solvent and resulted in only 49% of the spins being present in the resultant polyradical⁶⁰. The mechanism of degradation was not reported.

The poor solubility of some conjugated polyradicals has hindered the formation of high molecular weight polymer chains. For example, a polyradical containing ethynyl links (Figure 32) was found to have an average of seven monomer units in each chain⁶⁰. The low molecular weight is the result of the polyradical being insoluble in the solvent used for polymerisation. The polyradical has the correct ferromagnetic coupler between radicals (a meta substituted benzene ring) but only paramagnetic effects have been observed. The lack of spin interactions is attributed to a low spin concentration, because the radicals are present on every other repeat unit only. This means that there are just two or three radicals

per polymer chain, and the distance between them is quite large.

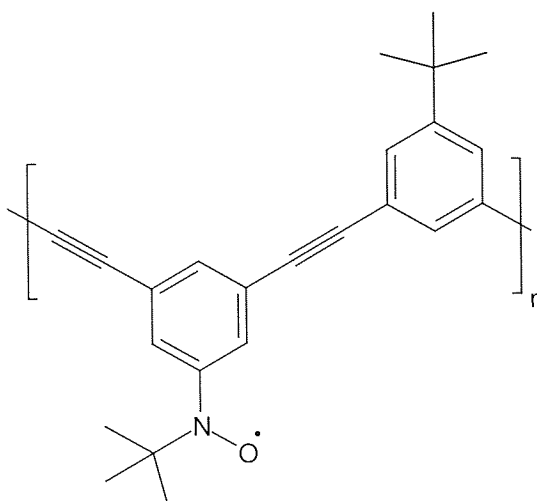


Figure 32 : Low molecular weight polyradical

A higher degree of polymerisation has been obtained using diacetylene links, in which the polymer chains are comprised of an average of 32 monomer units⁶¹, as shown in Figure 33. In this material however, the spin interactions were primarily dependent upon the precipitation method employed. When precipitated in hexane, paramagnetic spin interactions were found. However, removal of the solvent by vacuum gave a material exhibiting AFM spin interactions. A slight difference in the morphologies of the materials is the most likely explanation for the different magnetic behaviours.

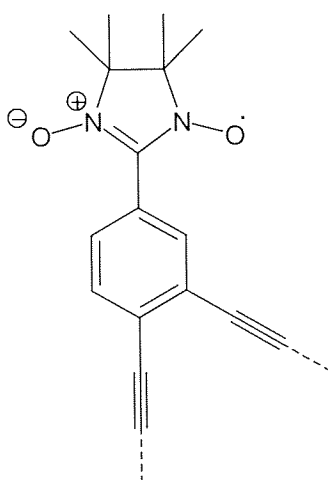


Figure 33 : Conjugated polyradical exhibiting AFM interactions

Higher average molecular weight polyradicals can be obtained using metal complexes as catalysts for polymerisation. The polymerisation of phenylacetylene bearing a nitronyl nitroxide group using such catalysts produced a polymer with a weight average molecular weight of 150,000⁶². Magnetic analysis of this material showed paramagnetic spin interactions, indicating that high molecular weight is not a significant factor for ferromagnetic spin exchange.

Steric hindrance has led to the radical being forced out of plane with the conjugated system in many polyradicals. A typical example is polyphenylacetylene bearing a pendant nitronyl nitroxide group⁶². Theoretically, the spin polarisation of this polyradical fulfils the requirements necessary for exchange interactions. However, no ferromagnetic spin interactions were observed. Molecular modelling of the structure showed that conjugation between the radical and backbone cannot occur because the nitronyl nitroxide group is twisted out of the plane of the phenyl ring, which prevents delocalisation. Furthermore, the phenyl ring is out of plane with the polymer backbone.

Other radicals that are more in plane with the backbone have been attached to polyphenylacetylene. This is exemplified by the incorporation of a phenoxy radical⁶³, as shown in Figure 34. Delocalisation of the spin into the polymer backbone was suggested by EPR analysis. However, analysis of the spin interactions, measured using a SQUID magnetometer, showed that the polyradical was paramagnetic. At temperatures lower than 30K antiferromagnetic interactions were found, which are thought to occur via through-space spin coupling. Molecular modelling of the polymer showed that conjugation between radicals was prevented, because the phenyl ring is not in plane with the backbone of the polymer.

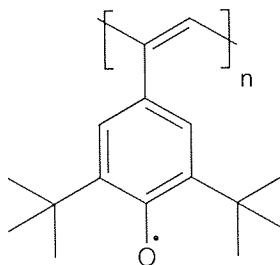


Figure 34 : Phenoxy radical on a polyphenylacetylene backbone

No spin interactions were observed for other radical groups such as nitroxide and galvinoxyl when attached to polyphenylacetylene⁶³. Non-interacting spins were also found in a conjugated polyimine, which had nitronyl nitroxides attached as pendant groups⁶⁴.

Therefore, the radical containing pendant group must be in plane with the backbone of the polymer if spins are to interact via a conjugated system. Furthermore, the radical must also be in plane with the pendant group.

1.5.7 Ferromagnetic spin interactions in polyradicals

It was realised that co-planarity between the radical and the backbone is essential for spin exchange. The polyphenylacetylene backbone does not permit this, because of steric congestion. Polyphenylenevinylene is better suited to conjugated polyradicals because the pendant groups are co-planar with the backbone.

Ferromagnetic spin exchange was first observed in polyphenylenevinylene bearing a pendant phenoxy radical^{65,66}, as shown in Figure 35. The phenoxy radical is almost co-planar with the phenyl ring, so spin delocalisation is possible. Steric protection of the radical by the tertiary butyl groups gave the polyradical sufficient stability to be isolated as a solid, at room temperature. The polyradical contained only 67% of the possible spins, because of incomplete oxidation. Delocalisation of the radical into the backbone of the polymer was observed using EPR analysis. Magnetic characterisation using SQUID showed that below 100K there were ferromagnetic interactions between spins. This suggests that conjugated radicals are tolerant of defects. However, the data reported was insufficient to determine whether ferromagnetic interactions occur throughout the bulk of the material.

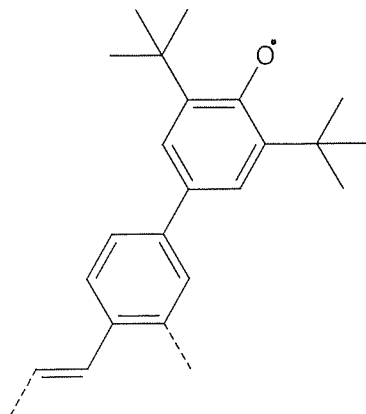


Figure 35 : Polyradical with ferromagnetic spin interactions

Theoretical modelling has shown that the spin polarisation of the repeat unit favours ferromagnetic coupling, as shown in Figure 36. The number of starred atoms is greater than the number of unstarred atoms. Theory also predicts that a higher degree of polymerisation leads to stronger ferromagnetic properties. Thus, the spin exchange is intramolecular, rather than intermolecular.

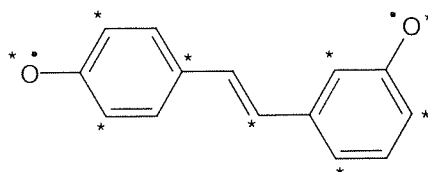


Figure 36 : Ferromagnetic spin interactions in a conjugated polyradical

Similar magnetic properties have been found in polyphenylenevinylene possessing a nitroxide group, indicating that planarity of the radical with the backbone is critical for the realisation of spin exchange⁶⁷.

1.5.8 Polyradicals utilising through-space spin interactions

Polyradicals designed to utilise dipolar (through-space) spin interactions are very rare. The strategy requires the pendant radical groups to be ordered, like those of a crystalline solid. The most effective design method is to employ liquid crystalline pendant groups⁶⁸. A TEMPO radical, when attached to a silicone polymer via a flexible spacer, as shown in Figure 37, was found to exhibit liquid crystalline behaviour. However, spin interactions

were paramagnetic only, which suggests that structural ordering of the radical species is not sufficient for magnetic interactions to occur.

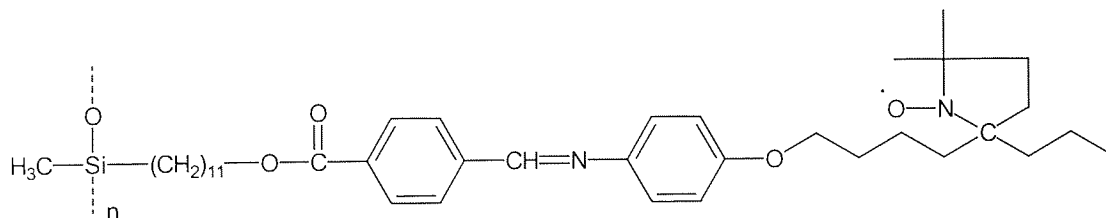


Figure 37 : A liquid crystalline polyradical

Another polyradical designed to utilise dipolar (through-space) coupling was comprised of a verdazyl stable radical and a polyiminomethylene backbone⁶⁹. The backbone exists in a helical conformation, which would result in stacking of the side groups. Electronic overlap may occur if there is a short contact distance between spins. However, paramagnetic behaviour was observed. It should be noted that less than 50% of the possible spins were present in the polyradical.

1.6 The strategy employed in this research

The aim of this work was to prepare an organic polymer that has ferromagnetic properties. It was noted previously, that it is not sufficient simply to create a polymer bearing pendant radical groups, but the radicals need a mechanism through which they can interact with one another. Most polyradicals in the literature employ the conjugated approach to the realisation of magnetic properties. This design strategy suffers from two major flaws, namely: the pendant group is not normally in plane with the backbone, and the radical is not in plane with the pendant group. Only by employing a polyphenylenevinylene backbone can spin exchange take place. However, the conditions used in the synthesis of this polymer tend to degrade the radicals. It is preferable for the polyradical to contain as many radicals as possible.

A different approach was used in this research, in which the design aspects of molecular magnets are integrated into a polyradical system. Bulk ferromagnetic properties are quite common in nitronyl nitroxide containing compounds. In these molecules, hydrogen bonding and “bridging” groups influence the magnetic properties. This project involved

the application of these design elements to polyradicals. If both nitronyl nitroxides and “bridging” group containing monomers could be co-polymerised then magnetic properties could be obtained.

Nitronyl nitroxide containing monomers are difficult to polymerise in good yields, because of incompatibilities with the polymerisation catalyst. The catalyst $\text{Rh}(\text{COD})(\text{NH}_3)\text{Cl}$ is known to give moderate yields of polyradical using a phenylacetylene based monomer. Higher yields of polyradical are required if co-polyradicals are to be prepared. In this research, the ligands around the rhodium are tailored to give increased yields of polymer.

It was essential to test the new catalyst with simple monomers, so that any incompatibilities could be characterised. Many phenylacetylene monomers were synthesised, because they were not commercially available. Polymerisation of these monomers allowed effective comparisons to be made between the new catalyst and those reported in the literature.

Several co-polyradicals were created utilising nitro or cyano “bridging” groups. Radicals could interact with “bridging” groups on the same chain, and “bridging” groups on a neighbouring chain. Thus, both intramolecular and intermolecular dipolar coupling could occur. The magnetic properties of these materials are investigated.

CHAPTER 2.
EXPERIMENTAL

2. EXPERIMENTAL

2.1 Chemicals and Sources

Name	Source	Grade	Abbreviation
(Bicyclo[2.2.1]hepta-2,5-diene)chlororhodium(I) dimer	Alfa	Unspecified	
1-(4-Iodophenyl)pyrrole	Maybridge	98%	
1-Ethynyl-4-fluorobenzene	Aldrich	99%	4FPA
2,3-Bis(hydroxylamino)-2,3-dimethylbutane sulphate	ACROS	Technical (85%)	BDBS
2,4-Dinitrophenylhydrazine	Aldrich	97%	2,4-DNP
2-Bromonaphthalene	Avocado	98%	
3,4-Dihydro-2 <i>H</i> -pyran	Aldrich	97%	DHP
3,4-Ethylenedioxyiodobenzene	Avocado	97%	
3,5-Dichloriodobenzene	Aldrich	99%	
3-Bromobenzaldehyde	Aldrich	97%	
3-Bromobenzonitrile	Aldrich	99%	
3-Hydroxyphenylacetylene	Lancaster	Technical	
3-Iodoanisole	Lancaster	98%	
3-Iodobenzylalcohol	Lancaster	99%	
3-Iodonitrobenzene	Aldrich	99%	
4-Bromo- γ -chlorobutyrophenone	Lancaster	98%	
4-Bromo-2-fluorobenzaldehyde	ACROS	98%	
4-Bromobenzaldehyde	Aldrich	99%	
4-Bromobenzonitrile	Aldrich	99%	
4-Bromiodobenzene	Avocado	97%	
4-Ethynylbiphenyl	Maybridge	98%	

4-Ethynyltoluene	Aldrich	97%	
4-Iodoaniline	Lancaster	98%	
4-Iodonitrobenzene	Lancaster	98%	
4-Iodophenol	Lancaster	98%	
4-Methoxyphenylacetylene	Maybridge	98%	4MeOPA
5-Bromopyrimidine	Aldrich	98%	
Ammonium hydroxide	Aldrich	30% in water	
Benzeneboronic acid	Aldrich	99%	BBA
Bis(triphenylphosphine)palladium (II) chloride	Lancaster	Unspecified	BTPPC
Copper(I) iodide	Lancaster	98%	
Ethyl-4-iodobenzoate	Avocado	98%	
Lead(IV) oxide	Aldrich	97%	
Phenylacetylene	Aldrich	98% *	PA
Potassium carbonate	Aldrich	99% (anhydrous)	
Pyridinium <i>p</i> -toluenesulfonate	Aldrich	98%	PTS
Trimethylsilylacetylene	Avocado	98%	TMSA

* Dried over calcium hydride for 12 hours and vacuum distilled to give a pale yellow liquid

2.2 Solvents and Sources

Name	Source	Grade	Abbreviation	Purification Procedure
Chloroform	Fisher	99% HPLC		
Dichloromethane	Laboratory stores	Lab	DCM	
Diethylether	Laboratory stores	Lab	Ether	
Ethanol	Laboratory stores	99%		Dried over Mg/I ₂
Hexane	Fisher	99% HPLC		
Methanol	Laboratory stores	Lab		
Tetrahydrofuran	Fisher	99% HPLC	THF	Dried over calcium hydride for 12 hours, then distilled under vacuum
Triethylamine	Aldrich	99%	TEA	Allowed to stand over potassium hydroxide pellets for 24 hours, then distilled using the vacuum line

2.3 Purification of Chemicals

2.3.1 Ethanol

Absolute ethanol was purified according to the literature procedure⁷⁰. The reflux apparatus for the purification of ethanol is shown in Figure 38 and consisted of a 2 necked, 1L flask fitted with a 100mL dropping funnel and reflux system. A water condenser and argon inlet/outlet bubbler were connected to the still. Magnesium turnings (2.5g), iodine (0.25g), and 50mL of absolute ethanol were added to the RBF. The grey suspension was refluxed, under argon, until the brown colour of iodine had disappeared, approximately 30-60 minutes. A further 500mL of absolute ethanol were added and the grey suspension was refluxed for 12 hours before use. Dry ethanol was removed through a 2 way Teflon tap fitted in the reflux section and used immediately.

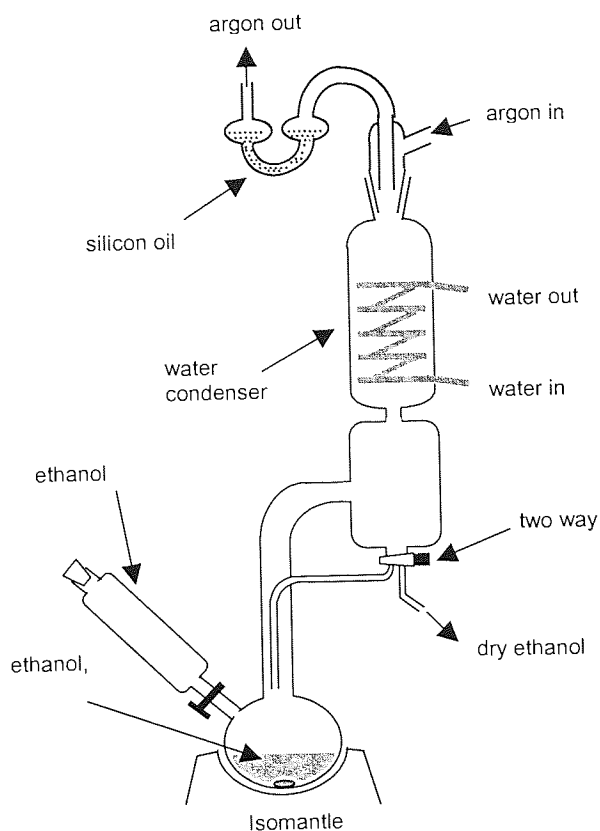


Figure 38 : Apparatus used to obtain dry ethanol

2.3.2 Distillation of solvents using a high vacuum line

A vacuum line was used to purify, degas, and distil solvents, under conditions that enabled many solvents/reagents to be distilled without heating. Highly flammable chemicals, such as phenylacetylene, can be distilled safely under vacuum.

The vacuum line consisted of a series of greaseless taps attached to a glass manifold, as shown in Figure 39. The manifold was connected to a mercury diffusion condenser and a high vacuum pump. Liquid-nitrogen traps were used on both sides of the mercury condenser to prevent stray vapours contaminating the manifold and vacuum pump.

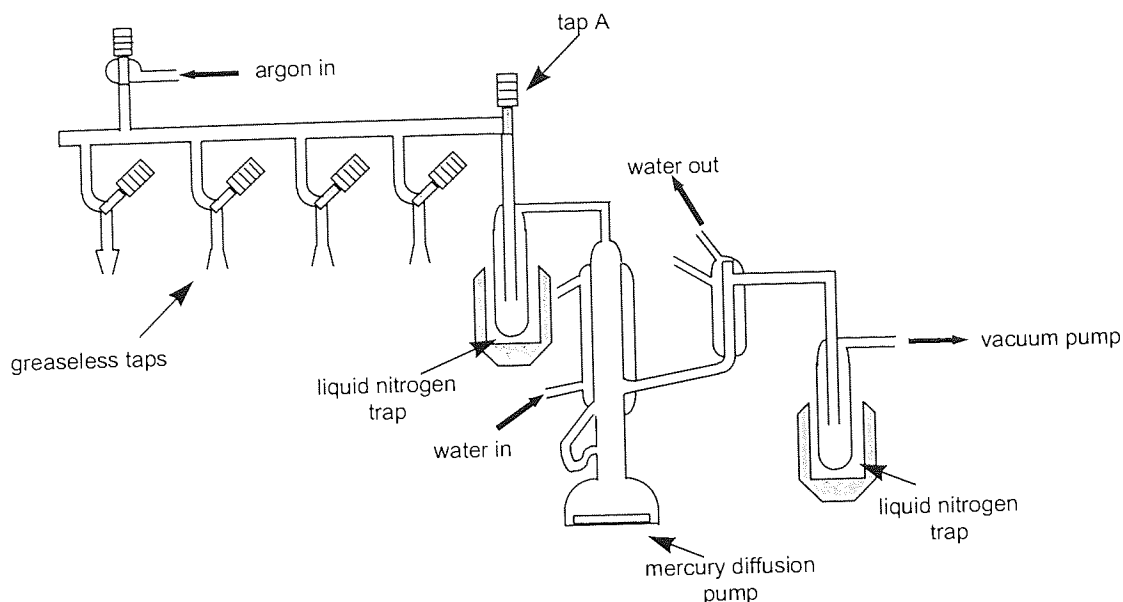


Figure 39 : High vacuum line used for distillation

Solvents were degassed using a freeze-thaw method before they could be distilled. A flask containing solvent was attached to the manifold and immersed in a Dewar of liquid nitrogen. When the contents were completely frozen, the flask was opened to the vacuum. Once all the air had been removed the manifold was isolated from the vacuum pump, by closing tap A. The Dewar of liquid nitrogen was removed and the contents of the flask allowed to thaw. Dissolved gases were removed from the liquid and then the contents were frozen and the procedure repeated. Closing the tap that connected the flask to the manifold isolated it.

A clean dry flask was attached to the manifold and then opened to the vacuum pump for 30 minutes to eliminate residual vapours. The dry flask was immersed in a Dewar of liquid nitrogen whilst still open to the vacuum. Once the flask was completely evacuated tap A was closed and the solvent flask opened to the manifold whereupon distillation into the frozen flask began. When the required amount had been distilled tap A was closed, and the freshly distilled solvent was thawed. The manifold and flask were flushed with argon. The flask was sealed using the greaseless tap and removed from the manifold, and the solvent was used immediately.

2.4 Characterisation Techniques

Although the structure determination techniques UV, IR, NMR, MS, SEC, and EA, are used throughout the project, they are well known and as such are not discussed in detail. More specialised EPR and SQUID analysis were carried out on substances containing free radicals. There is very sparse information about the SQUID technique because it uses the phenomenon of superconductivity and hence, is a relatively new technique for the measurement of magnetic fields. EPR has been known for much longer, and is well documented, so a fuller account of the technique is given.

2.4.1 Electron Paramagnetic Resonance (EPR)

The characterisation of a free radical cannot be accomplished using conventional NMR because paramagnetism leads to broadening of the signals. Instead a technique, called Electron Paramagnetic Resonance (EPR)⁷¹ was used to identify free radical species.

An unpaired electron can exist in two states, of which both are equal energy in the absence of an applied magnetic field. However, when a magnetic field is applied the electron can exist in two energy levels, parallel or anti-parallel to the field.

Electromagnetic radiation can be regarded as coupled electric and magnetic fields oscillating perpendicular to one another. When a molecule containing magnetic dipoles is irradiated with the magnetic component of microwaves, in the presence of a static magnetic field, interactions occur. Specifically, absorption will occur when the energy of incident radiation is equal to that of the energy-level separation.

In practice, for the detection of organic free radicals, it is common to keep the irradiation frequency constant and to sweep the magnetic field.

EPR can provide structural information of the free radical, and three parameters, g factor, linewidth, and hyperfine splitting describe this. For the purpose of this project only the latter is of importance. Hyperfine splitting arises from interaction of the unpaired electron and neighbouring magnetic nuclei, e.g. ^1H , ^{13}C , ^{14}N .

Professor J. C. Walton, of St-Andrews University, generously performed EPR analysis using a Bruker EMX 10/12 spectrometer operating at 9GHz with 100kHz modulation. Samples were examined in DCM, or THF solution in capillary tubes at ambient temperature (25°C). Prior of use each sample was degassed by bubbling nitrogen for 15 minutes. Polymeric free radicals were analysed in the solid state, and in DMF solution.

2.4.2 Gas Chromatography (GC)

GC analysis was performed with an ATI Unicam 610 Series gas chromatograph, and a flame ionisation detector. The column was a packed type, with silicon grease as the stationary phase. The oven temperature was set at a constant 150°C, or 200°C, or 250°C, depending upon the boiling point of the molecule.

2.4.3 Ultra Violet - Visible Spectrometry (UV)

UV-Vis spectra were obtained using a Perkin Elmer Lamda 12 spectrometer. DCM or CHCl₃ were used as the first choice solvent, other alternatives were THF, DMF, and DMSO. In this work it was used to measure the $\pi \rightarrow \pi^*$ electronic transitions of polyphenylacetylenes and other molecules. The absorption maximum (λ_{max}) provides an indication of the extent of conjugation in the polymer, in general, the longer the conjugation, the longer the wavelength of the absorption maximum (λ_{max}).

2.4.4 Infra Red Spectrometry (IR)

IR spectra were recorded on a Perkin Elmer FT-IR Paragon 1000. Solid samples were mixed with KBr and compressed into a disk. Liquid samples were analysed between two pre-formed NaCl disks.

2.4.5 Mass Spectrometry (MS)

Mass spectra were obtained using a HP 5989B MS Engine, with a HP 59987A Electrospray, and a HP 5890 Gas Chromatograph. MS may be performed using a number of different techniques but the one most used throughout this work was APCI (atmospheric pressure chemical ionisation), using methanol as solvent. APCI was used whenever possible because it allows the identification of a compound with

minimum fragmentation. The APCI technique protonates the compound, so the peak is found at one mass unit higher than the original compound, denoted as MH^+ . Where APCI failed, e.g. non-polar compounds, EI (electron impact) was used. EI substantially fragments the molecule and occasionally the parent ion cannot be observed. To decrease the amount of fragmentation a probe voltage of 50eV (rather than the normal 70eV) was sometimes used.

2.4.6 Nuclear Magnetic Resonance (NMR)

NMR spectra were obtained using a Bruker AC300MHz FT-NMR spectrometer and PENDANT⁷² pulse sequence. The ^{13}C spectra was proton decoupled using "composite pulse decoupling", which is similar to broadband decoupling. The PENDANT technique enhances the signal of an insensitive nucleus (^{13}C) by polarisation transfer from a sensitive nucleus (1H). PENDANT differentiates between types of substituted ^{13}C where -CH (tertiary) / -CH₃ (primary) are shown as positive signals and -C (quaternary) / -CH₂ (secondary) as negative signals. NMR analysis was carried out in deuterated chloroform (CDCl₃). Impurities in this solvent gave a characteristic peak in the 1H spectrum, a singlet at δ 7.24, and in the ^{13}C spectrum, three peaks at δ 77.43, δ 77.00, and δ 76.58.

2.4.7 Size Exclusion Chromatography (SEC)

SEC analysis was performed in duplicate by an external agency, RAPRA Technology Ltd, Shawbury, Shrewsbury, Shropshire, using a column (PLgel 2* mixed bed-B, 30cm, 10 microns) at a constant 30°C, with a flow-rate of 1.0mL/min, and THF as the solvent. The detector was of the refractive index type.

2.4.8 Superconducting Quantum Interference Device (SQUID)

Magnetic properties are best determined using a Superconducting Quantum Interference Device (SQUID)^{73,74,75}, because of its extremely high sensitivity to small magnetic fields. SQUID is able to perform susceptibility measurements down to a temperature of 1.8K, which is ideal for weak magnets where thermal energy can destroy magnetic properties.

There are at least three different types of SQUID instrument, RF (Radio Frequency), AC (Alternating Current), and DC (Direct Current), the simplest of which is the latter. A schematic diagram of a DC SQUID is shown in Figure 40. It consists of a superconducting loop where super-current enters at W and divides into two, part going to X and part going to Y, and then recombines at Z. X and Y are weakly conducting junctions (Josephson Junctions) through which super-current can tunnel. X is left unchanged whereas Y is subjected to a magnetic field (from a magnetic material). The super-current flow through junction Y is affected by a magnetic field and the difference in current is measured at Z. The difference in current can be related to the magnetic field strength at Y.

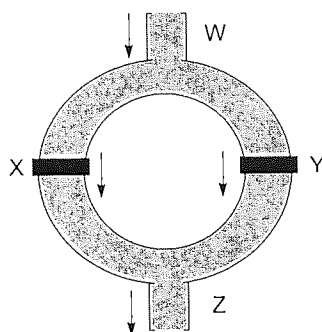


Figure 40 : Schematic of SQUID magnetometer

Dr Andrew Harrison, University of Edinburgh, performed susceptibility analyses with a Quantum Design MPMS₂ SQUID magnetometer. Samples were loaded into gelatine drug capsules, which in turn were held in a plastic drinking straw that had a negligible paramagnetic response. Data were taken over the temperature range 1.8-330K in an applied magnetic field of 1000Oe (or 0.1 T in SI units), and in some cases hysteresis loops were measured over the field range +/- 10,000 Oe (+/- 1 T) at various temperatures. Data were corrected for the diamagnetic response of the sample holder and of the constituent atoms in the sample, and calculated per gram of sample.

2.4.9 Elemental Analysis (EA)

MEDAC LTD, using a Carloerb 1106, performed C, H, and N elemental analysis in duplicate. Samples were combusted at an approximate temperature of 1000°C, and the resulting gases were separated using a GC and analysed using a thermoconductivity detector.

CHAPTER 3.
SYNTHESIS AND CHARACTERISATION OF
PHENYLACETYLENE MONOMERS

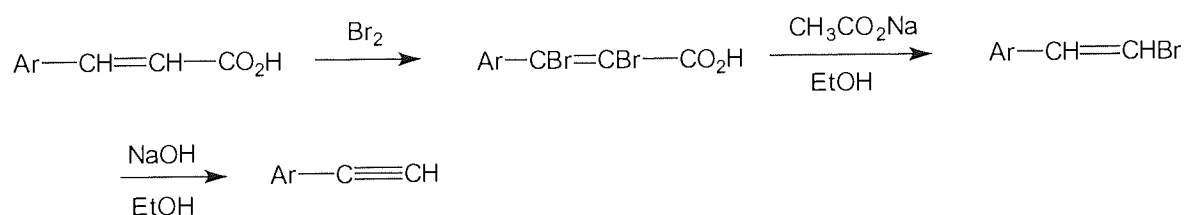
CHAPTER 3. SYNTHESIS AND CHARACTERISATION OF PHENYLACETYLENE MONOMERS

3. Objectives

To synthesise a wide range of functionalised phenylacetylene monomers that could be polymerised at a later stage. In particular, monomers with stable nitronyl nitroxide radicals, and monomers bearing a bridging group, such as nitro, cyano, and fluoro, were essential components of polyradicals.

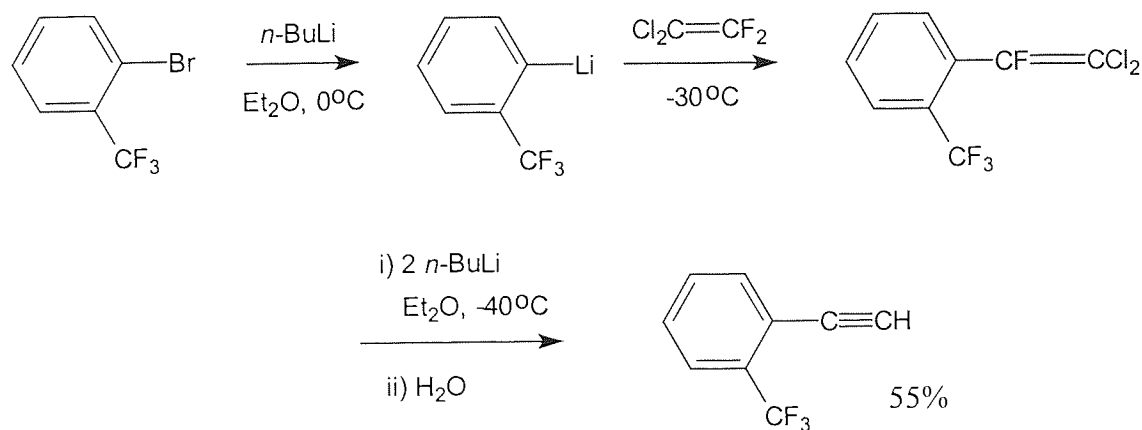
3.1 Classical synthesis of phenylacetylenes

Aryl alkynes can be prepared from methyl ketones, styrenes, and cinnamic acids (Scheme 3) using conventional dehydrohalogenation techniques⁷⁶, but the procedure suffers from poor yields and poor tolerance. The reactions are normally carried out under strongly basic conditions which can adversely affect base sensitive groups, such as esters.



Scheme 3 : Dehydrohalogenation of cinnamic acid to give phenylacetylene

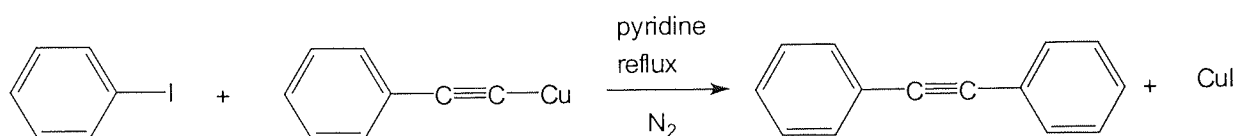
A different procedure for the synthesis of phenylacetylenes involves the addition of 1,1-dichloro-2,2-difluoroethylene to an aryl-lithium species⁷⁷, shown in Scheme 4, where the subsequent double de-halogenation generates the phenylacetylene in good yield. Again, the reaction is of limited scope because of the strong reagents employed (*n*-BuLi), which can interfere with functional groups sensitive to a strong base.



Scheme 4 : Synthesis of phenylacetylenes using de-halogenation

3.2 Synthesis of phenylacetylenes using palladium catalysed cross-coupling, or Sonogashira Coupling

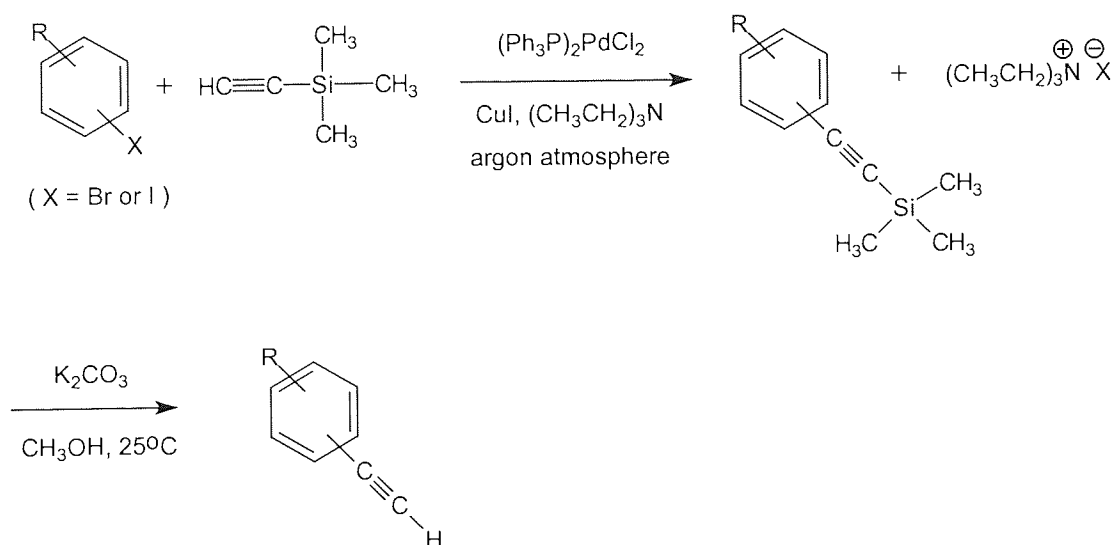
A more effective method involves the coupling of aryl iodides with a copper acetylide, in the Stephens Castro reaction⁷⁸, shown in Scheme 5. Under harsh reflux conditions the reaction generally gives good to excellent yields of the coupled product. However, the reaction can be hazardous because copper acetylides are explosively unstable under certain conditions, which can give rise to significant danger during the synthesis.



Scheme 5 : The Stephens Castro coupling reaction

Using a palladium catalyst the same reaction can be accomplished in high yields under milder conditions, as described by Heck⁷⁹. This reaction is sometimes referred to as Sonogashira coupling and this name will be used throughout this report. It is based upon the coupling of an aryl halide to trimethylsilylacetylene (TMSA), using a bistriphenylphosphinepalladium(II) chloride catalyst and triethylamine solvent, as shown in Scheme 6. Triethylamine not only acts as a solvent for the reaction but also as a base, and a scavenger of the hydrogen halide by-product. The reaction usually requires gentle

reflux, but it can sometimes be accomplished at room temperature by the addition of a catalytic amount of copper(I) iodide.



Scheme 6 : Synthesis of phenylacetylenes using the Sonogashira reaction

TMSA is used as a one end protected acetylene equivalent, to prevent double addition of the aryl halide. Deprotection of the trimethylsilyl group can be easily accomplished by mild hydrolysis conditions using potassium carbonate in methanol. Purification of this mixture by chromatography gives the phenylacetylene product.

The mild conditions used during the deprotection reaction are important because aromatic aldehydes are susceptible to the Canizzaro reaction in the presence of sodium hydroxide or other strong bases^(10 pp.1233-1235). Aldehyde functionality is essential for the subsequent synthesis of nitronyl nitroxide stable radicals, the target in this research.

The yield of coupled product obtained depends upon the nature of the halide, and also with the electron donating/withdrawing characteristics of any other substituents present on the ring. Excellent yields of the product can be obtained at room temperature when the starting material is an aryl iodide, or an aryl bromide that is deactivated towards electrophilic substitution. Aryl bromides possessing weak electron donor/withdrawing groups also give good yields, but require reflux conditions. Yields are dramatically reduced when the aryl bromide possesses a strong electron donor substituent, e.g. –

NR₂⁸⁰. Aryl chlorides are generally unreactive, although a few examples have been reported^{(79 pp.304),81}. To understand the order of reactivity of the halide, a consideration of the mechanism is required.

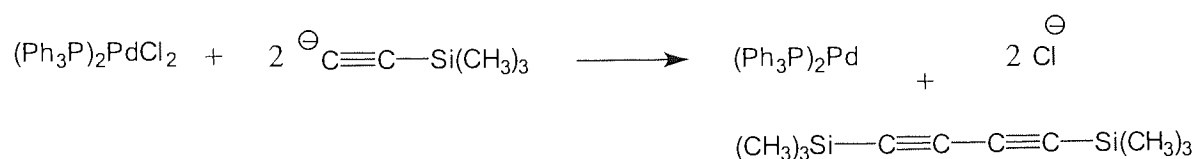
3.2.1 Mechanism of the Sonogashira coupling, and aryl halide reactivity

The *sp*-hybridised hydrogen of the terminal acetylene is acidic and can be removed by triethylamine, to give an acetylide, as shown in Scheme 7.



Scheme 7 : Loss of acetylenic hydrogen by triethylamine

The active catalyst in this case is bis(triphenylphosphine)palladium(0) which is formed by the reduction of bis(triphenylphosphine)palladium(II) chloride by two acetylides, resulting in the formation of the corresponding diacetylene as a by-product, as shown in Scheme 8. For this reason a slight excess of trimethylsilylacetylene is always required to maximise the yield of the product.



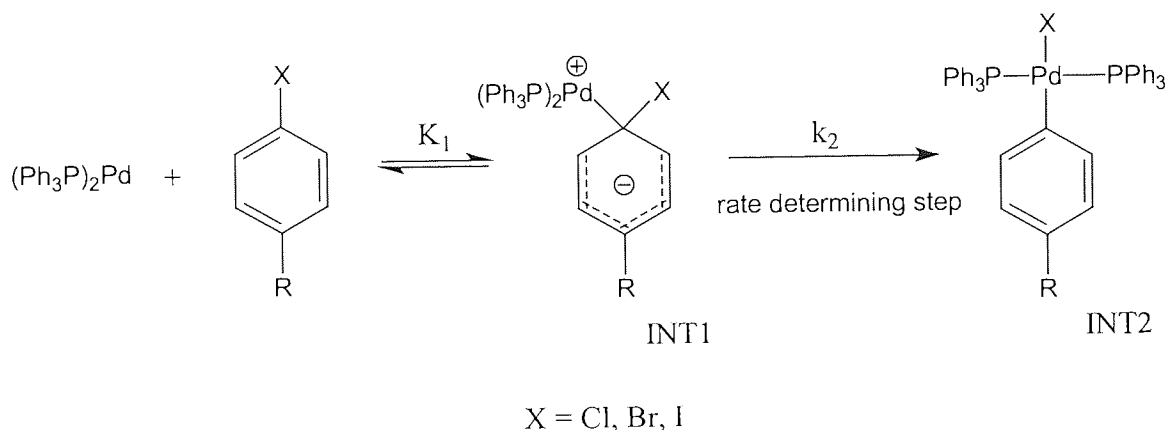
Scheme 8 : Formation of the active palladium(0) catalyst

The palladium(0) catalyst performs a nucleophilic attack on the aryl halide to give an intermediate (INT1), as shown in Scheme 9, which by spontaneously rearranges to a tetra-coordinate palladium(II) complex (INT2).

The equilibrium constant K_1 and the reactivity of the intermediate (INT1) determine the activity of the aryl halide in this scheme. Studies by Fitton showed that cleavage of the leaving halide group (X) from the aryl moiety, k_2 , is the rate determining step⁸¹. It was

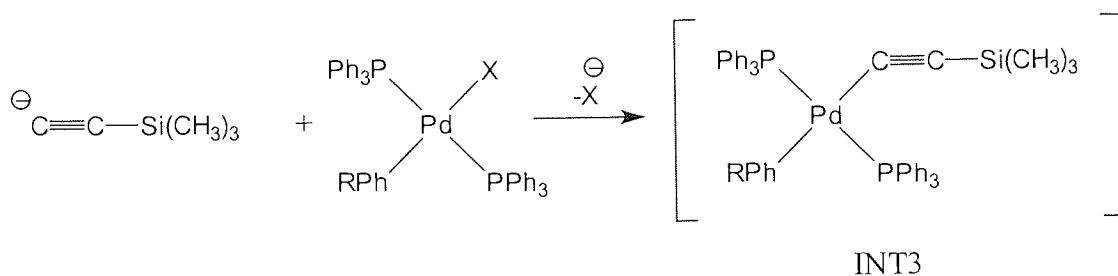
found that k_2 increased when changing the substituent X from chlorine, to bromine, and to iodine, in agreement with the proposed mechanism. The position of equilibrium is determined principally by the nature of R, electron withdrawing substituents favouring an increase in equilibrium constant K_1 . The order of reactivity of aryl halide was reported to be: *p*-nitro > *p*-nitrile > *p*-phenone > *p*-hydrogen, in agreement with the proposed mechanism.

This mechanism accounts for the poor reactivity of aryl chlorides and aryl bromides particularly those possessing a strong electron donating group. The C-Cl bond is stronger than both the C-Br and C-I bonds and thus causes a decrease in k_2 . Aryl bromides bearing a strong electron donating R group are thought to react poorly, because INT1 is destabilised, which decreases the equilibrium constant K_1 .



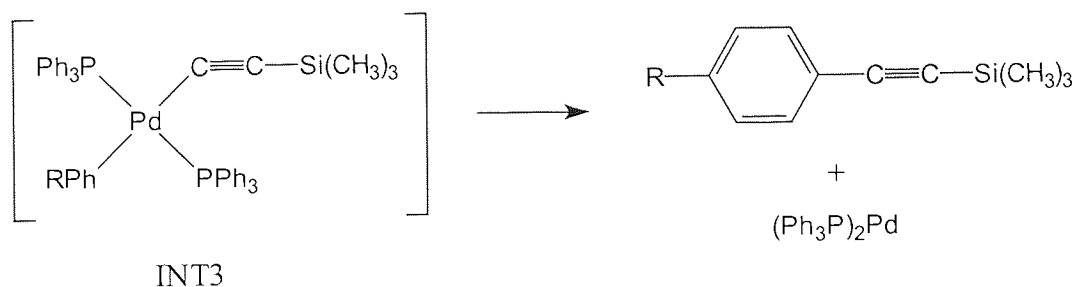
Scheme 9 : Oxidative addition of the aryl halide to the palladium(0) catalyst

Nucleophilic displacement of the halide by the acetylide gives the transient intermediate, INT3, as shown in Scheme 10.



Scheme 10 : Substitution of halogen for acetylide

Reductive elimination of INT3 produces the coupled product and regenerates the active catalyst, as shown in Scheme 11.



Scheme 11 : Reductive elimination to give the coupled product

3.2.2 Summary of the Sonogashira coupling reaction

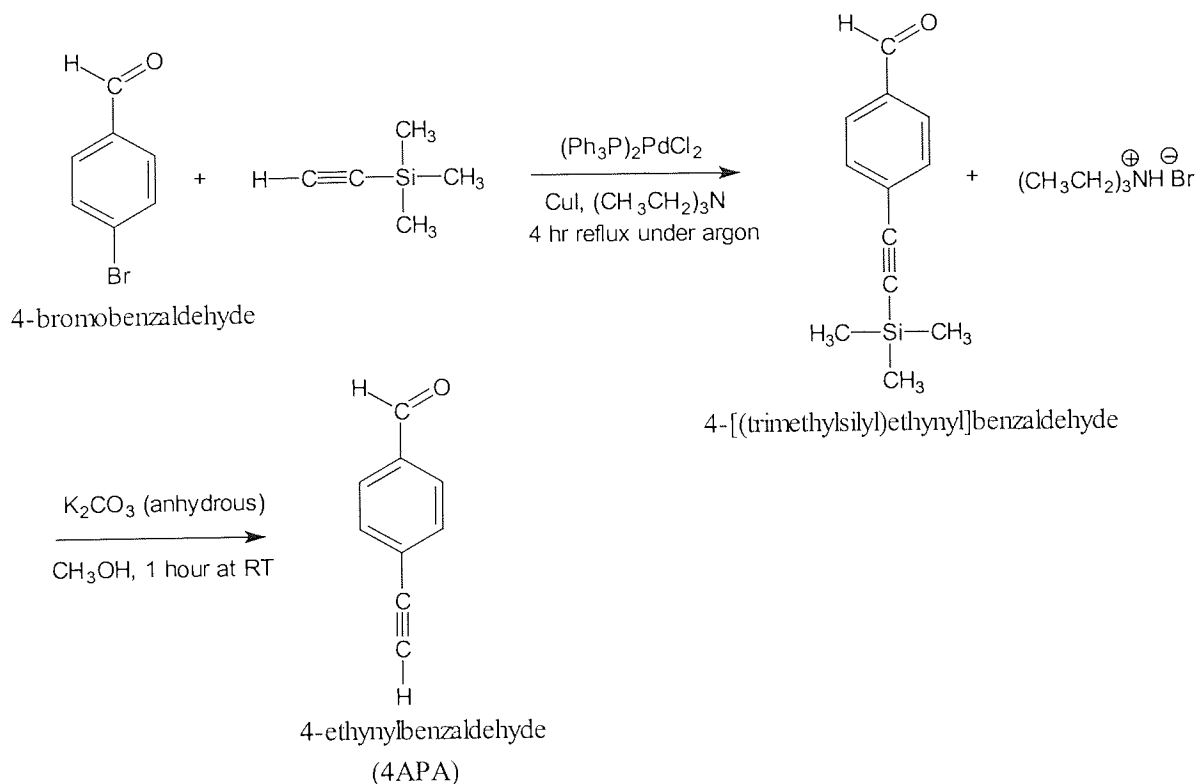
In conclusion, the efficiency of the Sonogashira coupling reaction is governed by the choice of halide starting material, where iodide and ring-deactivated bromides produce the best yields. Yields are generally high, conditions are mild, and the functional group interconversion is accomplished in just two steps. For these reasons, the Sonogashira coupling was employed throughout this project for the synthesis of substituted phenylacetylenes.

Recently it has been reported that THF/TEA is a better solvent system for the Sonogashira coupling of aromatic bromides, such that the reaction could be accomplished at room temperature, rather than under the reflux conditions usually employed⁸². The yields were higher or at least on a par with the conventional TEA procedure. No account of how THF increases the mildness/yields of the reaction was reported.

The timescale of the coupling reaction can be dramatically reduced to a few minutes using microwave radiation, but the procedure requires DMF as the solvent⁸³, which is difficult to remove completely using a conventional rotary evaporator.

Other developments have increased the scope even further so that the reaction can be accomplished successfully in aqueous media⁸⁴.

3.3 Typical synthesis of a phenylacetylene monomer, 4-ethynylbenzaldehyde



Scheme 12 : The synthesis of a phenylacetylene derivative, 4-ethynylbenzaldehyde (4APA)

A mixture of 4-bromobenzaldehyde 6.0g (32.43mmol), bistriphenylphosphine palladium(II) chloride (BTPPC) 0.1g (0.14mmol), copper (I) iodide 0.01g (0.05mmol), and triethylamine (100mL) was prepared in a single-neck 250mL RBF. The mixture was stirred magnetically under argon for 15 minutes. Trimethylsilylacetylene (TMSA) 3.35g (34.2mmol) was added to the flask, whereupon the mixture changed from yellow to orange and then to brown. The mixture was refluxed at 80°C for 4 hours under argon, allowed to cool to room temperature and filtered to yield an off-white solid (triethylammonium bromide). More catalyst, BTPPC 0.05g (0.07mmol) and copper(I) iodide 0.01g (0.05mmol) were added to the brown filtrate, and the mixture was refluxed for another 4 hours under argon. The brown mixture was filtered, and the filtrate was concentrated using a rotary evaporator to yield a brown solid. This was dissolved in ether (80mL) and washed with water (25mL) followed by saturated sodium chloride solution (25mL). The supernatant liquor was separated and dried with MgSO_4 (anhyd.) for 12 hours. The solution was filtered through a thin layer of silica gel, washed with ether (2*10mL), and the ether removed on a rotary evaporator to yield a brown solid. Purification by “flash”

column chromatography using CHCl_3 /hexane (1:1) gave a yellow crystalline product. Recrystallisation of the product from hot hexane gave pale yellow crystals of 4-[(trimethylsilyl)ethynyl]benzaldehyde 4.99g (24.70mmol), 76% yield. Analysis by IR, NMR, and MS analysis confirmed the identity of the compound.

Analytical data for 4-[(trimethylsilyl)ethynyl]benzaldehyde:- mp $64-65^\circ\text{C}$ (from hexane); $\nu_{\text{max}}/\text{cm}^{-1}$ 2966 (m, sharp, C-H), 2736 (w, sharp, -CHO), 2156 (m, sharp, $\text{C}\equiv\text{C}$), 1701 (s, sharp, Ar-CHO), 1250 (s, sharp, SiC-H), 842 (s, sharp, SiC-H); δ_{H} (300 MHz; CDCl_3) 9.93 (1 H, s, -CHO), 7.76 (2 H, d, Ph), 7.54 (2 H, d, Ph), 0.22 (9 H, s, Si-Me₃); δ_{C} (75 MHz; CDCl_3) 191.15 (-CHO), 135.39 (Ph), 132.27 (Ph), 129.24 (Ph), 129.11 (Ph), 103.67 ($\text{C}\equiv\text{C}$ -Ph), 98.79 ($\text{C}\equiv\text{C}$ -Si), -0.38 (Si-Me₃); m/z (APCI) 203 (MH^+).

4-[(Trimethylsilyl)ethynyl]benzaldehyde 4.95g (24.50mmol) was dissolved in methanol (50mL) and 1g of K_2CO_3 was added. The mixture was stirred magnetically under an argon atmosphere for 1 hour. Thin layer chromatography (TLC) was used to check the progress of the reaction; a typical chromatogram is shown in Figure 41.

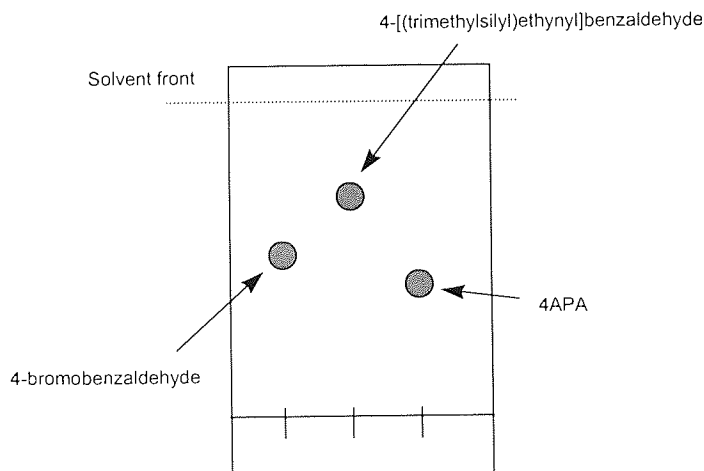


Figure 41 : TLC of 4APA (CHCl_3 1 : hexane 1)

When the reaction was complete the solvent was removed by rotary evaporation and a brown crystalline solid was obtained. This was dissolved in chloroform (50mL) and the solution filtered through a thin layer of silica gel. The yellow filtrate obtained was concentrated on a rotary evaporator to give a yellow solid. The yellow solid was purified by “flash” column chromatography using CHCl_3 /hexane (1:1) on silica gel to yield a pale

yellow crystalline solid. Recrystallisation from hot hexane gave very pale yellow crystals of 4-ethynylbenzaldehyde (4APA) 2.54g (19.56mmol), 60% overall yield. The identity of the product, 4APA, was confirmed using IR (Figure 42), NMR (Figure 43 and Figure 44), and MS (Figure 45) analysis.

Analytical data for 4APA:- mp 88-89°C (from hexane); $\nu_{\text{max}}/\text{cm}^{-1}$ 3218 (s, sharp, $-\text{C}\equiv\text{C}-\text{H}$), 1685 (s, sharp, Ar-CHO), 1604 (m, sharp, Ph); δ_{H} (300 MHz; CDCl_3) 9.98 (1 H, s, -CHO), 7.81 (2 H, d, Ph), 7.61 (2 H, d, Ph), 3.28 (1 H, s, $\equiv\text{C}-\text{H}$); δ_{C} (75 MHz; CDCl_3) δ 191.35 (-CHO), δ 135.85 (Ph), 132.63 (Ph), 129.43 (Ph), 128.21 (Ph), 82.56 (Ph-C \equiv), 81.06 ($\equiv\text{C}-\text{H}$); m/z (APCI) 131 (MH^+).

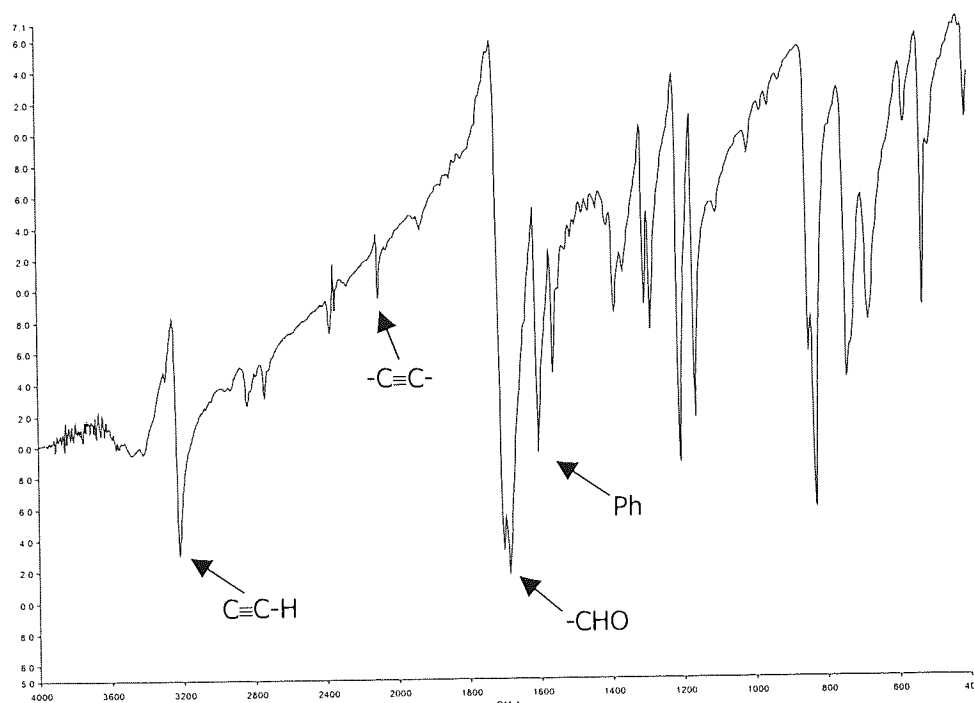


Figure 42 : Example IR of aldehydic monomer 4APA

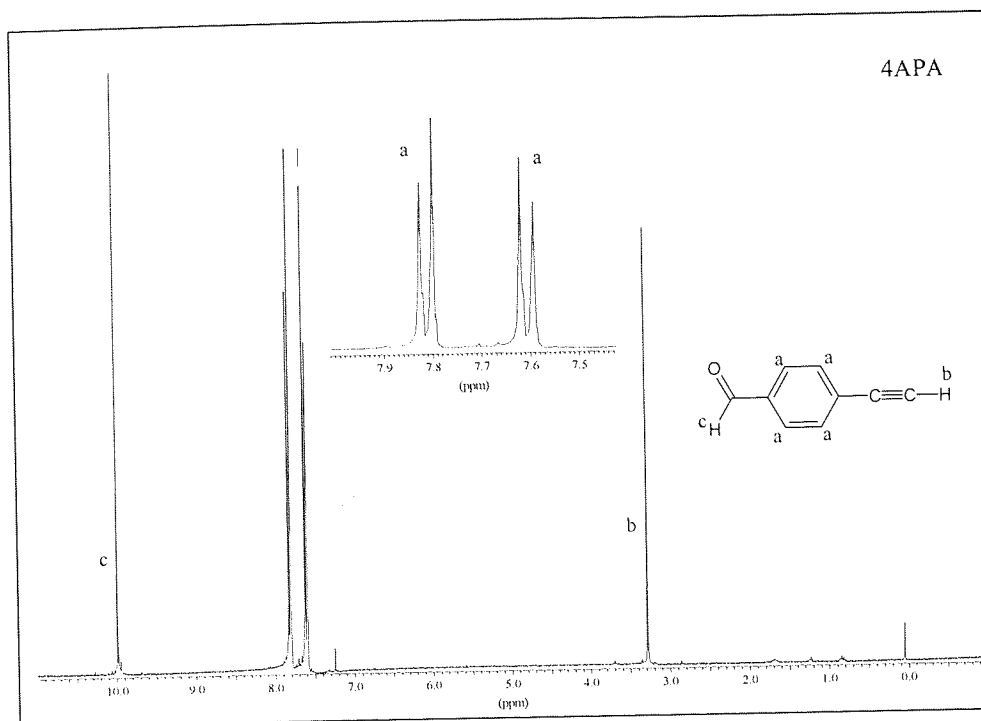


Figure 43 : Example ^1H NMR of aldehydic monomer 4APA

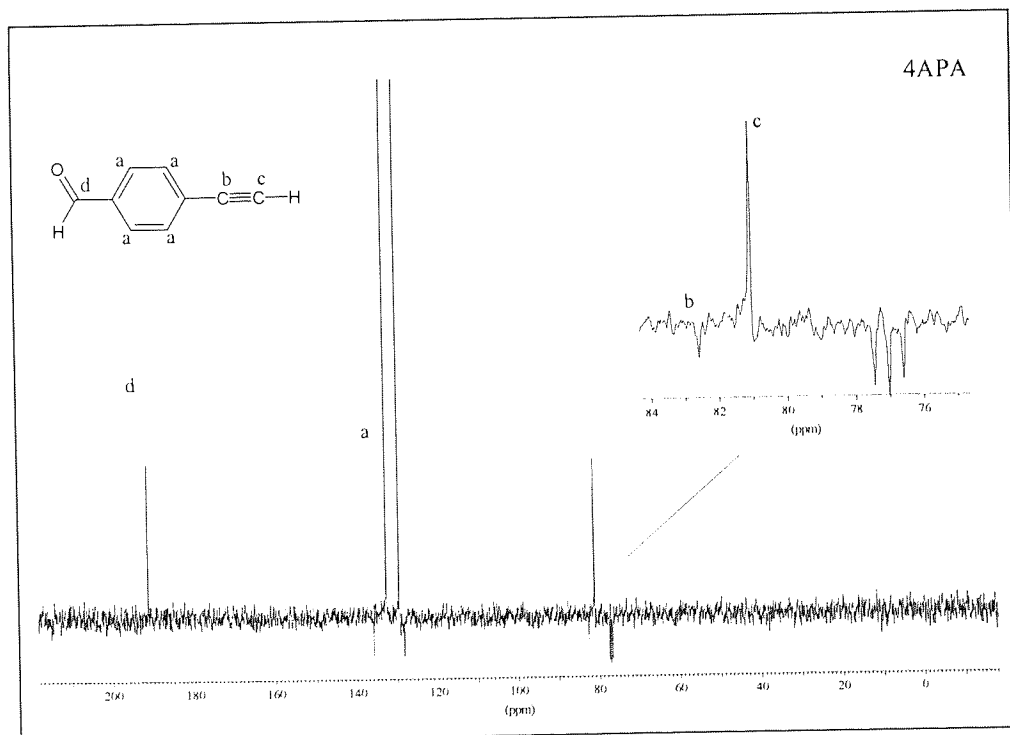


Figure 44 : Example ^{13}C NMR of aldehydic monomer 4APA

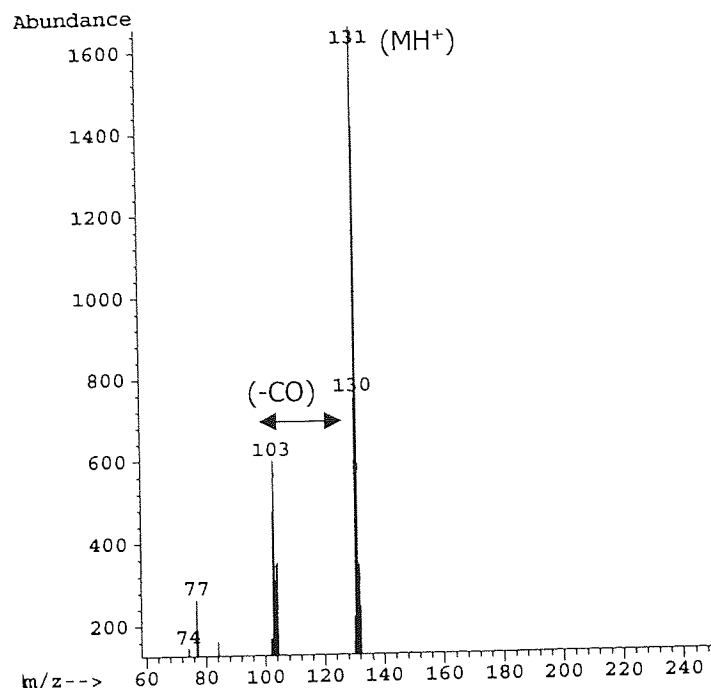


Figure 45 : Example mass spectrum (APCI) of aldehydic 4APA

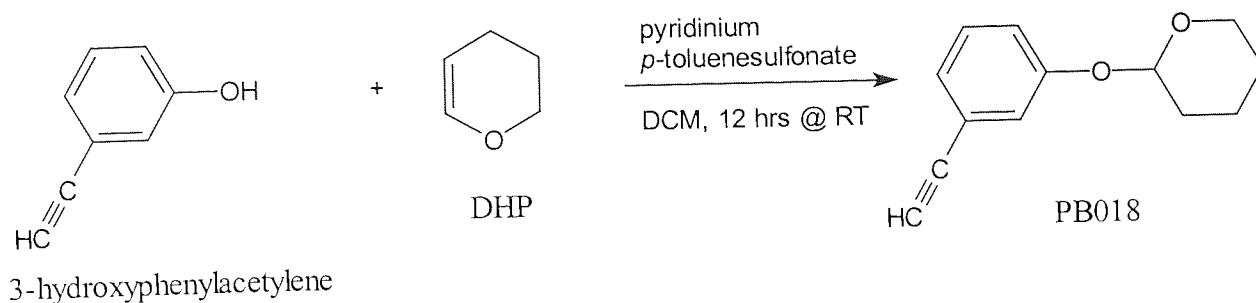
3.4 Derivatives of phenylacetylene monomers

During the course of this project several monomers were synthesised by derivatisation of existing phenylacetylenes. These derivatives were selected because the mild reaction conditions employed in their synthesis were not expected to destroy the alkyne group.

3.4.1 Synthesis of tetrahydro-2*H*-pyran phenylacetylene derivatives

Phenylacetylene monomers possessing hydroxyl groups were highly desirable because of their ability to hydrogen bond. However, problems were encountered during the synthesis of 4-hydroxyphenylacetylene (see 3.6.3) which were overcome by derivatising the hydroxyl group by reaction with 3,4-dihydro-2*H*-pyran (DHP). The resulting tetrahydropyran (THP) ethers were stable enough to be prepared and characterised successfully.

The reaction of an alcohol with DHP under mildly acidic conditions gives the THP ether in good yield⁸⁵, shown in Scheme 13.



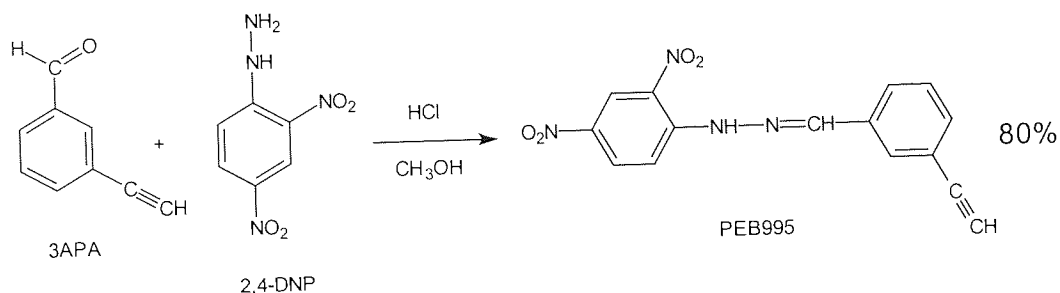
Scheme 13 : Synthesis of a THP derivative 2-(3-ethynylphenoxy)tetrahydro-2*H*-pyran (PB018)

3-Hydroxyphenylacetylene 0.50g (4.24mmol), 3,4-dihydro-2*H*-pyran (DHP) 0.50g (5.95mmol), pyridium *p*-toluenesulfonate (PTS) 0.1g, and 50mL of DCM were added to a 100mL RBF. The resultant yellow solution was stirred, magnetically, for 12 hours at room temperature. The formation of the product was monitored by TLC until the reaction was complete. The resultant yellow solution was concentrated using a rotary evaporator to a yellow oil that crystallised slowly. The oil was purified by “flash” column chromatography using CHCl_3 /hexane (1 :1) and gave PB018 as a pale yellow oil which crystallised slowly, 0.68g (3.37mmol) 80% yield.

Characterisation of PB018 was accomplished by IR, NMR, and MS analysis; mp 59-62°C (from EtOH); $\nu_{\text{max}}/\text{cm}^{-1}$ 3286 (s, sharp, $\text{-C}\equiv\text{C-H}$), 2948 (m, sharp, C-H), 2882 (w, sharp, $\text{O-CH}_2\text{-}$), 1583 (s, sharp, Ph), 1486 (m, sharp, Ph), 1252 (m, sharp, C-O); δ_{H} (300 MHz; CDCl_3) 7.22-7.19 (2 H, multiplet, Ph), 7.14-7.11 (1 H, split doublet, Ph), 7.07-7.03 (1 H, split doublet, Ph), 5.41-5.39 (1 H, t, THP), 3.91-3.83 (1 H, split triplet, THP), 3.63-3.56 (1 H, multiplet, THP), 3.10 (1 H, s, $\equiv\text{C-H}$), 2.02-1.93 (1 H, multiplet, THP), 1.86-1.81 (2 H, multiplet, THP), 1.73-1.54 (3 H, multiplet, THP); δ_{C} (75 MHz; CDCl_3) 156.62 (Ph), 129.14 (Ph), 125.25 (aromatic, 122.87 (Ph), 119.75 (Ph), 117.29 (Ph), 96.11 (THP), 83.37 (Ph-C \equiv), 76.93 ($\equiv\text{C-H}$) 61.73 (THP), 30.08 (THP), 24.97 (THP), 18.50 (THP); m/z (APCI) 203 (MH^+).

3.4.2 Synthesis of 2,4-dinitrophenylhydrazine derivative

Aldehydes can be derivatised by reaction with 2,4-dinitrophenylhydrazine (2,4DNP) under acidic conditions⁷⁰, shown in Scheme 14.



Scheme 14 : Synthesis of a 2,4DNP derivative of 3APA

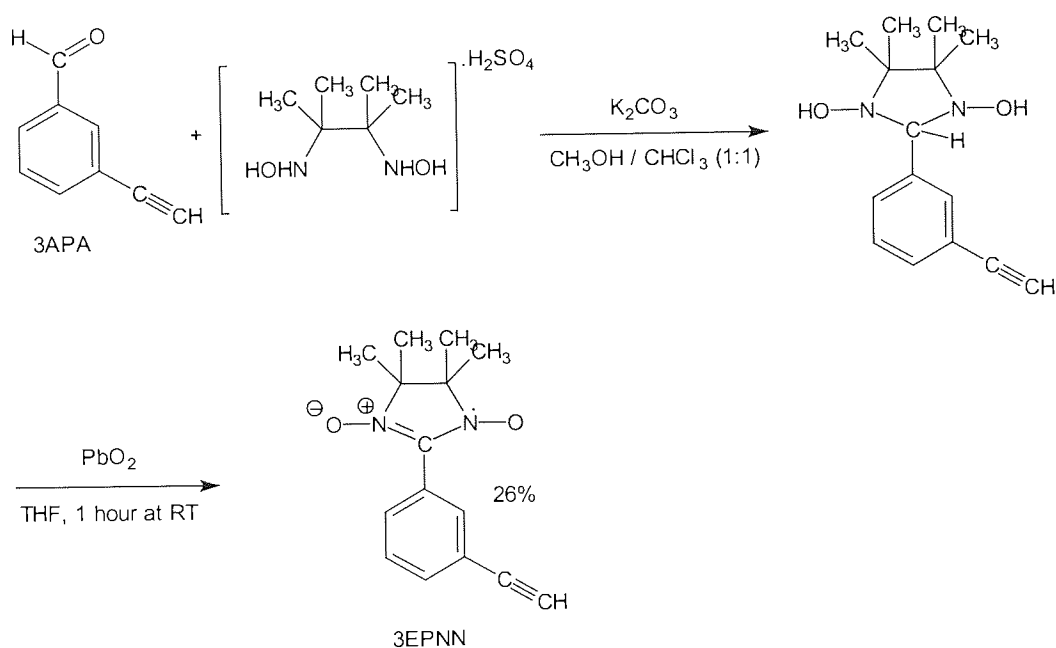
A solution of 3APA 0.3g (2.3mmol) in methanol (10mL) was prepared. To this was added a solution of 2,4DNP 0.6g (3.0mmol), methanol (8mL), and concentrated HCl (2mL). The combined solutions were allowed to stand at room temperature for 30 minutes. The orange suspension formed was filtered and evaporated to give orange crystals, which were then washed with methanol (2*5mL). Recrystallisation from THF/hexane (1:1) gave orange needle-like crystals of PEB995, 0.57g (1.8mmol), 80% yield.

Analytical data for PEB995: $\nu_{\max}/\text{cm}^{-1}$ 3286 (s, sharp, $\text{-C}\equiv\text{C-H}$), 3093 (w, sharp, Ph), 1618 (s, sharp, Ph), 1586 (s, sharp, Ar-NO_2), 1513 (s, sharp, Ph), 1329 (s, sharp, Ar-NO_2); δ_{H} (300 MHz; CDCl_3) 11.33 (1 H, s, -CH=N-), 9.14 (1 H, d, unassigned), 8.37 (1 H, split d, unassigned), 8.08 (2 H, s, unassigned), 7.89 (1 H, s, unassigned), 7.72 (1 H, d, unassigned), 7.56 (1 H, d, unassigned), 7.42 (1 H, t, unassigned), 3.15 (1 H, s, $\equiv\text{C-H}$); δ_{C} (75 MHz; CDCl_3) 146.51 (Ph), 134.29 (Ph), 130.88 (Ph), 130.10 (Ph), 129.06 (Ph), 127.89 (Ph), 123.47 (Ph), 116.83 (CH=N-), 82.63 (Ph- $\text{C}\equiv$).

PEB995 was probably impure, as there were several peaks in the ^1H NMR spectrum that could not be rationalised. Time did not permit the purification of the compound by column chromatography.

3.4.3 Synthesis of nitronyl nitroxide monomers

Originally, nitronyl nitroxides were synthesised by the reaction of an aldehyde with pure 2,3-bis(hydroxylamino)-2,3-dimethylbutane (BDBS) in refluxing methanol, and the resulting adduct was oxidised by lead dioxide in benzene¹⁷. This is a time consuming procedure, because pure BDBS has to be synthesised from starting materials, and this can take many days to complete. This procedure has now been superseded by stirring the commercially available sulphate salt of BDBS with an aldehyde in a chloroform/methanol mixture, shown in Scheme 15. Oxidation of the resultant slurry by lead dioxide in THF gives a yield of product equivalent to that obtained by the original method. This method was used throughout this project for the synthesis of nitronyl nitroxide monomers.



Scheme 15 : Synthesis of a nitronyl nitroxide monomer, 3-ethynylphenylnitronylnitroxide

During this reaction weighings and preparation were carried out in an inert atmosphere as a precautionary measure. A solution of 3APA 0.5g (3.85 mmol), BDBS 1.12g (3.87 mmol), and K_2CO_3 (1.0g), in 40mL of methanol/chloroform (1:1), was prepared in a 100mL RBF. The flask was sealed with Nesco® film and stirred magnetically at room temperature for 96 hours. The solvents were then removed using a rotary evaporator and the yellow solid formed was dissolved in THF (20mL, dry, degassed, and distilled). Lead(IV) oxide (1.0g) was added, the flask was quickly flushed with argon, and the

suspension stirred for 15 minutes. The black suspension was removed by filtration through a thin layer of silica gel; the residue was washed with THF (2*15mL), and the yellow filtrate collected. That the filtrate was yellow was an indication that oxidation had not occurred. To the yellow filtrate was added lead(IV) oxide (0.5g) and the suspension was again stirred for 15 minutes, when the colour changed to first green and then to blue. Two further batches of PbO₂ (2*0.5g) were added to the reaction during 30 minutes of stirring. The blue/black suspension was filtered through a thin layer of silica gel, and the residue washed with THF (2*15mL), to give a dark blue filtrate. The filtrate was collected and the solvent was removed using a rotary evaporator to give a blue oil. The oil was purified by "flash" column chromatography (CHCl₃ as eluent) and the product was obtained as a dark blue crystalline solid. Blue crystals were obtained by slow evaporation of a solution of the product in DCM. The crystals of 3EPNN were collected, and dried in a vacuum oven, 0.25g (0.98mmol), 26% yield. 3EPNN was characterised by IR (Figure 46 and Figure 47), MS (Figure 48) and EPR analysis (Figure 49).

Analytical data for 3EPNN; mp (from ether) 138-139°C⁶²; $\nu_{\max}/\text{cm}^{-1}$ 3206 (s, sharp, -C≡C-H), 2994 (w, sharp, C-H), 2922 (w, sharp, C-H), 2098 (w, sharp, -C≡C-), 1392 (w, sharp, unassigned), 1361 (s, sharp, N-O), 1310 (w, sharp, unassigned), 1214 (w, sharp, nitronyl nitroxide), 1165 (w, sharp, nitronyl nitroxide); m/z (APCI) 258 (MH⁺); EPR (in CHCl₃) showed 5 peaks in the ratio of 1:2:3:2:1.

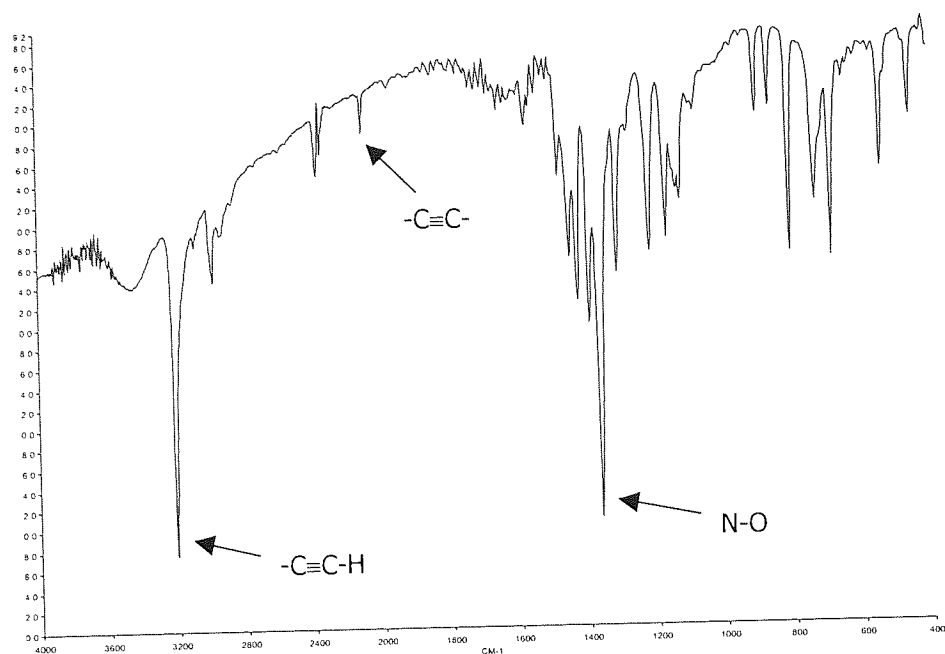


Figure 46 : IR spectrum of radical monomer 3EPNN

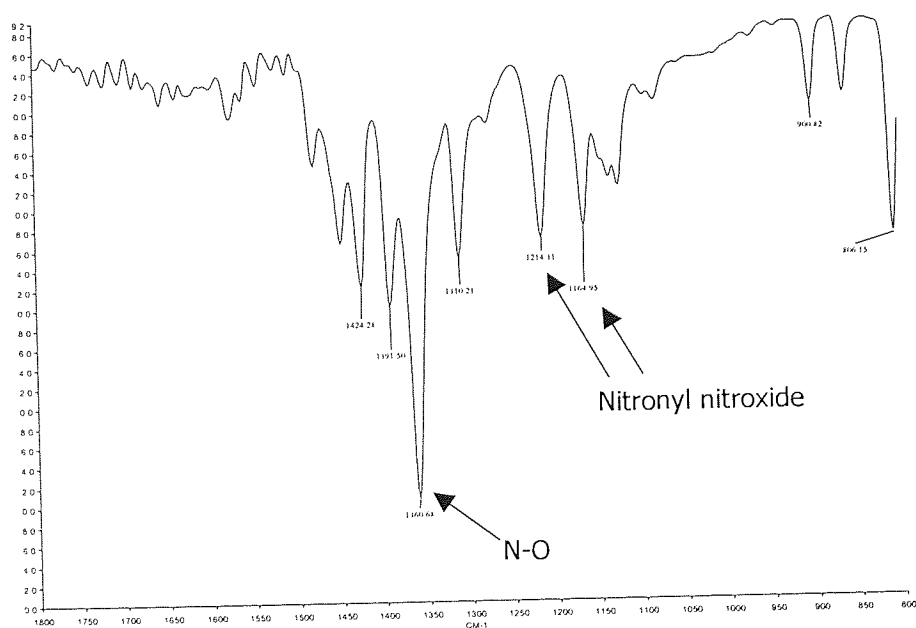


Figure 47 : IR spectrum (attenuated) of radical monomer 3EPNN

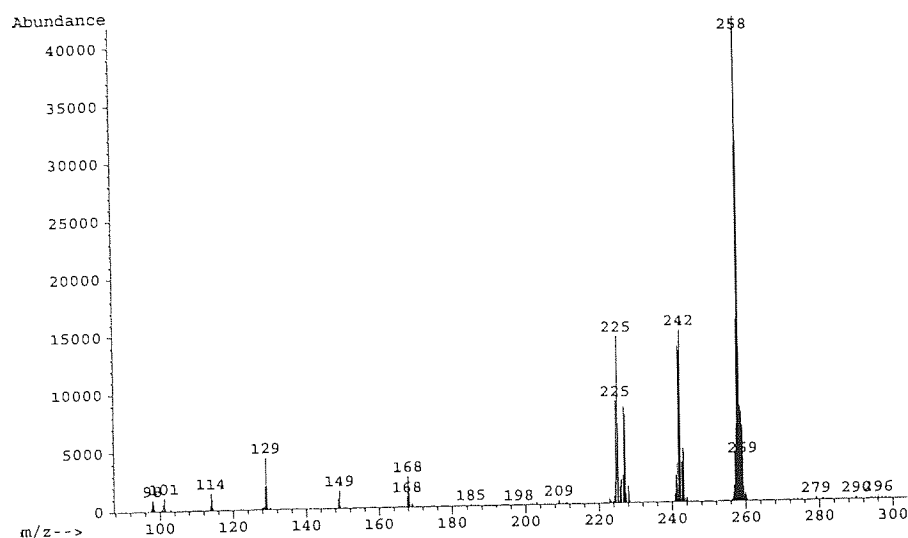


Figure 48 : Mass spectrum (APCI) of 3EPNN

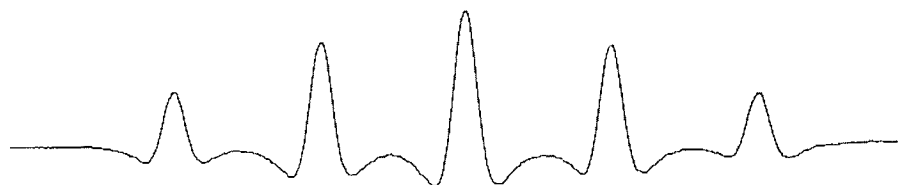
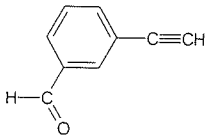
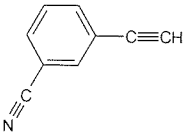
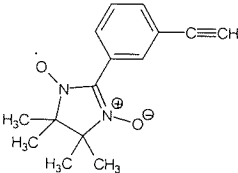
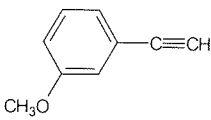
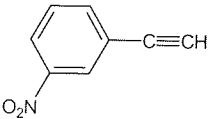
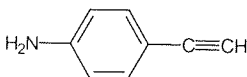
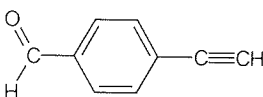
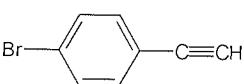
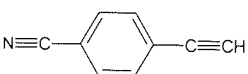
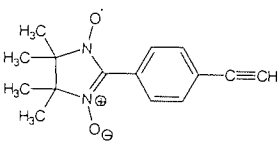


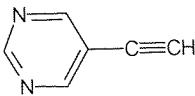
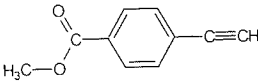
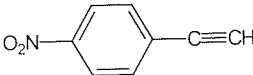
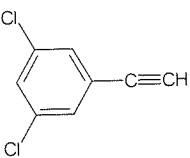
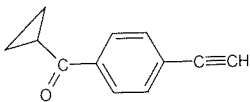
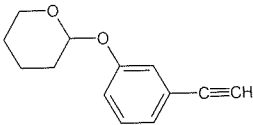
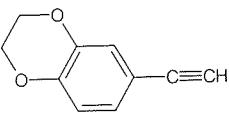
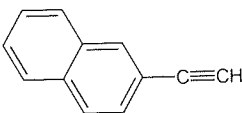
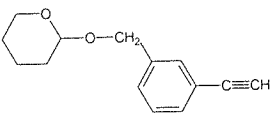

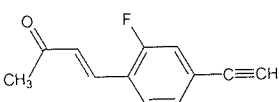
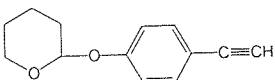
Figure 49 : EPR of monomer radical 3EPNN

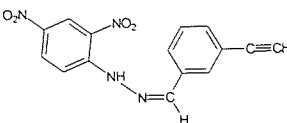
3.5 Introduction to the results

The Sonogashira coupling between alkynes and an aromatic halide is a much prized reaction because of its specificity, high yield, and good tolerance. However, most phenylacetylenes reported in the literature are simple derivatives and possess only one functional group. This project reproduces many of these monomers, but also progresses to a bi-functionalised phenylacetylene, where some problems were encountered. The monomers synthesised during the course of this work are summarised in Table 2.

Table 2 : Summary of phenylacetylene monomers

Code	Functional group	Structure	Name	Yield (%)
3APA	Aldehyde		3-ethynylbenzaldehyde	52
3CPA	Cyano		3-ethynylbenzonitrile	67
3EPNN	Nitronyl nitroxide		3-ethynylphenylnitronyl nitroxide	26
3MeOPA	Alcoxy (methyl)		3-ethynylanisole	91
3NPA	Nitro		3-ethynlnitrobenzene	90
4AMPA	Amine		4-ethynylaniline	65
4APA	Aldehyde		4-ethynylbenzaldehyde	61
4BrPA	Bromo		4-bromophenylacetylene	60
4CPA	Cyano		4-ethynylbenzonitrile	82
4EPNN	Nitronyl nitroxide		4-ethynylphenylnitronyl nitroxide	36

5EPYM	Pyrimidine		5-ethynylpyrimidine	55
4MEPA	Ester (methyl)		methyl-4-ethynylbenzoate	63
4NPA	Nitro		4-ethynylnitrobenzene	78
DCPA	Chloro		3,5-dichlorophenylacetylene	76
PB014	Ketone (cyclopropyl)		cyclopropyl-4-ethynylphenyl ketone	82
PB018	THP ether		2-(3-ethynylphenoxy)tetrahydro-2H-pyran	80
PB029	Ethylenedioxy		3,4-ethylenedioxyphenylacetylene	89
PB032	Naphthalene		2-ethynyl-naphthalene	78
PB054	THP ether		2-(3-ethynylbenzyloxy)tetrahydro-2H-pyran	85
PB055	Pyrrole		1-(4-ethynylphenyl)pyrrole	77
PEB923B	Ketone, fluoro		1-(4-ethynyl-2-fluorophenyl)but-1-en-3-one	27
PEB943	THP ether		2-(4-ethynylphenoxy)tetrahydro-2H-pyran	84

PEB995	DNPH		2,4-DNP derivative of 3APA	80
--------	------	---	-------------------------------	----

The first objective was to synthesise some simple phenylacetylene monomers that were already known, e.g. 3-methoxyphenylacetylene (3MeOPA), 2-ethynylnaphthalene, and 4-bromophenylacetylene (4BrPA). 4BrPA was synthesised from 4-iodobromobenzene, but there was a possibility that TMSA would couple to both halides, to give a mixture of mono and diethynyl products. To minimise this possibility, the procedure was conducted at room temperature where only iodo derivatives are sufficiently reactive to couple with TMSA. No diethynyl products were obtained, which illustrates that iodo aromatics can undergo Sonogashira coupling in the presence of a bromo group, when the reaction conditions are selected carefully.

The difference in reactivity between the bromo and iodo anilines is highlighted by the yields of 4-ethynylaniline (4AMPA) obtained from 4-iodoaniline (65%) in this work, and those obtained by Yashima from 4-bromoaniline (30%)⁸⁰. This is an example of the choice of starting material having a substantial effect on the yield of product. Bromo compounds that possess a more strongly electron donating group react poorly, when compared with the equivalent iodo compound. For this reason iodo starting materials were preferred. When the iodo starting material could not be acquired commercially, the bromo equivalent was used, but care was taken to avoid strong donating substituents, such as $-NR_2$, or $-OR$. When bromo starting materials were used, the Sonogashira coupling was always carried out under reflux conditions, to maximise the yield of product.

Analysis of the phenylacetylene monomers by NMR, MS, and IR analysis confirmed the structures of the products. The synthetic technique was carried out successfully and yields of products compared favourably with those reported in the literature. However, it was essential to carry out all experimental manipulations under an inert atmosphere, to minimise brown by-products. These unwanted side-reactions probably originated from the effect of atmospheric oxygen which can couple alkynes to form a diacetylene, by the Glaser reaction^(10 pp.714-715).

Once a good synthetic method had been established, monomers possessing “bridging groups” were prepared, as shown in Table 3.

Table 3 : Phenylacetylene monomers synthesised possessing a bridging group

Bridging group required	Monomer synthesised
Nitro - NO ₂	4-nitrophenylacetylene (4NPA),
	3-nitrophenylacetylene (3NPA)
Cyano – CN	4-cyanophenylacetylene (4CPA),
	3-cyanophenylacetylene (3CPA)
Hydroxyl – OH	Attempted 4-hydroxyphenylacetylene
Fluoro – F	1-Ethynyl-4-fluorobenzene (acquired commercially)

For the synthesis of monomers bearing a nitronyl nitroxide group, it was first necessary to prepare 4-ethynylbenzaldehyde (4APA) or 3-ethynylbenzaldehyde (3APA), which were obtained in good yield. These aldehydic monomers were further derivatised to the nitronyl nitroxide (4EPNN) and (3EPNN) respectively. Although the yields obtained for the conversion of an aldehyde monomer to a nitronyl nitroxide seem quite low (36% and 26% respectively) they are comparable with those reported in the literature⁶². These monomers were vital constituents of co-polyradicals, the target of this project.

Other monomers were prepared during the course of this research, and are reported because they, and their subsequent polymers, are novel materials.

3.6 By-products obtained

Some monomers exhibited side-reactions during the synthesis procedure, and these are now described.

3.6.1 Side-reactions with the ethyl ester group

A monomer bearing an ethyl ester (ethyl-4-ethynylbenzoate, as shown in Figure 50) was synthesised during initial testing of the MCAT catalyst. However, the monomer obtained using conventional Sonogashira coupling did not correspond to that of the expected product.

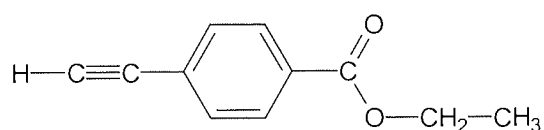


Figure 50 : Structure of ethyl-4-ethynylbenzoate

The product was investigated first by MS analysis, which showed that the compound had a molecular weight of 14 Daltons less than that expected for ethyl-4-ethynylbenzoate. The magnitude of this mass loss corresponds to that of a CH_2 . Structural elucidation of the unknown product was accomplished using NMR analysis (Figure 51 & Figure 52), which showed the presence of a terminal alkyne, an aromatic ring, a carbonyl, and a CH_3 . The absence of a CH_2 group in the NMR spectra confirms that suggested by the MS analysis. Functional group identification by IR spectroscopy showed that the carbonyl was actually an ester group. The product will be referred to as 4MEPA from hereon.

Analytical data for 4MEPA : 4MEPA was synthesised from ethyl-4-iodobenzoate and was obtained as pale yellow crystals (63%); mp (from hexane) $91\text{--}92^\circ\text{C}$ (lit. mp $92.5\text{--}93.5^\circ\text{C}$ ⁸⁶ (from sublimation)); $\nu_{\text{max}}/\text{cm}^{-1}$ 3243 (s, sharp, $\text{--C}\equiv\text{C--H}$), 2102 (w, sharp, $\text{--C}\equiv\text{C--}$), 1703 (s, sharp, $\text{--CO}_2\text{--}$), 1606 (w, sharp, Ph), 1279 (s, sharp, C-O), 1109 (m, sharp, C-O); δ_{H} (300 MHz; CDCl_3) 7.97 (2 H, d, Ph), 7.53 (2 H, d, Ph), 3.21 (1 H, s, $\equiv\text{C--H}$); δ_{C} (75 MHz; CDCl_3) 166.36 (carbonyl), 132.02 (Ph), 130.06 (Ph), 129.40 (Ph), 126.68 (Ph), 82.73 (Ph- $\text{C}\equiv$), 80.01 ($\equiv\text{C--H}$), 52.24 (CH_3); m/z (EI) 160 (M^+).

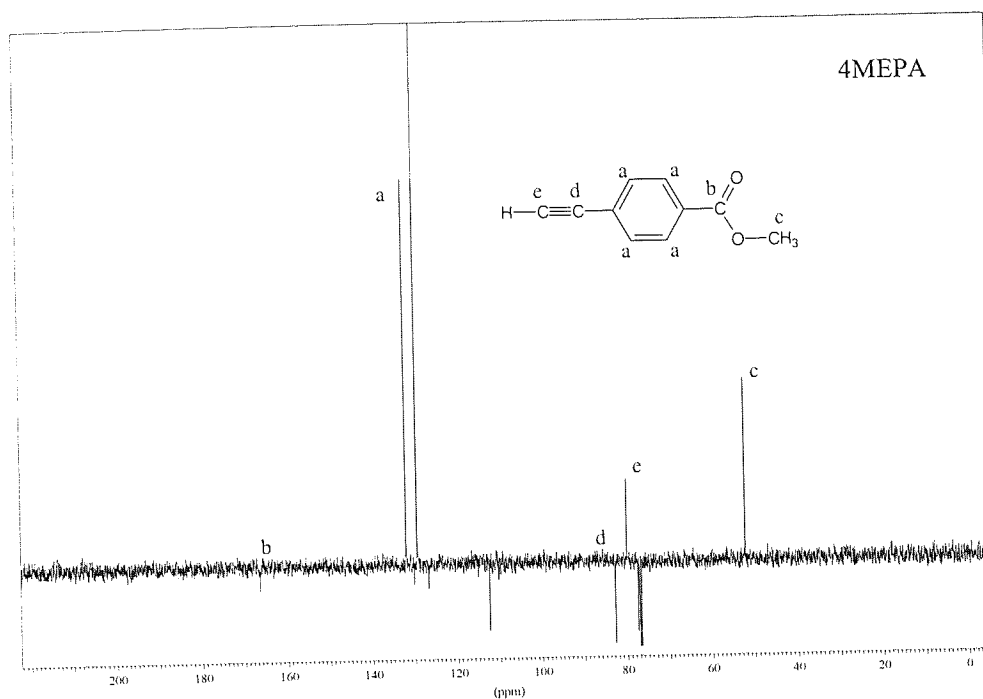


Figure 51 : ^{13}C NMR of trans-esterified monomer 4MEPA

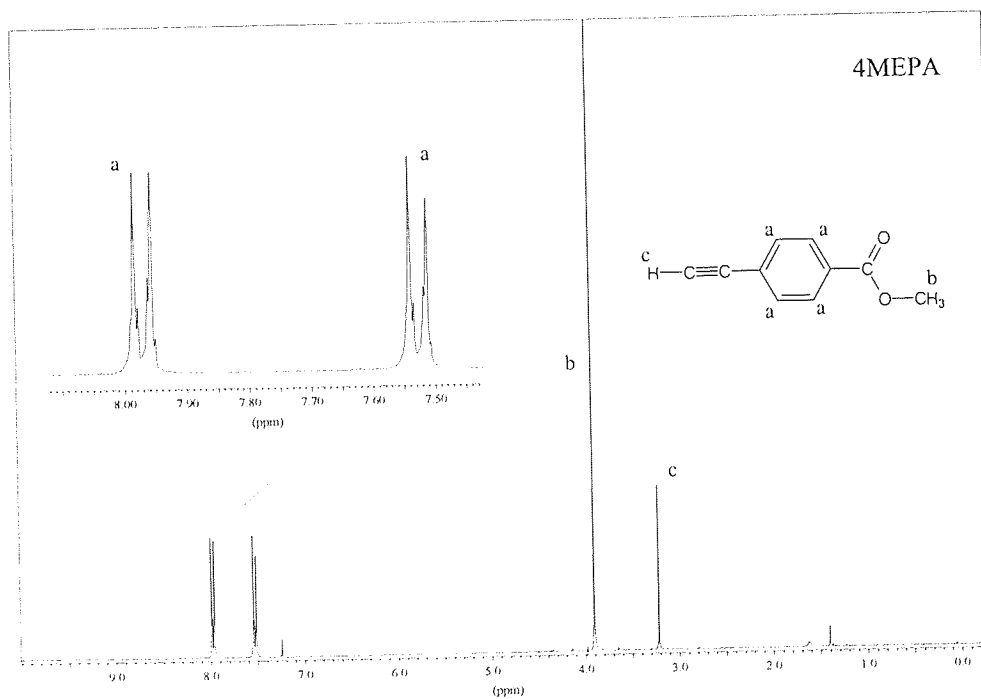


Figure 52 : ^1H NMR of trans-esterified monomer 4MEPA

The interpretation of these analyses suggested that the compound was a phenylacetylene derivative, but that it no longer possessed an ethyl ester group. Instead, the product was a methyl ester, and was identified as methyl-4-ethynylbenzoate (4MEPA), Figure 53.

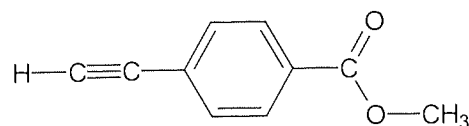


Figure 53 : Structure of product methyl-4-ethynylbenzoate (4MEPA)

It was necessary to ascertain the stage at which transformation of ethyl to methyl ester had occurred. If the change had taken place during the palladium coupling, then the trimethylsilyl intermediate (PEB121) should also be a methyl ester, shown in Figure 54. ^1H and ^{13}C NMR spectra (Figure 55, and Figure 56) showed that both CH_2 and CH_3 were present, suggesting that the compound contained an ethyl ester. This was confirmed by MS analysis, which showed that the molecular weight of PEB121 corresponded to that of an ethyl ester. Hence, the intermediate PEB121 was identified as ethyl-4-trimethylsilylethynylbenzoate.

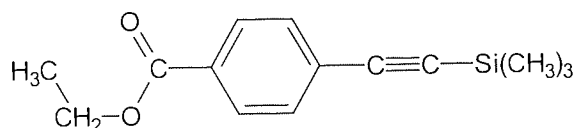


Figure 54 : Structure of intermediate ethyl ester (PEB121)

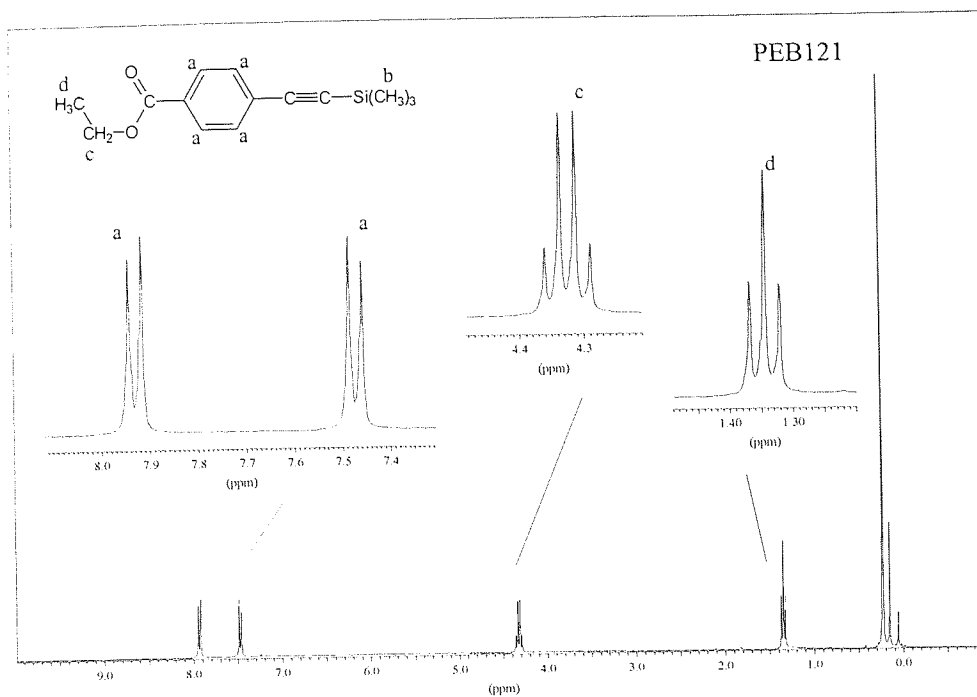


Figure 55 : ¹H NMR of ethyl ester intermediate PEB121

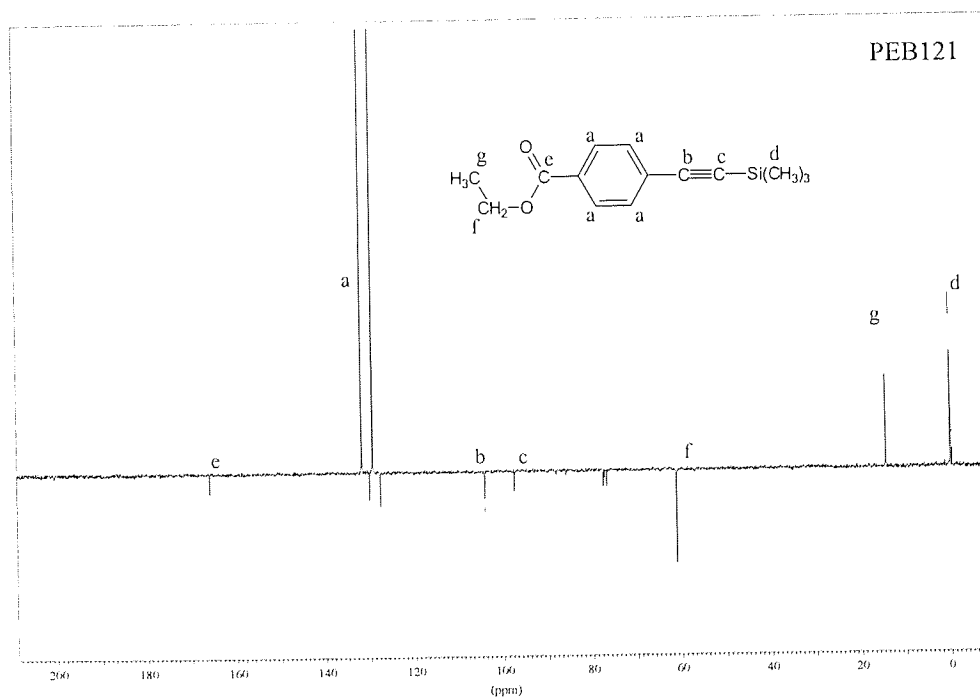
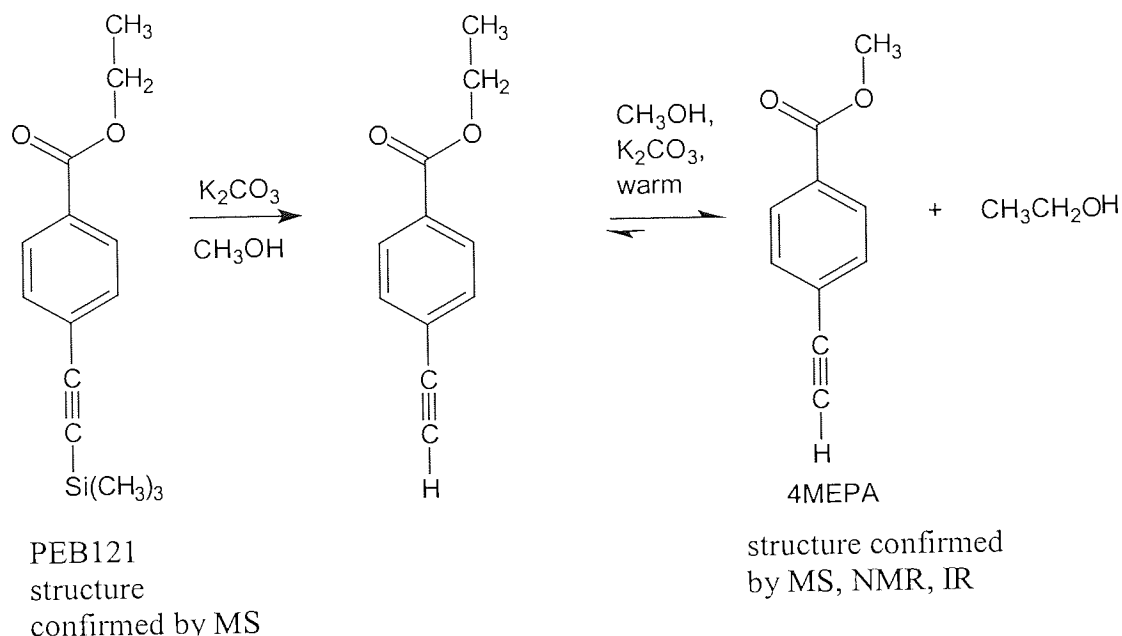


Figure 56 : ¹³C NMR of ethyl ester intermediate PEB121

The transformation from ethyl to methyl ester must have occurred during the deprotection using K_2CO_3 /methanol. Esters can undergo trans-esterification, when in the presence of an acid/base catalyst and a large excess of an alcohol^(10 pp.397-398), shown in Scheme 16. An equilibrium of both methyl and ethyl esters is created, but because of the large excess of methanol the former is favoured.

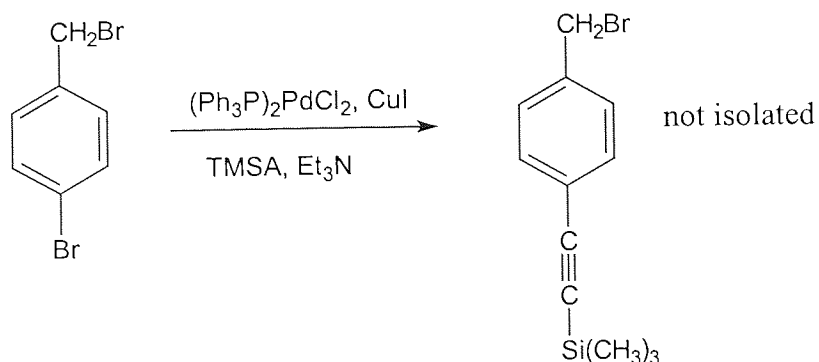


Scheme 16 : Possible trans-esterification of esters during deprotection in methanol

This highlighted a deprotection problem with hydrolysis-sensitive groups, such as esters.

3.6.2 TEA salt formation of a reactive benzylbromide

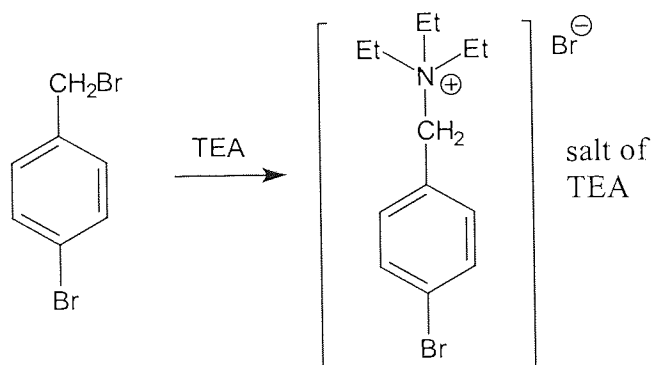
Another problem was encountered during the synthesis of a monomer bearing a benzylbromide function, as shown in Scheme 17. The palladium/TEA reaction was refluxed as usual and the mixture the solid was removed by filtration. The filtrate was concentrated using a rotary evaporator to give, unexpectedly, a very small amount (about 0.1g) of a yellowish solid from about 5.0g of starting material. IR analysis of this yellow solid showed that the peaks corresponding to silicon were absent.



Scheme 17 : Attempted synthesis of a phenylacetylene monomer bearing a benzylbromide group

It was considered possible that the yellowish solid was actually the palladium catalyst, BTPPC, and that the substituted benzyl bromide had been filtered out as the TEA salt. This was confirmed by a test experiment in which the substituted benzyl bromide compound was added to 10mL of TEA, whereupon it dissolved, but after 10 seconds a white solid precipitate was formed, as shown in Scheme 18. The white solid was removed by filtration, and added to water when it dissolved fully. No formal analysis was carried out, but all these observations pointed towards the benzylbromide forming a salt with TEA, which then precipitates out of solution.

The formation of a salt is the only example of a side-reaction that occurred during Sonogashira coupling, but it highlights the fact that molecules containing reactive halides are unsuitable for conversion to phenylacetylenes using the conventional solvent TEA.

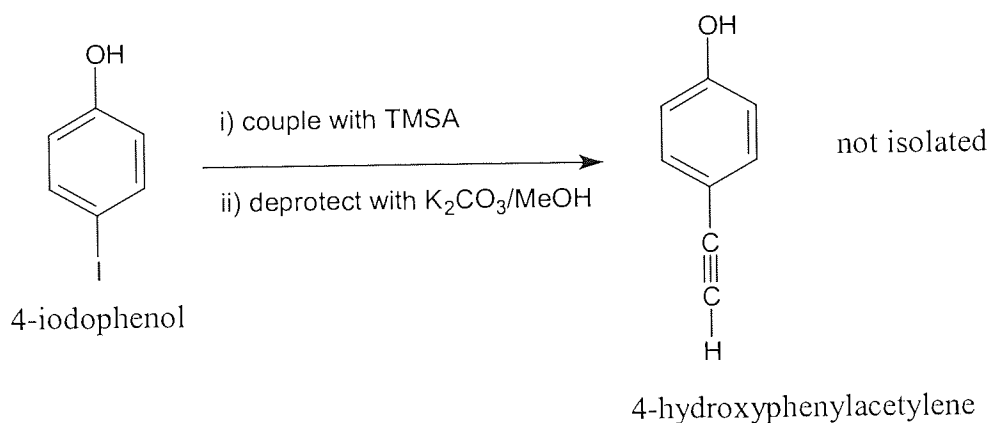


Scheme 18 : TEA salt formation of a benzylbromide compound

3.6.3 Attempted synthesis of 4-hydroxyphenylacetylene

The synthesis of a hydroxyl functionalised monomer was attempted, because the group may act as a bridging moiety in organic magnets³². It was envisaged that the hydroxyl group could be incorporated into a co-polyradical to facilitate hydrogen bonding and hence magnetic interactions.

Sonogashira coupling of the commercially available 4-iodophenol starting material gave the product as a yellow oil, as shown in Scheme 19. A period of about seven days elapsed before purification of this crude product obtained was attempted. Over a period of 72 hours the yellow oil was exposed to light and air, whereupon it changed to an insoluble black solid. MS analysis found no trace of the monomer in this black solid.



Scheme 19 : Attempted preparation of 4-hydroxyphenylacetylene

NMR analysis was not carried out because the product was insoluble in a wide range of solvents, but it was assumed that a type of autopolymerisation had occurred. To circumvent this problem, iodophenols were converted to tetrahydropyran (THP) derivatives. It was envisaged that upon polymerisation, the THP derivatives could be deprotected to regenerate the hydroxyl function.

3.6.4 Condensation reaction of an *o*-fluorobenzaldehyde (PEB923B)

An attempt was made to integrate a stable free radical and a “bridging group” into one compound. The starting material 4-bromo-2-fluorobenzaldehyde was reacted with TMSA and deprotected, using the normal Sonogashira procedure. The reaction mixture was purified using “flash” column chromatography, from which pale yellow crystals were obtained. IR analysis showed an absence of an aldehyde group in the crystalline product. Confirmation of the structure of the product was provided by MS analysis which showed the compound isolated had a molecular weight of 188. This represents an increase of 40 mass units in excess of the expected molecule, 4-ethynyl-2-fluorobenzaldehyde (molecular weight 148) (shown in Figure 57).

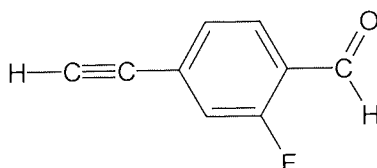


Figure 57 : Structure of 4-ethynyl-2-fluorobenzaldehyde

The structural interpretation of this unknown compound was made difficult because fluorine (^{19}F) couples to both ^1H and ^{13}C giving a complex NMR spectrum, as shown in Figure 58 and Figure 59. ^{13}C NMR analysis showed that there were peaks corresponding to $\text{C}=\text{O}$ (ketone), a terminal alkyne, and a CH_3 . The 198ppm chemical shift of the carbonyl is higher than that of a normal ketone, but conjugated ketones, such as 2-cyclohexen-1-one (198ppm), are known to give higher chemical shift values⁸⁷. Conjugation with the alkene is the cause of the higher ppm value, because it affects the π electron distribution of the carbonyl group. This change of local magnetic environment results in a chemical shift that is further downfield than normal.

^1H NMR analysis confirmed the presence of a terminal alkyne group, and also revealed a peak that corresponded to a CH_3 . No signal was found that corresponded to the hydrogen of an aldehyde group (approximately $\delta 10\text{ppm}$).

Analytical data for PEB923B : obtained as yellow needle-like crystals (27%); mp 97-98.5°C (from EtOH); $\lambda_{\text{max}}(\text{CHCl}_3)/\text{nm}$ 350; $\nu_{\text{max}}/\text{cm}^{-1}$ 3192 (m, sharp, $\equiv\text{C-H}$), 1670 (s, sharp, $\text{C}=\text{C}-\text{CO}-$), 1612 (m, sharp, Ph), 1500 (m, sharp, Ph), 1363 (m, sharp, COCH_3); $\delta_{\text{H}}(300 \text{ MHz}; \text{CDCl}_3)$ 7.53 (1 H, d, unassigned), 7.46 (1 H, t, unassigned), 7.20 (1 H, d, unassigned), 7.15-7.11 (1H, split doublet, unassigned), 6.70 (1 H, d, unassigned), 3.21 (1 H, s, $\equiv\text{C-H}$), 2.32 (3 H, s, methyl); $\delta_{\text{C}}(75 \text{ MHz}; \text{CDCl}_3)$ 197.90 ($\text{C}=\text{O}$), 162.13-158.77 (unassigned), 134.37 (Ph), 129.64-129.56 (split singlet, Ph), 128.34-128.35 (split singlet, Ph), 128.17-128.133 (split singlet, Ph), 119.58 ($\text{C}=\text{C}$), 119.27 ($\text{C}=\text{C}$), 81.76-81.72 (split singlet, $\text{Ph}-\text{C}\equiv$), 80.35 ($\equiv\text{C-H}$); $^1\text{H}-^{13}\text{C}$ NMR correlation spectrum was used to provide additional confirmation; m/z (EI) 188 (M^+).

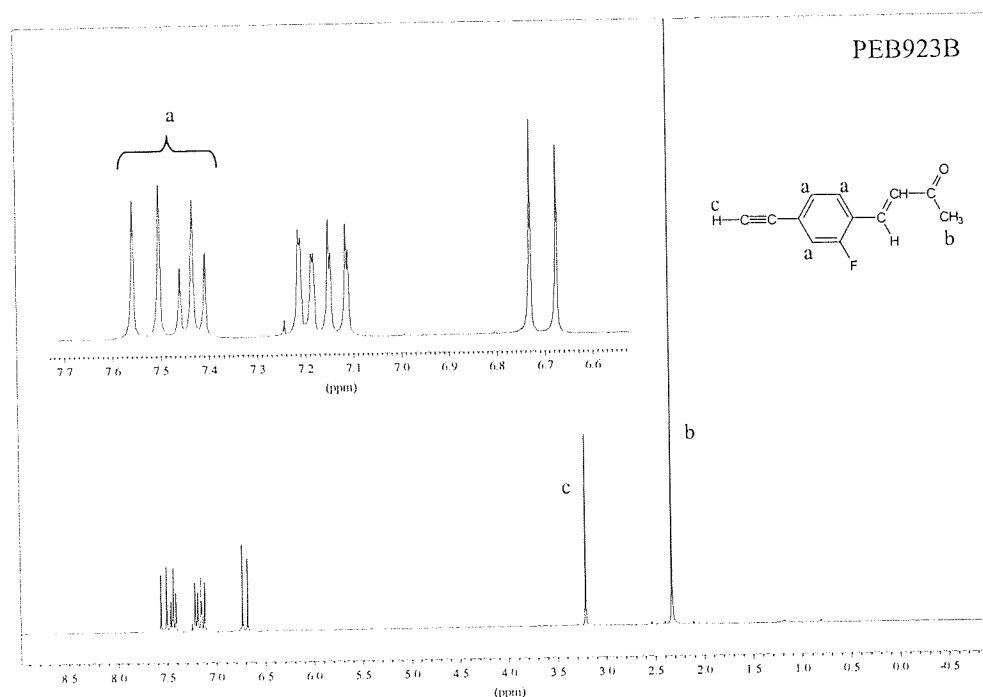


Figure 58 : ^1H NMR of condensation product PEB923B

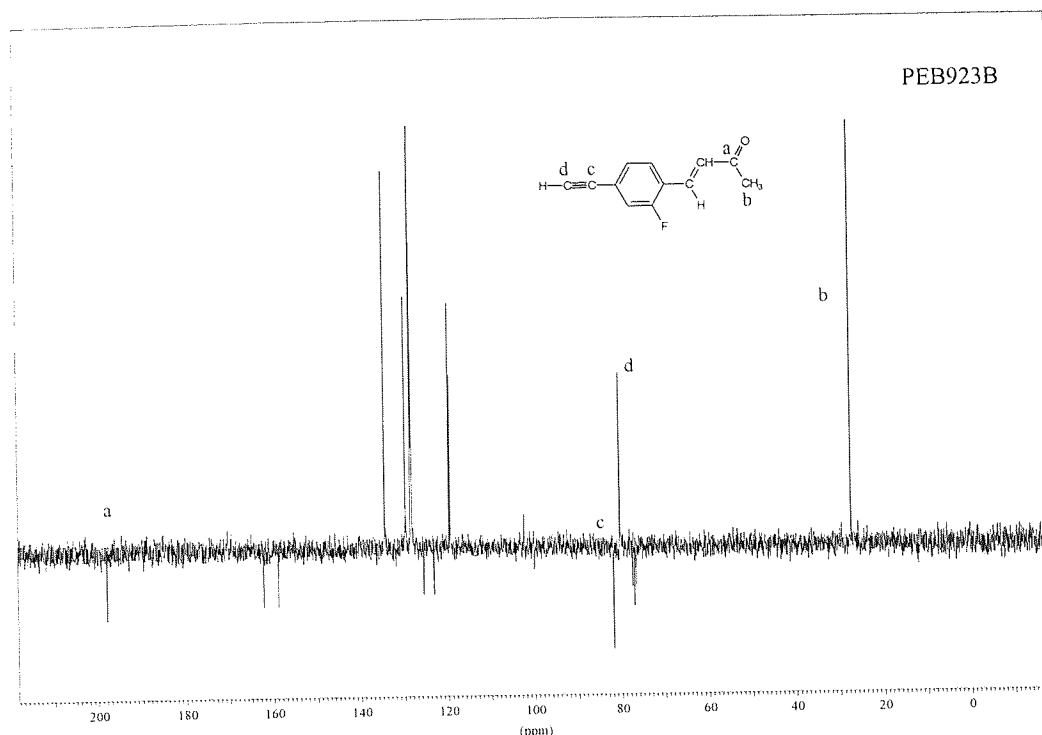


Figure 59 : ^{13}C NMR of condensation product PEB923B

After much consideration of the analytical data it was decided that the structure of the product was that of 1-(4-ethynyl-2-fluorophenyl)but-1-en-3-one (PEB923B), shown in Figure 60.

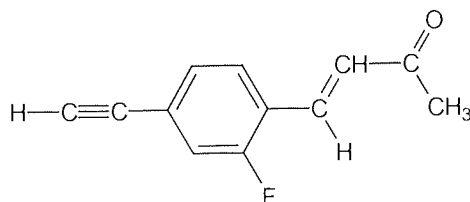
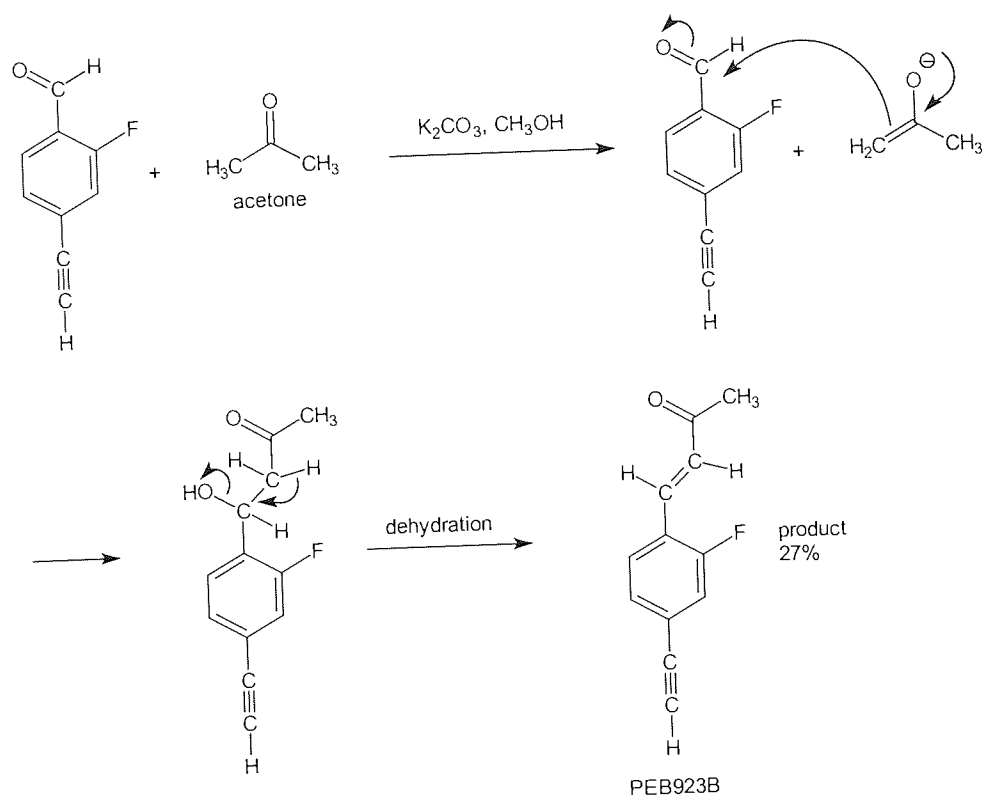


Figure 60 : Structure of product 1-(4-ethynyl-2-fluorophenyl)but-1-en-3-one (PEB923B)

The compound is probably the product of a mixed aldol condensation (Claisen-Schmidt reaction) between the aromatic aldehyde and acetone^(10 pp.940-941). Acetone was used as a general washing solvent, but in this case it acted as a reagent rather than as a solvent. A possible mechanism for this condensation reaction is shown in Scheme 20.

Under the basic conditions employed acetone was able to generate the enol-anion form which could perform a nucleophilic attack on the aromatic aldehyde. The intermediate alcohol spontaneously dehydrates because of the drive towards conjugation, giving the product PEB923B.

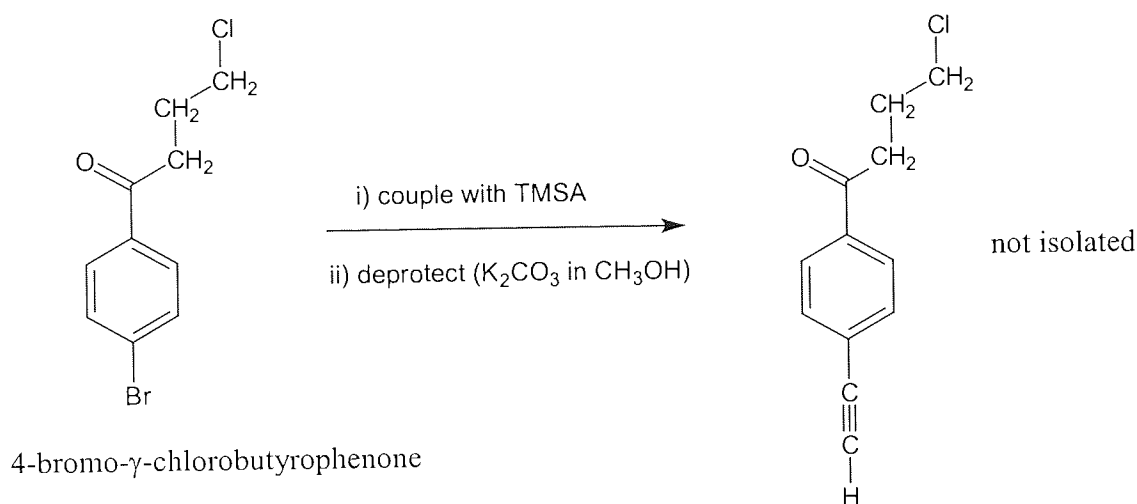


Scheme 20 : Condensation of 4-ethynyl-2-fluorobenzaldehyde with acetone

As a result of this condensation mechanism observed, it was imperative that any synthesis of this compound in the future should require the complete elimination of acetone from the procedure.

3.6.5 Unexpected product from an alkyl chloride monomer (PB014)

The synthesis of a monomer possessing an chloroalkyl group was attempted, so that new functionalities could be attached using a simple nucleophilic substitution, eliminating the need for Sonogashira coupling. A suitable commercially available starting material, 4-bromo- γ -chlorobutyrophenone, was reacted using the conventional procedure, as shown in Scheme 21. There was a possibility that TEA would form a salt with the chloroalkyl as described previously for a substituted benzylbromide, but this did not occur.



Scheme 21 : Attempted synthesis of an alkyl chloride functionalised monomer

A pale yellow crystalline solid was obtained (PB014), but MS analysis of the product showed that the compound had a molecular weight of 170 Daltons, thirty-six less than expected. In addition, the chlorine isotopic pattern was absent. A loss of 36 mass units corresponded to the molecular weight of HCl, and it was supposed that dehydrohalogenation had occurred to give an alkene function. However, on examination of the NMR this was proved not to be the case, as the 1H spectrum contained no peaks that corresponded to an alkene (6-7ppm region), see Figure 61. The 1H alkyl splitting of the product was expected to be triplet, quintet, and triplet, but it was found to be two quintets and a septet. Three different alkyl carbons were expected in the ^{13}C spectrum, but only 2 different alkyl carbons were found, see Figure 62. The ^{13}C PENDANT NMR technique shows not only chemical shift, but also indicates the number of bonds of each carbon atom. This was used to show that one type of alkyl carbon was a CH (tertiary) or CH_3

(primary), and the other type was a C (quarternary) or CH₂ (secondary). Furthermore, the PENDANT ¹³C spectrum revealed that the carbonyl at 200ppm was a ketone. Two separate effects can explain this unusually high shift of the ketone group. The first is that the cyclopropyl ring can “act as an alkene” in its electronic properties, which results in conjugation effects^(10 pp.151-152). The other important factor is that the ketone group is directly attached to the benzene ring and may be susceptible, therefore, to the influence of ring currents.

Analytical data for PB014; pale yellow crystalline solid (82% yield); mp 69-70°C (from EtOH); λ_{max}(DCM)/nm 290; ν_{max}/cm⁻¹ 3247 (s, sharp, -C≡C-H), 3103 (w, sharp, Ph), 2107 (m, sharp, -C≡C-), 1658 (s, sharp, ketone), 1599 (s, sharp, Ph), 1405 & 1386 (cyclopropane ring); δ_H(300 MHz; CDCl₃) 7.88 (2 H, d, Ph), 7.51 (2 H, d, Ph), 3.23 (1 H, s, ≡C-H), 2.57 (1 H, septet with unusual splitting, C-H), 1.19 (2 H, quintet with unusual splitting, -CH₂-), 1.02-0.96 (2 H, overlapping splitting pattern, -CH₂-); δ_C(75 MHz; CDCl₃) 199.58 (C=O), 137.41 (Ph), 132.02 (Ph), 127.71 (Ph), 126.32 (Ph), 82.68 (Ph-C≡), 80.16 (≡C-H), 17.07 (-CH-), 11.79 (-CH₂-); m/z (EI) 170 (M⁺) chlorine isotopic pattern absent.

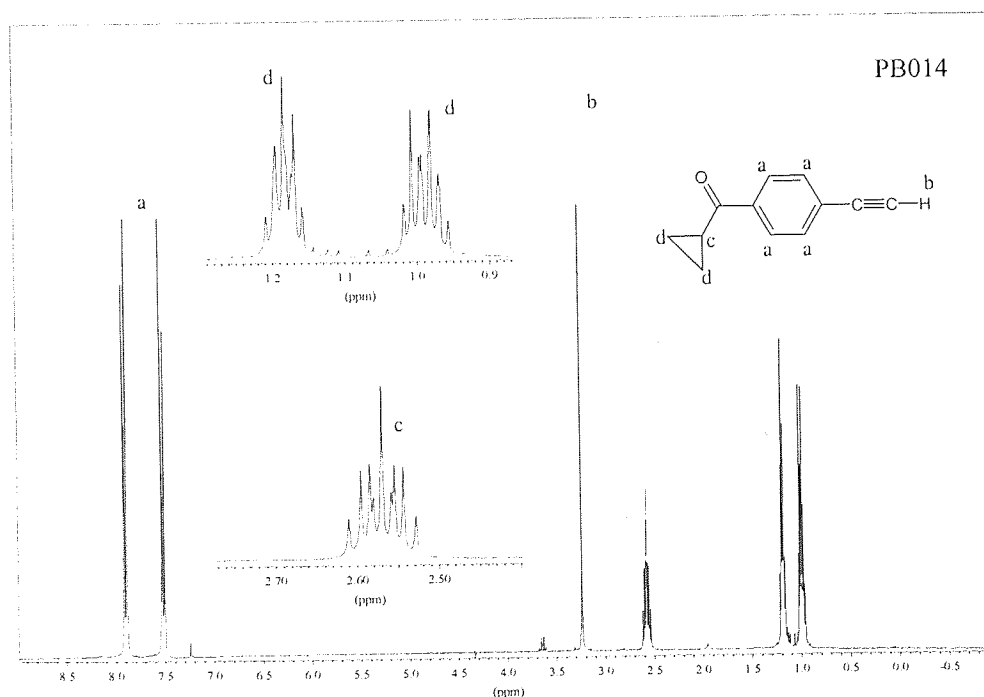


Figure 61 : ¹H NMR of cyclised monomer PB014

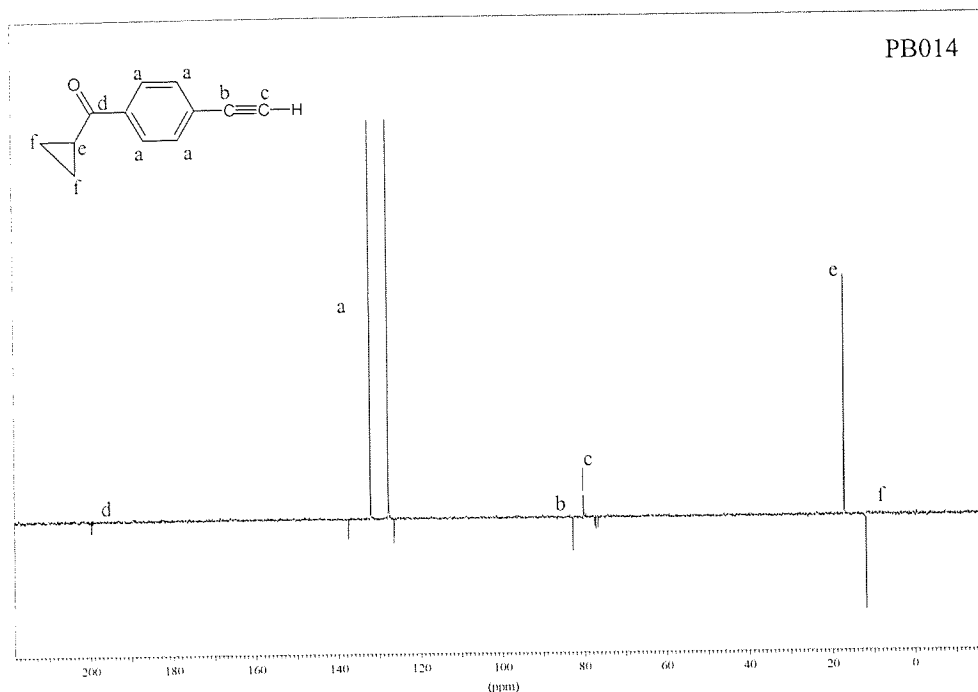


Figure 62 : ^{13}C NMR of cyclised monomer PB014

The culmination of this characterisation implied that the product was a phenylacetylene derivative bearing a ketone group, two CH_2 , and one CH. As there was no alkene function the structure had to include a cyclopropyl ring structure. Hence, the most likely structure of the product was cyclopropyl-4-ethynylphenyl ketone (Figure 63).

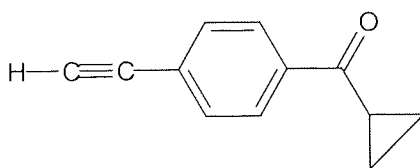


Figure 63 : Cyclised product cyclopropyl-4-ethynylphenyl ketone (PB014)

It is interesting to note that the splitting patterns of the two quintets in the ^1H NMR spectrum are not identical. In most organic molecules only one magnetic environment is observed because the bonds in the molecule are rotating about their axis. This rotation is so fast that the NMR spectrometer can only detect an “average” magnetic environment for each nucleus. The quintets in PB014 correspond to that of the CH_2 's of the cyclopropyl

group, thus implying that there are two different magnetic environments in this ring. It can be assumed therefore, that the cyclopropyl ring is fixed in space. This may be explained by considering that the highly strained bond angles that exist in the ring can also distort the bonding orbitals. This distortion gives the orbitals some π character, which can overlap with the π system of the neighbouring ketone group. It is this π overlap that is responsible for the non-rotation of the cyclopropyl ring.

It is necessary to visualise the structure of this compound in three dimensions in order to explain how the different magnetic environments of the hydrogen atoms arise, as shown in Figure 64. The two hydrogens H_a are equivalent because they are approximately the same distance away from the carbonyl group, and they are on the same side of the cyclopropyl ring. The distance between the oxygen atom and the hydrogens on the under-side of the cyclopropyl ring, H_b , is much greater than for H_a . Thus, the hydrogens H_b give rise to a separate magnetic environment to that of H_a .

The splitting patterns are more complicated than a simple quintet, because the geminal hydrogens on the methylene carbons are different. Each hydrogen atom, therefore, couples to every other hydrogen atom in the ring, which in turn are split by other hydrogen atoms. A full explanation of "ABX" coupling is beyond the scope of this work, but Williams & Flemming⁸⁷ provides a good account.

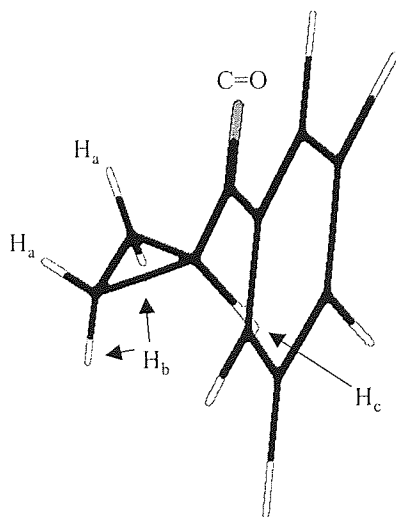


Figure 64 : Atomic structure of cyclopropyl derivative PB014

To ascertain the stage at which cyclisation had taken place, NMR and MS analyses were carried out on the intermediate trimethylsilyl derivative PEB997 (Figure 65). An isotopic pattern corresponding to the presence of a chlorine atom was found by MS analysis, and the peak was of correct molecular weight. The expected ^1H NMR splittings were found for a $-\text{CH}_2-\text{CH}_2-\text{CH}_2-$ structure, as shown in Figure 66. Further evidence was provided by the ^{13}C NMR spectrum which showed 3 peaks corresponding to CH_2 , see Figure 67. It was concluded that PEB997 was of correct molecular weight and structure, i.e. it was uncyclised.

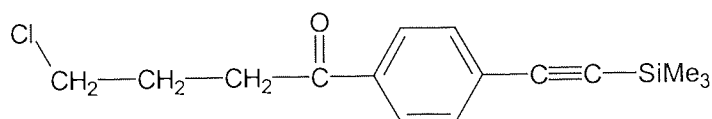


Figure 65 : Structure of the uncyclised trimethylsilyl intermediate PEB997

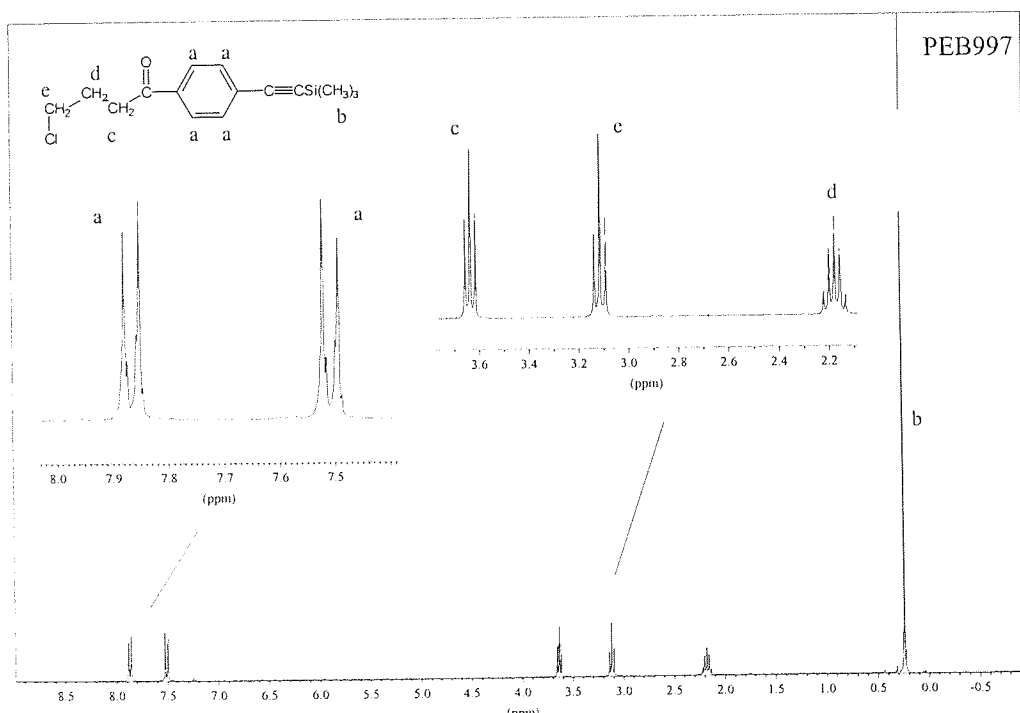


Figure 66 : ^1H NMR of trimethylsilyl intermediate PEB997

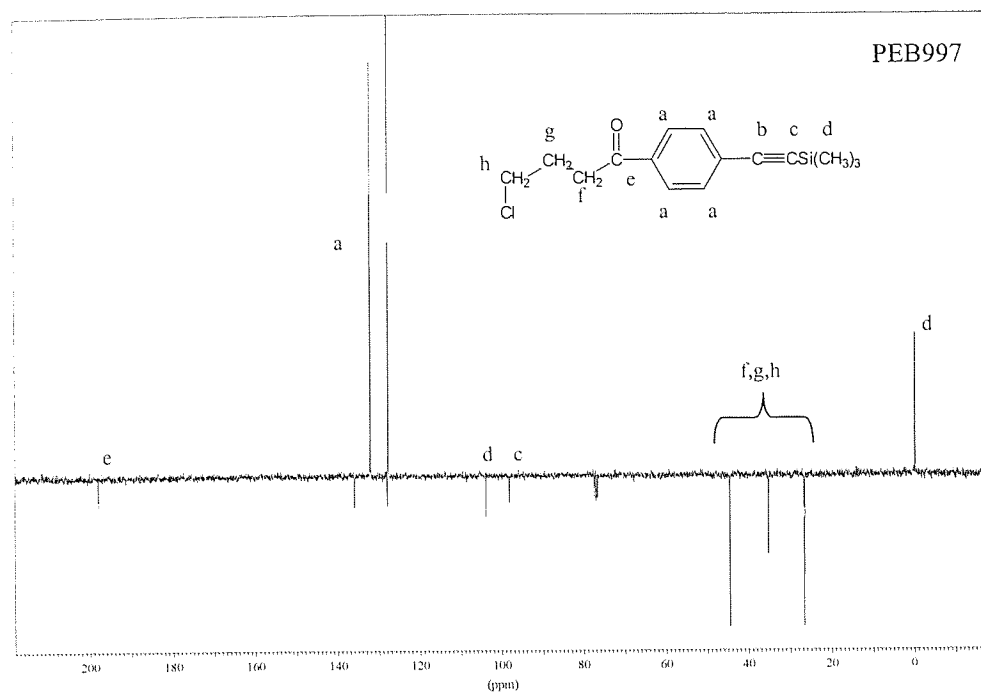
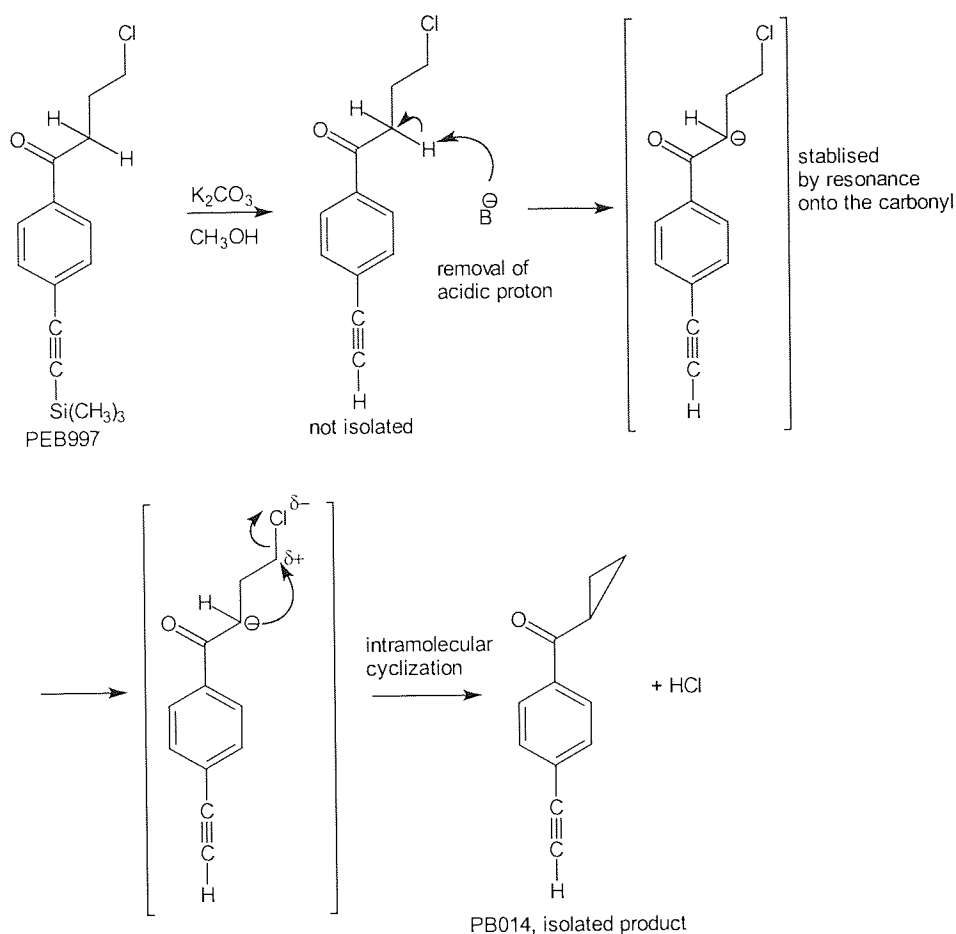


Figure 67 : ^{13}C NMR of uncyclised trimethylsilyl intermediate

Therefore, intramolecular cyclisation must have occurred during the deprotection to $\text{K}_2\text{CO}_3/\text{methanol}$, to give the cyclopropane product (PB014). This cyclisation was unexpected, but it can be explained by using a classical “Neighbouring-Group mechanism”^(10 pp.308-312), as shown in Scheme 22. A neighbouring-group (NG) can be defined as a group (close to the carbon undergoing attack) which has a lone pair of electrons, such as O, N, or S. The NG in this reaction is the enolate anion, which is formed under the basic conditions employed. Performing an intramolecular cyclisation by an $\text{S}_{\text{N}}2$ nucleophilic attack on the alkyl chloride relieves this instability of this enolate anion. In addition, cyclisation is made easier because the chloride ion is an excellent leaving group.

Although the cyclopropyl ring is very strained, it is quite common for this size of ring to be formed in these NG type mechanisms.



Scheme 22 : Neighbouring-group mechanism for the intramolecular cyclisation of PB014

3.7 Recommendations for Sonogashira coupling

The synthesis of phenylacetylene monomers was accomplished successfully, with yields close to those reported in literature. However, some molecules possessing less-conventional functional groups exhibited side reactions during deprotection in K_2CO_3 /methanol, such as trans-esterification, cyclisation, and the formation of condensation adducts. Deprotection using non-basic conditions, such as tetrabutylammonium fluoride in THF, could have eliminated these unwanted side-reactions⁸⁸. No problems were encountered with the palladium catalyst, but TEA was found to form salts with reactive halides.

CHAPTER 4.
POLYMERS AND POLYRADICALS

CHAPTER 4. POLYMERS AND POLYRADICALS

4.1 Overview

In this chapter an overview of the synthesis and properties of polyphenylacetylene is described. Polyphenylacetylene has attracted much attention during the last twenty years because of its potential application in areas such as electrical conductivity⁸⁹, chiral recognition⁸⁰, non-linear optics⁹⁰, and magnetism⁶². Its main feature is a conjugated backbone, with pendant phenyl groups. The three most common forms of polyphenylacetylene are discussed, in which the structure is determined primarily by the choice of polymerisation catalyst. An appreciation of the various catalyst systems is given, with those based upon rhodium generally giving the best yields and tolerance of functional groups. Some catalysts are intolerant of groups such as nitro or nitronyl nitroxide, both of which are important in this research. Of vital importance to both the yield and/or tolerance are the coordinated ligands around the catalyst. A rhodium catalyst was synthesised using a new arrangement of ligands, and this catalyst was used to co-polymerise stable radicals with “bridging group” monomers. Magnetic characterisation of these materials revealed several interesting and unusual effects, and some account is made to explain these.

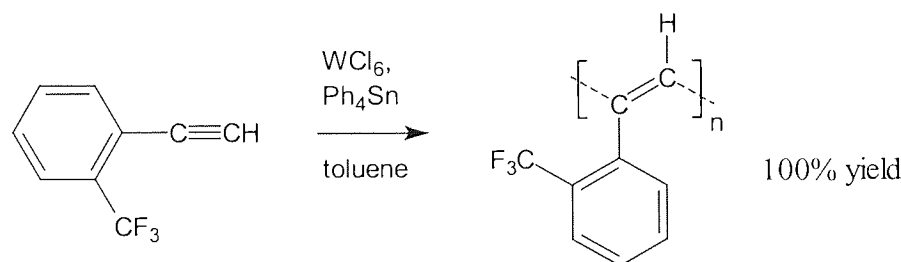
4.1.1 Thermal polymerisation

The simplest method of synthesising polyphenylacetylenes (PPAs) is to heat a phenylacetylene monomer for 3 hours at 250°C, in a high boiling solvent⁹¹. Good yields are obtained, but the polymers are of very low molecular weight (500 to 1600 Daltons). The conditions employed in this radical polymerisation are very harsh, which limits the range of monomers that can be polymerised. Monomers bearing certain functional groups, such as nitronyl nitroxide, are incompatible with this method of polymerisation because they degrade in the presence of other free radical species. In addition, the high temperature conditions can decompose some functional groups, such as primary amide or tetrahydropyran.

4.1.2 Metathesis catalysts

Polyphenylacetylene obtained from thermal polymerisation has low molecular weight and no stereoregularity. Stereochemistry is very important in polyphenylacetylenes because the carbon-carbon double bond of the backbone is able to exist in more than one configuration. The backbone configuration plays an important part in the solubility, conjugation, and colour of polyphenylacetylenes. Thus, it is highly desirable to control these factors. Control of the stereochemistry, and sometimes molecular weight can be achieved using a catalyst.

The first catalysts to be tested with phenylacetylene were those already known to be active in ROMP, such as WCl_6 ⁹², $\text{W}(\text{CO})_6/\text{h}\nu$ ⁹³, MoCl_5 ⁹⁴, and MoCl_4 ⁹⁵. These catalysts give good yields of stereoregular polyphenylacetylene, or its simple derivatives, but the average molecular weight of the polymer obtained is usually only moderate (100,000 Daltons approximately). The molecular weight of the polymer can reach 1 million Daltons by the presence of a bulky substituent ortho to the alkyne, such as an *o*- CF_3 ⁷⁷ or an *o*- $\text{Si}(\text{CH}_3)_3$ ⁹² group, as shown in Scheme 23. The electron donating or withdrawing effect of the ortho substituent has a minimal influence on the reactivity of the alkyne.



Scheme 23 : Polymerisation of *o*- CF_3 phenylacetylene by WCl_6 - Ph_4Sn

The standard metathesis catalysts offer only minimal control of average molecular weight, with polydispersities in the range of 2 to 5. Some applications, such as non-linear optics, demand a low polydispersity of polymer. This was achieved by Schrock, using a molybdenum(VI) based catalyst^{96,97}, shown in Figure 68. This system gave low polydispersities (in the range of 1.04 to 1.07) whilst retaining a high yield of polymer.

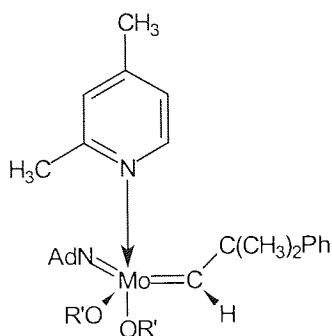


Figure 68 : Schrock type catalyst

Metathesis catalysts, however, suffer from several disadvantages, the most obvious being the requirement of an ortho substituent, which imposes severe limitations on the spatial arrangement of functional groups about the structure of the monomer. Another disadvantage is that the polymer backbone is known to possess defects, which can reduce the length of conjugated sequences⁸⁸. These catalysts are also sensitive to nitrogen containing solvents, such as nitrobenzene and benzonitrile, in which polymerisation is inhibited⁹². Further evidence for this poisoning effect of nitro groups was provided by the attempted polymerisation of *p*-nitrophenylacetylene (4NPA), using WOCl_4 , which did not yield any polymer⁹⁸. Successful polymerisation of 4NPA was achieved using WOCl_4 with Me_4Sn as the co-catalyst, but the highest yield obtained was only 56%. Of more importance to this project is the fact that some functional groups containing basic nitrogen atoms, such as nitroxide inhibited polymerisation⁵⁸.

Furthermore, metathesis catalysts can be sensitive to oxygen containing solvents, such as anisole or acetophenone, in which no metathesis took place⁷⁷. This lack of tolerance towards some functional groups has lead to the search for other catalysts that can polymerise a wider range of monomers.

Other catalyst complexes such as those based on neodymium⁹⁹ and iridium¹⁰⁰ have been reported, but only give moderate yields of polyphenylacetylene at best. This is because these catalysts have a tendency to produce cyclotrimers, rather than polymers.

4.1.3 Rhodium catalysts

Furlani reported that good yields of polyphenylacetylene could be obtained utilising a rhodium complex, bis(cycloocta-1,5-diene)- $\mu\mu'$ -dichlorodirhodium $[\text{Rh}(\text{COD})(\text{Cl})]_2$ ¹⁰¹ (Figure 69). The highest yields (>90%) were obtained using the strong base NaOH as co-catalyst. This system is quite flexible, in that the polymerisation can take place in solvents of different polarity, such as benzene or THF. However, the use of the NaOH co-catalyst is detrimental to the polymerisation of certain monomers, because base sensitive groups could be hydrolysed during polymerisation (e.g. ester).

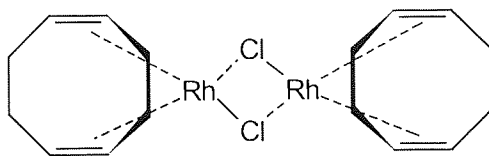


Figure 69 : $[\text{Rh}(\text{COD})(\text{Cl})]_2$ catalyst for polymerisation of phenylacetylene

Monomers containing nitro groups, which posed a problem for metathesis catalysts, can be polymerised by Furlani's $[\text{Rh}(\text{COD})\text{Cl}]_2/\text{NaOH}$ system. This was demonstrated by the polymerisation of 4NPA to give a high yield of polymer (80%)¹⁰².

It was found that the NaOH co-catalyst of Furlani's system could be omitted by the use of triethylamine as the solvent. A system comprised of (bicyclo[2.2.1]hepta-2,5-diene)chlororhodium(I) dimer, or $[\text{Rh}(\text{NBD})(\text{Cl})]_2$ ¹⁰³ (Figure 70), in TEA gave extremely high molecular weight PPA ($>10^6$ Daltons by SEC) in excellent yield (100%). This catalyst system employs a 2,5-norbornadiene (NBD) ligand, instead of Furlani's COD ligand, because NBD is known to give higher yields and lower polydispersity^{104,105}. It is unclear exactly how the NBD ligand influences the yield and molecular weight of the polymer, but two important points have been suggested. Firstly, NBD is smaller sterically than COD; secondly, the NBD is both a stronger π back-bonding acceptor and a stronger σ donor. Such steric and electronic effects may affect the stability and reactivity of the rhodium complex.

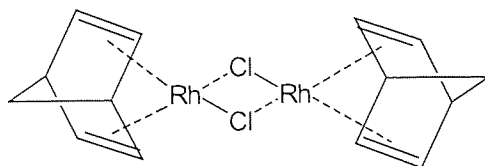


Figure 70 : Popular polymerisation catalyst $[\text{Rh}(\text{NBD})\text{Cl}]_2$

4.1.3.1 Living Polymerisation using $[\text{Rh}(\text{NBD})(\text{OCH}_3)]_2$

Kishimoto developed a highly efficient rhodium catalyst $[\text{Rh}(\text{NBD})(\text{OCH}_3)]_2$ (Figure 71) by replacing the bridging chlorines of $[\text{Rh}(\text{NBD})\text{Cl}]_2$ with methoxy groups¹⁰⁵. High yields of PPA (>98%) were obtained within 1 hour at room temperature using THF as the solvent. The additives 4-dimethylaminopyridine and triphenylphosphine were required to obtain very low polydispersities (<1.2 by SEC). By performing experiments involving sequential monomer addition there was a distinct shift in average molecular weight, whilst the polydispersity remained low. The greater control of the average molecular weight allows useful polymer structures, such as block co-polymers, to be synthesised.

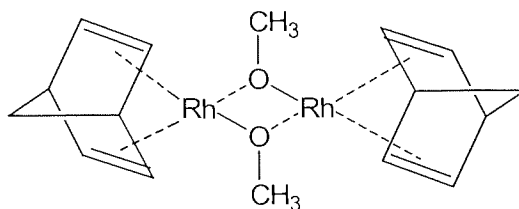
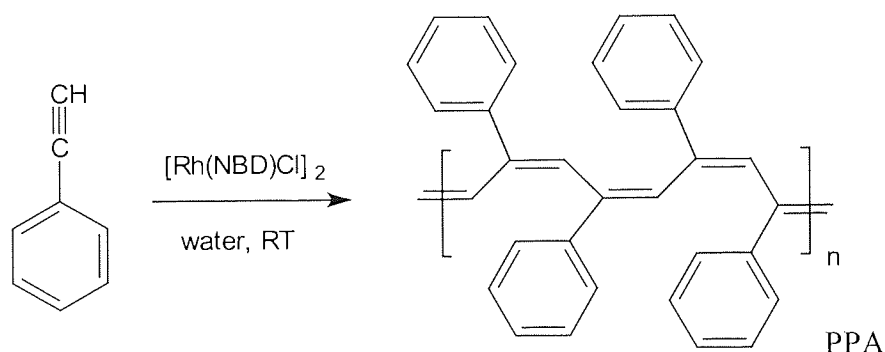


Figure 71 : $[\text{Rh}(\text{NBD})\text{OCH}_3]_2$ "Living" type rhodium catalyst

4.1.3.2 Polymerisation by rhodium catalysts in water

Water can be used as the catalyst medium for some types of rhodium catalyst, such as $[\text{Rh}(\text{NBD})\text{Cl}]_2$, in which polymerisation takes place at the aqueous-solvent interface and generally gives a good yield of polymer¹⁰⁶ (as shown in Scheme 24). The water has two purposes, to behave as a solvent for the rhodium complex, and as a co-catalyst. The role of water as a co-catalyst was confirmed by performing a polymerisation using an identical

catalyst but with toluene as the solvent, which generated only a trace amount of polymer (1% yield). This water based system was shown to have several advantages over conventional organic solvent systems. The catalyst solution can be used repeatedly without depletion in the yield of polymer obtained, which decreases the amount of expensive rhodium wasted. Of more importance is that the polymerisation can be carried in an open flask in the presence of air. Films of polymer can easily be obtained by dropping a solution of monomer onto the surface of the water phase. This system makes the synthesis of PPAs very simple, but it does have two important drawbacks. Polyphenylacetylene obtained from this catalyst system can be insoluble in common organic solvents, whereas those obtained from other systems are soluble. Furthermore, it can be envisaged that the complete removal of water from the polymer matrix would be difficult to achieve.



Scheme 24 : Polymerisation of PPA in water using a rhodium complex

4.1.4 Polymerisation of phenylacetylene bearing a stable nitronyl nitroxide radical

Fujii *et al.* found that conventional rhodium(I) catalysts were ineffective for the polymerisation of phenylacetylene bearing a nitronyl nitroxide group⁶². It is thought that the polymerisation is inhibited because the basic nitrogen atom blocks the active site. This most likely occurs by coordination of the nitrogen moiety to the metal centre, in preference to the alkyne. The $\text{Rh}(\text{NBD})\text{Cl}_2/\text{TEA}$ system, which generally gives a high yield of polymer, was not tested, presumably because nitronyl nitroxides are known to be unstable in the presence of TEA⁶⁰. These problems were overcome by the use of a rhodium(I) complex which contained a basic ligand (ammonia), $\text{Rh}(\text{COD})(\text{NH}_3)\text{Cl}$ (Figure 72). This

catalyst was moderately effective for the polymerisation of a nitronyl nitroxide containing monomer (42% yield of polymer) when using ethanol as the solvent.

The ammonia ligand is thought to modify the electron density on the rhodium(I) centre, by donation of its lone pair of electrons, which leads to a better tolerance of a monomer bearing a nitronyl nitroxide group.

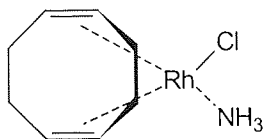


Figure 72 : $\text{Rh}(\text{COD})(\text{NH}_3)\text{Cl}$ - a catalyst tolerant of nitronyl nitroxide groups

4.1.5 Synthesis of co-polymers by rhodium catalysts

The problems of insolubility associated with some homopolymers of substituted phenylacetylene have led to research into co-polymerisation. The polymer of 4NPA is highly desirable because of its enhanced conductivity compared to PPA, but it is completely insoluble in all common organic solvents. 4NPA was copolymerised with phenylacetylene in an attempt to produce materials that have better solubility in organic solvents. This was accomplished in good yield (70%) using $[\text{Rh}(\text{COD})\text{Cl}]_2$ under high reflux conditions¹⁰². In a ratio of 1:1, these monomers gave a random co-polymer of partial solubility. Increasing the ratio of phenylacetylene to 4NPA led to better solubility, such that a co-polymer using a ratio of phenylacetylene:4NPA (3:1) was found to be soluble in common organic solvents.

To alleviate insolubility problems of the homopolymer of 4-(*N,N*-dimethylamino)phenylacetylene (Figure 73) it was co-polymerised with 4-nitrophenylacetylene (4NPA), or 4-chlorophenylacetylene¹⁰⁷. These random co-polymers were obtained in good yield (greater than 75%) and were soluble (except when 4NPA was used as the co-monomer) in common organic solvents. A lesser proportion of 4-(*N,N*-dimethylamino)phenylacetylene was found in the co-polymer than that expected. This can be explained by considering that one monomer is more reactive towards the catalyst than the other. No attempt was made to explain how the substituent group altered the reactivity of the monomer.

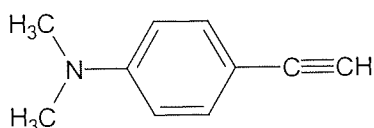


Figure 73 : The monomer 4-(*N,N*-dimethylamino)phenylacetylene

4.2 Polymerisation mechanism of phenylacetylene

It can be rationalised from the review of rhodium complexes that the nature of the diene ligand is of critical importance in obtaining good molecular weight and low polydispersity. In order to gain further insight into how this may occur a mechanism of polymerisation is required.

4.2.1 Hydrogen transfer mechanism

Escudero *et al.* first proposed a mechanism for the polymerisation of phenylacetylene using a rhodium centre, but provided no physical data to support their theory¹⁰⁸. Furthermore, the credibility of this mechanism was diminished further because it is based on the results obtained from a non-standard rhodium catalyst, di- μ -pentafluorothiophenolate bis(1,5-cyclooctadiene) rhodium(I). This catalyst gave results that are not consistent with those reported in the literature. Monomers that normally polymerise successfully were found to give very low yields, e.g. 4-methylphenylacetylene polymerises in 18% yield only. In addition, it was reported by Escudero that polymerisation was inhibited by benzaldehyde. Unfortunately this observation was based on unpurified benzaldehyde, which can contain a small, but sometimes significant amount

of benzoic acid. Carboxylic acids are generally used in the literature to quench polymerisations, because they destroy rhodium complexes.

However, this mechanism deserves consideration because some of its conclusions have subsequently been proved correct. A complete appraisal of this mechanism is not possible in this report, because Escudero provided minimal description of the steps involved. An overview of this mechanism is now given.

Association of a monomer unit to the rhodium complex to give the intermediate OW1 is the initial step, as shown in Figure 74.

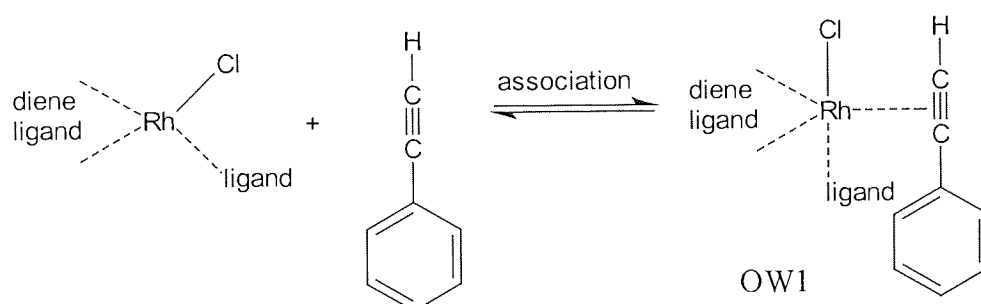


Figure 74 : Association of phenylacetylene to the rhodium centre

The bonding mode of the monomer now changes from one that is coordinated to the carbon-carbon triple bond OW1, to one that has two coordinate bonds OW2 (one from each carbon), as shown in Figure 75.

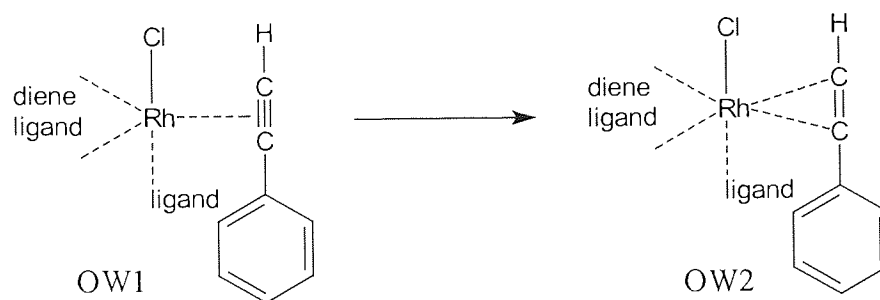


Figure 75 : Change of bonding mode of the monomer

Propagation occurs by the association of a second molecule to OW2. Hydrogen transfer from the newly associated monomer to the di-coordinated monomer occurs, as shown in Figure 76.

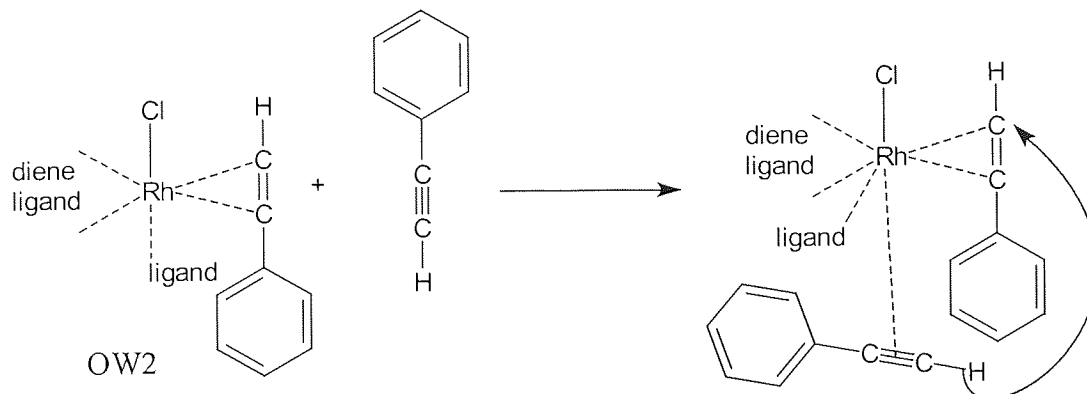


Figure 76 : Propagation - hydrogen transfer from monomer to polymer

A rearrangement of the intermediate OW3 gives the polymer unit OW4, as shown in Figure 77. Propagation is repeated for a number of times.

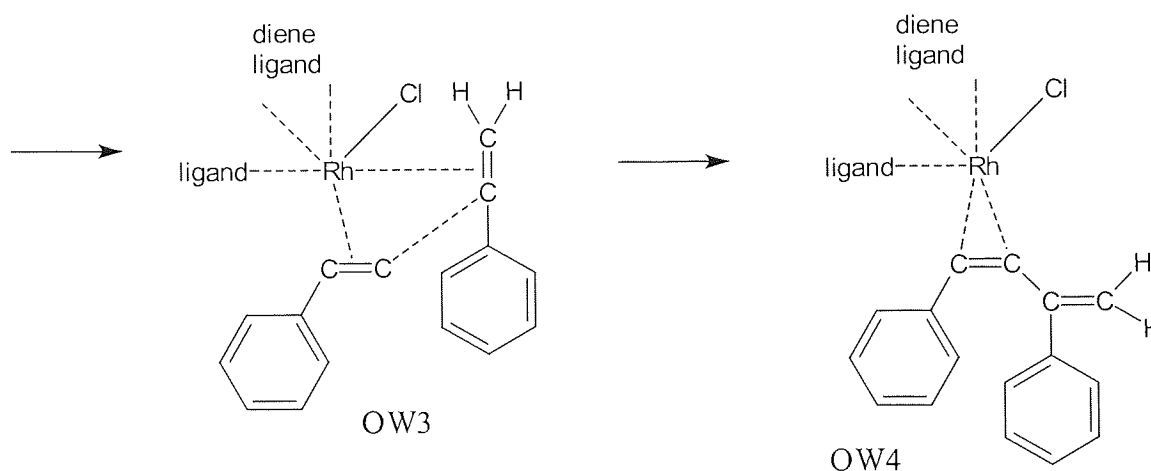


Figure 77 : Rearrangement to give polymer

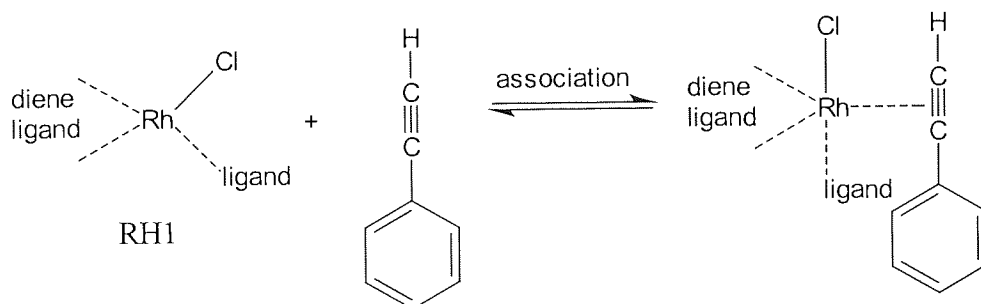
Escudero gave no account of how termination might occur.

It was theorised by Escudero that only phenylacetylenes have the correct acidity to facilitate this hydrogen transfer mechanism. This corresponds with that in the literature, in which polymerisation of alkylacetylenes by rhodium complexes are rarely successful.

4.2.2 Monomer insertion mechanism

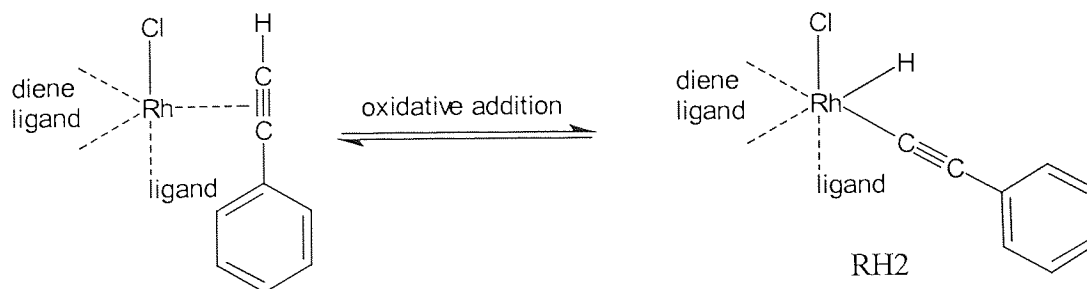
More recently, Schneidermeier *et al.* proposed a much simpler mechanism which was supported by kinetic experiments, computer modelling, and solid-state ^{13}C NMR^{109,110}. Polymerisation proceeds via a coordination type mechanism comprised of four steps.

The rhodium(I) catalyst, RH1, forms a coordinate bond with the triple bond of phenylacetylene, as shown in Scheme 25.



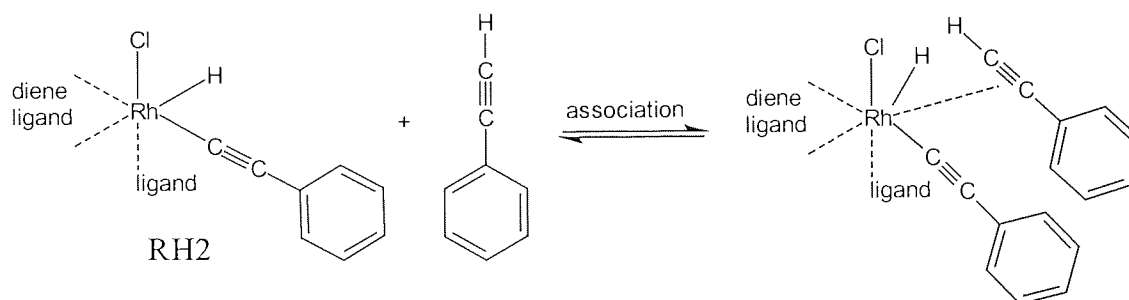
Scheme 25 : Association of phenylacetylene with rhodium(I) centre

Oxidative addition of the coordinated phenylacetylene to the rhodium(I) centre generates a rhodium(III) complex (RH2), as shown in Scheme 26.



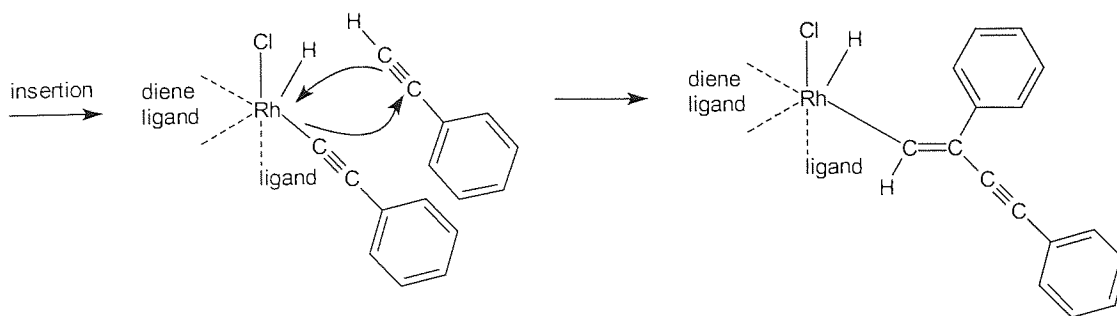
Scheme 26 : Oxidative addition of phenylacetylene to give a rhodium(III) centre

Propagation occurs by the coordination of RH2 to another molecule of phenylacetylene, as shown in Scheme 27, which was proved to be the rate-determining step of the polymerisation, because of steric crowding around the catalyst centre. The steric size of the diene ligand was found to be important for the formation of high average molecular weight PPA. COD gave lower molecular weight polymers than those obtained using NBD. This was ascribed to the increased crowding around the rhodium centre caused by the sterically larger COD.



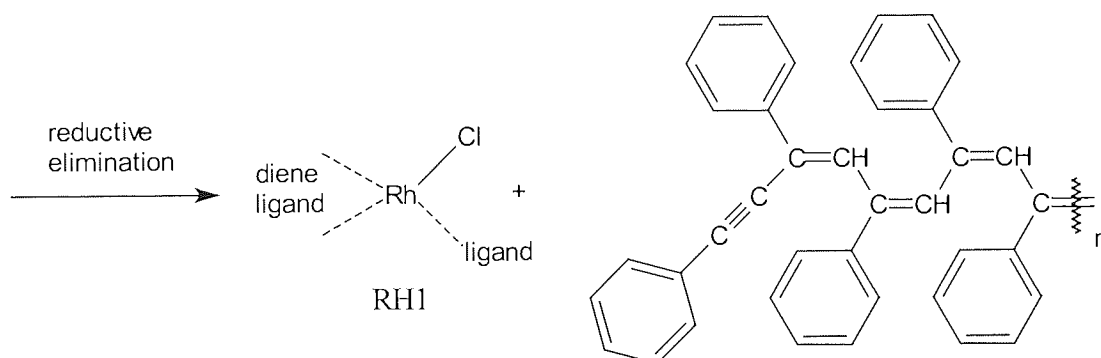
Scheme 27 : Propagation – association of another molecule of phenylacetylene

Insertion of the coordinated phenylacetylene gives the polymer repeat unit, as shown in Scheme 28. The propagation and insertion steps are repeated for a number of times.



Scheme 28 : Insertion of coordinated phenylacetylene

Reductive elimination of the catalyst/polymer complex gives the polymer product, and regenerates the rhodium(I) complex RH1, as shown in Scheme 29.



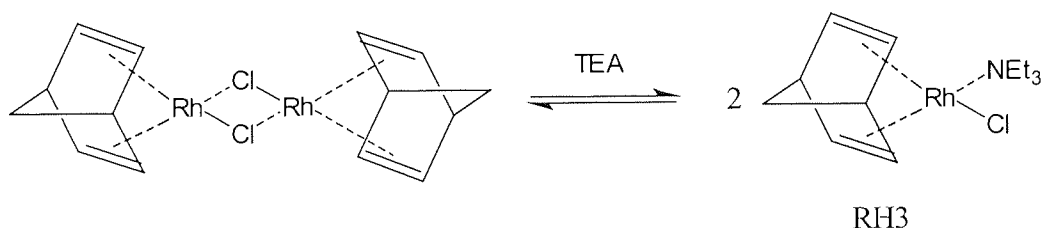
Scheme 29 : Reductive elimination – to give PPA and reform the rhodium(I) centre

However, this mechanism should be considered only as a guide, because it does not account for two important factors. There is no adequate explanation for the increased yields observed by the use of triethylamine as the solvent, and how the addition of an ammonia ligand gives better tolerance towards some functional groups.

4.2.1 The role of the solvent during polymerisation with rhodium complexes

Tabata conducted research into the role of solvents during polymerisation, and it was found that the choice of solvent employed can have a marked effect on the yield, average molecular weight, and colour of the polymer¹¹¹. Solvents can be split into two groups, those that coordinate to the rhodium complex (TEA and ethanol/methanol), and those that do not (THF and benzene).

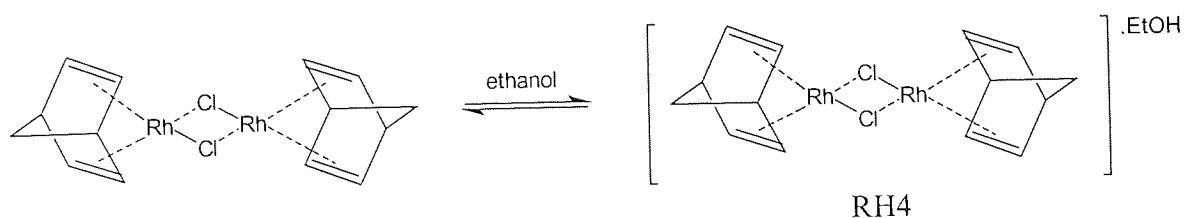
Dissociation of dimeric rhodium complexes occurs in the presence of TEA, as shown in Scheme 30. It is this catalyst-TEA complex RH3 that is thought to be the catalyst active during polymerisation. The high molecular weights achieved by this system are attributed to the presence of a very efficient propagation step.



Scheme 30 : Rhodium complex with triethylamine

A similar dissociation also occurs using alcohol solvents, but to a lesser extent because it is thought that the catalyst-alcohol complex may exist in equilibrium with the uncoordinated rhodium complex. However, the nature of this coordinated species remains unknown, and it is best represented as RH4, as shown in Scheme 31.

No evidence of coordination for benzene or THF was reported. It is safe to assume that these solvents function as a solvent for the dimeric rhodium catalyst and the polymer only.



Scheme 31 : Rhodium complex with alcohol

4.3 Types of structure and properties of polyphenylacetylene

Polyphenylacetylene exists in at least three different tautomeric forms. These tautomers are the result from the differences in stereochemistry about the carbon-carbon double bond of the polymer backbone. The structure of the polymer obtained is always dependent upon the choice of catalyst used. There are three main types, *trans-trans*, *cis-trans* and *cis-cis*. This nomenclature is based upon the conjugated backbone, and it must be considered that a carbon-carbon double bond alternating with a carbon-carbon single bond is only a representation. The real structure is probably a hybrid of this, so in these representations the configurations of both bonds are required.

4.3.1 Trans-trans PPA from metathesis catalysts

All known metathesis catalysts give a “*trans-trans*” polymer, where the double bond of the backbone is in a *trans* configuration, the carbon-carbon single bond is also in the *trans* configuration⁶³, as shown in Figure 78. The *trans* structure of the backbone results in substantial conjugation, giving this polymer a distinctive red/brown colour. The pendant group of each monomer unit is on the same side as its neighbour, giving rise to steric congestion when the chain is elongated. The strain is alleviated by twisting of the pendant phenyl group, so that it is out of plane with the backbone. Conjugation between pendant groups is therefore assumed to be weak, because of the lack of co-planarity.

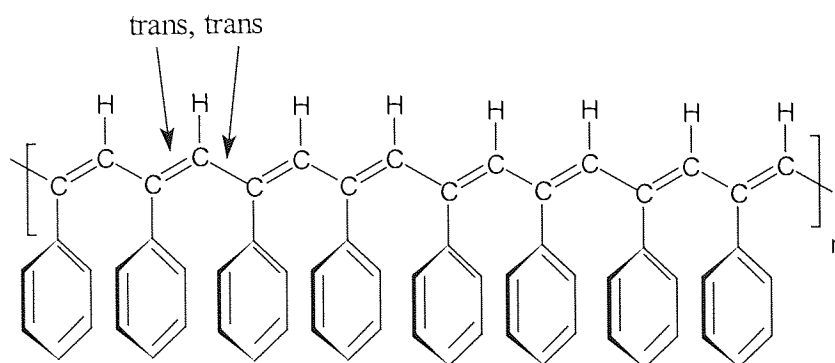


Figure 78 : The structure of *trans-trans* PPA from metathesis catalysts

4.3.1.1 Colours and solubility

The solubility of *trans-trans* polyphenylacetylene in common organic solvents, such as toluene, or THF is usually very good. When the monomer possesses a bulky ortho group the backbone structure remains unchanged, but the colour and solubility of the polymer can change. This is exemplified by PPA bearing an *o*-CF₃⁷⁷ which is dark brown and *o*-Si(CH₃)₃⁹² which is dark purple. The solubility of halogen containing polymers is usually very poor; e.g. PPA possessing chloro groups at the 2,4, and 6 positions was reported to be insoluble in all common solvents¹¹².

Characterisation of *trans-trans* PPA is quite difficult because analysis by NMR always gives very broad signals. The reason for this broadening has not been fully investigated but it is reasonable to assume that the twist of the phenyl groups is not the same from neighbour to neighbour. This could result in slightly different magnetic environments for the ring hydrogen atoms, and hence very broad signals.

4.3.2 Cis-trans PPA from rhodium catalysts

Rhodium catalysts are the main source of the *cis-trans* tautomer of PPA. Its backbone structure consists of a carbon-carbon double bond in the *cis* configuration, and the carbon-carbon single bond is in the *trans* configuration, as shown in Figure 79. This backbone configuration results in a structure in which each monomer unit is on the opposite side of the chain from both its nearest neighbours. Although the pendant groups are not as close as those in the *trans-trans* form, there is still significant steric congestion, which results in

a slight dihedral twist of the phenyl group from the plane of the backbone. Hence the conjugation between the phenyl ring and the backbone is prevented. Thus, any substituent will not be conjugated with the main polymer structure and so there will be no through-bond interaction between pendant rings.

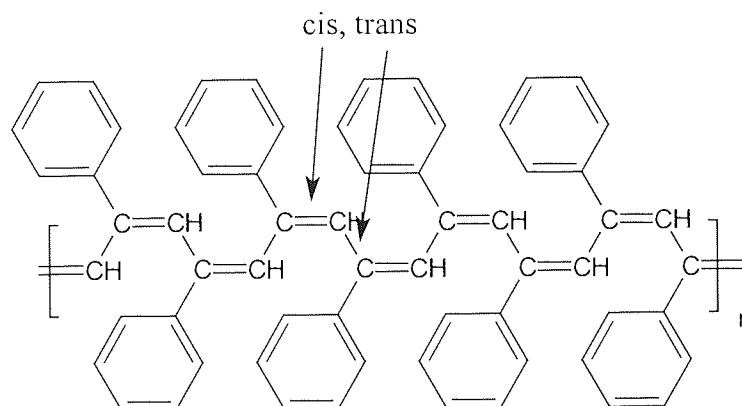


Figure 79 : The structure of *cis-trans* PPA as obtained from rhodium catalysts

4.3.2.1 Colours and solubility

The colour of *cis-trans* PPA is generally yellow, but it can be obtained as bright orange depending upon the ligands of the catalyst and the solvent system used. *Cis-trans* PPA is readily soluble in common organic solvents, such as THF or DCM, but when the phenyl ring is substituted with a functional group, solubility can be affected greatly. This is exemplified by poly(4-methoxyphenylacetylene) which is soluble in common solvents, whereas poly(4-methylphenylacetylene) is insoluble in all common organic solvents. The most common monomers which produce soluble polymers are listed in Table 4, and those generating partially soluble or insoluble polymers are shown in Table 5.

Table 4 : Soluble derviatives of polyphenylacetylene

Substituent
3-methoxy ¹⁰⁴
3-methyl ester ¹⁰⁴
4-chloro ¹¹³
4-methoxy ¹⁰⁴
4-methyl ester ¹⁰⁴
4-methyl ketone ¹¹³

Table 5 : Insoluble derivatives of polyphenylacetylene

Substituent
3-amino ⁸⁰
4-amino ⁸⁰
4-cyano ¹¹³
4-dimethylamino ⁸⁰
4-ethynylpyridine ⁸⁰
4-methyl ¹⁰³
4-nitro ¹¹³

Although there is no clear pattern of solubility, it is reasonable to suggest that polymers bearing a highly polar functional group will tend to be insoluble, whereas those possessing a flexible, less polar, substituent tend to be more soluble.

It should also be noted that the nature of the substituent group also affects the colour of the polymer; highly polar substituent groups, such as nitro or amino, are brown rather than yellow polymers. There is no satisfactory explanation available to account for this.

4.3.2.2 Characterisation

Cis-trans PPA is highly stereoregular, when synthesised by rhodium catalysts, and the polymer gives a well defined ^1H NMR spectrum allowing easy characterisation. Some broadening can occur, and this is usually a function of the solvent system used during synthesis. It has also been reported that broadening can occur when the polymer is repeatedly dissolved in a solvent and then precipitated in methanol¹⁰¹. This was attributed to a relaxing of strain, giving rise to more disorder in the polymer structure.

4.3.2.3 Crystallisation of *cis-trans* to give *cis-cis* polyphenylacetylene

Cis-trans PPAs are amorphous materials when first made and they are generally soluble in common organic solvents. Some polymers that possess a rigid, or a highly polar ring substituent can be insoluble. These insoluble polymers can sometimes undergo a colour change upon exposure to conventional solvents. This is exemplified by the change from yellow to red for the insoluble *p*-CH₃ PPA when it was immersed in either chloroform or toluene¹⁰³. The red form of this material was found to be 75-80% crystalline by X-ray analysis. It is thought that this red material is the “*cis-cis*” form of polyphenylacetylene, although the nature of this solvent induced change was unaccounted for. The *cis-cis* form of PPA is shown in Figure 80. The stereochemistry about the carbon-carbon double bond is that of a *cis* configuration, and that of the carbon-carbon single bond is also in the *cis* configuration. This backbone configuration gives rise to a helix type structure. If the intramolecular pitch distance is very short then solvent molecules could be excluded from penetrating the backbone and thus result in an insoluble material.

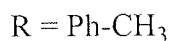
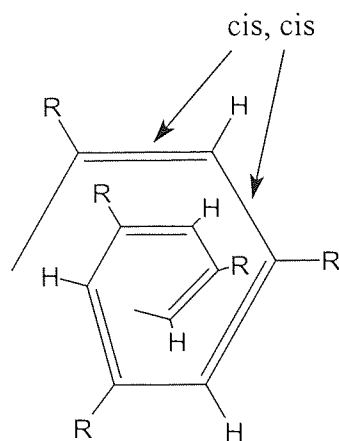
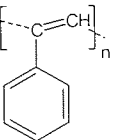
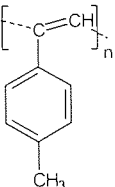
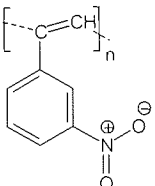
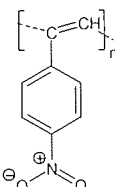


Figure 80 : The *cis-cis* form of polyphenylacetylene

4.4 Introduction to the results

The living catalyst $[\text{Rh}(\text{NBD})(\text{OCH}_3)]_2$ was first considered as a suitable catalyst in this project, because it was known to produce good yields of polymer and exhibited excellent control of molecular weight. This was the first catalyst system to be tested, and it was found to be successful for the polymerisation of phenylacetylene, as shown in Table 6. However, this system possessed one major flaw, it did not catalyse the polymerisation of 4-nitrophenylacetylene. This was an important point because the presence of nitro groups is essential for use in co-polyradical work. The fact that 3-nitrophenylacetylene was found to polymerise in 97% yield suggests that the nitro group in the para position has a deactivating influence on the alkyne. This theory led to the investigation of the effects of ring substituents on the alkyne, refer to Chapter 5. The incompatibility of 4-nitrophenylacetylene with this catalyst was not investigated further. A new catalyst that had more tolerance towards functional groups was sought.

Table 6 : Results using $[\text{Rh}(\text{NBD})(\text{OCH}_3)_2]$

Derivative	Structure	Code	% Yield	Soluble in
N/A		PEB791	98 *	DCM, THF
4-methyl		PEB796	98	N/A
3-nitro		PEB792	97%	N/A
4-nitro		PEB864	0 *	N/A

(* = performed in duplicate)

4.4.1 Design of a new catalyst

From the literature review it became apparent that none of the catalysts fitted the requirements necessary for the synthesis of polymers containing nitro groups. The characteristics of the ideal catalyst were as follows:-

1. it must give good yields of polymer (>70%).
2. the polymers obtained should be of moderate to high molecular weight.
3. it does not require the use of triethylamine, because nitronyl nitroxide stable radicals degrade in this solvent.
4. it should tolerate a wide range of functional groups, including nitronyl nitroxide.
5. polymerisation should be possible preferably at ambient temperature.

Metathesis catalysts are intolerant of functional groups, such as nitro, which precludes their use in this project. Rhodium catalysts are superior in this respect, but the solvents/conditions employed in most of these systems are unsuitable for nitronyl nitroxide radicals, e.g. an amine solvent. The catalyst that best fitted the requirements of this work was that employed by Fujii, $\text{Rh}(\text{COD})(\text{NH}_3)\text{Cl}$, as this was tolerant of nitronyl nitroxide groups. This catalyst requires ethanol and ambient temperatures for polymerisation, which is ideal for this work. However, the yield of polymer obtained from this catalyst was too low (42%) to warrant its use in the synthesis of co-polyradicals, the target of this research.

With no suitable catalyst available from the literature, it was therefore necessary to develop one that would fulfil the requirements of this project.

There are three important factors in the chemistry of the rhodium catalysts under consideration, the diene ligand, the donor ligand, and the solvent. It was noted from a review of the literature that the NBD diene gives a better yield, molecular weight, and polydispersity of polymer compared to the equivalent COD. Better tolerance of nitronyl nitroxides could be obtained by changing the ligand from the standard chloro to an ammonia ligand. It was also noted that the rhodium complex that employed an ammonia ligand could operate in ethanol, avoiding the use of triethylamine. It was envisaged that a rhodium catalyst bearing these attributes would give good yields and good tolerance.

The novel catalyst $\text{Rh}(\text{NBD})(\text{NH}_3)\text{Cl}$, shown in Figure 81, was synthesised by a modification of the literature procedure¹¹⁴ and hereafter will be referred to as MCAT.

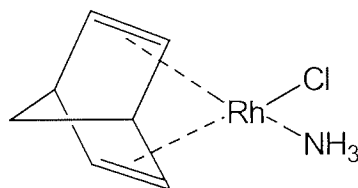
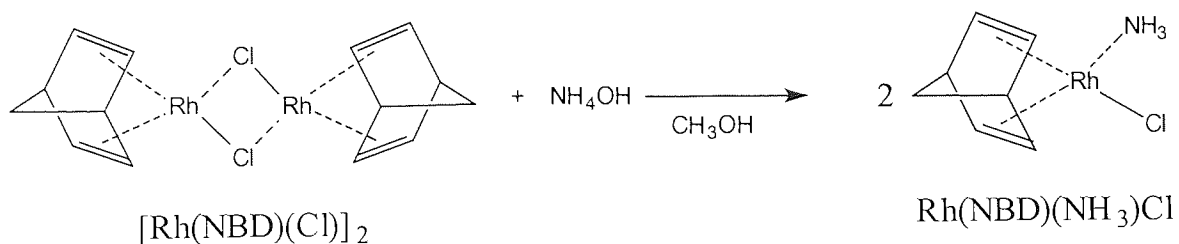


Figure 81 : Structure of novel catalyst $\text{Rh}(\text{NBD})(\text{NH}_3)\text{Cl}$ - (MCAT)

4.4.2 Synthesis of novel catalyst Rh(NBD)(NH₃)Cl - (MCAT)



Scheme 32 : Synthesis of novel catalyst for the polymerisation of phenylacetylenes, Rh(NBD)(NH₃)Cl - (MCAT)

To a suspension of [Rh(NBD)Cl]₂ 0.25g (0.55mmol) in 40mL of degassed methanol was added ammonium hydroxide (0.3mL). The suspension was stirred vigorously until the solid had dissolved, giving a yellow solution. This yellow solution was then filtered and concentrated using a rotary evaporator. A yellow powder was precipitated upon addition of this concentrated solution to ethanol (50mL). The yellow suspension was filtered, and the yellow powder obtained was dried in a vacuum oven, to give 0.12g (0.49mmol) of Rh(NBD)(NH₃)Cl. The overall yield was 45%.

Analytical data for Rh(NBD)(NH₃)Cl : λ_{max} (acetone)/nm 395; (Found: C, 33.67; H, 4.37; N, 4.58. C₇H₁₁ClNRh requires C, 33.97; H, 4.48; N, 5.66); δ_{H} (300 MHz; acetone-*d*₆ and DMSO-*d*₆) the spectrum showed many broad lines which made characterisation difficult, as shown in Figure 82.

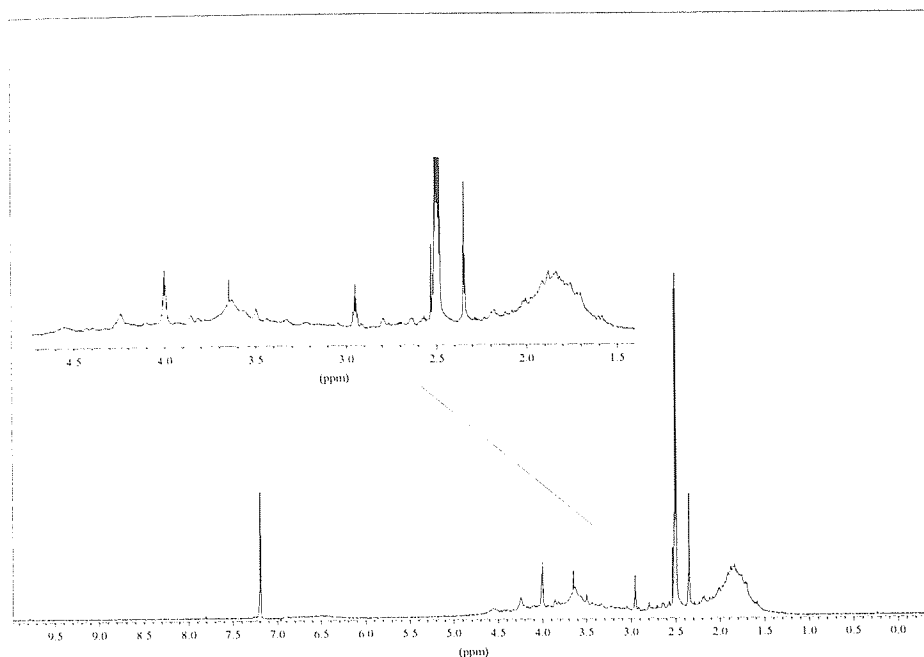


Figure 82 : ^1H NMR spectrum of polymerisation catalyst $\text{Rh}(\text{NBD})(\text{NH}_3)\text{Cl}$ - (MCAT)

MCAT is fully soluble in ethanol, but only partially soluble in THF. Characterisation of MCAT by ^1H NMR proved fruitless, as the spectrum consisted of broad lines. The only successful analytical technique was elemental analysis, but this revealed that the quantity of nitrogen was inconsistent with that of a pure compound. Hence, MCAT was impure. This considered, it remained a viable proposition for the polymerisation of phenylacetylene derivatives, and would represent a significant advance if successful.

4.4.3 Use of the novel catalyst MCAT

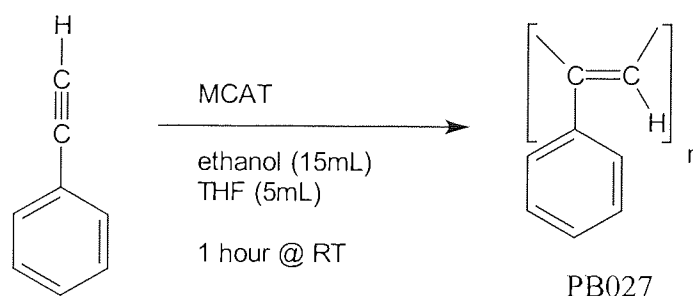
Before any novel polymers could be prepared it was essential to test MCAT with phenylacetylene, and some simple derivatives, to determine the conditions and solvent system that would best suit this catalyst.

4.4.3.1 Solvents and conditions employed

Ethanol was the ideal choice of solvent, because it dissolved MCAT completely to give a yellow solution. However, monomers possessing nitronyl nitroxide are only partially soluble in pure ethanol, so the polarity of the solvent had to be reduced by the use of THF as co-solvent. It was found that ethanol:THF (3:1) was the ideal mixture, because nitronyl nitroxide monomers, and most other types of monomer were soluble in the system. MCAT was also soluble in this system.

The possibility that water could act as a co-catalyst could not be discounted, so to minimise this possibility the polymerisation was conducted under an inert atmosphere. The polymerisation time was initially set at 1 hour, although this could be altered if the yield of polymer was low. Polymerisation was carried out at room temperature using a monomer:MCAT ratio of approximately 100:1.

4.5 Example synthesis of polyphenylacetylene using MCAT (PB027)



Scheme 33 : Synthesis of a polyphenylacetylene (PB027)

All equipment was oven dried at 100°C for 12 hours before use. To a 2 neck 100mL RBF was added $\text{Rh}(\text{NBD})(\text{NH}_3)\text{Cl}$ 0.005g, and a magnetic stirrer bar. The side-neck was plugged using a Suba-Seal cap. The RBF was attached to, and evacuated, using the vacuum line. Once evacuated, the vacuum line and RBF were flushed with argon. Super-dry ethanol, 10mL, was admitted through the Suba-Seal cap using a syringe. The catalyst solution was stirred for 15 minutes at RT, to give a yellow solution. Closing the appropriate tap on the vacuum line isolated the RBF. The vacuum line was then re-evacuated.

A fresh solution of Rh(NBD)(NH₃)Cl catalyst was prepared for each polymerisation reaction, although this can lead to inaccuracies owing to the very small amount of rhodium catalyst used. This may have been overcome by making an ethanolic stock solution of the catalyst. However, dry ethanol is very hygroscopic and difficult to store for a length of time. To minimise the water content of the polymerisation, the solution of catalyst was always freshly prepared.

The side-neck of a two-neck RBF was plugged using a Suba-Seal cap and attached to the manifold of a vacuum line. Having evacuated the RBF and flushed it with argon, phenylacetylene 0.30g (2.94mmol) and ethanol (5mL) were administered via a syringe. Freshly distilled dry THF (5mL) was administered in the same manner. The solution of monomer was repeatedly taken up in a syringe and expelled to facilitate mixing.

The solution of monomer was drawn up into a syringe, and the appropriate tap was closed to eliminate the now redundant flask. The isolator tap of the catalyst flask was opened to the argon supply to prevent pressure build-up, and the solution of monomer injected. The polymerisation mixture was stirred vigorously. Immediately, the colour became a darker yellow, and after 2 minutes cloudiness had begun to develop. A yellow precipitate had formed after 5 minutes. After 1 hour, the yellow suspension was added to 100mL of methanol, to aid precipitation. Filtration of the fine yellow suspension gave PB027 as a yellow/orange solid, which was dried in a vacuum oven for 6 hours at 40°C. PB027 was obtained as a yellow/orange solid, 0.25g, 83% (compared to mass of monomer), and was soluble in DCM, and THF. The polymer PB027 was characterised by UV, IR, NMR (Figure 83 and Figure 84), and SEC (Figure 85).

Analytical data for PB027 : λ_{max} (CHCl₃)/nm 460; ν_{max} /cm⁻¹ 3051 (w, sharp, Ph), 1595 (w, sharp, Ph), 1488 (m, sharp, Ph), 1442 (m, sharp, unassigned); δ_{H} (300 MHz; CDCl₃) 6.96-6.94 (3 H, split singlet, Ph), 6.65-6.63 (2 H, split singlet, Ph), 5.85 (1 H, s, -C=CH-); δ_{C} (75 MHz; CDCl₃) 142.84 (Ph), 139.24 (Ph), 131.81 (=CH-), 127.76 (Ph), 127.52 (Ph), 126.68 (Ph); SEC (Mw = 200,500 ; Mn = 37,200 ; Pd = 5.4).

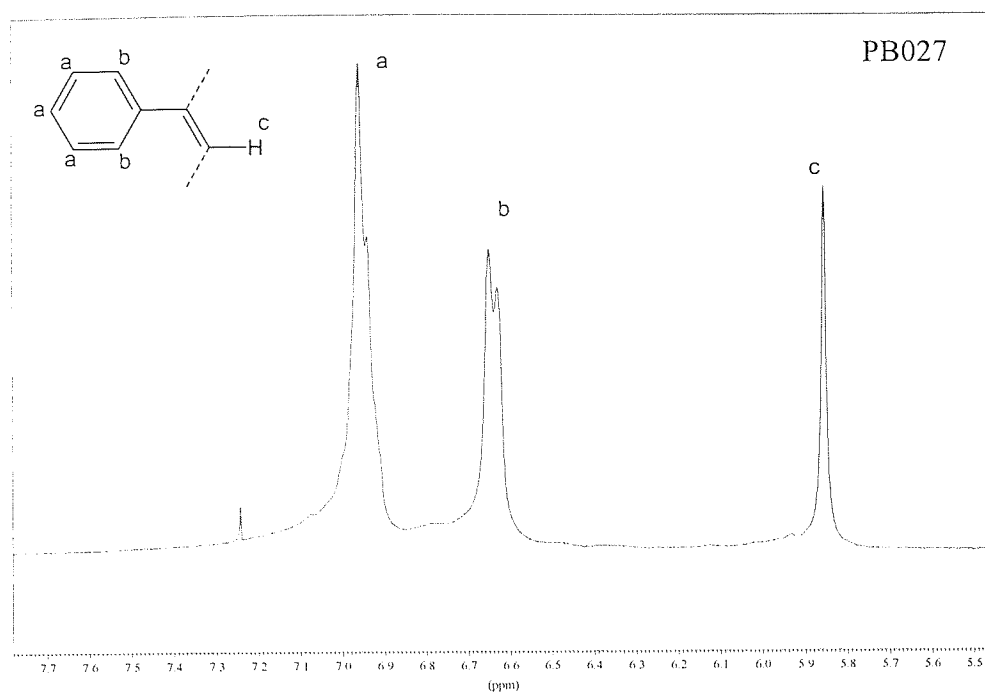


Figure 83 : ^1H NMR of polyphenylacetylene obtained using MCAT - (PB027)

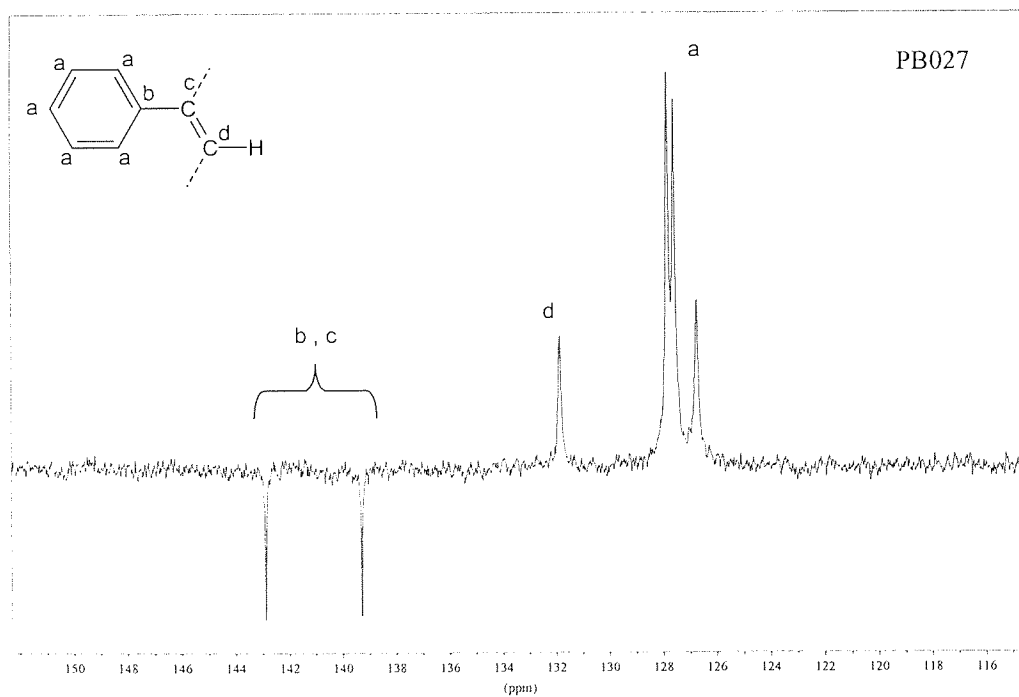


Figure 84 : ^{13}C NMR of polyphenylacetylene obtained using MCAT - (PB027)

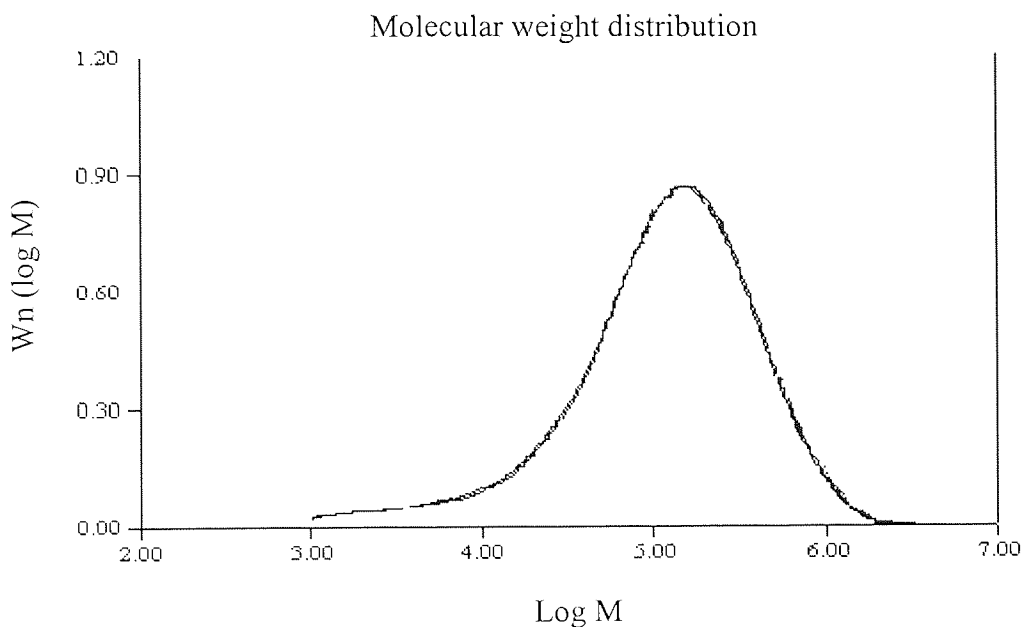


Figure 85 : SEC analysis of polyphenylacetylene - PB027

4.5.1 Interpretation and comments

IR analysis of PB027 gave only a small amount of information. It showed that there were peaks that corresponded to the phenyl group (around 1500 and 1600cm^{-1}). The peak corresponding to the alkene backbone was found at approximately 1700cm^{-1} , but this signal was difficult to identify because it was very weak. A peak corresponding to that of an alkyne (3300cm^{-1}) was absent, indicating that there was no monomer present in PB027.

The ^1H NMR shows a very sharp peak at $\delta 5.85$ corresponding to the vinyl proton of the polymer backbone. The sharpness of this peak is indicative of a highly stereoregular polymer. The chemical shift of the peak corresponds to that of a vinyl proton in the *cis* configuration, indicating that PB027 is likely to be a *cis-trans* type polyphenylacetylene. No peaks corresponding to that of NBD were found, which implies that the diene ligand is not incorporated into the polymer structure.

The polystyrene equivalent average molecular weight of PB027 was reasonably high (200500), but the polydispersity was broad. This was better than the catalyst system of $\text{Rh}(\text{COD})(\text{NH}_3)\text{Cl}$ in water¹⁰⁶, which was reported to give an average molecular weight of only 23300. It can also be compared with the average molecular weight reported for the

[Rh(NBD)Cl]₂/TEA system¹¹, which can reach values in excess of 10⁶. The broad polydispersity of PB027 could be the result from impure MCAT, which may contain more than one initiation species. It is important to note that molecular weight determination of polyphenylacetylenes by SEC should only be used as a guide because of the difference in hydrodynamic volume between it and polystyrene, on which the calibration is usually based. The chromatogram also shows that no oligomeric or other low molecular weight species are formed during polymerisation.

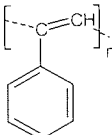
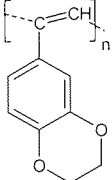
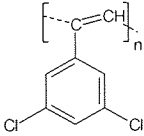
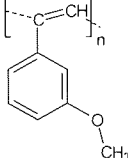
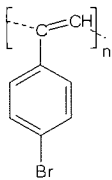
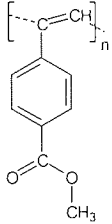
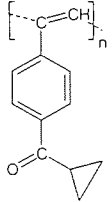
The yield of PB027 obtained was good (83%), but it is lower than that obtained using TEA or Kishimoto's "living" catalyst system which can produce yields in excess of 98%. This result showed that the catalyst/conditions employed can be considered to be successful for the polymerisation of phenylacetylene. This lower yield could be attributed to an impurity in the monomer, or that the time of polymerisation was too short.

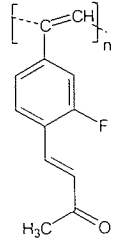
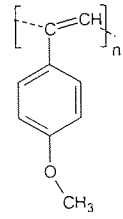
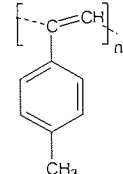
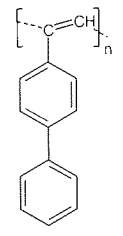
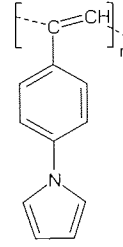
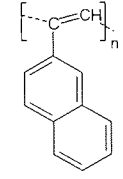
No firm conclusion about the efficiency of MCAT could be rationalised from this one result, so some simple derivatives of phenylacetylene were also polymerised.

4.6 Polymerisation of some simple derivatives of phenylacetylene

Some simple derivatives of phenylacetylene were polymerised using MCAT, e.g. monomers containing 4-methyl, 4-methyl ester, 4-methoxy, and 3-methoxy groups. These monomers were chosen so that comparisons could be made between the MCAT catalyst and those known in the literature. Using monomers bearing more unusual functional groups, such as ethylenedioxy, a conjugated ketone, or a pyrrole ring, the scope of the polymerisation was extended further. The results of these polymerisations are summarised in Table 7.

Table 7 : Results of the polymerisation of some simple derivatives of phenylacetylene

Derivative	Structure	Mw	Code	Colour	% Yield	Soluble in	Insol in
N/A		200,000	PB027	Y	83	DCM, THF	N/A
3,4-ethylenedioxy		N/A	PB031	Y/O	40	N/A	All tested
3,5-dichloro		N/A	PEB992	Y/O	94	DCM ^p	THF
3-methoxy ¹¹⁵		213,000	PB035	Y	70 ^l	DCM, THF	N/A
4-bromo		N/A	PB017	Y/O	91 *	N/A	All tested
4-ester (methyl) ¹¹⁶		248,000	PEB988	Y/O	98	DCM, THF	N/A
4-ketone (cyclopropyl)		N/A	PB024	Y/O	97 *	DCM, THF ^p	N/A

4-ketone, and 3-fluoro		N/A	PB026	Red	98	N/A	All tested
4-methoxy ¹¹⁵		214,000	PB033	Y/O	91	DCM ^w , THF ^w	
4-methyl ¹¹³		N/A	PB008	O	94 *	THF ^p	N/A
4-phenyl		N/A	PEB985	O	92 *	N/A	All tested
4-pyrrole		N/A	PB057	Y/O	86	N/A	All tested
Naphthalene		N/A	PB044	Y/O	68	N/A	All tested

(* = average of two polymerisation; ^l = incomplete precipitation; ^p = partial solubility; ^w = warming required)

4.6.1 Characterisation and interpretation

Only the polymers bearing a 3-methoxy, a 4-methoxy, or a 4-methyl ester group were found to be soluble in common organic solvents. The insoluble polymers PB008 (4-methyl) and PB044 (2-ethynylnaphthalene) were found to change colour from yellow to red upon exposure to chloroform or toluene. These changes of colour are usually associated with the formation of a crystalline material (red) from an amorphous one (yellow). Normally, polyphenylacetylenes are yellow when isolated from the catalyst solution, but in the case of the conjugated ketone derivative (PB026) the polymer was already red. This implies that a crystalline morphology is very favourable for this polymer.

Most of these polymers were obtained in near quantitative yields, which were as good as those reported using Kishimoto's "living" catalyst and $[\text{Rh}(\text{NBD})(\text{Cl})]_2/\text{TEA}$. The yield of the 3-methoxy derivative (PB035) was lower because of difficulties encountered during filtration of the polymer suspension. Another polymerisation that gave a low yield was that of the ethylenedioxy derivative PB031 (40%). The poor yield of this polymer could be attributed to either a lower affinity of the catalyst towards this monomer, or to an impurity in the monomer compound. However, NMR analysis of the monomer found no evidence of impurities.

The average molecular weights of all of these polymers were approximately in the range of 200,000 to 248,000 as determined by SEC. The electron donating/withdrawing nature of the substituent group did not significantly affect the molecular weight of the polymer. This suggests that the average molecular weight of the polymer is a function of the catalyst and/or conditions employed, and not that of the monomer.

^1H NMR analysis was used to probe the stereochemistry of the soluble polymers. An example spectrum of the polymer PB024 is shown in Figure 86. A sharp peak (approximately $\delta 6\text{ppm}$) corresponding to that of the vinyl proton is found in all instances. This indicates that the *cis-trans* structure of the polymers is not markedly influenced by the presence of ring substituents.

These polymerisations showed that MCAT is able to tolerate halides (Br, Cl, and F), carbon-carbon double bonds, ketone, and conjugated ketone groups.

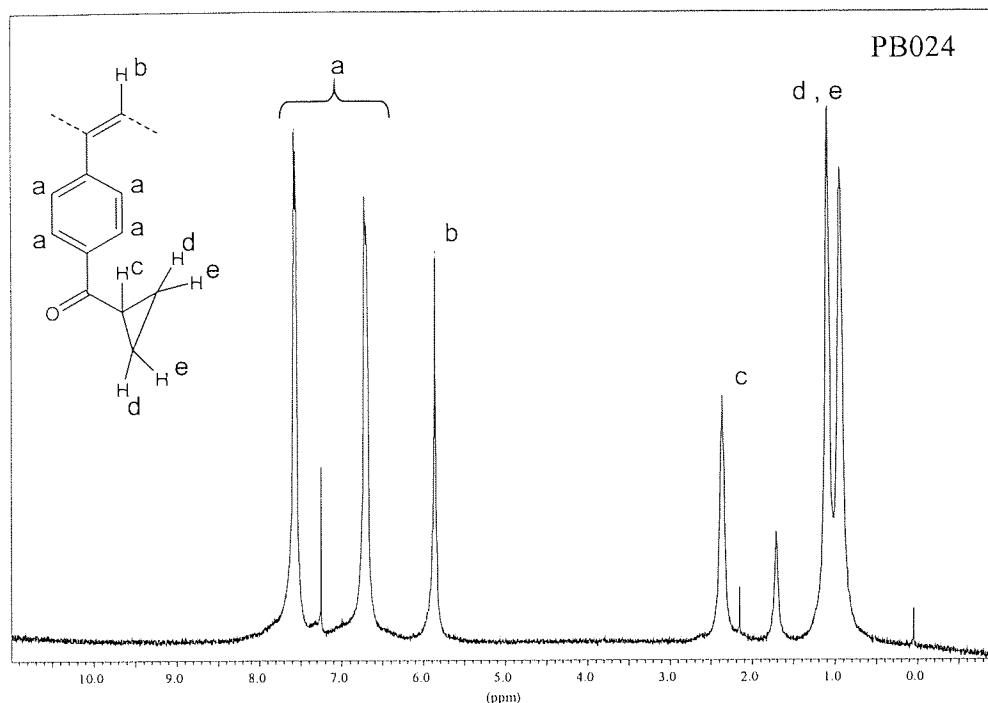


Figure 86 : ^1H NMR of polyphenylacetylene bearing a cyclopropyl-ketone group (PB024)

4.6.2 Line broadening in the ^1H NMR of poly(4-methoxyphenylacetylene)

The ^1H NMR of poly(4-methoxyphenylacetylene) (PB033) was unusual because the peaks were broad, particularly at the base of the peak, as shown in Figure 87. From the literature, this is attributed either to the formation of a paramagnetic radical species, or to an inhomogeneous polymer structure. The latter is the more likely explanation, as a similar spectrum was obtained using $\text{Rh}(\text{NBD})\text{Cl}_2/\text{benzene}$ and the line broadening was attributed to the incorporation of *trans* sequences in the polymer backbone¹¹¹.

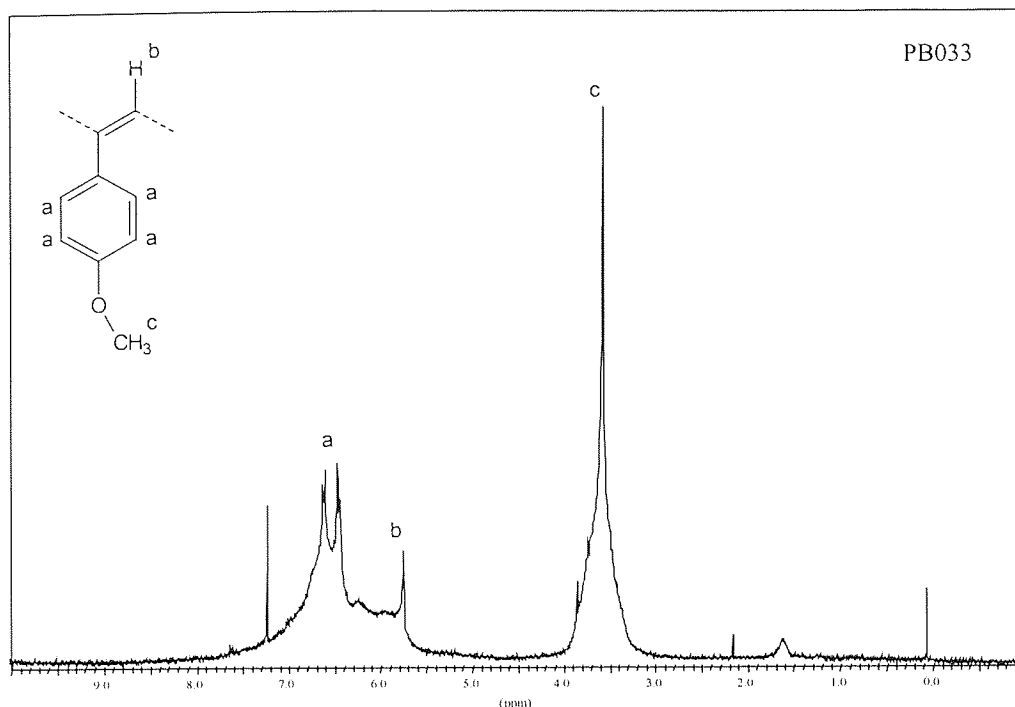


Figure 87 : Example of line broadening in the ^1H NMR of 4-(methoxy)phenylacetylene – PB033

4.6.3 Poly 1-(4-ethynylphenyl)pyrrole : A polymer exhibiting changes of colour in different solvents

MCAT is also able to polymerise N-substituted pyrroles in excellent yield, as shown by the polymer PB057. Interestingly however, the colour of the polymer was found to change when exposed to different solvents.

This polymer PB057 was first obtained as a yellow/orange solid (from ethanol/THF). On exposure to THF, the solid remained insoluble, but immediately changed to red. This was not specific to THF, but was also found to occur in benzene, toluene, and DMF. By itself this was not of great significance, until a fresh sample was exposed to DCM. The solid remained insoluble, but instantly changed to black. A black insoluble solid was also obtained from exposure to CHCl_3 .

To ascertain if these changes are reversible a simple experiment was performed. PB057 was pre-treated in THF to give a red product, which was then exposed to DCM whereupon it became black instantly. The black solid was re-exposed to THF, but the black colour remained. A diagram of these colour changes is shown in Figure 88.

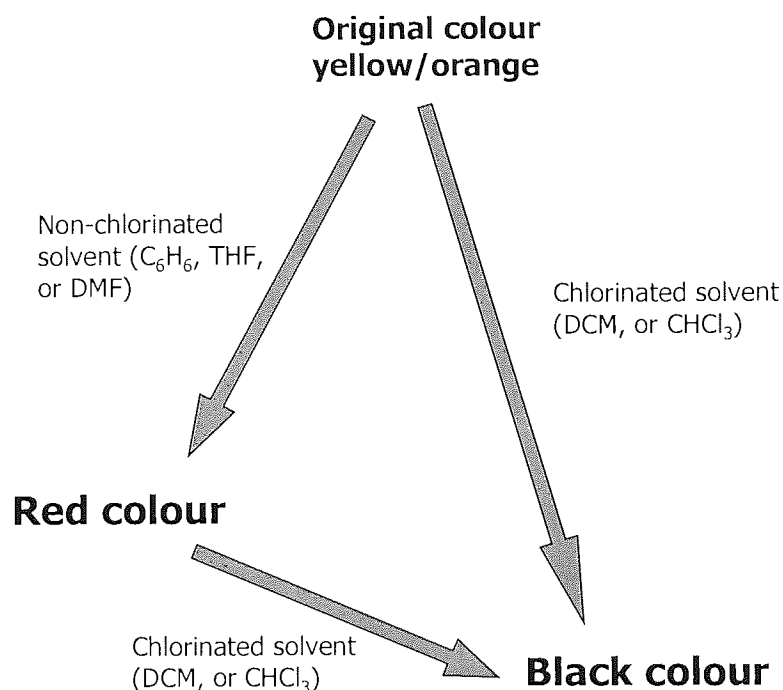


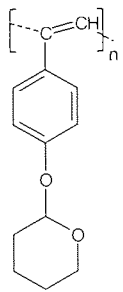
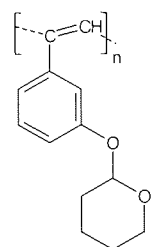
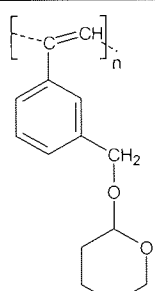
Figure 88 : Colour changes of poly 1-(4-ethynylphenyl)pyrrole (PB057)

It is reasonable to assume that a structural change occurs from amorphous to crystalline in PB057 when exposed to non-chlorinated solvents. In chlorinated solvents, the polymer changes to black. There are no reports of such phenomena in the literature, but it is reasonable to assume that a solvation of the polymer occurs.

4.7 Synthesis of polymers bearing a THP group

The presence of a hydroxyl functional group is highly desirable for its ability to act as a bridging group in organic radicals³². However, during monomer synthesis it was found that 4-hydroxyphenylacetylene was unstable, and underwent autopolymerisation. In an attempt to obtain hydroxyl functionalised polymers, monomers that possessed a THP group were synthesised. The polymerisation of these monomers is now reported, as shown in Table 8.

Table 8 : Summary of polymers containing a THP group

Derivative	Structure	Mw	Code	Colour	% Yield	Soluble in	Insol in
THP ether		255,500	PB013	O	87	DCM, THF ^P	
THP ether		232,500	PB038	O	92	DCM, THF	
THP ether		202,000	PB059	Y/O	43 ^I	DCM, THF	

(^I = incomplete precipitation during synthesis; ^P = partially soluble)

4.7.1 Characterisation of THP derivatives

These polymers were obtained in excellent yield, except PB059, which was assumed to possess an impurity, although none was found by NMR analysis.

Excellent solubility of these polymers was found in common organic solvents, such as DCM or THF. SEC analyses showed that the average molecular weights were very similar to those obtained for other derivatives (200,000 to 255,500). This indicates that the THP group did not poison the catalyst or interfere with the polymerisation mechanism. An example ¹H NMR spectrum of polymer PB038 is shown in Figure 89. Interpretation of this spectrum was difficult, because the peaks were broad and tended to overlap, which

resulted in unidentifiable multiplets. As noted before, this broadening can result from structural irregularities, such as the incorporation of some *trans* sequences into the backbone.

Time did not allow these polymers to be deprotected to their corresponding hydroxyl functions.

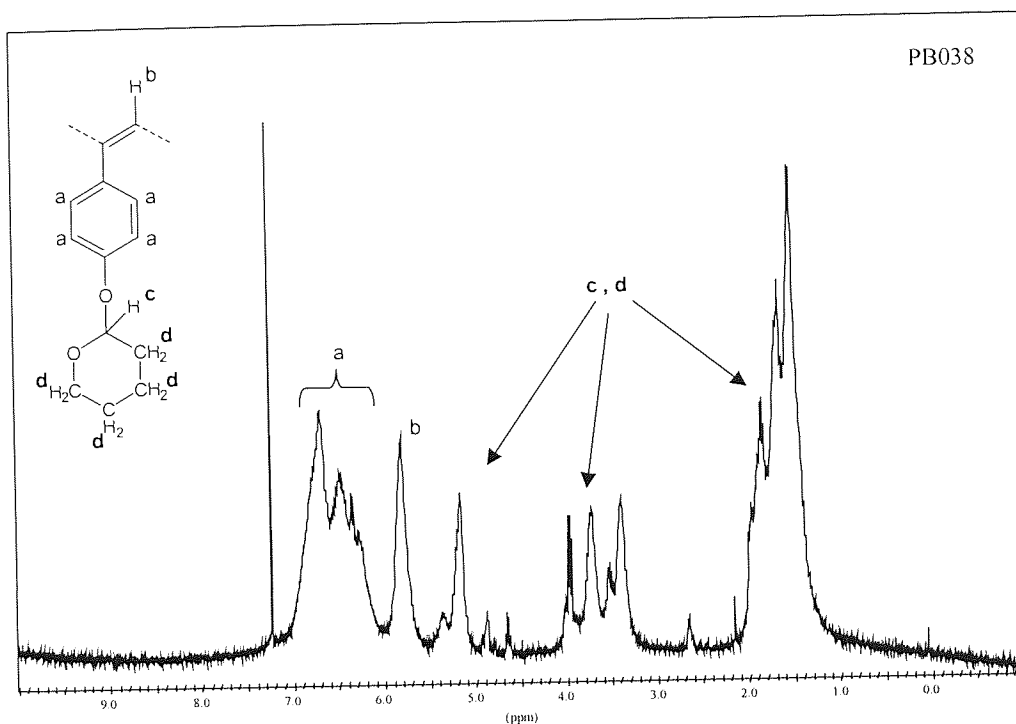
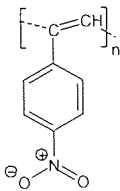
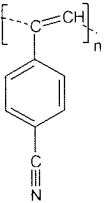
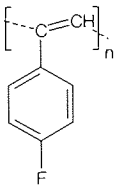


Figure 89 : ^1H NMR of a polymer bearing a THP group - (PB038)

4.8 Synthesis of polymers bearing a bridging group

Before co-polyradicals were synthesised, it was necessary to determine the tolerance of MCAT towards “bridging groups”. Monomers bearing a nitro, cyano, or a fluoro group were polymerised using MCAT using the conditions designated previously for PB027. A summary of these polymerisations is shown in Table 9.

Table 9 : Summary of polymers containing bridging groups

Derivative	Structure	Mw	Code	Colour	% Yield	Soluble in	Insol in
Nitro ¹⁰²		N/A	PB036	Brown	76	N/A	All tested
Cyano ¹¹³		N/A	PEB956	Brown	25 *	DMF	All else
Fluoro		201,000	PB049	Y	95	DCM, THF	

(* = average of two polymerisations)

Poly(4-nitrophenylacetylene) (PB036) was obtained as a brown solid, in good yield. It was completely insoluble in all solvents tested, including warm nitrobenzene and warm DMSO. This is consistent with that reported by Furlani, but a higher yield was reported for the $[\text{Rh}(\text{COD})\text{Cl}]_2/\text{NaOH}$ catalyst system using reflux conditions for 3 days¹⁰². It is likely that allowing a longer time of polymerisation could have increased the yield obtained in this work.

The polymer poly(4-cyanophenylacetylene) (PEB956) was also obtained as a brown solid, which exhibited partial solubility in hot DMF. There has been only one reported successful synthesis of this polymer¹¹³. This is probably because, as found in this work, that the yield of polymer obtained is very low, approximately 25%. To verify this result, the synthesis of PEB956 was repeated, and the yield was found to be almost identical. The monomer was analysed by NMR, MS, and IR but no impurities were found. It was unlikely therefore, that an impure monomer was the reason for the low yield of polymer. The low yield of polymer may be explained by considering that the triple bond of the

cyano group may coordinate to the rhodium centre, in a similar way to that of an alkyne, as shown in Figure 90. Once coordinated, the normal mechanism of polymerisation cannot ensue because of the lack of a terminal hydrogen (refer to the mechanism of polymerisation Scheme 26). This would result in the active site of the catalyst becoming blocked, and polymerisation would stop. The cyano group may therefore act as a poison for the catalyst.

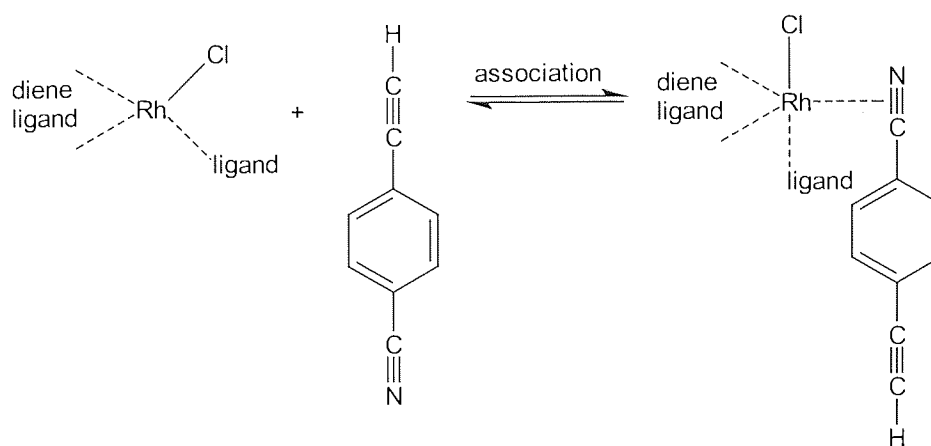


Figure 90 : "Poisoning" effect of the cyano group

The fluorine containing monomer was expected to give an insoluble polymer, because of solubility problems previously encountered in this work with other polymers bearing halide groups. Surprisingly, poly(4-fluorophenylacetylene) (PB049) was found to be fully soluble in DCM or THF. This suggests that the size of the halogen has a large influence on the solubility, where the smallest halide is the most soluble. The electronegativity of the halogen is not of marked importance.

The polystyrene equivalent Mw of PB049 was 201,000, which is the same as most of the polymers synthesised using MCAT. The polydispersity was found to be very broad, with a value of 11. It was impossible to ascertain whether the polymer was that of a stereoregular *cis-trans* type, because the ^1H NMR showed very broad peaks (Figure 91). This broadening probably originates from those reasons discussed previously for poly(4-methoxyphenylacetylene), namely a structural disorder of the polymer backbone.

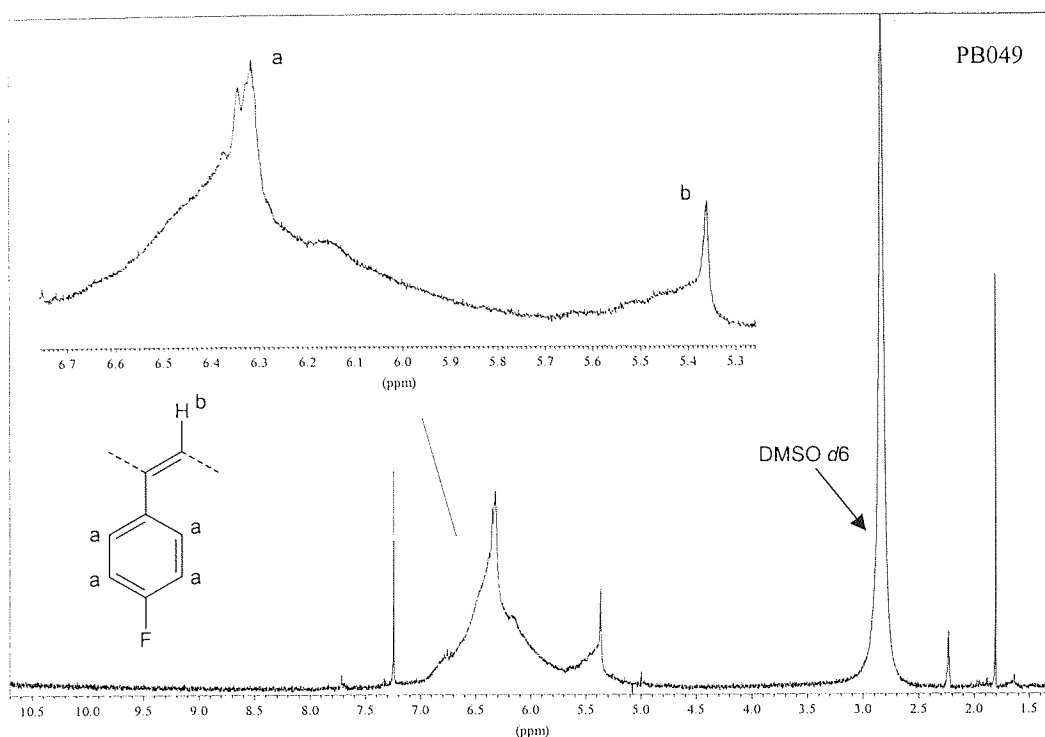


Figure 91 : ^1H NMR of poly(4-fluorophenylacetylene)

4.9 Enhancement of polymer yield

The phenyl boronic acid group was found to act as a “bridging group” in the literature⁴⁶, so it was desirable to integrate this moiety into a monomer. A phenylacetylene monomer bearing this group would have been difficult to synthesise because boronic acid groups are well known to react under the conditions of Sonogashira coupling¹¹⁷. However, it was envisaged that a homopolymer of a nitronyl nitroxide could be synthesised in the presence of BBA to give a polyradical that was doped with a “bridging” molecule. Before this synthesis was attempted it was essential to test whether MCAT would be tolerant of BBA. Firstly, phenylacetylene was polymerised in the presence of BBA using an approximate ratio of phenylacetylene:BBA:MCAT (100:20:1), in the conventional EtOH/THF (3:1) mixture.

4.9.1 Synthesis of polyphenylacetylene in the presence of BBA

The experimental procedure was carried out in exactly the same manner as that described previously for in section 4.5 but BBA 0.10g (0.82mmol) was added to the solution of monomer prior to mixing with the catalyst. The yield of polymer PB047 was 95%.

Analytical data for PB047; $\lambda_{\max}(\text{DCM})/\text{nm}$ 440; $\nu_{\max}/\text{cm}^{-1}$ 1700 (w, sharp, $-\text{C}=\text{C}-$), 1595 (w, sharp, Ph), 1489 (m, sharp, Ph); $\delta_{\text{H}}(300 \text{ MHz}; \text{CDCl}_3)$ 6.98-6.93 (3 H, split singlet, Ph), 6.64-6.62 (2 H, split singlet, Ph), 5.84 (1 H, s, $-\text{C}=\text{CH}-$); $\delta_{\text{C}}(75 \text{ MHz}; \text{CDCl}_3)$ 142.84 (Ph), 139.26 (Ph), 131.82 ($=\text{CH}-$), 127.76 (Ph), 127.52 (Ph), 126.70 (Ph); SEC ($M_w = 117,500$; $M_n = 35,250$; $Pd = 3.3$).

4.9.2 Characterisation and interpretation of PB047

The ^1H NMR spectrum of PB047 (shown in Figure 92) was very similar to that of PPA synthesised using just MCAT (PB027), showing no signal corresponding to that of BBA. The integrated values of the ^1H NMR signals were correct for that corresponding to polyphenylacetylene only. This means that BBA was not present in the polymer obtained. The IR of PB047 was examined for the strong signal of boronic acids, which is usually around 1350cm^{-1} , but signals at this characteristic wavelength were absent. This provided additional confirmation that BBA was absent from the polymer matrix. The BBA must have been lost during synthesis/purification, probably when the precipitated polymer was washed with methanol.

The yield of polymer obtained was excellent (95%), which was considerably higher than that obtained without BBA (PB027, 83% yield). This result showed that the BBA/MCAT system can give comparable yields with that of Kishimoto's $[\text{Rh}(\text{NBD})(\text{OCH}_3)]_2$ and $[\text{Rh}(\text{NBD})\text{Cl}]_2/\text{TEA}$, both of which are renowned for their high yields (95% and greater).

Analysis of the molecular weight of PB047 showed that it was approximately half of that obtained without BBA (PB027), 117500 compared to 200500. As described previously, all the polymers synthesised without BBA had a molecular weight greater than 200,000 and this was a function of the catalyst or conditions employed. Therefore, BBA must alter the nature of the catalyst, or the conditions. Conclusions cannot be rationalised from this

data alone, and further work was beyond the scope of this project. However, some possibilities can be proposed.

Firstly, BBA may coordinate to MCAT, giving a new catalyst complex that is a more effective initiator than MCAT itself. Another possibility is that the presence of BBA increases the occurrence of transfer reactions. Both of these hypotheses would result in a reduction in molecular weight of the polymer obtained.

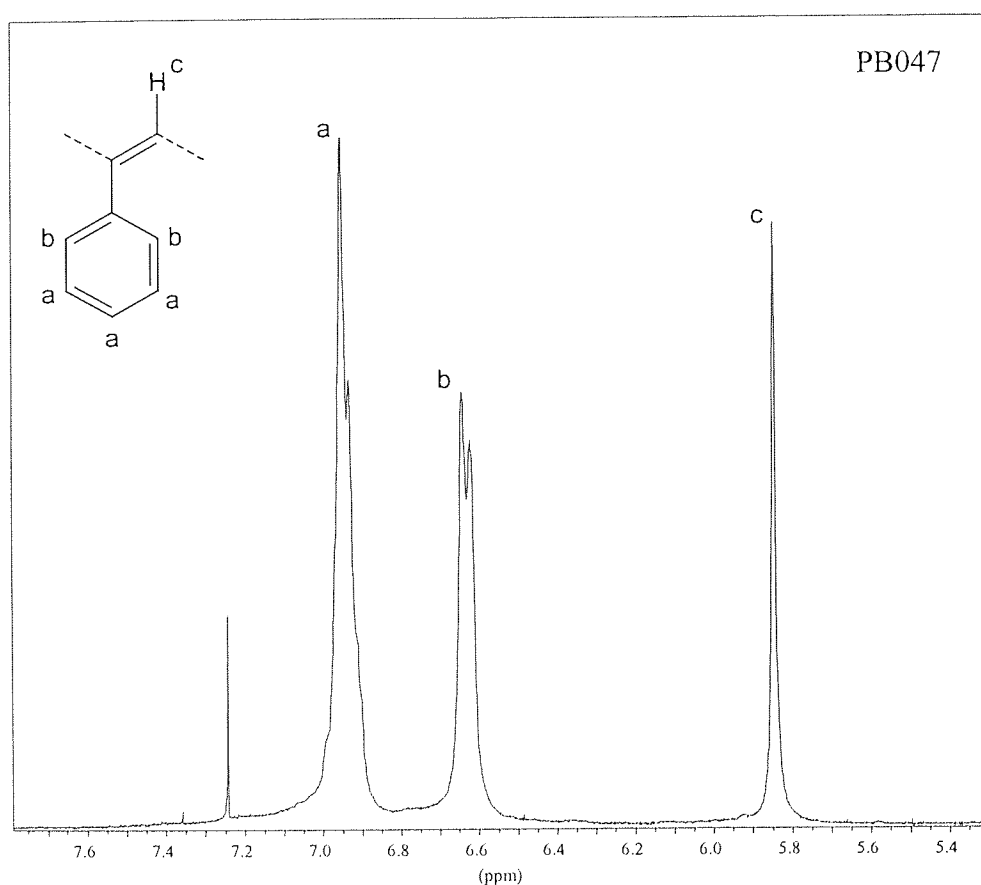


Figure 92 : ^1H NMR of PPA using BBA co-catalyst (PB047)

4.9.3 Synthesis of a polymer bearing a 2,4-dinitrophenylhydrazine group

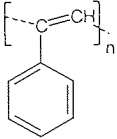
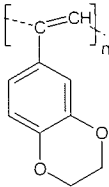
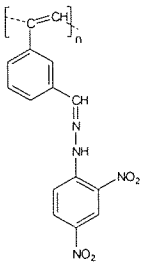
To obtain further clarification that the BBA/MCAT gave better yields than MCAT alone, it was necessary to polymerise a monomer that gave a poor yield using just MCAT. The monomer bearing an ethylenedioxy group (PB029) was selected, as the yield of polymer (PB031) obtained was particularly low when polymerised with MCAT alone. This monomer was polymerised using the BBA/MCAT to give the polymer PB054, as shown in Table 10.

The yield of polymer obtained was markedly higher (63%) than that of the original method (40%, PB031). This 23% increase in yield confirmed that enhanced yields can be obtained by the use of this BBA/MCAT system.

Furthermore, the MCAT/BBA system also proved to be moderately successful for the polymerisation of a monomer bearing a 2,4-DNP group. This group was envisaged to be difficult to polymerise because the basic nitrogen atom would be expected to block the active site of the catalyst. To effect polymerisation the solvent mixture had to be altered to EtOH/THF (1:1) because the monomer exhibited poor solubility in the conventional EtOH/THF (3:1) mixture. The polymer, PB056, was obtained as a red/brown solid, and was found to be completely insoluble in all common organic solvents tested. The monomer, however, was fully soluble in THF or DCM. Apart from the lack of solubility of PB056 there was no other indication that polymer had been formed. Elemental analysis revealed that the CHN ratio was in good agreement with theoretical calculations. The IR spectrum revealed the presence of a terminal alkyne, which corresponded to that of the monomer compound. This implied that the polymer was impure.

IR was used to examine both of these polymers (PB054, PB056), and no trace of BBA was found.

Table 10 : Summary of polymers synthesised using the BBA/MCAT system

Derivative	Structure	Mw	Code	Colour	% Yield	Soluble in	Insol in
N/A		N/A	PB047	O	95	DCM, THF	
Ethylenedioxy		N/A	PB054	Y/O	63	DCM ^{p w} , THF ^{p w}	
2,4-dinitrophenyl-hydrazine		N/A	PB056	Red/ brown	53	N/A	All tested

(^p = partial solubility; ^w = warming required)

4.10 Inhibition of polymerisation

Normally, substituent groups do not affect the yield of polymer, but an inhibition of polymerisation was found to occur with two phenylacetylene monomers, i.e. 5-ethynylpyrimidine (5EPYM) and 4-ethynylaniline (4AMPA). After evaporation, NMR and MS analysis of the polymerisation mixtures showed that only the monomer compound was present, no polymerisation had occurred. This is in agreement with that reported by Yashima⁸⁰, in which the polymer of 4AMPA was obtained in a yield of 12% only (using methanol as solvent). Furthermore, low yields of polymer were obtained using the monomer 4-pyridylacetylene, which is similar in structure to 5EPYM.

Yashima did not account for the difficulty in polymerisation of these monomers, but it can be postulated that the substituents block the active site of the catalyst. This "poisoning effect" is most likely to occur because the nitrogen atoms have an exposed lone pair of electrons, which may preferentially coordinate to the catalyst instead of the alkyne, as shown in Figure 93.

An experiment was performed with 4AMPA, in which the monomer was allowed to react with the MCAT catalyst. No solid had formed in the polymerisation mixture, indicating that polymerisation had not taken place. Phenylacetylene was added to this 4AMPA/MCAT mixture to determine if the catalyst was in some way inhibited by the presence of 4AMPA. No polymer was isolated after 1 hour, which confirms that the amine substituent was inhibiting polymerisation. This implies that the theory of a "poisoning effect" by preferential coordination of the nitrogen atom to the catalyst centre is correct.

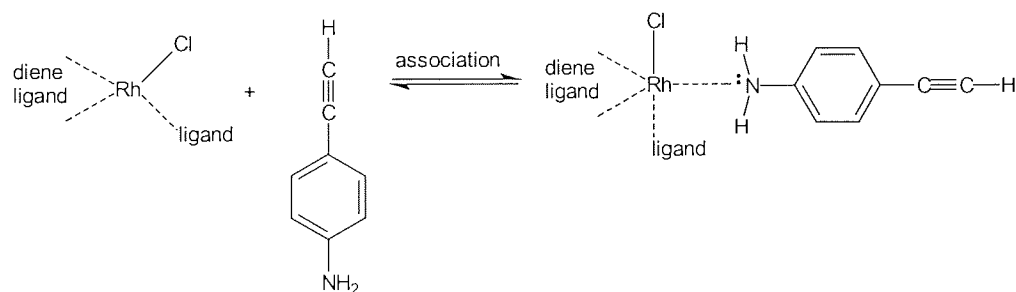


Figure 93 : Possible mechanism for the "poisoning" effect of amine groups

4.11 Summary of the novel catalyst MCAT

The catalyst system of MCAT/EtOH/THF has been shown to be very effective, with good to excellent yields, reasonable molecular weight, short polymerisation time, all at room temperature. Most functional groups can be tolerated without degradation in yield, with the exception of the cyano group. The system was capable of polymerising monomers possessing either an electron donating or an electron withdrawing group. The polymers obtained were a highly stereoregular form of the *cis-trans* polyphenylacetylene structure. Some substituent groups containing a nitrogen atom were found to inhibit polymerisation, probably by poisoning the catalyst.

Yields were markedly increased by the addition of BBA to the system, but it was not incorporated into the polymer structure. Therefore, BBA functions as a co-catalyst. The polymers were of approximately half the molecular weight compared to that obtained using MCAT only.

4.12 The synthesis of co-polyradicals

Initially, co-polyradicals were synthesised using a 1:1 ratio of 1:1 of “bridging group” to nitronyl nitroxide. This was extended in some cases to a 2:1 ratio, respectively. Generally, the co-monomers bore their substituents at the 4- position, but magnetic properties can be affected by the morphology of the polymer, as found by Swoboda⁶¹. To test this, monomers with substituents at the 3- position were also co-polymerised.

It has been shown previously that MCAT does not permit effective control of molecular weight, which implies that it is impossible to prepare block co-polymers. Therefore, the co-polyradicals obtained in this work were of the random type.

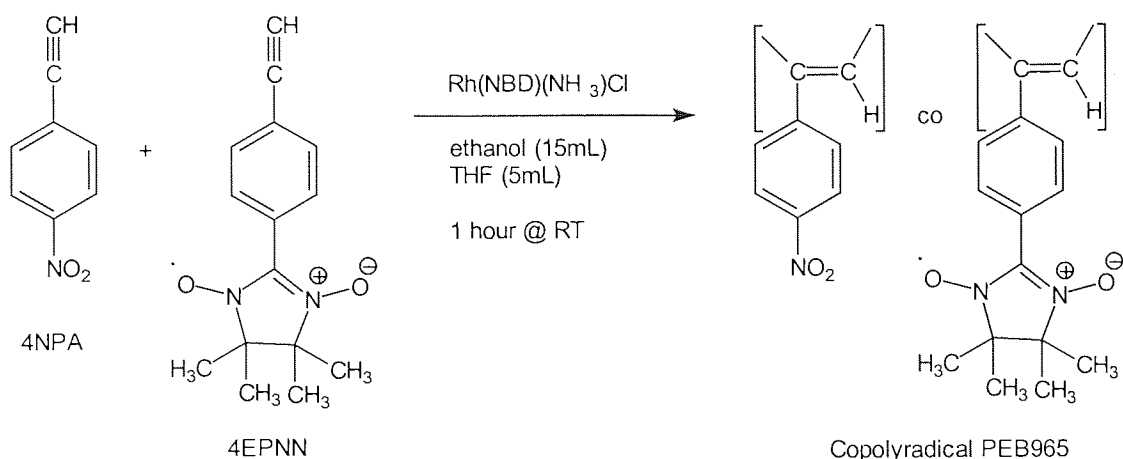
BBA was omitted from these syntheses so that any magnetic properties could be safely assigned to a function of the co-polyradical only.

4.12.1 Example synthesis of a copolyradical - poly 4NPA co 4EPNN

It was imperative that all possible sources of metal contamination, particularly nickel, were eliminated from the synthetic procedure, because traces of nickel could interfere with the estimation of magnetic behaviour. For this reason, all handling of the radical monomers and the resultant co-polyradicals was conducted using Teflon coated spatulas.

The polymerisation vessel and stirrer bar were allowed to stand in concentrated nitric acid for 1 hour, washed thoroughly with water, and then acetone. All equipment was dried overnight at 100°C prior to use. Co-polyradicals and radical monomers were stored in glass sample vials with plastic tops and seals.

An example synthesis of a co-polyradical is shown in Scheme 34.



Scheme 34 : Synthesis of a copolyradical PEB965

The monomers 4NPA 0.57g, and 4EPNN 0.10g were prepared in the monomer-RBF. The blue solution of monomers was added to the catalyst-RBF and stirred magnetically under argon. After 1 minute the polymerisation mixture became cloudy, and a green precipitate began to form. After 1 hour the green suspension was poured into methanol (100mL) to aid precipitation. This green suspension was filtered and washed twice with 15mL portions of methanol to give PEB965 as a green solid 0.13g, 83% overall yield. PEB965 was characterised using IR (Figure 94 and Figure 95), EPR (Figure 96 and Figure 97), and SQUID. The data/graphs from SQUID analysis are not shown here, as this will be described later in this report.

Analytical data for PEB965; $\nu_{\text{max}}/\text{cm}^{-1}$ 2984 (w, sharp, C-H), 1704 (w, sharp, C=C), 1593 (m, sharp, Ph), 1517 (s, sharp, Ph), 1342 (s, broad, NO₂ and overlap with nitronyl nitroxide), 1216 (w, sharp, nitronyl nitroxide), 1165 (nitronyl nitroxide), 1105 (nitronyl nitroxide); other peaks 3447 (m, broad, residual water); EPR (distorted five line spectrum); SQUID (108% spin per C₂₃H₂₂N₃O₄ formula unit – calculated by Dr A. Harrison).

4.12.1.1 Characterisation and interpretation

Usually, the most useful structural characterisation technique for polymers is NMR. The presence of a paramagnetic species, in this case a nitronyl nitroxide group, relaxes hydrogen atoms faster than normal. This results in a broadening of the NMR spectrum, and as such is of minimal use for these co-polyradicals.

Functional group identification was performed using IR, which showed peaks corresponding to the nitronyl nitroxide group. The presence of the nitronyl nitroxide group was confirmed using EPR analysis, which showed a 1:2:3:2:1 signal pattern, as shown in Figure 96. There was no evidence for the delocalisation of spin on to the aromatic ring, or polymer backbone. Hence, it can be rationalised that the nitronyl nitroxide groups are not conjugated to each other or to the “bridging groups”. This was expected, because Fujii obtained similar results for a homopolymer of PPA bearing a nitronyl nitroxide⁶². Poor conjugation is apparent because not only are the nitronyl nitroxide groups out of plane with the aromatic ring, but the aromatic ring is also out of plane with the backbone. The baseline of the EPR spectrum is slightly distorted, which could result from the poor solubility of the polyradical in DMF.

Information regarding molecular weight is not available because of the poor solubility of this co-polyradical.

It was essential to test the compatibility of nitronyl nitroxide monomers with the MCAT system because some literature catalysts/solvents are known to degrade them⁶⁰. The spin concentration per formula unit (radical monomer plus bridging monomers) of PEB965 was analysed by extrapolation of the SQUID data, which revealed that there was negligible degradation (108% spin per formula unit). The details and theory are not described in this report, but Dr Andrew Harrison, of Edinburgh University generously performed these calculations. The slight excess of spin in the polymer signifies that a greater proportion of the stable radical group is incorporated into the structure of the co-polymer in comparison to the “bridging group” monomer.

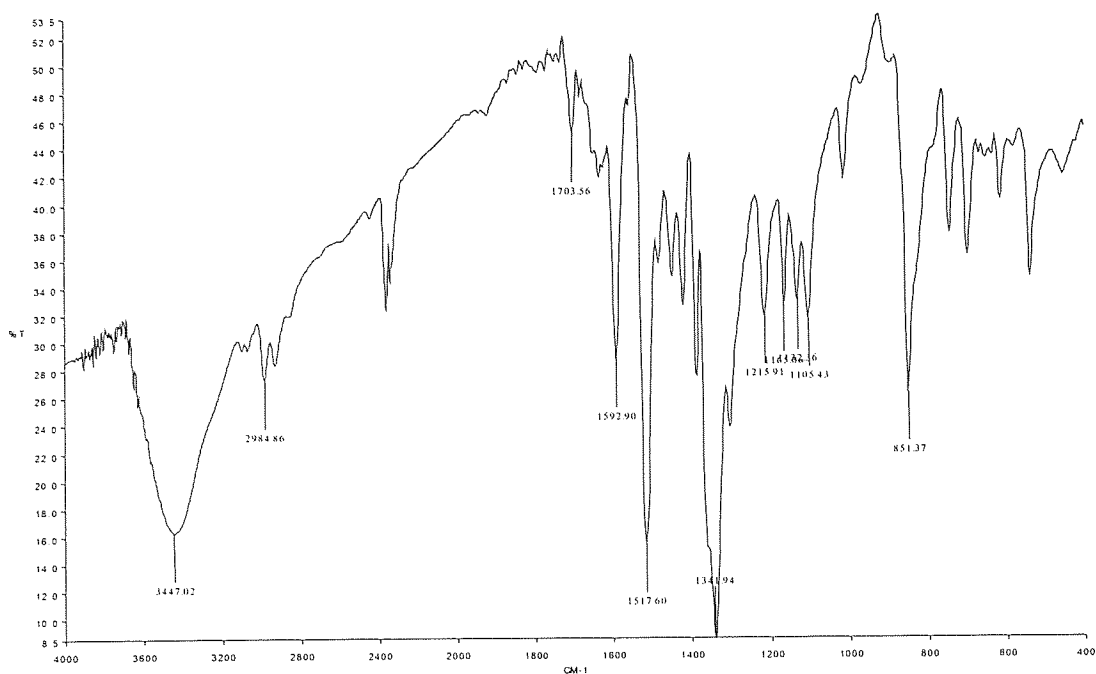


Figure 94 : IR of co-polyradical PEB965

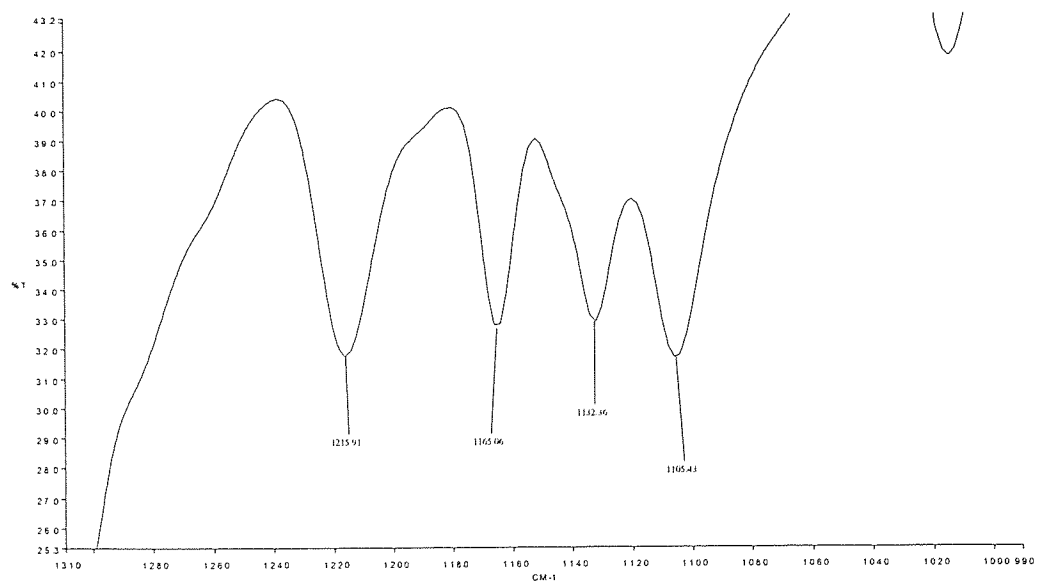


Figure 95 : IR signature peaks of nitronyl nitroxide radical (PEB965)

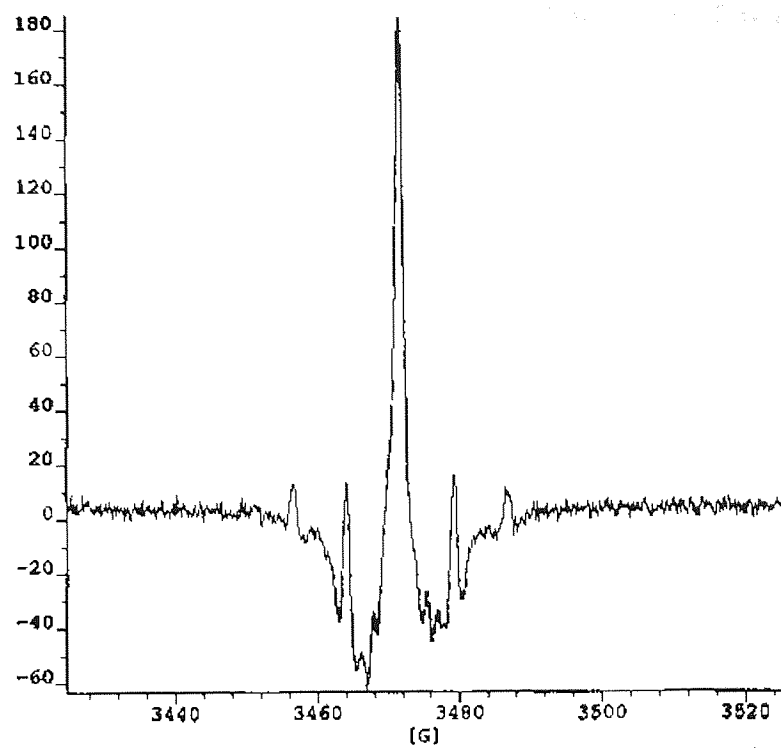


Figure 96 : Solution state EPR of PEB965

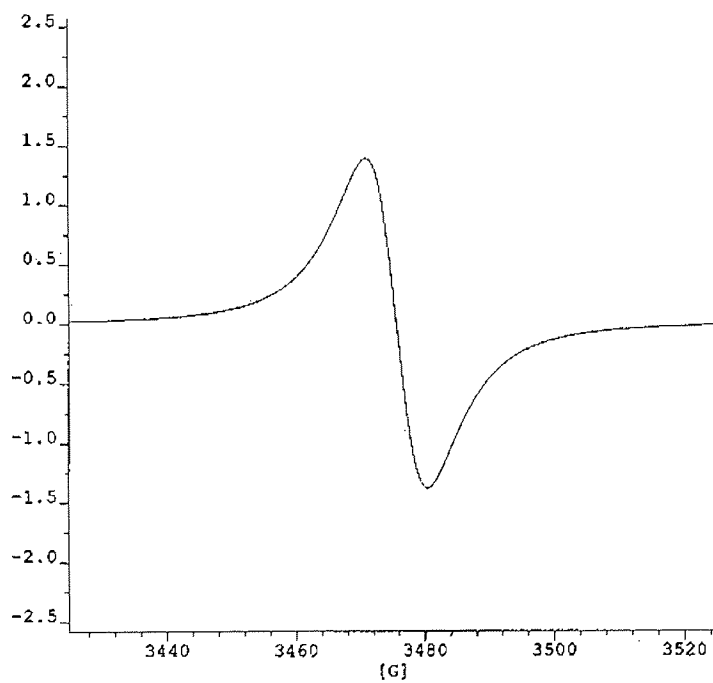


Figure 97 : Solid state EPR of PEB965

4.12.2 Improvement of Polymerisation Procedure - elimination of metal contact

Although the technique described previously for the synthesis of co-polyradicals gave good yields of polymer, it also suffered from a flaw that was initially overlooked. The transfer of monomer solution to the catalyst solution was accomplished using a conventional syringe bearing a metal needle. This contact, although only brief, constituted a possible source of metal contamination, and therefore a new procedure was required which reduced this to a minimum.

This was accomplished using some Teflon tubing and a 3-way Omnifit® valve, as shown in Figure 98. The glass tip of a syringe was attached to the third port of the valve and was used to administer solvents into the flasks.

The monomer solution was mixed magnetically using a Teflon coated magnet for five minutes, and was then taken up into the syringe. The contents of the syringe were then injected into the catalyst solution by changing the valve configuration. The polymerisation solution was stirred magnetically under an inert atmosphere for 1 hour at RT. Precipitation and analysis were carried as described previously.

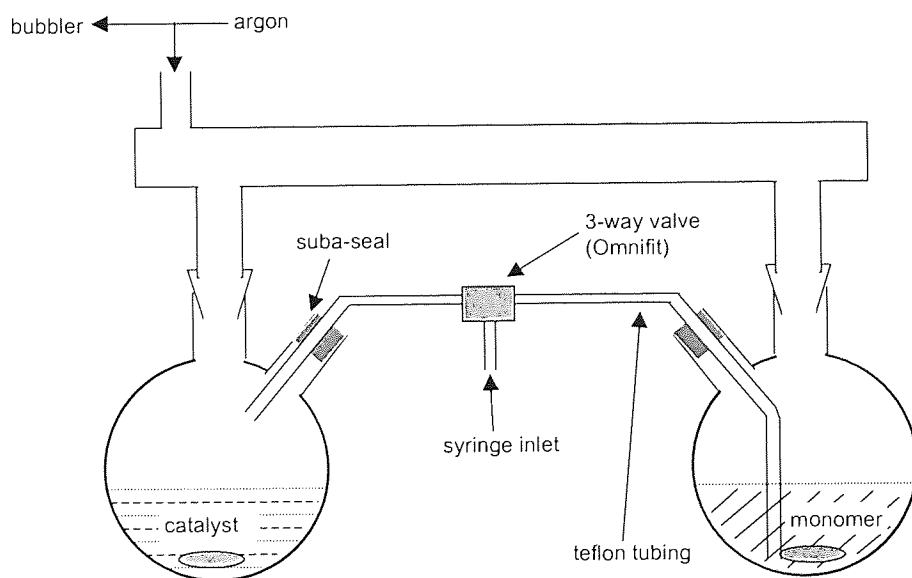


Figure 98 : Polymerisation apparatus for minimum metal contact

4.13 Results of co-polyradicals

Several co-polyradicals that possessed a 4-nitronyl nitroxide and a 4-“bridging group” were synthesised, and these are summarised in Table 11. Co-polyradicals using the 3-isomers were also prepared, and these are summarised in Table 12.

The yields of co-polyradicals obtained were generally moderate to good, demonstrating the effectiveness of the MCAT/EtOH/THF system. No reduction in yield was found by employing a co-monomer bearing a cyano group, which contrasts with the severely low yields obtained for the formation of the homopolymer.

The nitronyl nitroxide radicals remained intact during polymerisation, and the percentage spin was found to be in the range of 86 to 109% of the theoretical value. This is in good agreement with that found by Fujii using the $\text{Rh}(\text{COD})(\text{NH}_3)\text{Cl}$ catalyst⁶², in which minimal degradation took place. This implies that the MCAT/solvent system utilised in this project was very effective in yield and tolerance towards nitronyl nitroxide containing monomers.

Table 11 : Summary of copolyradicals using 4EPNN

Co-monomer	Group	Ratio (Mon:Rad)	Code	% Yield	Soluble in	% Spins per unit ^A
4FPA	F	1:1	PB065	58 ^{1, O}	DCM, THF	
4CPA	CN	1:1	PEB963	91	DMF	98
4CPA	CN	1:1	PB067	76 ^O	DMF	89
4CPA	CN	2:1	PB034	64	DMF	
4NPA	NO ₂	1:1	PEB965	83	N/A	108
4NPA	NO ₂	2:1	PB020	72	N/A	86
4NPA	NO ₂	2:1	PB064	61 ^O	N/A	85

(^A = by Dr A. Harrison; ¹ = incomplete precipitation; ^O = using the Omnifit procedure)

Table 12 : Summary of copolyradicals using 3EPNN

Co-monomer	Group	Ratio (Mon:Rad)	Code	% Yield	Soluble in	% Spins per unit ^A
3CPA	CN	1:1	PEB967	67	DMF	109
3NPA	NO ₂	1:1	PB028	57	N/A	89

(^A = calculated by Dr A. Harrison)

4.13.1 Physical properties of the co-polyradicals

All the co-polyradicals were obtained as green powder-like solids. Those that contained a nitro “bridging group” were found to be insoluble in all common organic solvents. Better solubility was observed for cyano “bridging groups”, where these co-polyradicals were soluble in highly polar, non-hydrogen bonding solvents such as DMF or DMSO. Interestingly, the most soluble co-polyradical was that which contained a fluorine co-monomer. This product was found to dissolve in common solvents such as DCM and THF.

4.14 A homopolyradical

Fujii’s Rh(COD)(NH₃)Cl was the only catalyst in the literature that was able to polymerise a phenylacetylene bearing a nitronyl nitroxide successfully⁶². The polymerisation, however, was marred by the low yield obtained (42%). This result was used as a benchmark for MCAT, and so a homopolyradical of 4EPNN was synthesised with the high yielding MCAT/BBA system. 4EPNN was polymerised using the Omnifit method to give the polyradical PB066, as shown in Table 13.

Analytical data for PB066; $\nu_{\text{max}}/\text{cm}^{-1}$ 2985 (w, sharp, C-H), 1601 (w, sharp, Ph), 1421 (m, sharp, unassigned), 1388 (m, sharp, unassigned), 1356 (w, slightly broad, nitronyl nitroxide or BBA), 1300 (m, sharp, unassigned), 1214 (m, sharp, nitronyl nitroxide), 1164 (w, sharp, nitronyl nitroxide), 1130 (m, sharp, nitronyl nitroxide).

The polyradical PB066 was obtained as a dark green solid, which was insoluble in all common organic solvents. These properties corresponded to those already reported by Fujii for this polymer⁶². However, the 66% yield obtained in this work was significantly greater than that obtained by Fujii. The IR spectrum was difficult to interpret because signals from BBA and the nitronyl nitroxide overlap with each other (approximately 1350cm⁻¹). SQUID analysis was more satisfactory since it revealed that the number of spins present was almost quantitative for a structure composed of nitronyl nitroxide monomer units, i.e. BBA was absent from the polymer. This also indicates that there was no degradation of the nitronyl nitroxide group during polymerisation. The magnetic properties of this polyradical are discussed later in this chapter.

Table 13 : Result of the synthesis of a homopolyradical

Radical Monomer	Colour	Code	Yield (%)	Soluble in	% Spins per unit ^A
4EPNN	Dark green/black	PB066 ^O	66	N/A	97

(^A = calculated by Dr A. Harrison; ^O = using the Omnifit procedure)

4.15 Magnetic characterisation by SQUID

It was expected that some through-space interactions could occur between the nitronyl nitroxide and the “bridging group”. This can sometimes be observed using EPR, but the data requires detailed analysis and an in-depth knowledge of the technique and substance in question. A more effective method is to examine the substance using a SQUID magnetometer. This is a highly sensitive device used for the detection of magnetic fields, making it ideal for the materials prepared in this work.

The SQUID analysis can reveal many attributes of a material, such as susceptibility, hysteresis, magnetic interactions, and other effects. However, the amount of data and graphs generated by each material analysed is very large and it is impractical to report all of these. As such, only the non-standard results will be discussed in detail.

4.15.1 The Curie Weiss law and its use

Before describing the magnetic properties of the co-polyradicals it is necessary to define the terms used in the characterisation data.

The magnetisation (M), or net induced magnetic moment, is proportional to the applied magnetic field, H, as shown in Equation 1. The proportionality constant is termed the molar magnetic susceptibility, χ .

$$M = \chi H$$

Equation 1 : Relationship of magnetisation to susceptibility

The susceptibility has a dependence on temperature, T, which is characterised by the Curie expression shown in Equation 2. The Curie constant, C, is defined by Equation 3, where N is Avogadro's number, S is the spin quantum number, g is the Lande factor, μ_B is the Bohr Magneton, and k_B is the Boltzmann constant.

$$\chi = \frac{C}{T}$$

Equation 2 : The Curie expression

$$C = \frac{Ng^2\mu_B^2S(S+1)}{3k_B}$$

Equation 3 : Definition of the Curie constant

Different types of bulk magnetic behaviour can be differentiated using the Curie Weiss Law, as shown in Equation 4. The Weiss constant, Θ , can be determined by a linear extrapolation of a plot of χ^{-1} against T. Paramagnetic materials have a Weiss constant of zero, whereas negative values indicate an antiferromagnet, and positive values a ferromagnet.

$$\chi = \left(\frac{C}{T - \Theta} \right)$$

Equation 4 : The Curie Weiss law

Interactions between spins can be revealed by examination of the effective spin moment, μ_{eff} , which is defined by Equation 5.

$$\mu_{\text{eff}} = 2.83\sqrt{\chi T}$$

Equation 5 : Definition of effective spin moment

4.15.2 Symbols used in graphs

H = applied field (in Oe)

M = magnetisation

χ = molar magnetic susceptibility

μ_{eff} = effective magnetic moment

T = temperature (K)

FC = field cooled

ZFC = zero field cooled

All data were obtained under ZFC conditions, unless specified.

4.15.3 Paramagnetic co-polyradicals

It was assumed that the molecular weight of the co-polyradicals should be reasonably high (100,000 to 240,000 Daltons) based solely on previous experiments. If ferromagnetic spin interactions occur among the stable radicals, then very high spin polymers are obtained. However, in this work all but one of the co-polyradicals were found to be paramagnetic. A paramagnetic material is one where there is no bulk magnetic behaviour because the spins are orientated in random directions.

By plotting the susceptibility (χ) against temperature (T) it is normal to observe a straight line between 100K and 300K, because the thermal energy is much greater than that energy of spin alignment, as shown in Figure 99. At lower temperatures χ begins to increase, and below 10K susceptibility rises very rapidly. This means that the alignment of spins throughout the material increases because the thermal energy is insufficient to destroy all spin coupling, and more of the material is becoming spin-aligned as the temperature decreases. This data plot is known as a Curie Curve, and is typical of a purely paramagnetic material.

Spin interactions involving the bulk of the material are easily observed in a plot of $1/\chi$ against T. For purely paramagnetic behaviour the intercept should be 0K, which is a feature of most of the co-polyradicals obtained in this work. A typical data plot showing bulk paramagnetic behaviour is also shown in Figure 99.

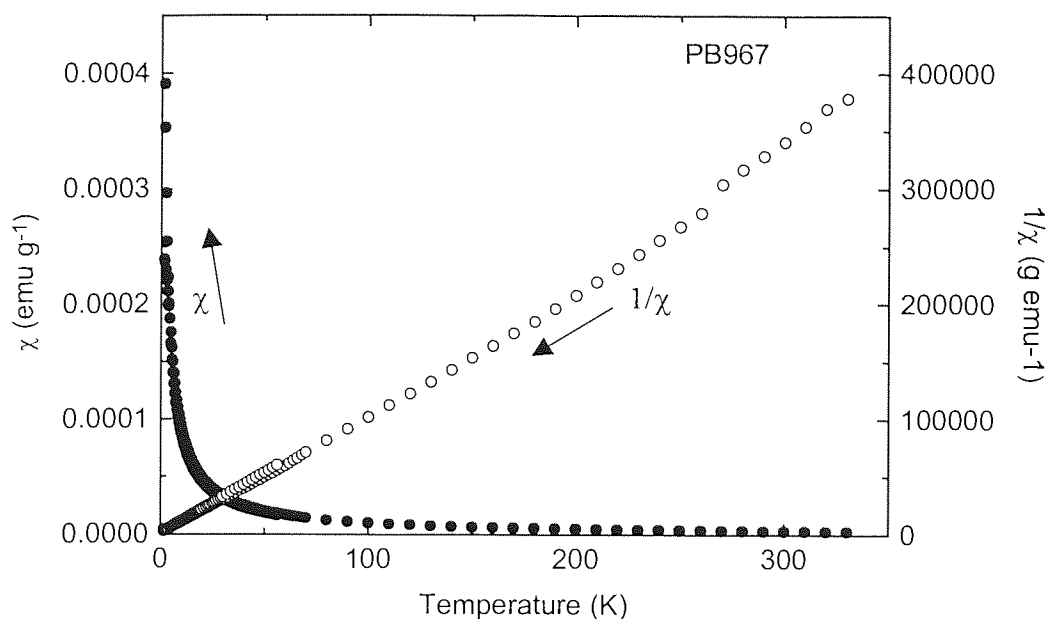


Figure 99 : Typical SQUID plot showing paramagnetism

Susceptibility graphs only reveal bulk interactions, or long-range order. Short-range spin interactions are more effectively displayed by a plot of the effective spin moment μ_{eff} against T , as shown in Figure 100. The plot is horizontal in the range of 50K to 300K, which signifies that the spins are acting independently, i.e. paramagnetic interactions are occurring in this temperature region. For most of the co-polyradicals prepared in this project the line deviates downwards below 50K, indicating that there is a net loss of spin moment, which is the result of spin cancellation. This type of effect is indicative of weak antiferromagnetic interactions occurring between the spins at very low temperatures. These AFM interactions arise from intermolecular dipolar (through-space) coupling between polymer chains¹¹⁸.

These PM and AFM properties are consistent with many other polyradicals in the literature, such as Fujii's polyradical of 4EPNN⁶², or a PPA bearing a galvinoxyl stable radical⁶³, or a conjugated polymer bearing a nitroxide¹¹⁹.

These results mean that the fluoro, nitro, and cyano substituted co-monomers did not introduce any long-range ferromagnetic interactions, as they are known to do for some molecular stable radicals. However, there are some interesting short-range magnetic properties in a few co-polyradicals and these are now described.

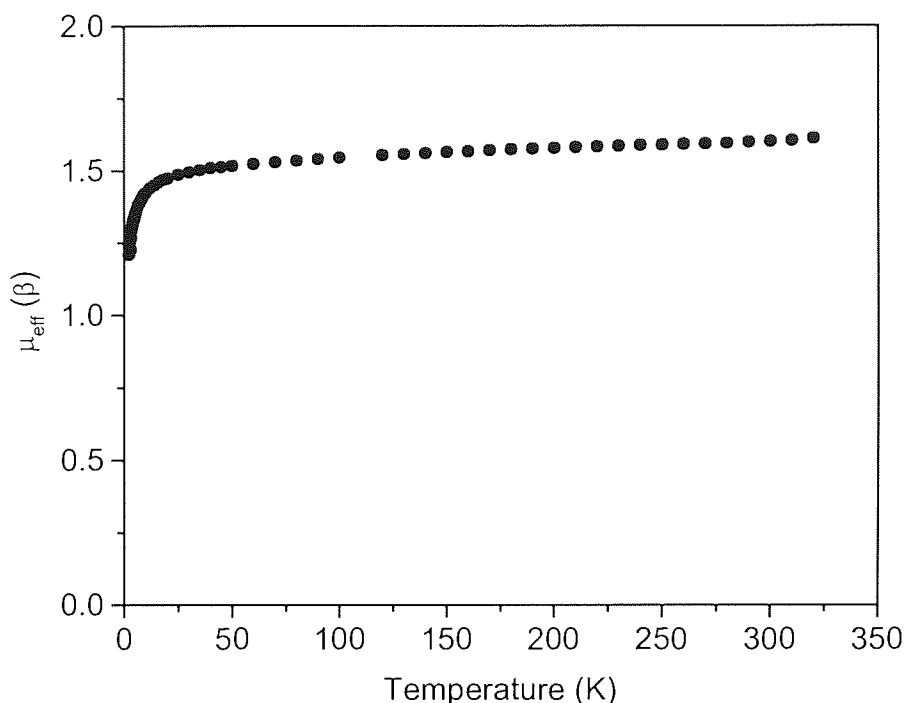


Figure 100 : SQUID plot showing weak antiferromagnetic interactions (PB066)

4.15.4 An antiferromagnet

Upon examination of the plot of $1/\chi$ against T for the cyano containing co-polyradical PEB963, it became obvious that this material was not paramagnetic. The Weiss constant is a negative value because the data plot does not intercept T at 0K, as shown in Figure 101. This is the classical sign of a material possessing bulk, short-range, antiferromagnetic properties.

Interactions between neighbouring spins were examined using a plot of μ_{eff} against T , shown in Figure 102. This plot shows that the number of spins is constant between 50K to 300K, which is indicative of paramagnetic spin interactions. Below 50K the plot deviates

downwards, which signifies the presence of antiferromagnetic interactions. This deviation becomes very steep below 25K, which is consistent with the onset of very strong antiferromagnetic interactions.

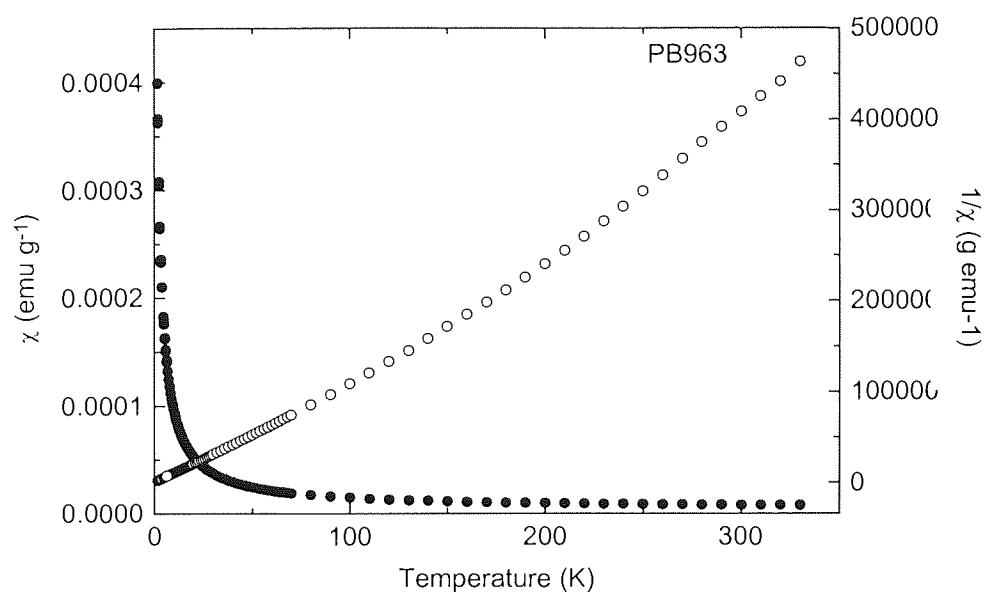


Figure 101 : SQUID plot of antiferromagnet PEB963

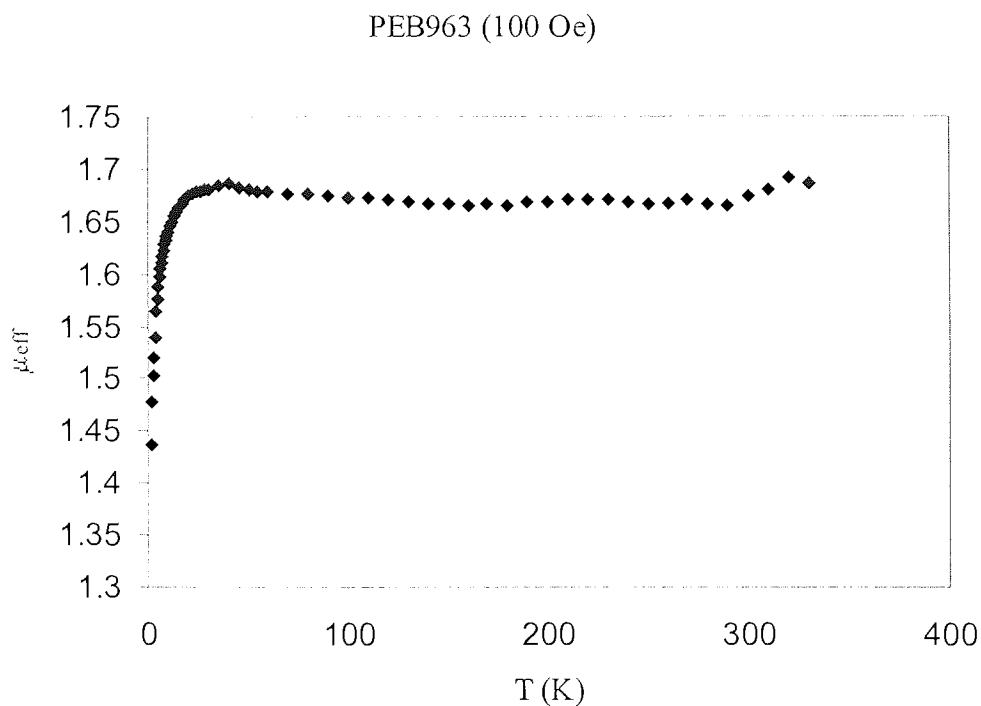


Figure 102 : SQUID plot showing antiferromagnetic interactions

This behaviour suggests that the material contains two different magnetic regions. A small, but significant, part of the co-polyradical must contain spins that are coupled antiferromagnetically. In this case, the AFM coupling is short range, implying that these AFM regions are not limited to two or three spin sites, but probably consist of 10 or more. The rest of the material must contain spins that are randomly orientated, i.e. paramagnetic, because there is no discernible reduction in μ_{eff} between RT and 50K. As the temperature is lowered below 50K, it can be envisaged that the antiferromagnetic regions tend to propagate through the material (Figure 103). This would result in a decrease of μ_{eff} , which gives a material where the type of spin alignment is predominantly AFM.

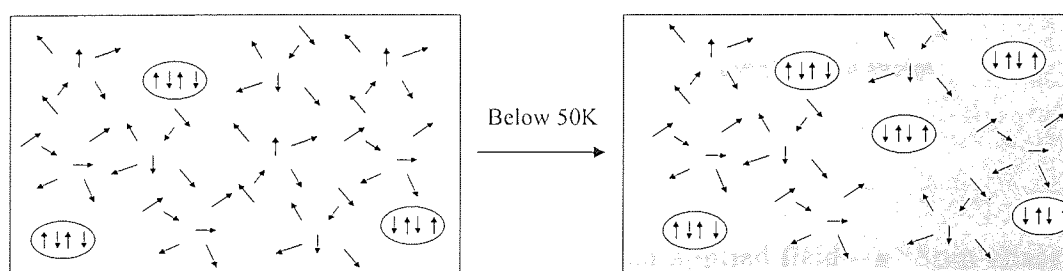


Figure 103 : Propagation of AFM coupling

This co-polyradical is most unusual, because it is generally accepted that structural disorder in amorphous solids makes them unsuitable for spin coupling¹²⁰. Therefore, it can be hypothesised that these short-range AFM properties are a function of small, ordered regions in the material. The cyano groups must have a vital role in the AFM coupling, because these magnetic properties are not found in any other co-polyradicals. Research by Kinoshita has found that the cyano group can act as a “bridge” between nitronyl nitroxides in an analogous manner to those of a nitro group⁴⁰. It is possible that this intermolecular “bridging” occurs in the co-polyradical PEB963 but it is favourable for the cyano bridge to align the nitronyl nitroxides antiferromagnetically, as shown in Figure 104.

Further work on this co-polyradical is required to determine a more in-depth explanation.

Similar magnetic properties were found to occur in PB067, which was synthesised by the Omnifit procedure using the same co-monomers in the same ratio as those of PEB963. This indicates that these magnetic properties are most likely to be a function of the co-polyradical than a contaminant.

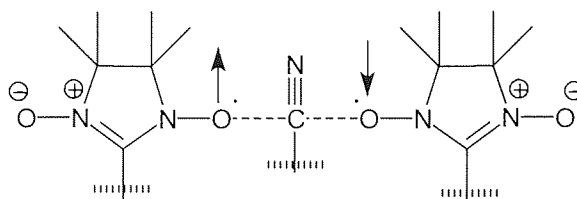


Figure 104 : AFM spin coupling through a “bridging” cyano group

4.15.5 Enhanced magnetisation upon cooling in an applied field – a “Spin Glass”

An attempt was made to induce the spins of an amorphous co-polyradical (PEB965) to align, by performing a SQUID experiment where the sample was cooled in the presence of an applied magnetic field (FC conditions). It was found that below 10K there was a significant increase in magnetisation under those conditions (1000 Oe magnetic field) compared to that obtained under ZFC conditions, as shown in Figure 105.

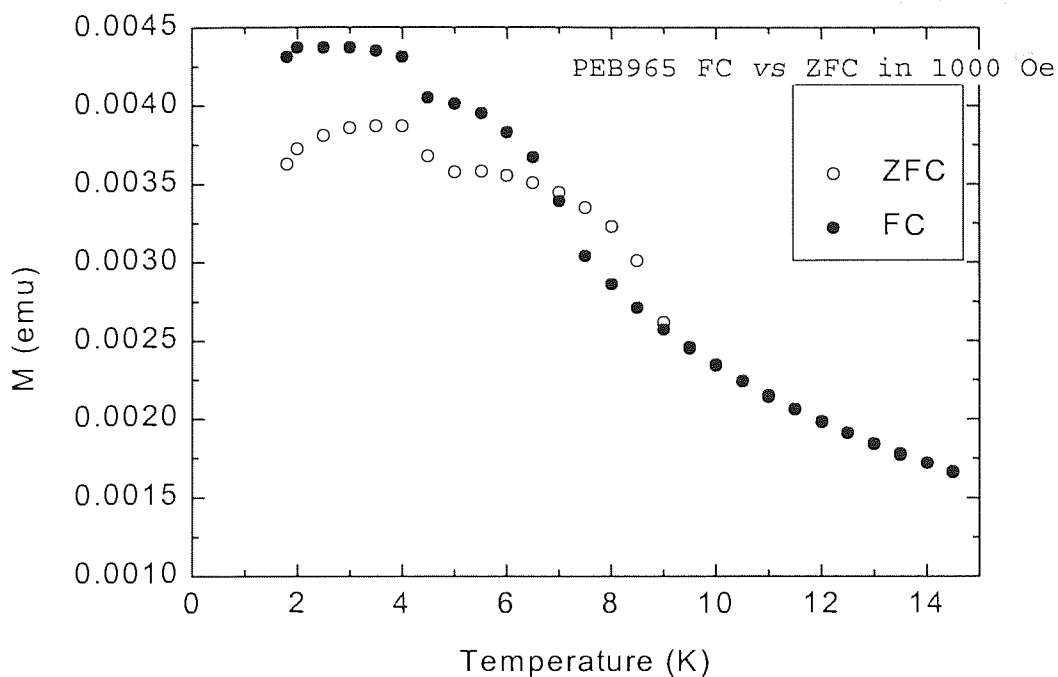


Figure 105 : SQUID of PEB965 obtained under FC and ZFC conditions

A molecular magnet developed by Mitsumori *et al* provided an insight into how these magnetisation properties may occur¹²¹. It was comprised of a stable nitronyl nitroxide radical and a manganese complex (Figure 106), and this gave a similar magnetisation plot to that obtained for PEB965. Mitsumori found that magnetisation of the material dramatically increased at 11K under FC conditions, and this was associated with the FM alignment of spins. Under ZFC conditions the magnetisation was significantly lower. Although a full account was not reported, the main feature of this material was the manganese complex, which acts as a “bridge” between spins. The spin alignment, however, was found to be favourable for certain parts of the material only and the rest of the spins remained paramagnetic. Only 30% of the total spins were observed to align, indicating that even in this crystalline complex there are regions which are just unfavourable for FM spin alignment.

In effect, small “pockets” of the material became magnetised, but there is no long-range order. This type of behaviour is commonly referred to as a “Spin Glass” system⁷³. A pictorial representation of a typical spin glass is shown in Figure 107. A typical system bears some residual magnetisation when the applied magnetic field is removed. To further verify the spin glass nature of PEB965 measurement of residual magnetisation is required, but time did not permit this analysis in this project.

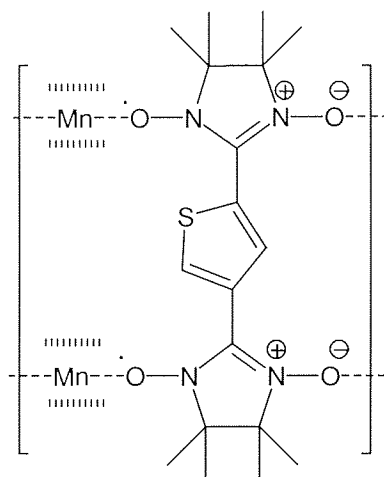


Figure 106 : A manganese bridging group

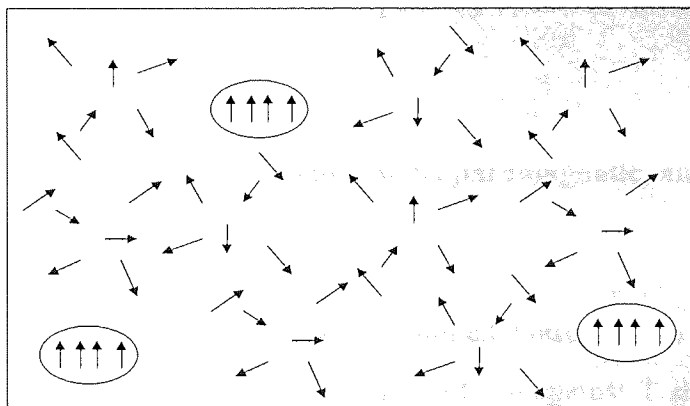


Figure 107 : Representation of a "Spin Glass"

It is reasonable to assume that a similar spin coupling takes place in PEB965, but the “bridge” in this case is a nitro group, as shown Figure 108. The magnitude of magnetisation is substantially lower than that observed in Mitsumori’s manganese complex, implying that the spin alignment in PEB965 is only favourable for a small fraction of the material. It is most likely that these effects are the result of intermolecular spin coupling, i.e. between polymer chains.

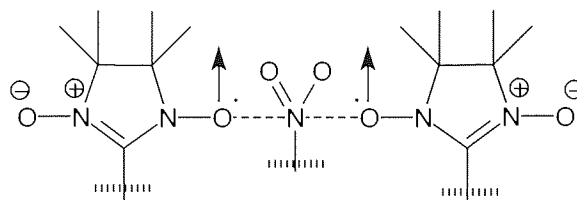


Figure 108 : Possible coupling in spin glass PEB965

The spin glass properties of PEB965 serve to illustrate that the nitro bridging group can be effective in co-polyradicals, just as they are in molecular magnets. However, the “bridging” effect is most likely to be very dependent upon the morphology of the polymer. This hypothesis is substantiated further by the fact that molecular magnets such as 4NPNN, have different magnetic properties depending upon the internal structure of the crystals²⁷.

4.14.6 A co-polyradical exhibiting ferromagnetic, paramagnetic, and antiferromagnetic interactions

The cyano containing co-polyradical PB034 exhibited unusual spin interactions when cooled in the presence of an applied field. A plot of μ_{eff} against T shows that there are three different interactions and these occur in distinctive temperature regions, as shown in Figure 109. In the range of 100K to 300K the plot shows an upward deviation, which reaches a maximum at 100K. Between 100K and 50K a horizontal line is observed. Below 50K the effective moment begins to drop, and the gradient of this curve becomes increasingly steep at lower temperatures.

When a sample is cooled in an applied field it is expected that this will encourage the spins to align in the direction of the field, resulting in ferromagnetic interactions. Surprisingly, an increase in spin moment was found to occur with the application of a weak field (100 Oe), which is synonymous with the presence of FM interactions. It is unusual to observe this behaviour at such high temperatures. In the literature, they are usually reported to occur below 100K⁴⁶. There is no increase in effective spin moment from 100K, suggesting that there are only certain regions of the material favourable for ferromagnetic coupling. Once these are saturated the susceptibility will remain constant, as seen in the plot between 100K and 50K. The loss of spin moment below 50K is typical of antiferromagnetic interactions resulting from through-space spin coupling.

A similar plot was reported by Nishide for a conjugated polynitroxide and the FM interactions were explained by spin coupling through a conjugated system (spin polarisation)⁶⁷. It is unlikely that this occurs in PB034 because the substituent groups are out of plane with the backbone. It is most likely, therefore, that the origins of these magnetic effects must be attributable to either dipolar or exchange interactions using the cyano group as a "bridge". In molecular magnets, such as 4NPNN, the FM interactions are the result of exchange and dipolar coupling, which are affected by the structural arrangement in the crystal²⁷. 4NPNN can exist in at least four different crystalline states, and each state has different magnetic characteristics. Therefore, it can be postulated that the interactions present in this co-polyradical are the result of the polymer morphology, such that regions of the materials are favourable for FM spin coupling.

The possibility of contamination cannot be ruled out, because time did not permit a repetition of this experiment using the Omnifit procedure. If, for example, the contaminant were a metal such as cobalt or iron, then this would be expected to account for the FM interactions. However, the onset of AFM coupling at low temperature is inconsistent with that of a metallic impurity. Hence, it is most likely that these properties are a function of the polymer and as such, represents a significant advance in the field of magnetic polymers.

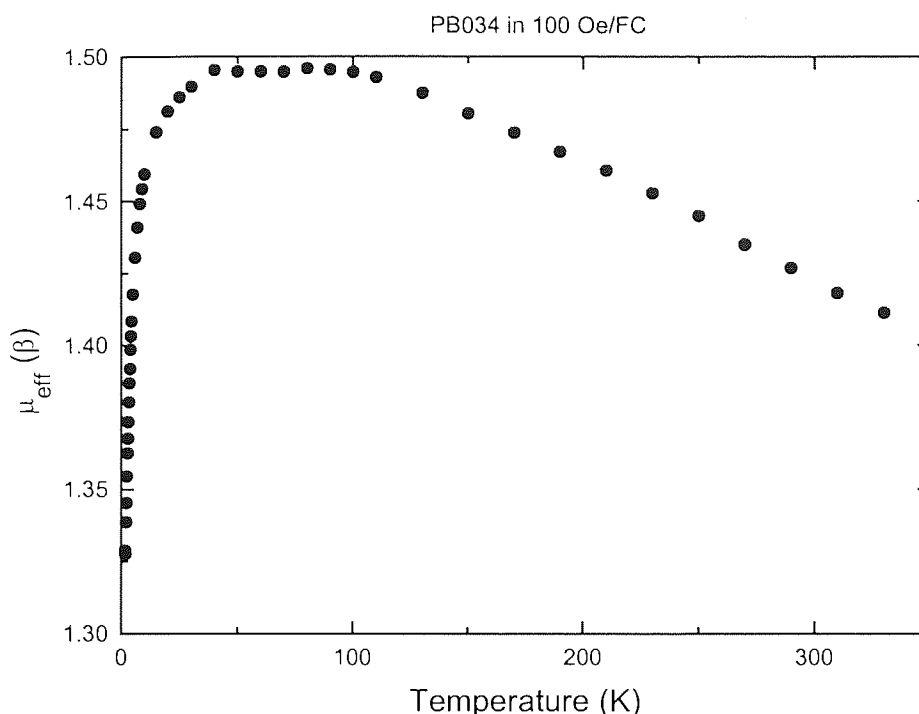


Figure 109 : SQUID showing ferro, para, and antiferromagnetic interactions

4.15.7 Co-polyradicals exhibiting weak and strong antiferromagnetism

Under FC and ZFC conditions unusual behaviour was observed for the nitro containing co-polyradical PB064, as shown in Figure 110. Under ZFC conditions the susceptibility of the co-polyradical began to increase at temperatures lower than 10K, which is normal behaviour for a paramagnetic material. As described previously, when a field is applied the spins in the material are encouraged to align in the direction of the field, resulting in FM interactions. This experiment was performed on PB064 under a weak field (100 Oe), and the susceptibility exhibited only a small increase below 10K. Furthermore, a susceptibility maximum was reached at 3K and below this a decrease was observed.

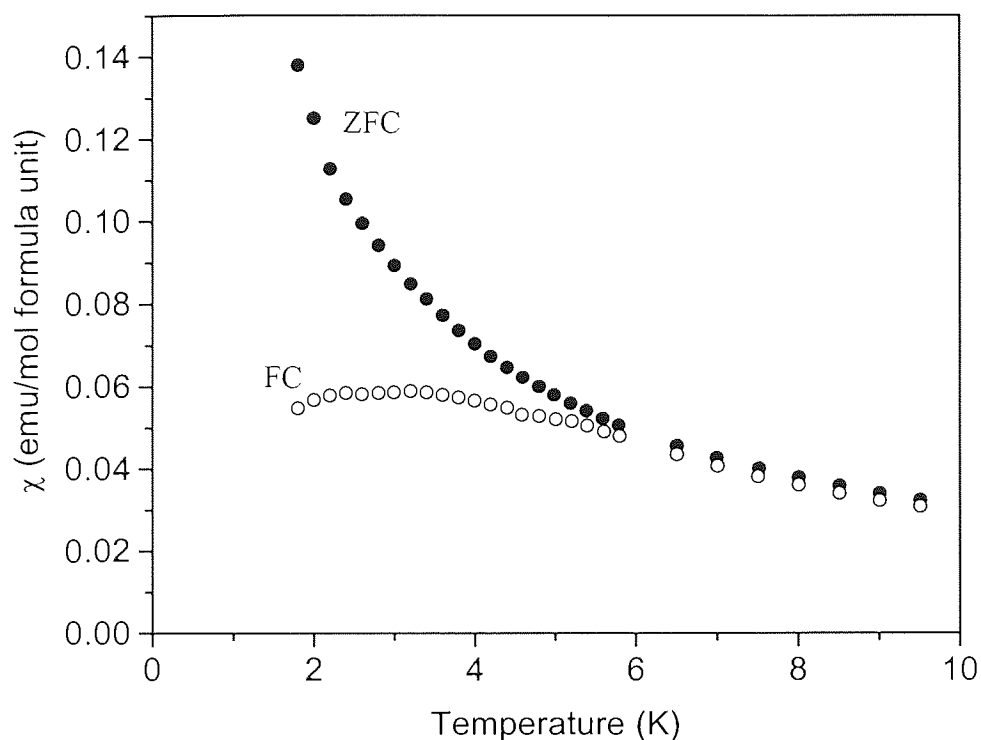


Figure 110 : Unusual FC and ZFC magnetic properties (PB064)

Further insight was sought using a plot of χT against T , as shown in Figure 111. This type of graph is the most common in the literature, and is well known to reveal spin interactions. Generally, a horizontal plot is indicative of paramagnetic spin interactions, a downward slope that of antiferromagnetic interactions, and an upward slope as ferromagnetic interactions. It can be seen from the plot that under both ZFC and FC conditions there is a downward slope, which is indicative of antiferromagnetic interactions in the region of 300K to 10K. Below 10K the plots of ZFC and FC were found to be markedly different, as shown in Figure 112. The AFM interactions were significantly greater under FC conditions than under ZFC. This implies that the applied field is encouraging the spins to align opposite to each other, rather than in the direction of the applied field. This behaviour is highly unusual, because it is energetically favourable for the spins to align in the direction of the field.

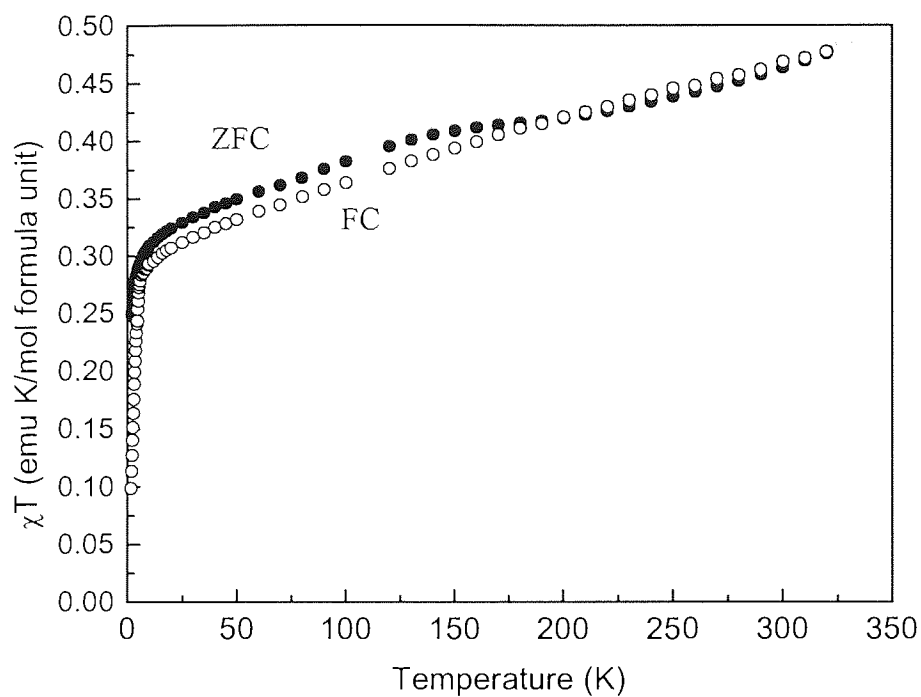


Figure 111 : Spin interactions 300K to 2K (PB064)

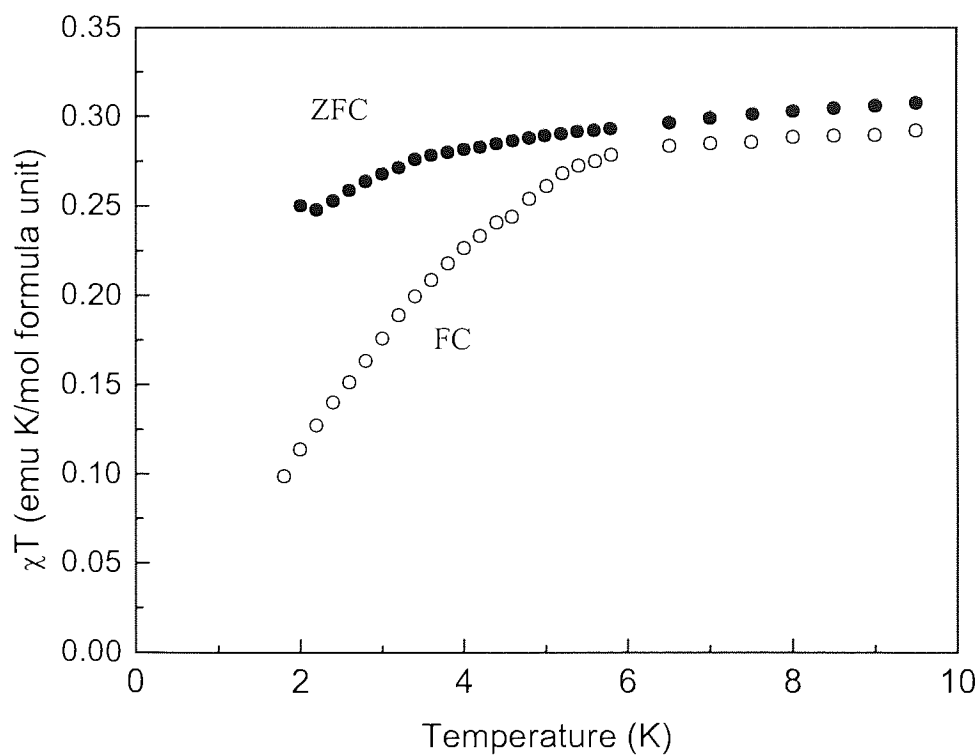


Figure 112 : AFM spin interactions (PB064)

Almost identical spin interactions were found to be operating in another nitro containing co-polyradical, PB028. A plot of χ against T showed exactly the same curve under FC/ZFC conditions (Figure 113) in comparison to that PB064 (Figure 110). The morphology of PB028 should be significantly different to that of PB064, because its ring substituents are in the meta rather than the para position. The only link between these two materials is that they both employ co-monomers bearing a nitro “bridging group”.

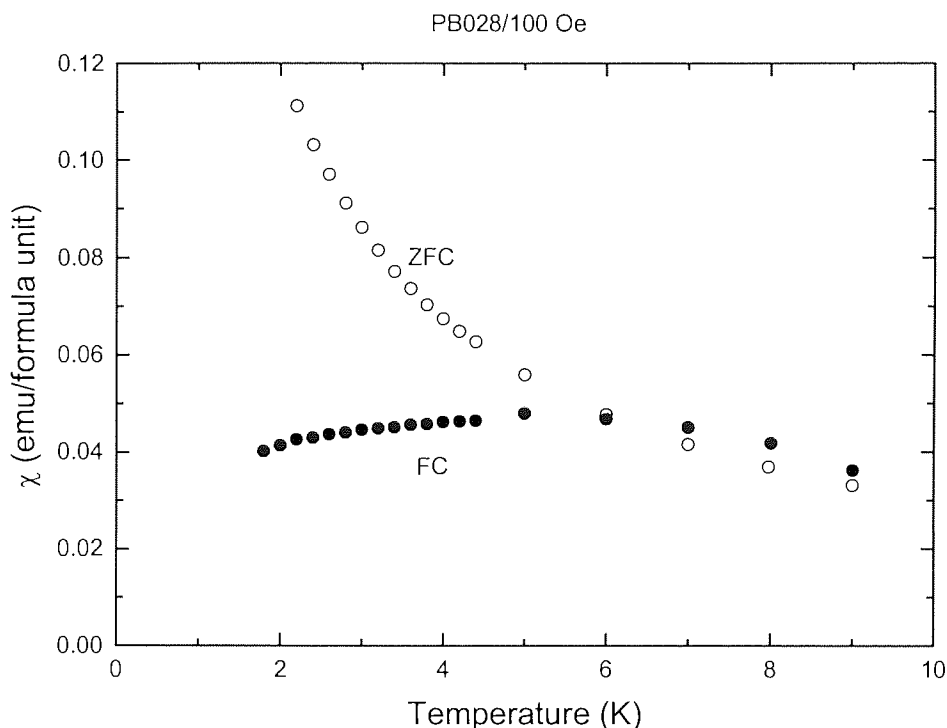


Figure 113 : Unusual magnetic behaviour in PB028

It is difficult to account for these unusual properties because nothing similar has been reported for other polyradical systems. However, it may be possible to explain this phenomenon by consideration of dipolar interactions between spins^{122,123}. At low temperatures, in zero applied field, some of the spins in these materials exhibit weak antiferromagnetic interactions, but the majority of the spins experience paramagnetic interactions. The effective spin moment is significantly reduced with the application of an applied field, which suggests that a new magnetic phase is being formed. This may take the form of a “striped phase” in which there is short range magnetic order in a stripe of the material but its neighbouring stripe has short range magnetic order in the opposite direction. The spins of neighbouring stripes would then cancel each other out. This

“striped phase” magnetism occurs because its ground state energy is less than that of the corresponding spin aligned phase. It is thought that this effect originates from a competition between short-range attractive forces that lead to local alignment and longer-range repulsive forces that lead to a competitive anti alignment. It is also known that under an applied magnetic field of a critical magnitude a change of phase from “striped” to a “bubble lattice” can take place, as shown in Figure 114. The “bubble lattice” takes its name from the fact that materials having this magnetic property were/are used in the “bubble” memory (permanent memory) of computers.

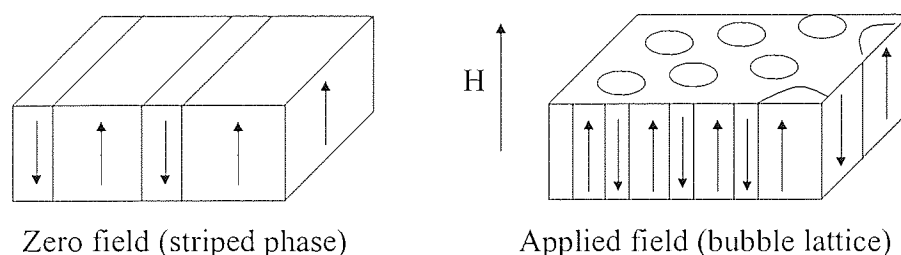


Figure 114 : Formation of a "bubble" phase

A plot of the inverse susceptibility against temperature illustrates the change of magnetic phase in PB064 more effectively, as shown in Figure 115. The ZFC data shows a straight line, which intercepts the temperature axis at a negative value. This is characteristic of bulk antiferromagnetic interactions. At about 6K the FC data begins to show a significant slope upwards from the ZFC plot. The data cannot be extrapolated to the temperature axis, which is highly unusual. This means that under an applied field and decreasing temperature the material is undergoing a change of magnetic phase from a weak antiferromagnet to a very strong antiferromagnet. Furthermore, both of these properties are a function of the bulk of the material. This lends weight to the hypothesis of the formation of a “stripe phase” or “bubble lattice” at temperatures lower than 6K.

Theoretical modelling of these co-polyradicals is required to reveal which of these effects occur, but this is beyond the scope of this research.

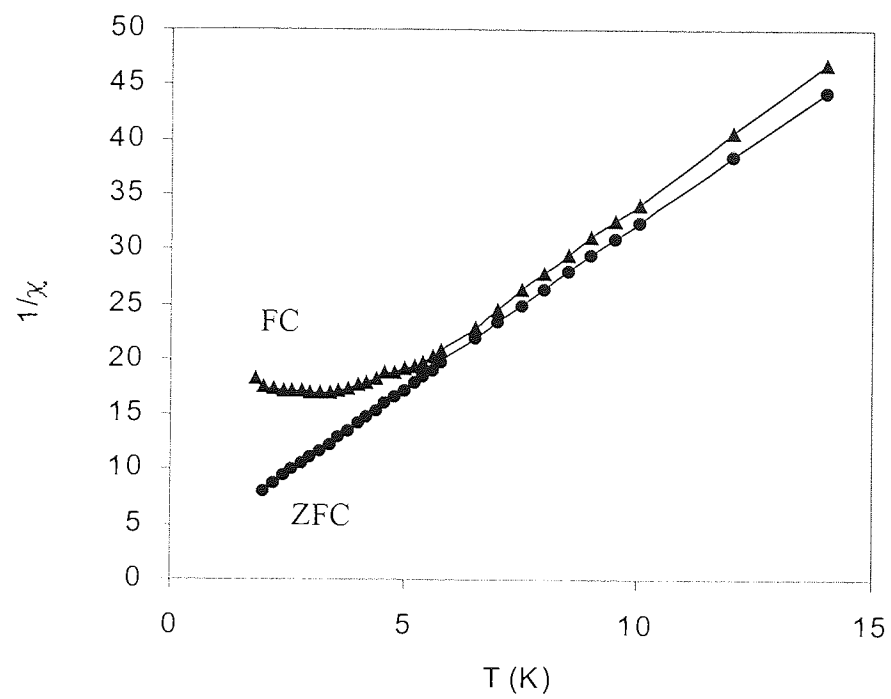


Figure 115 : Change of magnetic phase in PB064

4.16 Summary of magnetic effects

Several co-polyradicals were synthesised in moderate to excellent yields using the MCAT catalyst. Most of these materials exhibited bulk paramagnetism, but one was found to have antiferromagnetic properties in the bulk. Short-range FM interactions were found in a nitro containing co-polyradical. A co-polyradical that could be magnetised under an applied field was found, and two co-polyradicals were found to exhibit a change of phase under an applied magnetic field at low temperature. The origin of these magnetic effects is most likely to occur by a through-space coupling via the "bridging group". Magnetic spin interactions were only observed in co-polyradicals that contained either cyano or nitro "bridging groups". No unusual magnetic properties were found in the case of a fluoro containing co-polyradical.

It is interesting to note that altering the ratio of "bridging group" to the stable radical can change the magnetic properties of a co-polyradical significantly. This is exemplified by the difference between the co-polyradical with a 1:1 ratio of nitro:nitronyl niroxide (PEB965), to that of a 2:1 ratio co-polyradical (PB064). Small regions of the former can be made to ferromagnetically align under an applied magnetic field, whereas the spins of the latter become strongly antiferromagnetic under an applied magnetic field. It seems likely, therefore, that the magnetic properties of these co-polyradicals are predominantly dependent upon electrostatic forces in the material.

CHAPTER 5.
CHEMICAL SHIFTS OF PHENYLACETYLENES

5. CHEMICAL SHIFTS OF PHENYLACETYLENES

5.1 Introduction

In this research, the monomer 4-nitrophenylacetylene did not polymerise in the presence of $[\text{Rh}(\text{NBD})(\text{OCH}_3)]_2$, a catalyst reported to be very efficient for the polymerisation of phenylacetylene. However, the polymerisation of 3-nitrophenylacetylene gave 98% yield of polymer, suggesting that electronic factors affecting the terminal alkyne may play a significant part in determining the polymerisability of the monomer.

In the literature, it has been suggested that the polymerisabilities of some phenylacetylene monomers were related to the chemical shift of the terminal acetylenic hydrogen atom⁸⁰. No formal conclusion was drawn from this data, but it is likely that the ring substituent group affects the electron density of the terminal acetylene.

An in-depth study of how substituent groups alter the chemical shift of the terminal alkyne was undertaken.

5.1.1 Techniques of measurement

The determination of substituent induced electronic changes in phenylacetylenes has been traditionally based on measurements such as acidity¹²⁴, and the addition of arylthiyl radicals¹²⁵. However the results from these types of measurements are inconclusive. Newer methods use spectroscopy, such as NMR analysis¹²⁶. The high precision of modern NMR has made this the technique of choice, where ^{13}C NMR analysis has become the de-facto standard because of problems associated with solvent interactions using ^1H NMR¹²⁷. The chemical shift of a nucleus is sensitive to the surrounding environment of electrons. Changes in this environment will give rise to a change in the value of the chemical shift. Thus, NMR is a sensitive probe for electronic changes resulting from different ring substituents.

5.1.2 Substituent Induced Chemical Shifts

Dawson has investigated the substituent induced chemical shift, SCS, of phenylacetylenes and reported that both resonance and polar effects are important in para substituted phenylacetylenes¹²⁶. Resonance effects operate when the ring is para substituted, because of the need for the substituents to conjugate.

Polarisation effects can be rationalised as the π -polarisation induced by a remote substituent dipole. Conjugation is not necessary, because the polarisation of one π electron system is known to affect a remote π electron system without an intervening conjugated π system¹²⁸.

Dawson did not adequately investigate the magnitudes of these SCS effects. In this project a series of meta substituted phenylacetylenes, including three electron donating substituents and three electron withdrawing substituents, was devised to provide insight into these electronic changes. The same substituents are also examined in the para position so that a comparison of the magnitude and the type of effects can be made. Direct resonance effects are excluded by changing the position of the substituent from para to meta leaving π -polarisation SCS effects only.

Any relation between the SCS of the substituents and the polymerisability of the phenylacetylene will be discussed.

5.2 Experimental

The spectrometer frequency of carbon was set at 75.45MHz. The samples were pulsed 480 times, using a relaxation delay of 3 seconds. The ^{13}C spectra were proton decoupled using "composite pulse decoupling". Samples were not degassed. All analyses were carried out at room temperature in deuterated chloroform (CDCl_3) using a maximum concentration of 10%. The spectra were calibrated so that the middle peak of CDCl_3 was set at 77.00ppm relative to TMS.

Assignment of the alkyne signals was possible using the PENDANT spectra, see Figure 116 for an example of 4-nitrophenylacetylene, **18**. The terminal carbon of the alkyne gave a positive signal and the non-terminal carbon a negative signal. No correction was applied for the biphenyl molecule, **9**. Solvent induced shifts were assumed to be minimal. The experimental error for ^{13}C NMR spectra was found to be ± 0.1 ppm, obtained by analysing the same molecule three times.

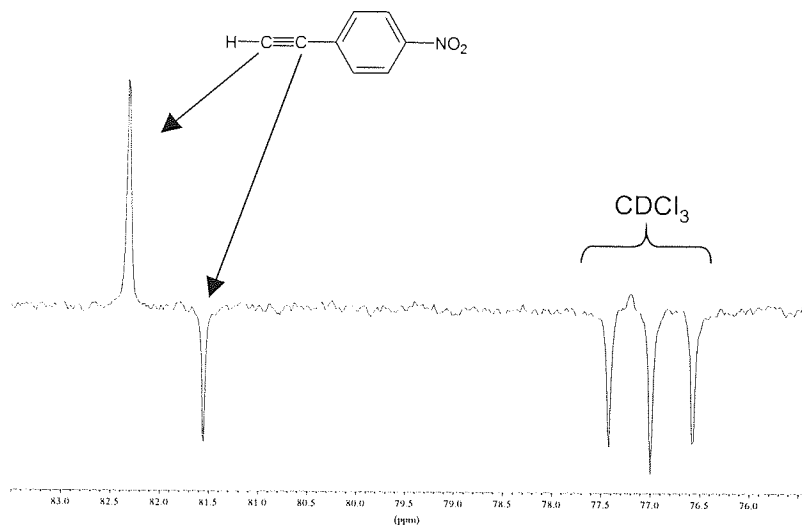


Figure 116 : attenuated ^{13}C PENDANT NMR spectrum of 4NPA in CDCl_3

5.3 Results

The notation used in the following discussion is represented in Figure 117. The ^{13}C NMR shifts and polymerisability are summarised in Table 14.

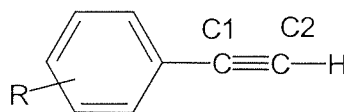


Figure 117 : Key to NMR data

Table 14 : ^{13}C NMR shifts of the terminal acetylenic carbon C2, and the non-terminal C1 (δ in ppm relative to TMS), of substituted phenylacetylenes.

Entry	R	C2	C1	Polymerisable?
1	<i>p</i> -NH ₂	74.91	84.37	No
2 ^a	<i>p</i> -OCH ₂ CH ₂ CH ₂ CH ₃	75.67	83.72	Yes
3	<i>p</i> -O-THP	75.82	83.61	Yes
4 ^b	<i>p</i> -CH ₃	76.47	83.76	Yes
5	<i>m</i> -NH ₂	76.61	83.83	No
6	<i>m</i> -OCH ₂ CH ₂ CH ₂ CH ₃	76.83	83.57	Yes
7	<i>m</i> -O-THP	76.93	83.37	Yes
8	<i>p</i> -H	77.20	83.56	Yes
9 ^a	<i>p</i> -C ₆ H ₅	77.81	83.52	Yes
10	<i>m</i> -CHO	78.86	81.98	Yes
11	<i>p</i> -ethynyl	79.09	82.98	No
12	<i>m,m'</i> dichloro	79.66	80.87	Yes
13	<i>m</i> -CN	79.75	81.03	Yes
14	<i>m</i> -NO ₂	79.89	81.04	Yes
15	<i>p</i> -CO ₂ CH ₃	80.02	82.74	Yes
16	<i>p</i> -CHO	81.06	82.56	Yes
17	<i>p</i> -CN	81.54	81.78	Yes
18	<i>p</i> -NO ₂	82.33	81.56	Yes

^a obtained from Maybridge. ^b obtained from Aldrich.

THP = the tetrahydro-2*H*-pyran derivative of the corresponding phenol.

5.4 Discussion

Magnetic anisotropy contributions from the substituents are assumed to be negligible, as described by Dawson¹²⁶. Modification of the ring current by the substituent was also assumed to be insignificant¹²⁷. Ortho substituents were deliberately excluded because of known complications from magnetic anisotropy and steric effects¹²⁹.

5.4.1 Electron donating groups at the para position

Electron donating groups in the para position relative to the triple bond shield C2, as seen in compounds **1-4**, and the effect increases with increasing donor strength. It can be seen that a primary amine group shields the terminal alkyne more effectively than a butoxy group, which in turn is more powerful than the methyl group. Substituents in the para position are in conjugation, so the strongest resonance donor has the greatest effect. The shielding of C2 occurs by extension of the resonance contributions of the donating group into the conjugated triple bond. Polarisation of the π electrons in the conjugated system is presumed to be minimal, because the donating groups studied do not possess a significant dipole.

The SCS changes of C1 in the series of **1-4** are negligible. Delocalisation of the charge from the substituent group over the conjugated system does not place any formal charge on C1 and hence the effects under discussion do not affect the electron shielding of this atom.

5.4.2 Electron donating groups at the meta position

Electron donating groups in the meta position **5-7** also lead to shielding of C2, but to a far lesser extent than in the para position. The strongest donor substituent has the greatest effect, which suggests resonance type interactions. Direct resonance interactions are not possible because substituents in the meta positions are not conjugatively linked. π -polarisation effects in systems **5-7** are very small because the donating groups studied do not possess a significant dipole moment. A similar effect was found in meta substituted benzene molecules, as reported by Bromilow¹³⁰. The precise mechanism of resonance transmission from the meta position was not reported. These resonance effects, "secondary resonance", are significantly weaker than direct resonance but are strong

enough to be observed. Using iterative calculations, Reynolds has also confirmed the presence of secondary resonance in meta substituted styrenes¹³¹.

It must be emphasised that this interpretation of the donating meta substituents is based on the series **5-7** that is identical to the donating para substituents **1-3**, and as such supports secondary resonance contributions. However, the differences in SCS between the donating meta substituents are very close to the experimental error of ¹³C NMR analysis. Hence, a definitive explanation is impractical using the NMR data in isolation.

5.4.3 Electron withdrawing groups in the para position

Electron withdrawing groups in the para position, such as compounds **15-18**, deshield C2, and the effect increases with increasing recognised acceptor strength. Thus, a nitro group induces a greater SCS than a cyano group. The SCS of para substituted phenylacetylenes is known to be the product of two effects, resonance and π -polarisation. Resonance effects operate between 1,4- substituents because they are conjugated. It is C2 of the alkyne that is directly conjugated with the para substituent, and it is this carbon that is most perturbed. The effect of resonance is demonstrated by the series **15-18**, where a stronger resonance acceptor exerts a larger perturbation of C2. π -polarisation effects also apply to C2, but these will be superimposed upon the resonance effects..

A “reverse” SCS occurs with C1 in which the shielding increases with increasing acceptor strength, e.g. nitro groups shield C1 more strongly than a cyano group. The reverse SCS of C1 can be explained by considering that the substituents are not only electron withdrawing groups, but they are also dipoles. These dipoles can effect a polarisation of the π electrons in the conjugated system¹²⁸, as shown in Figure 118. The polarisation effect is transmitted through space, and so C1 does not require direct conjugation. Hamer has described evidence for the existence of π -polarisation in a substituted styrene series¹³².

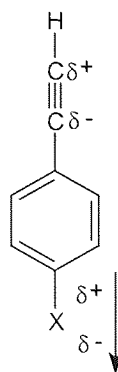


Figure 118 : schematic of π -polarisation

Normally, in phenylacetylenes, C2 is more significantly shielded than C1, but this effect is reversed when a nitro group is para to the alkyne (**18**). This reversal occurs because of the powerful resonance acceptor properties of the nitro group which are manifested in the deshielding of C2 only. It is important to emphasise that this is not a formal change of alkyne bond polarity, as suggested by Izawa *et al.*¹³³, but a substituent induced change peculiar to NMR analysis.

5.4.4 Electron withdrawing groups in the meta position.

Electron withdrawing groups in the meta position (**10**, **12-14**) deshield C2, and the effect increases with increasing acceptor strength. Since direct resonance interactions between 1,3- aromatic substituents are absent, the deshielding of C2 must be attributable to π -polarisation of the electron system, as reported by Reynolds for styrene derivatives¹³¹. As already mentioned previously, the electron withdrawing groups studied all possess a significant dipole that engenders a polarisation of the π electron system. The polarisation effect modifies the distribution of π electrons about the acetylene carbons C1 and C2. The ¹³C NMR data shows that substituents containing stronger dipoles exert the largest deshielding of C2 from the meta position, which reinforces the concept of π -polarisation. The strength of the polarisation is greater for meta substituents in comparison to para substituents, because of the closer proximity of meta substituents to C2¹²⁸.

Although direct resonance plays no role in redistributing electrons from C2, a secondary type may operate, as described previously for donating meta substituents. This effect will be superimposed upon π -polarisation because the substituents studied possess dipoles, and are resonance acceptors. However the magnitude of SCS effects observed are far greater than those anticipated for secondary resonance only. Thus, it can be concluded that the major SCS effect is from π -polarisation. Additional problems are encountered because of the small shift dispersity for the substituents studied, where the difference in SCS of C2 (between **13** and **14**) is sometimes close to the experimental error of ^{13}C NMR.

5.4.5 Comparison of para and meta SCS

Difficulties arise when considering each type of substituent series individually because of the superposition of resonance, secondary resonance, and π -polarisation effects. By consideration of the NMR changes that occur on changing the substituent position from meta to para, an assessment of the relative magnitudes can be made.

Direct resonance is a considerably more potent effect than secondary resonance. By comparing the SCS changes of donating substituents in the meta and para positions this becomes evident, because the former induce secondary resonance and the latter direct resonance. For example, C2 of *m*-NH₂ (**5**) is shifted -0.59ppm, whereas the same carbon centre of *p*-NH₂ (**1**) is shifted by -2.29ppm. A comparison of other donating groups, **6-7** vs **2-3**, shows a similar trend. Thus the probe site C2 is relatively insensitive to changes in the strength of secondary resonance, whereas direct resonance has a much greater influence.

Assignment of SCS effects for para ring substituents that possess a dipole moment is difficult because direct resonance and π -polarisation operate simultaneously. Resonance plays no direct role in meta substituents, as previously described, so SCS effects can be ascribed to π -polarisation. The strength of the dipole has a direct influence on the SCS of C2, and this is seen in the compounds *m*-CHO (**10** +1.66ppm), *m*-CN (**13** +2.55ppm), and *m*-NO₂ (**14** +2.69ppm).

Electron withdrawing dipolar substituents in the para position should exert both π -polarisation and direct resonance effects. We have already discussed π -polarisation effects of dipolar substituents in the meta position, so any further SCS change can be attributed to a concomitant direct resonance effect. The SCS of substituents in the para position are significantly greater than those in the meta position, as shown by the compounds *p*-CHO (**16** +3.86ppm), *p*-CN (**17** +4.34ppm), *p*-NO₂ (**18** +5.13ppm). These values are approximately two to three times greater than the meta series discussed previously, compounds (**10**, **13**, **14**). The large influence of direct resonance is clearly observed by the SCS difference between *m*-NO₂ (**14**) and *p*-NO₂ (**18**), an increased SCS of +2.44ppm in the para position. Hence, both direct resonance and π -polarisation operate simultaneously, and both are equally important.

5.5 Polymerisability in relation to the NMR data

Most phenylacetylenes in this study were amenable to polymerisation by the MCAT/EtOH/THF system. There is no relation between the ¹³C NMR of the terminal alkyne and the polymerisability of the monomer. The polymerisability is more related to the ring substituent, in which those containing a sterically unhindered nitrogen atom bearing its lone pair of electrons do not polymerise well, if at all. The nitrogen containing molecule may act as a ligand by coordination to the catalyst centre in preference to the alkyne.

5.6 Conclusion

In summary, both the type of substituent, and the position of substitution affect the SCS of phenylacetylenes. Regardless of position, donors shield, and acceptors deshield C2 respectively. Donor substituents in the meta position induce secondary resonance, whereas dipole acceptors exhibit π -polarisation. Furthermore, the latter has a greater influence than the former. Donors in the para position exert direct resonance, and dipole acceptors exhibit direct resonance and π -polarisation. Both of these effects are comparable in magnitude in this position. There was no link between ^{13}C NMR data and the polymerisability of the monomer.

CHAPTER 6.
CONCLUSION AND FURTHER WORK

CHAPTER 6. CONCLUSION AND FURTHER WORK

6.1 Conclusion

Most polyradicals reported in the literature are paramagnetic because there is no mechanism by which their spins can interact with each other. Spin alignment through a conjugated π system has proved difficult to achieve because electron spin density tends to be localised on the radical species. The vision encompassing this project however was to integrate both a nitronyl nitroxide radical and a bridging group into a polymeric material. The bridging groups (nitro or cyano) would provide a pathway through which neighbouring spins can interact magnetically other than by delocalisation through a chain. Before these polyradicals could be prepared however, it was essential to develop a catalyst that could polymerise phenylacetylene monomers bearing a nitronyl nitroxide in good yield.

Initial trials with a very efficient catalyst described in the literature, $[\text{Rh}(\text{NBD})(\text{OCH}_3)]_2$ showed that polymerisation did not occur when the phenylacetylene possessed a bridging strongly electron withdrawing nitro group in the para position. The incompatibility of 4-nitro groups was not investigated further. In addition, there has been only one successful polymerisation of phenylacetylenes bearing nitronyl nitroxides radicals reported in the literature, using $\text{Rh}(\text{COD})(\text{NH}_3)\text{Cl}$. However, the yields of polymer were too low (40%) for it to be used in the synthesis of co-polymers in this research. A high yielding catalyst with good tolerance of nitronyl nitroxides was therefore required, so a new catalyst had to be synthesised. The yield and tolerance of rhodium catalysts are primarily determined by the ligands about the catalyst centre. Changing the ligand of a rhodium catalyst from COD to NBD tends to result in a significant increase in the yield of polymer obtained. Incorporating ammonia as a ligand into the catalyst also tends to give increased tolerance towards nitronyl nitroxide radicals. In this research both of these ligands were built into a new catalyst complex, $\text{Rh}(\text{NBD})(\text{NH}_3)\text{Cl}$ (MCAT). MCAT was synthesised successfully in a simple one step reaction, which gave the product in moderate yield.

Phenylacetylene and its simple derivatives were first polymerised in order to assess the effectiveness of the MCAT catalyst. The yields of polymers obtained were high (80% to 98%) using a system comprised of MCAT/ethanol/THF. Furthermore, monomers bearing functional groups such as halide, ketone, conjugated ketone, tetrahydropyran ethers, pyrrole, alkoxy, and esters were tolerated without a reduction in polymer yield. High weight average molecular weight polymers were obtained in each instance, with Mw in the range of 200,000 to 250,000. The MCAT catalyst also gave high yields of polymer containing a nitro bridging group (76% yield), which is a significant improvement over literature catalysts. However, a marked reduction in polymer yield was encountered when the monomer possessed a cyano group (25% yield). This "poisoning" effect is most likely to originate from the electronic similarities between a terminal alkyne and a cyano group, resulting in a blocking of the polymerisation mechanism. Experimental evidence from other nitrogen containing monomers also suggested that nitrogen atoms bearing a lone pair of electrons tend to inhibit polymerisation. Preferential coordination of the nitrogen to the rhodium centre is the most likely cause of the "poisoning" effect.

During assessment of MCATs tolerance towards functional groups it was discovered that the presence of benzene boronic acid (BBA) increased the yields of polymers in general by as much as 20%. The enhanced reactivity of the MCAT/BBA system was utilised in the polymerisation of a normally unreactive monomer, phenylacetylene bearing a 2,4-dinitrophenylhydrazine substituent, with reasonable success (53% yield). This catalyst system however also resulted in a reduction of the weight average molecular weight of the polymers, approximately 50% compared to those obtained from the MCAT only system. This reduction in molecular weight means that this catalyst system either is a more efficient initiator than MCAT alone or that more transfer reactions are occurring during polymerisation. It is unclear from this research which of these possibilities is occurring. It was found that BBA was not incorporated into the matrices of the polymers indicating that it acts as a co-catalyst. Polymerisation of a monomer bearing a nitronyl nitroxide using the MCAT/BBA system showed that the yield was 25% greater than that reported in the literature, thus showing that this system is the most efficient polymerisation catalyst known for phenylacetylenes bearing nitronyl nitroxide substituents.

The synthesis of co-polyradicals was initiated once a polymerisation system that could tolerate nitronyl nitroxides had been established. The co-polyradicals were designed to utilise dipolar (through-space) spin coupling, which is effective in molecular magnets. The spin coupling units or "bridging groups" utilised in this research were nitro, cyano, or fluoro groups. Monomers possessing these substituents were co-polymerised with monomers bearing nitronyl nitroxides using the MCAT system. The yields of co-polyradicals were remarkably high (70% to 90%) with no significant reduction in yield when using a cyano co-monomer.

The magnetic properties of these co-polyradicals were investigated, and several were found to possess interesting magnetic properties. One material that employed a nitro bridging groups (1:1 with respect to the nitronyl nitroxide radical) could be magnetised under the application of an external magnetic field, albeit at very low temperatures. This material is not naturally ferromagnetic but some magnetism can be induced artificially, such systems are known as spin glasses. The importance of the bridging group in the materials was demonstrated by changing the ratio of nitro group to nitronyl nitroxide from 1:1 to 2:1. This material, by contrast, was naturally a weak antiferromagnet but under an applied magnetic field became a very strong antiferromagnet. This was a highly unusual result, and has been interpreted as a rare type of magnetic material in which strips of spins align in opposite directions to their neighbouring strips.

The bridging groups are a necessity for the realisation of magnetic properties, as the homopolymer of phenylacetylene possessing a nitronyl nitroxide radical was paramagnetic and no unusual magnetic properties were found.

The highlight of this project was a co-polyradical containing cyano bridging groups in which short-range ferromagnetic interactions were found. Examination of the total spin moment showed a gradual increase when cooled from 300K to 100K, which is the signature of weak, but significant, ferromagnetic interactions. This result demonstrates that spin alignment through bridging groups can give rise to magnetic interactions in polymers. All literature reports of polyradicals that were designed to utilise through-space interactions failed to observe anything but paramagnetism. The materials prepared in this research therefore represent a significant advance towards a ferromagnetic polymer with long-range interactions.

6.2 Further work

Further work should be carried out using other co-monomers bearing "bridging" groups that are able to hydrogen bond, such as boronic acid, or hydroxyl groups. Hydrogen bonding could provide a mechanism through which spins exchange. It could also influence the morphology of the polyradical. The synthesis of these monomers will require careful consideration because the functional groups are either unstable or incompatible with respect to the conventional Sonogashira coupling.

The effect of increasing the density of the radicals and "bridging" groups should be investigated. Both of these groups should be incorporated into one monomer. This can be envisaged in *m*-nitrophenylacetylene bearing a nitronyl nitroxide at the other meta position. The cyano group would be more difficult to integrate into a monomer radical, because of incompatibilities with the synthesis of nitronyl nitroxides. This could be overcome using "protecting group" chemistry, in which the cyano group is regenerated after the nitronyl nitroxide is formed. A polyradical using this strategy would guarantee that a radical has an adjacent "bridging" group.

Further work is required to determine whether or not the conjugated backbone is necessary for magnetic interactions using the through-space design philosophy. If the magnetic properties are a result of interactions between radicals and "bridging" monomers then the conjugated backbone is superfluous. This could be tested by co-polymerising monomers based on styrene, rather than phenylacetylene. Magnetic properties may be enhanced by the incorporation of a long spacer group between the radical/"bridging" groups and

the polymer backbone. This would allow the groups to assemble in a liquid crystalline fashion. Magnetic spin interactions could be obtained if three dimensional ordering were to take place.

The use of benzenboronic acid as a co-catalyst for the polymerisation of phenylacetylenes ought to be examined. NMR experiments should indicate whether this co-catalyst complexes with the rhodium catalyst. Kinetic experiments would be required to determine if BBA stabilises a mechanistic pathway, or if it changes the polarity of the solvent system. Although ethanol is a good co-catalyst by itself, when it is combined with BBA increased yields are obtained. Theoretical modelling may reveal whether the boron atom modifies the electron density on its OH, compared to a normal alcohol group. This work would be of considerable value, as there are very few catalysts that polymerise phenylacetylenes in very high yields.

The poisoning effect of nitrogen containing monomers is worthy of further study. A polymer bearing a primary amine group would be of great significance, because of the ability of the group to form hydrogen bonds. Nitrogen atoms bearing lone pairs of electrons tend to inhibit polymerisation. NMR evidence could be used to determine if the nitrogen atom coordinates to the rhodium. A ligand of the catalyst could also be displaced, altering the steric and electronic factors of the catalyst. This is a distinct possibility, as the catalyst used in this research was formed by reaction with ammonia. If the ligands about the catalyst could be tailored to reduce the affinity towards nitrogen atoms, then not only could many novel polymers be prepared but it also may give increased yields of nitronyl nitroxide containing polyphenylacetylene. At the time of writing, the highest known yield obtained is the one reported in this research.

REFERENCES

- 1 Parker, R. J. (1990), *Advances in Permanent Magnetism*, USA, Wiley, pp. 1-14.
- 2 Miller, J., Epstein, A. (1990), "Magnetism Without Metals", *New Scientist*, **23rd June**, 52-56.
- 3 Crystal, B. (1997), "Your Flexible Friend", *New Scientist*, **8th Nov**, 42-45.
- 4 Miller, J. S., Epstein, A. J. (1994), "Organic and Organometallic Molecular Materials - Designer Magnets", *Angew. Chem. Int. Ed. Engl.*, **33**, 385-415.
- 5 Miller, J. S., Epstein, A. J. (1996), "Molecular and Polymeric Magnets", *Chemistry and Industry*, **15th Jan**, 49-53.
- 6 Dougherty, D.A. (1991), "Spin Control in Organic Molecules", *Acc. Chem. Res.*, **24**(3), 88-94.
- 7 Kollmar, C., Kahn, O. (1993), "Ferromagnetic Spin Alignment in Molecular Systems : An Orbital Approach", *Acc. Chem. Res.*, **26**(5), 259-265.
- 8 Turek, P., Nozawa, K., Shiomi, D., Awaga, K., Inabe, T., Maruyama, Y., Kinoshita, M. (1991), "Ferromagnetic Coupling in a New Phase of the *p*-Nitrophenyl Nitronyl Nitroxide Radical", *Chem. Phys. Lett.*, **180**, 327-331.
- 9 Crayston, J. A., Iraqi, A., Walton, J. C. (1994), "Polyradicals: Synthesis, Spectroscopy and Catalysis", *Chem. Soc. Rev.*, **23**(3), 147-155.
- 10 March, J. (1992), *Advanced Organic Chemistry* (4th edition), USA, Wiley.
- 11 Keana, J. F. (1978), "Newer Aspects of the Synthesis and Chemistry of Nitroxide Spin Labels", *Chem. Rev.*, **78**(1), 37-63.
- 12 Ballester, M. (1967), "Inert Carbon Free Radicals", *Pure Appl. Chem.*, **15**, 123-151.
- 13 Nonhebel, D. C., Walton, J. C. (1974), *Free-radical Chemistry*, Cambridge University Press, Great Britain, pp. 118.
- 14 Mukai, K., Nedachi, K. (1993), "Magnetic Properties of 1,5-Dimethylverdazyl Radicals. Evidence for the Ferromagnetic Exchange Interaction in 3-(4-chlorophenyl)-1,5-dimethyl-6-thioxoverdazyl Radical Solid", *Chem. Phys. Lett.*, **214**(6), 559-562.
- 15 Patel, M. K., Huang, J., Kaszynski, P. (1995), "Design of New Stable Radicals for Molecular Magnetic Materials", *Mol. Cryst. Liq. Cryst.*, **271**, 87-97.
- 16 Katritzky, A. R., Belyakov, S. A. (1994), "Syntheses of 3-(Substituted) -2,4,6-Triphenylverdazyls", *Can. J. Chem.*, **72**, 1849-1856.

- 17 Ullman, E. F., Osiecki, J. H., Boocock, D. G. B., Darcy, R. (1972), "Studies of Stable Free Radicals. X. Nitronyl Nitroxide Monoradicals and Biradicals as Possible Small Molecule Spin Labels", *J. Am. Chem. Soc.*, **94**(20), 7049-7059.
- 18 Angeloni, L., Caneschi, A., David, L., Fabretti, A., Ferraro, F., Gatteschi, D., Lirzin, A., Sessoli, R. (1994), "Crystal Structures, Magnetic and Non-linear Optical Properties of Methoxyphenyl Nitronyl-Nitroxide Radicals", *J. Mater. Chem.*, **4**(7), 1047-1053.
- 19 Kusaba, Y., Tamura, M., Hosokoshi, Y., Kinsolita, M., Sawa, H., Kato, R., Kobayashi, H. (1997), "Isolation of Crystals of a Planar Nitronyl Nitroxide Radical: 2-phenylbenzimidazol-1-yl N,N'-dioxide (PIBDO)", *J. Mater. Chem.*, **7**(8), 1377-1382.
- 20 Yamanaka, S., Kawakami, T., Nagao, H., Yamaguchi, K. (1995), "Theoretical Studies of Spin Populations on Nitronyl Nitroxide, Phenyl Nitronyl Nitroxide and P-NPNN", *Mol. Cryst. Liq. Cryst.*, **271**, 19-28.
- 21 Zheludev, A., Barone, V., Bonnet, M., Delley, B., Grand, A., Ressouche, E., Rey, P., Subra, R., Schweizer, J. (1994), "Spin Density in a Nitronyl Nitroxide Free Radical. Polarized Neutron Diffraction Investigation and ab Initio Calculations", *J. Am. Chem. Soc.*, **116**(5), 2019-2027.
- 22 Bonnet, M., Luneau, D., Ressouche, E., Rey, P., Schweizer, J., Wan, M., Wang, H., Zheludev, A. (1995), "The Experimental Spin Density of Two Nitrophenyl Nitroxides: A Nitronyl Nitroxide and an Imino Nitroxide", *Mol. Cryst. Liq. Cryst.*, **271**, 35-53.
- 23 Nakano, M., Yamada, S., Yamaguchi, K. (1998), "Negative Second Hyperpolarizability of the Nitronyl Nitroxide Radical", *Bull. Chem. Soc. Jpn.*, **71**(4), 845-850.
- 24 Hamachi, K., Matsuda, K., Itoh, T., Iwamura, H. (1998), "Synthesis of an Azobenzene Derivative Bearing Two Stable Nitronyl Nitroxide Radicals as Substituents and its Magnetic Properties", *Bull. Chem. Soc. Jpn.*, **71**(12), 2937-2943.
- 25 Awaga, K., Inabe, T., Nagashima, U., Maruyama, Y. (1989), "Two Dimensional Network of the Ferromagnetic Organic Radical, 2-(4-Nitrophenyl)-4,4,5,5-tetramethyl-4,5-dihydro-1H-imidazol-1-oxyl 3-N-Oxide", *J. Chem. Soc., Chem. Commun.*, 1617-1618.
- 26 Tamura, M., Nakazawa, Y., Shiomi, D., Nozawa, K., Hosokoshi, Y., Ishikawa, M., Takahashi, M. (1991), "Bulk Ferromagnetism in the β -phase Crystal of the p-Nitrophenyl Nitronyl Nitroxide Radical", *Chem. Phys. Lett.*, **186**(4,5), 401-404.

- 27 Allemand, P. M., Fite, C., Srdanov, G., Keder, N., Wudl, F., Canfield, P. (1991), "On the Complexities of Short Range Ferromagnetic Exchange in a Nitronyl Nitroxide", *Synthetic Metals*, **41-43**, 3291-3295.
- 28 Nakatsuji, S., Anzai, H. (1997), "Recent Progress in the Development of Organomagnetic Materials Based on Neutral Nitroxide and Charge Transfer Complexes Derived from Nitroxide Radicals", *J. Mater. Chem.*, **7**(11), 2161-2174.
- 29 Caneschi, A., Ferraro, F., Gatteschi, D., Lirzin, A., Novak, M. A., Rentschler, E., Sessoli, R. (1995), "Ferromagnetic Order in the Sulfur-Containing Nitronyl Nitroxide Radical, 2-(4-Thiomethyl)-phenyl-4,4,5,5-tetramethylimidazoline-1-oxyl-3-oxide, NIT(SMe)Ph", *Adv. Mater.*, **7**(5), 476-478.
- 30 Pei, Y., Kahn, O., Aebbersold, M. A., Ouahab, L., Le Berre, F., Pardi, L., Tholence, J. L. (1994), "Synthesis, Crystal Structure, Magnetic Properties, and Spin Densities of a Triazole-Nitronyl-Nitroxide Radical", *Adv. Mater.*, **6**(9), 681-683.
- 31 Matsushita, M. M., Izuoka, A., Sugawara, T. (1996), "Ferromagnetic Spin Ordering Along Intermolecular Hydrogen Bonds of a Hydroquinone Derivative Carrying a Nitronyl Nitroxide", *Mol. Cryst. Liq. Cryst.*, **279**, 139-144.
- 32 Cirujeda, J., Mas, M., Molins, E., Lanfranc de Panthou, F., Laugier, J., Park, J., Paulsen, C., Rey, P., Rovira, C., Veciana, J. (1995), "Control of the Structural Dimensionality in Hydrogen-bonded Self-assemblies of Open-shell Molecules. Extension of Intermolecular Ferromagnetic Interactions in α -Phenyl Nitronyl Nitroxide Radicals into Three Dimensions", *J. Chem. Soc., Chem. Commun.*, 709-710.
- 33 Chiarelli, R., Novak, M. A., Rassat, A., Tholence, J. L. (1993), "A Ferromagnetic Transition at 1.48K in an Organic Nitroxide", *Nature*, **363**, 147-149.
- 34 Yoshizawa, K., Hoffman, R. (1995), "The Role of Orbital Interactions in Determining Ferromagnetic Coupling in Organic Molecular Assemblies", *J. Am. Chem. Soc.*, **117**(26), 6921-6926.
- 35 Lanfranc de Panthou, F., Luneau, D., Laugier, J., Rey, P. (1993), "Crystal Structures and Magnetic Properties of a Nitronyl Nitroxide and of Its Imino Analogue. Crystal Packing and Spin Distribution Dependence of Ferromagnetic Intermolecular Interactions", *J. Am. Chem. Soc.*, **115**(20), 9095-9100.
- 36 Takeda, K., Konishi, K., Masafumi, T., Kinoshita, M. (1995), "Magnetism of the β -Phase *p*-Nitrophenyl Nitronyl Nitroxide Crystal", *Mol. Cryst. Liq. Cryst.*, **273**, 57-66.
- 37 Hosokoshi, Y., Tamura, M., Kinoshita, M., Sawa, H., Kato, R., Fujiwara, Y., Ueda, Y. (1994), "Magnetic Properties and Crystal Structure of the *p*-Fluorophenyl Nitronyl

Nitroxide Radical Crystal: Ferromagnetic Intermolecular Interactions Leading to a Three-dimensional Network of Ground Triplet Dimeric Molecules", *J. Mater. Chem.*, **4**(8), 1219-1226.

- 38 Sugano, T., Tamura, M., Kinoshita, M., Sakai, Y., Ohashi, Y. (1992), "Ferromagnetic Intermolecular Interaction in an Organic Radical 3-Quinolyl Nitronyl Nitroxide (3-QNNN)", *Chem. Phys. Lett.*, **200**(3), 235-240.
- 39 Okumura, M., Yamaguchi, K., Awaga, K. (1994), "Ferromagnetic Intermolecular Interaction of the Cation Radical of the *m*-N-methylpyridinium Nitronyl Nitroxide. A CASSCF Study", *Chem. Phys. Lett.*, **228**, 575-582.
- 40 Hosokoshi, Y., Tamura, M., Sawa, H., Kato, R., Kinoshita, M. (1995), "Two-dimensional Ferromagnetic Intermolecular Interactions in Crystals of the *p*-Cyanophenyl Nitronyl Nitroxide Radical", *J. Mater. Chem.*, **5**(1), 41-46.
- 41 Cirujeda, J., Hernandez-Gasio, E., Lan-Franc de Pantahou, F., Laugier, J., Mas, M., Molins, E., Rovira, C., Novoa, J. J., Rey, P., Veciana, J. (1995), "The Hydrogen Bonding Strategy. A New Approach Towards Purely Organic/Molecular Ferromagnets", *Mol. Cryst. Liq. Cryst.*, **271**, 1-12.
- 42 Hernandez, E., Mas, M., Molins, E., Rovira, C., Veciana, J. (1993), "Hydrogen Bonds as a Crystal Design Element for Organic Molecular Solids with Intermolecular Ferromagnetic Interactions", *Angew. Chem. Int. Ed. Engl.*, **32**(6), 882-884.
- 43 Veciana, J., Cirujeda, J., Rovira, C., Molins, E., Novoa, J. J. (1996), "Organic Ferromagnets. Hydrogen Bonded Supramolecular Magnetic Organizations Derived from Hydroxylated Phenyl α -Nitronyl Nitroxide Radicals", *J. Phys. I*, **6**(12), 1967-1986.
- 44 Romero, F. M., Ziessel, R., Cian, A., Fischer, J., Turek, P. (1996), "Synthesis, Crystal Structure and Magnetic Properties of Novel Stable Nitronyl-Nitroxide Pyridine-Based Radicals", *New J. Chem.*, **20**(9), 919-924.
- 45 Lang, A., Pei, Y., Ouahab, L., Kahn, O. (1996), "Synthesis, Crystal Structure, and Magnetic Properties of 5-Methyl-1,2,4-Triazole-Nitronyl Nitroxide: A One-Dimensional Compound with Unusually Large Ferromagnetic Intermolecular Interactions", *Adv. Mater.*, **8**, 60-62.
- 46 Akita, T., Mazaki, Y., Kobayashi, K. (1995), "Ferromagnetic Spin Interaction in a Crystalline Molecular Complex Formed by Inter-heteromolecular Hydrogen Bonding: a 1 : 1 Complex of Phenyl Nitroxide Radical and Phenylboronic Acid", *J. Chem. Soc., Chem. Commun.*, **18**, 1861-1862.
- 47 Akita, T., Mazaki, Y., Kobayashi, K. (1996), "Ferromagnetic Spin Interaction Through the Inter-Heteromolecular Hydrogen Bond: a 1:1 Crystalline Complex of

- Phenylboronic Acid and Phenyl Nitronyl Nitroxide", *Mol. Cryst. Liq. Cryst.*, **279**, 39-45.
- 48 Katulevskii, Y. A., Magrupov, M. A., Muminov, A. A. (1992), "Peculiarities of Magnetic Resonance in Organic Ferromagnet of Pyrolyzed Polyacrylonitrile", *J. Non-Crystalline Solids*, **142**, 155-158.
 - 49 Miller, J. S. (1992), "The Quest for Magnetic Polymers - Caveat Emptor", *Adv. Mater.*, **4**(4), 298-300.
 - 50 Miller, J. S. (1992), "The Quest for Magnetic Polymers - Caveat Emptor", *Adv. Mater.*, **4**(6), 435-438.
 - 51 Ito, A., Ota, K., Tanaka, K., Yamabe, T. (1995), "*n*-Alkyl Group-Substituted Poly(*m*-aniline)s: Syntheses and Magnetic Properties", *Macromolecules*, **28**(16), 5618-5625.
 - 52 Rossitto, F. C., Lahti, P. M. (1993), "Poly[3,5-di-*tert*-butyl-4-[(2,4,6-tri-*tert*-butyl-phenyl)oxalato] phenylacetylene: A Photochemical Precursor to a Conjugated Polyradical", *Macromolecules*, **26**(23), 6308-6309.
 - 53 Miura, Y., Inui, K., Yamaguchi, F., Inoue, M., Teki, Y., Takui, T., Itoh, K. (1992), "Molecular Design, Synthesis, and Magnetic Characterization of Poly(phenylacetylene) with π -Toporegulated Pendant Nitronyl Nitroxide Radicals as Models for Organic Superpara- and Ferromagnets", *J. Polym. Sci., Polym. Chem. Ed.*, **30**, 959-966.
 - 54 Endo, T., Takuma, K., Takata, T., Hirose, C. (1993), "Synthesis and Polymerisation of 4-(Glycidyoxy)-2,2,6,6-tetramethylpiperidine-1-oxyl", *Macromolecules*, **26**(12), 3227-3229.
 - 55 Vlietstra, E. J., Nolte, R. J. M., Zwikker, J. W., Drenth, W., Meijer, E. W. (1990), "Synthesis and Magnetic Properties of a Rigid High Spin Density Polymer with Piperidine-N-Oxyl Pending Groups", *Macromolecules*, **23**(4), 946-948.
 - 56 Cao, Y., Wang, P., Hu, Z., Li, S., Zhang, L. (1988), "Magnetic Characterization of Organic Ferromagnet -Poly-BIPO and its Analogue", *Solid State Comm.*, **68**(9), 817-820.
 - 57 Rajca, A. (1994), "Organic Diradicals and Polyradicals : From Spin Coupling to Magnetism ?", *Chem. Rev.*, **94**(4), 871-893.
 - 58 Dulong, L., Lutz, S. (1993), "Polymerization of Acetylene Derivatives with Nitroxyl Radical Pendant Groups", *Makromol. Chem. Rapid Commun.*, **14**, 147-153.

- 59 Alexander, C., Feast, W. J., Friend, R. H., Sutcliffe, L. H., (1992), "Electron Paramagnetic Resonance and Magnetic Susceptibility Studies of New Substituted Poly(acetylene) Derivatives", *J. Mater. Chem.*, **2**(4), 459-465.
- 60 Miura, Y., Ushitani, Y. (1993), "Synthesis and Characterisation of Poly(1,3-phenyleneethynylene) with Pendant Nitroxide Radicals", *Macromolecules*, **26**(25), 7079-7082.
- 61 Swoboda, P., Saf, R., Hummel, K., Hofer, F., Czaputa, R. (1995), "Synthesis and Characterization of a Conjugated Polymer with Stable Radicals in the Side Groups", *Macromolecules*, **28**(12), 4255-4259.
- 62 Fujii, A., Ishida, T., Koga, N., Iwamura, H. (1991), "Syntheses and Magnetic Properties of Poly(phenylacetylenes) Carrying a (1-Oxido-3-oxy-4,4,5,5-tetramethyl-2-imidazolin-2-yl) Group at the Meta or Para Position of the Phenyl Ring", *Macromolecules*, **24**(5), 1077-1082.
- 63 Nishide, H., Kaneko, T., Igarashi, M., Tsuchida, E., Yoshioka, N., Lahti, P. M. (1994), "Magnetic Characterization and Computational Modeling of Poly(phenylacetylene)s Bearing Stable Radical Groups", *Macromolecules*, **27**(11), 3082-3086.
- 64 Ragossnig, H., Saf, R., Hummel, K. (1996), "Synthesis and Characterization of Polyradicals with a Polyimine Backbone and Nitronyl Nitroxide Side Groups", *Eur. Polym. J.*, **32**(11), 1307-1312.
- 65 Nishide, H., Kaneko, T., Nii, T., Katoh, K., Tsuchida, E., Yamaguchi, K. (1995), "Through-Bond and Long-Range Ferromagnetic Spin Alignment in a π -Conjugated Polyradical with a Poly(phenylenevinylene) Skeleton", *J. Am. Chem. Soc.*, **117**(1), 548-549.
- 66 Kaneko, T., Toriu, S., Nii, T., Tsuchida, E., Nishide, H. (1995), "Poly[(N-Oxyamino) and (Oxyphenyl)phenylenevinylene)s: Magnetically Coupled Polyradicals in the Chain", *Mol. Cryst. Liq. Cryst.*, **272**, 153-160.
- 67 Nishide, H., Kaneko, T., Toriu, S., Kuzumaki, Y., Tsuchida, E. (1996), "Synthesis of and Ferromagnetic Coupling in Poly(phenylenevinylene)s Bearing Built-in *t*-Butyl Nitroxides", *Bull. Chem. Soc. Jpn.*, **69**(2), 499-508.
- 68 Allgaier, J., Finkelmann, H. (1994), "Synthesis and Magnetic Properties of Mesogenic Side-Chain Polymers Containing Stable Radicals", *Macromol. Chem. Phys.*, **195**, 1019-1030.
- 69 Bosch, J., Rovira, C., Veciana, J., Castro, C., Palacio, F. (1993), "Synthesis and Study of a Stable Polyradical Macromolecule with a Helical Structure. A Poly(iminomethylene) with Verdazyl Radicals as Side Groups", *Synthetic Metals*, **55-57**, 1141-1146.

- 70 Vogel, A. I. (1956), *Practical Organic Chemistry* (3rd edition), Longmans, USA.
- 71 Wertz, J. E., Bolton, J. R. (1986), *Electron Spin Resonance. Elemental Theory and Practical Applications*, McGraw-Hill, USA.
- 72 Homer, J., Perry, M.C. (1994), "New Method for NMR Signal Enhancement by Polarization Transfer, and Attached Nucleus Testing", *J. Chem. Soc. Chem. Commun.*, **4**, 373-374.
- 73 Crangle, J. (1991), *Solid State Magnetism*, Great Britain, Edward Arnold.
- 74 Clarke, J. (1994), "SQUIDS", *Scientific American*, **August**, 36-43.
- 75 Gallop, J. C. (1991), *SQUIDS, the Josephson Effects and Superconducting Electronics*, IOP Publishing Ltd, England.
- 76 Mesnard, D., Bernadou, F., Miginiac, L. (1981), "Selection Methods for the Unequivocal Synthesis of Alkynes. Part 3. Arylacetylenes and 1-Arylalk-1-ynes", *J. Chem. Res. (S)*, **9**, 270-271.
- 77 Masuda, T., Hamano, T., Higashimura, T. (1988), "Synthesis and Characterization of Poly[[*o*-(trifluoromethyl)phenyl]acetylene]", *Macromolecules*, **21**(2), 281-286.
- 78 Stephens, R. D., Castro, C. E. (1963), "The Substitution of Aryl Iodides with Cuprous Acetylides. A Synthesis of Tolanes and Heterocyclics", *J. Org. Chem.*, **28**, 3313-3315.
- 79 Heck, R. F. (1985), *Palladium Reagents in Organic Synthesis*, Academic Press Ltd, San Diego.
- 80 Yashima, E., Maeda, Y., Matsushima, T., Okamoto, Y. (1997), "Preparation of Polyacetylenes Bearing an Amine Group and Their Application to Chirality Assignment of Carboxylic Acids by Circular Dichromism", *Chirality*, **9**, 593-600.
- 81 Fitton, P., Rick, E.A. (1971), "The Addition of Aryl Halides to Tetrakis(Triphenylphosphine) Palladium(0)", *J. Organomet. Chem.*, **28**, 287-291.
- 82 Thorand, S., Krause, N. (1998), "Improved Procedures for the Palladium-Catalyzed Coupling of Terminal Alkynes with Aryl Bromides (Sonogashira Coupling)", *J. Org. Chem.*, **63**(23), 8551-8553.
- 83 Larhed, M., Hallberg, A. (1996), "Microwave-Promoted Palladium-Catalyzed Coupling Reactions", *J. Org. Chem.*, **61**(26), 9582-9584.
- 84 Bleicher, L., Cosford, N. D. P. (1995), "Aryl- and Heteroaryl-Alkyne Coupling Reactions Catalyzed by Palladium on Carbon and CuI in an Aqueous Medium", *Synlett*, **November**, 1115-1116.

- 85 Miyashita, N., Toshikoshi, A., Grieco, P. A. (1977), "Pyridinium p-Toluenesulfonate. A Mild and Efficient Catalyst for the Tetrahydropyranylation of Alcohols", *J. Org. Chem.*, **42**, 3772-3774.
- 86 Austin, W. B., Bilow, N., Kelleghan, W. J., Lau, K. S. Y. (1981), "Facile Synthesis of Ethynylated Benzoic Acid Derivatives and Aromatic Compounds via Ethynyltrimethylsilane", *J. Org. Chem.*, **46**(11), 2280-2286.
- 87 Williams, D. H., Fleming, I. (1989), *Spectroscopic Methods in Organic Chemistry*, McGraw-Hill, London.
- 88 Le Moigne, J., Hilberer, A., Strazielle, C. (1992), "Poly(phenylacetylene) Derivatives for Nonlinear Optics", *Macromolecules*, **25**(24), 6705-6710.
- 89 Ogale, K., Wilson, M. L., Ehrlich, P. (1987), "Temperature and Field-dependence of Electron Currents in Films of *trans*-Polyphenylacetylene", *Polymer*, **28**, 587-592.
- 90 Neher, D., Kaltbeitzel, A., Wolf, A., Bubeck, C., Wegner, G. (1991), "Linear and Non-linear Optical Properties of Substituted Polypphenylacetylene Thin Films", *J. Phys. D: Appl. Phys.*, **24**, 1193-1202.
- 91 Wentworth, S. E., Bergquist, P. R. (1985), "Regiospecifically Substituted Poly(phenylacetylenes) as Potential Chemical Detectors", *J. Polym. Sci, Polym. Chem. Ed.*, **23**, 2197-2203.
- 92 Masuda, T., Hamano, T., Tsuchihara, K., Higashimura, T. (1990), "Synthesis and Characterization of Poly[[*o*-(trimethylsilyl)phenyl]acetylene]", *Macromolecules*, **23**, 1374-1380.
- 93 Yoshida, T., Abe, Y., Masuda, T., Higashimura, T. (1996), "Polymerization and Polymer Properties of (*p*-*tert*-Butyl-*o*,*o*-dimethylphenyl)acetylene", *J. Polym. Sci, Polym. Chem. Ed.*, **34**, 2229-2236.
- 94 Seki, H., Masuda, T. (1995), "Polymerization of [*o*-n-(Perfluorohexyl)phenyl]acetylene and Polymer Properties", *J. Polym. Sci, Polym. Chem. Ed.*, **33**, 1907-1912.
- 95 Mizumoto, T., Masuda, T., Higashimura, T. (1993), "Polymerization of [*o*-(Trimethylgermyl)phenyl]acetylene and Polymer Characterization", *J. Polym. Sci, Polym. Chem. Ed.*, **31**, 2555-2561.
- 96 Schrock, R. R., Luo, S., Lee, J. C., Zanetti, N. C., Davis, W. M. (1996), "Living Polymerization of (*o*-(Trimethylsilyl)phenyl)acetylene by Molybdenum Imido Alkylidene Complexes", *J. Am. Chem. Soc.*, **118**(16), 3883-3895.

- 97 Schrock, R. R., Lou, S., Zanetti, N. C., Fox, H. F. (1994), "Living Polymerization of (*o*-(Trimethylsilyl)phenyl)acetylene Using "Small Alkoxide" Molybdenum(VI) Initiators", *Organometallics*, **13**(9), 3396-3398.
- 98 Sedlacek, J., Vohlidal, J., Cabioch, S. Lavastre, O., Dixneuf, P., Balcar, H., Sticha, M. (1998), "Polymerization of *p*-Nitrophenylacetylene with Metathesis Catalysts. Photoelectrical Properties of Phenylacetylene/*p*-Nitrophenylacetylene Copolymer", *Macromol. Chem. Phys.*, **199**, 155-161.
- 99 Yang, M., Zhan, X., Zhao, J., Shen, Z. (1995), "Simultaneous Polymerization and Formation of Polyphenylacetylene Film by Nd(P₂₀₄)₃-Fe(AA)₃-Al(*i*-Bu)₃ Combined Catalyst System", *J. Polym. Sci, Polym. Chem. Ed.*, **33**, 1873-1879.
- 100 Lee, S., Shim, S., Kim, T. (1996), "Catalytic Polymerization of Phenylacetylene by Cationic Rhodium and Iridium Complexes of Ferrocene-based Ligands", *J. Polym. Sci, Polym. Chem. Ed.*, **34**, 2377-2386.
- 101 Furlani, A., Napoletano, C., Russo, M. V., Camus, A., Marisch, N. (1989), "The Influence of the Ligands on the Catalytic Activity of a Series of Rh^I Complexes with Phenylacetylene: Synthesis of Stereoregular Poly(phenyl) Acetylene", *J. Polym. Sci, Polym. Chem. Ed.*, **27**, 75-86.
- 102 Russo, M. V., Furlani, A., D'Amato, R. (1998), "Synthesis and Properties of *p*-Nitrophenylacetylene-Phenylacetylene Copolymers", *J. Polym. Sci, Polym. Chem. Ed.*, **36**, 93-102.
- 103 Yang, W., Tabata, M., Kobayashi, S., Yokota, K., Shimizu, A. (1991), "Synthesis of Ultra-High-Molecular-Weight Aromatic Polyacetylenes with [Rh(norbornadiene)Cl]₂-Triethylamine and Solvent-Induced Crystallization of the Obtained Amorphous Polymers", *Polymer Journal*, **23**(9), 1135-1138.
- 104 Kishimoto, Y., Itou, M., Miyatake, T., Ikariya, T., Noyori, R. (1995), "Polymerization of Monosubstituted Acetylenes with a Zwitterionic Rhodium(I) Complex, Rh⁺(2,5-norbornadiene)[η⁶-C₆H₅)B⁻(C₆H₅)₃]", *Macromolecules*, **28**(19), 6662-6666.
- 105 Kishimoto, Y., Miyatake, T., Ikariya, T., Noyori, R. (1996), "An Efficient Rhodium(I) Initiator for Stereospecific Living Polymerization of Phenylacetylenes", *Macromolecules*, **29**(14), 5054-5055.
- 106 Tang, B. Z., Poon, W. H., Leung, S. M., Leung, W. H., Peng, H. (1997), "Synthesis of Stereoregular Poly(phenylacetylene)s by Organorhodium Complexes in Aqueous Media", *Macromolecules*, **30**(7), 2209-2212.
- 107 Lindgren, M., Lee, H., Yang, W., Tabata, M. Yokota, K. (1991), "Synthesis of Soluble Polyphenylacetylenes containing a Strong Donor Function", *Polymer*, **32**(8), 1531-1534.

- 108 Escudero, A., Vilar, R., Salcedo, R., Ogawa, T. (1995), "Effects of Substituent Groups and Substituted Benzenes on the Polymerization of Phenylacetylenes Initiated by Di- μ -pentafluorothiophenolate bis(1,5-cyclooctadiene) Rhodium(I)", *Eur. Polym. J.*, **31**(11), 1135-1138.
- 109 Schniedermeier, J., Haupt, H.-J. (1996), "New Rhodium(I)-(π)-chelate Complexes with Coordinated Amidine Bases (dbu, dbn) and Their Catalytic Properties to Polymerize Phenylacetylene", *J. Organomet. Chem.*, **506**, 41-47.
- 110 Hirao, K., Ishii, Y., Terao, T., Kishimoto, Y., Miyatake, T., Ikariya, T., Noyori, R. (1998), "Solid-State NMR Study of Poly(phenylacetylene) Synthesized with a Rhodium Complex Initiator", *Macromolecules*, **31**(11), 3405-3408.
- 111 Tabata, M., Yang, W., Yokota, K. (1994), " ^1H -NMR and UV Studies of Rh Complexes as a Stereoregular Polymerization Catalysts for Phenylacetylenes: Effects of Ligands and Solvents on Its Catalyst Activity", *J. Polym. Sci., Polym. Chem. Ed.*, **32**, 1113-1120.
- 112 Yoshimura, T. (1993), "Polymerization of *o*-chloro and *o*-bromo-substituted Phenylacetylenes and Polymer Properties", *Polymer Bulletin*, **31**, 511-516.
- 113 Katayama, H., Yamamura, K., Miyaki, Y., Ozawa, F. (1997), "Stereoregular Polymerization of Phenylacetylenes Catalyzed by [Hydridotris(pyrazolyl)borato]rhodium(I) Complexes", *Organometallics*, **16**, 4497-4500.
- 114 Zassinovich, G., Mestroni, G., Camus, A. (1975), "Diolefinic Complexes of Rhodium(I) and Iridium(I) with Nitrogen-containing Ligands", *J. Organomet. Chem.*, **91**, 379-388.
- 115 Tabata, M., Sone, T., Sadahiro, Y., Yokota, K., Nozaki, Y. (1998), "Pressure-Induced Cis to Trans Isomerization of Aromatic Polyacetylenes Prepared Using a Rh Complex Catalyst: A Control of π -Conjugation Length", *J. Polym. Sci., Polym. Chem. Ed.*, **36**, 217-223.
- 116 Kishimoto, Y., Eckerle, P., Miyatake, T., Ikariya, T., Noyori, R. (1994), "Living Polymerization of Phenylacetylenes Initiated by $\text{Rh}(\text{C}=\text{CC}_6\text{H}_5)(2,5\text{-norbornadiene})[\text{P}(\text{C}_6\text{H}_5)_3]_2$ ", *J. Am. Chem. Soc.*, **116**(26), 12131-12132.
- 117 Miyaura, N., Suzuki, A. (1995), "Palladium-Catalyzed Cross Coupling Reactions of Organoboron Compounds", *Chem. Rev.*, **95**(7), 2457-2483.
- 118 Nath, K., Taylor, P. L. (1991), "Electronic Structure and Magnetic Properties of Some Possible Organic Ferromagnetic Polymers", *Mol. Cryst. Liq. Cryst.*, **205**, 87-100.

- 119 Miura, Y., Issiki, T., Ushitani, Y., Teki, Y., Itoh, K. (1996), "Synthesis and Magnetic Behaviour of Polyradical: poly(1,3-phenyleneethynylene) with (π)-toporegulated Pendant Stable Aminoxy and Imine *N*-oxide-aminoxy Radicals", *J. Mater. Chem.*, **6**(11), 1745-1750.
- 120 Palacio, F., Ramos, J., Castro, C. (1993), "Magnetic Polymers", *Mol. Cryst. Liq. Cryst.*, **232**, 173-194.
- 121 Mitsumori, T., Inoue, K., Koga, N., Iwamura, H. (1995), "Exchange Interaction between Two Nitronyl Nitroxide or Iminyl Nitroxide Radicals Attached to Thiophene and 2,2'-Bithienyl Rings", *J. Am. Chem. Soc.*, **117**, 2467-2478.
- 122 Whitehead, J. P., De Bell, K. (1994), "Stability of Striped Phases in Two-Dimensional Dipolar System", *J. Phys.: Condens. Matter.*, **6**, L731-L734.
- 123 Garel, T., Doniach, S. (1982), "Phase Transitions with Spontaneous Modulation - the Dipolar Ising Ferromagnet", *Phys. Rev. B*, **26**, 325-329.
- 124 Dessy, R. E., Okuzumi, Y., Chen, A. (1962), "The Acidities of Some Weak Acids", *J. Am. Chem. Soc.*, **84**, 2899-2904.
- 125 Ito, O., Fleming, M. D. C. M. (1989), "Substituent Effects on the Free-radical Addition Reactions of Arylthiyl Radicals and Arylacetylenes", *J. Chem. Soc. Perkin Trans. II*, **6**, 689-693.
- 126 Dawson, D. A., Reynolds, W. F. (1975), "Investigations of Substituent Effects by Nuclear Magnetic Resonance Spectroscopy and All-valence Electron Molecular Orbital Calculations. IV. 4-Substituted Phenylacetylenes", *Can. J. Chem.*, **53**, 373-382.
- 127 Hamer, G. K., Peat, I. R., Reynolds, W. F. (1973), "Investigation of Substituent Effects by Nuclear Magnetic Spectroscopy and All-valence Electron Molecular Orbital Calculations. I. 4-Substituted Styrenes", *Can. J. Chem.*, **51**, 897-914.
- 128 Bromilow, J., Brownlee, R. T. C., Craik, D. J., Fiske, P. R., Rowe, J. E., Sadek, M. (1981), "Carbon-13 Substituent Chemical Shifts in the Side-chain Carbons of Aromatic Systems: the Importance of π -Polarization in Determining Chemical Shifts", *J. Chem. Soc. Perkin Trans. II*, **5**, 753-759.
- 129 Spiesecke, H., Schneider, W. G. (1961), "Substituent Effects on the C^{13} and H^1 Chemical Shifts in Monosubstituted Benzenes", *J. Chem. Phys.*, **35**(2), 731-738.
- 130 Bromilow, J., Brownlee, R. T. C., Craik, D. J., Sadek, M. (1986), "Non-additive Carbon-13 NMR Substituent Chemical Shifts", *Magn. Res. Chem.*, **24**, 862-871.
- 131 Reynolds, W. F., Gomes, A., Maron, A., MacIntyre, D. W., Tanin, A., Hamer, G. K., Peat, I. R. (1983), "Substituent-induced Chemical Shifts in 3- and 4-substituted

Styrenes : Definition of Substituent Constants and Determination of Mechanisms of Transmission of Substituent Effects by Iterative Multiple Linear Regression", *Can. J. Chem.*, **61**, 2376-2384.

- 132 Hamer, G. K., Peat, G. K., Reynolds, W. F. (1973), "Investigation of Substituent Effects by Nuclear Magnetic Spectroscopy and All-valence Electron Molecular Orbital Calculations. I. 4-Substituted α -Methylstyrenes and α -*t*-Butylstyrenes", *Can. J. Chem.*, **51**, 915-926.
- 133 Izawa, K., Okuyama, T., Fueno, T. (1973), "Carbon-13 NMR Spectra of 1-Arylpropynes and 1-Arylpropenes. Transmission of the Electronic Effects of Substituents Through Carbon-Carbon Triple and Double Bonds", *Bull. Chem. Soc. Jap.*, **46**, 2881-2883.

APPENDIX

CHARACTERISATION OF PHENYLACETYLENE MONOMERS

4-Ethynylaniline (4AMPA)

4AMPA was synthesised from 4-iodoaniline and was obtained as pale brown crystals (65%); mp 100.5-101.5°C; $\nu_{\max}/\text{cm}^{-1}$ 3484 (s, sharp, -NH₂), 3386 (s, sharp, -NH₂), 3258 (s, sharp, -C≡C-H), 2096 (m, sharp, -C≡C-), 1616 (s, sharp, Ph), 1512 (s, sharp, Ph); δ_{H} (300 MHz; CDCl₃) 7.28 (2 H, d, Ph), 6.57 (2 H, d, Ph), 3.81 (2 H, br s, NH₂), 2.96 (1 H, s, ≡C-H); δ_{C} (75 MHz; CDCl₃) 147.06 (Ph), 133.46 (Ph), 114.58 (Ph), 111.20 (Ph), 84.44 (Ph-C≡), 74.98 (≡C-H); m/z (APCI) 118 (MH⁺).

3-Ethynylbenzaldehyde (3APA)

3APA was synthesised from 3-bromobenzaldehyde and was obtained as off-white crystals (52%); mp (from hexane) 76-77°C; $\nu_{\max}/\text{cm}^{-1}$ 3250 (s, sharp, -C≡C-H), 2851 (w, sharp, Ar-CHO), 1697 (s, sharp, CHO), 1595 (m, sharp, Ph); δ_{H} (300 MHz; CDCl₃) 9.98 (1 H, s, CHO), 7.97 (1 H, s, Ph), 7.85 (1 H, d, Ph), 7.71 (1 H, d, Ph), 7.49 (1 H, t, Ph), 3.15 (1 H, s, ≡C-H); δ_{C} (75 MHz; CDCl₃) 186.57 (CHO), 132.80 (Ph), 131.61 (Ph), 128.58 (Ph), 124.73 (Ph), 124.33 (Ph), 118.51 (Ph), 77.39 (Ph-C≡), 74.27 (≡C-H); m/z (EI) 130 (M⁺).

4-Bromophenylacetylene (4BrPA)

4BrPA was synthesised from 4-bromoiodobenzene and was obtained as white crystals (60%); mp (from hexane) 62-63°C; $\nu_{\max}/\text{cm}^{-1}$ 3263 (s, sharp, -C≡C-H), 1483 (s, sharp, Ph); δ_{H} (300 MHz; CDCl₃) 7.46-7.42 (2 H, split d, Ph), 7.35-7.32 (2 H, split d, Ph), 3.13 (1 H, s, ≡C-H); δ_{C} (75 MHz; CDCl₃) 133.47 (Ph), 131.52 (Ph), 123.07 (Ph), 120.95 (Ph), 82.52 (Ph-C≡), 78.37 (≡C-H); m/z (EI) 180 (M⁺, ⁷⁹Br), 182 (M⁺, ⁸¹Br).

3-Ethynylbenzonitrile (3CPA)

3CPA was synthesised from 3-bromobenzonitrile and was isolated as yellow crystals (67%); mp 45-46°C (from hexane); $\nu_{\max}/\text{cm}^{-1}$ 3292 (s, sharp, $-\text{C}\equiv\text{C}-\text{H}$), 3065 (w, sharp, Ph), 2230 (m, sharp, $\text{Ar}-\text{C}\equiv\text{N}$); δ_{H} (300 MHz; CDCl_3) 7.71 (1 H, s, Ph), 7.66 (1 H, d, Ph), 7.60 (1 H, d, Ph), 7.42 (1 H, t, Ph), 3.19 (1 H, s, $\equiv\text{C}-\text{H}$); δ_{C} (75 MHz; CDCl_3) 131.41 (Ph), 130.65 (Ph), 127.27 (Ph), 124.55 (Ph), 118.96 ($-\text{C}\equiv\text{N}$), 113.12 (Ph), 108.12 (Ph), 76.42 (Ph- $\text{C}\equiv$), 75.14 ($\equiv\text{C}-\text{H}$); m/z (APCI) 128 (MH^+).

4-Ethynylbenzonitrile (4CPA)

4CPA was synthesised from 4-bromobenzonitrile and was obtained as white crystals (82%); mp 153-154°C; $\nu_{\max}/\text{cm}^{-1}$ 3235 (s, sharp, $-\text{C}\equiv\text{C}-\text{H}$), 2226 (m, sharp, $\text{Ar}-\text{C}\equiv\text{N}$), 1600 (w, sharp, Ph), 1496 (w, sharp, Ph); δ_{H} (300 MHz; CDCl_3) 7.57 (4 H, quartet, Ph), 3.29 (1 H, $\equiv\text{C}-\text{H}$); δ_{C} (75 MHz; CDCl_3) 132.62 (Ph), 131.98 (Ph), 126.93 (Ph), 118.23 ($-\text{C}\equiv\text{N}$), 112.25 (Ph), 81.81 (Ph- $\text{C}\equiv$), 81.56 ($\equiv\text{C}-\text{H}$); m/z (EI) 127 (M^+).

3,5-Dichlorophenylacetylene (DCPA)

DCPA was synthesised from 3,5-dichloriodobenzene and was obtained as off-white crystals (76%); mp 81-83°C; $\nu_{\max}/\text{cm}^{-1}$ 3288 (m, sharp, $-\text{C}\equiv\text{C}-\text{H}$), 3070 (w, sharp, Ph), 1558 (s, sharp, Ph), 1412 (m, sharp, unassigned), 855 (m, sharp, Ph); δ_{H} (300 MHz; CDCl_3) 7.33 (3 H, s, Ph), 3.14 (1 H, s, $\equiv\text{C}-\text{H}$); δ_{C} (75 MHz; CDCl_3) 134.87 (Ph), 130.29 (Ph), 129.24 (Ph), 124.85 (Ph), 80.87 (Ph- $\text{C}\equiv$), 79.66 ($\equiv\text{C}-\text{H}$); m/z (APCI) 171 (MH^+ , ^{35}Cl), ^{35}Cl 173 (MH^+ , ^{35}Cl ^{37}Cl).

4-Ethynylphenylnitronyl nitroxide (4EPNN)

4EPNN was synthesised from 4APA and green crystals were obtained from slow evaporation of a concentrated DCM solution (36%); mp (from benzene) 158-159°C; $\nu_{\max}/\text{cm}^{-1}$ 3211 (s, sharp, $-\text{C}\equiv\text{C}-\text{H}$), 2994 (w, sharp, C-H), 2922 (w, sharp, C-H), 2098 (w, sharp, $-\text{C}\equiv\text{C}-$), 1387 (w, sharp, unassigned), 1361 (s, sharp, N-O), 1302 (m, sharp, unassigned), 1166 (m, sharp, nitronyl nitroxide), 1130 (w, sharp, nitronyl nitroxide); m/z (APCI) 258 (MH^+); EPR (in CHCl_3) showed 5 peaks in the ratio of 1:2:3:2:1.

5-Ethynylpyrimidine (5EPYM)

PEB899 was synthesised from 5-bromopyrimidine and was obtained as white crystals (55%); mp (from hexane) 81-82°C; $\nu_{\max}/\text{cm}^{-1}$ 3167 (s, sharp, $-\text{C}\equiv\text{C}-\text{H}$), 2103 (m, sharp, $-\text{C}\equiv\text{C}-$), 1545 (s, sharp, Ph), 1410 (s, sharp, Ph); δ_{H} (300 MHz; CDCl_3) 9.09 (1 H, s, Ph), 8.74 (2 H, s, Ph), 3.37 (1 H, s, $\equiv\text{C}-\text{H}$); δ_{C} (75 MHz; CDCl_3) 159.16 (Ph), 157.07 (Ph), 84.42 ($\equiv\text{C}-\text{H}$), 76.75 (Ph- $\text{C}\equiv$); m/z (EI) 104 (M^+).

3-Ethynylnitrobenzene (3NPA)

*** BEWARE : 3NPA gave a highly exothermic reaction when heated in air ***

3NPA was synthesised from 3-iodonitrobenzene and was obtained as a pale yellow liquid (90%); $\nu_{\max}/\text{cm}^{-1}$ 3289 (s, sharp, $-\text{C}\equiv\text{C}-\text{H}$), 3083 (m, sharp, Ph), 1531 (s, sharp, Ar- NO_2), 1354 (s, sharp, Ar- NO_2); δ_{H} (300 MHz; CDCl_3) 8.31-8.30 (1 H, split s, Ph), 8.18 (1 H, split d, Ph), 7.78-7.75 (1 H, split s, Ph), 7.50 (1 H, t, Ph), 3.20 (1 H, s, $\equiv\text{C}-\text{H}$); δ_{C} (75 MHz; CDCl_3) 137.76 (Ph), 129.37(Ph), 126.94 (Ph), 123.85 (Ph), 123.55 (Ph), 81.04 (Ph- $\text{C}\equiv$), 79.89 ($\equiv\text{C}-\text{H}$); m/z (EI) 147 (M^+).

4-Ethynylnitrobenzene (4NPA)

4NPA was synthesised from 4-iodonitrobenzene and was obtained as a pale yellow crystalline solid (78%); mp 147-148°C; $\nu_{\max}/\text{cm}^{-1}$ 3252 (m, sharp, $-\text{C}\equiv\text{C}-\text{H}$), 3106 (w, sharp, Ph), 2106 (w, sharp, $-\text{C}\equiv\text{C}-$), 1511 (s, sharp, Ar- NO_2), 1344 (s, sharp, Ar- NO_2); δ_{H} (300 MHz; CDCl_3) 8.18 (2 H, d, Ph), 7.62 (2 H, d, Ph), 3.34 (1 H, s, $\equiv\text{C}-\text{H}$); δ_{C} (75 MHz; CDCl_3) 147.46 (Ph), 132.92 (Ph), 128.86 (Ph), 123.35 (Ph), 82.33 ($\equiv\text{C}-\text{H}$), 81.55 (Ph- $\text{C}\equiv$); m/z (GCMS) 147 (M^+).

3-Ethynylanisole (3MeOPA)

3MeOPA was synthesised from 3-iodoanisole and was obtained as a pale yellow liquid (91%); $\nu_{\max}/\text{cm}^{-1}$ 3291(s, sharp, $-\text{C}\equiv\text{C}-\text{H}$), 2958 (w, sharp, C-H), 2834 (w, sharp, $-\text{OCH}_3$), 2107 (w, sharp, $-\text{C}\equiv\text{C}-$), 1577 (s, sharp, Ph), 1482 (s, sharp, Ph), 1283 (s, sharp, C-O), 1260 (s, sharp, unassigned), δ_{H} (300 MHz; CDCl_3) 7.23 (1 H, t, Ph), 7.11-7.08 (1 H, split doublet, Ph), 7.03-7.02 (1 H, split singlet, Ph), 6.92-6.88 (1 H, split doublet, Ph), 3.77 (3 H, s, OCH_3), 3.08 (1 H, s, $\equiv\text{C}-\text{H}$); δ_{C} (75 MHz; CDCl_3) 159.20 (Ph), 129.35 (Ph), 124.56

(Ph), 123.01 (Ph), 116.90 (Ph), 115.30 (Ph), 83.51 (Ph-C \equiv), 77.00 (\equiv C-H), 55.13 (OMe); m/z (EI) 132 (M^+); GC (150°C) 99.5% pure.

The non-terminal alkyne carbon peak was superimposed with the centre peak of CDCl₃ (also 77.00ppm). To accurately identify this peak a separate NMR experiment was carried out using a coupled ¹³C pulse sequence (including full NOE build-up). Using this technique the non-terminal alkyne carbon couples with the hydrogen to give a doublet, with the centre of the splitting identified as the original peak. This was recorded as δ 77.00ppm for the non-terminal alkyne.

2-(4-ethynylphenoxy)tetrahydro-2H-pyran (PEB943)

PEB943 was synthesised from 4-iodophenol and DHP, and was obtained as a white crystalline solid (76%); $\nu_{\max}/\text{cm}^{-1}$ 3279 (m, sharp, -C \equiv C-H), 2942 (m, sharp, C-H), 2869 (w, sharp, -O-CH₂-), 2106 (w, sharp, -C \equiv C-), 1604 (s, sharp, Ph), 1505 (s, sharp, Ph), 1239 (s, sharp, C-O); δ_{H} (300 MHz; CDCl₃) 7.44-7.40 (2 H, d, Ph), 7.01 (2 H, d, Ph), 5.42 (1 H, t, THP), 3.90-3.82 (1 H, split triplet, THP), 3.63-3.56 (1 H, multiplet, THP), 3.02 (1 H, s, -C \equiv C-H), 2.05-1.91 (1 H, multiplet, THP), 1.88-1.83 (2 H, multiplet, THP), 1.75-1.54 (3 H, multiplet, THP); δ_{C} (75 MHz; CDCl₃) 157.36 (Ph), 133.41 (Ph), 116.24 (Ph), 114.88 (Ph), 96.08 (THP), 83.61 (Ph-C \equiv), 75.82 (\equiv C-H), 61.92 (THP), 30.14 (THP), 25.04 (THP), 18.55 (THP); m/z (EI) 202 (M^+).

3,4-Ethylenedioxyphenylacetylene (PB029)

PB029 was synthesised from 3,4-ethylenedioxyiodobenzene and was obtained as a pale yellow liquid (89%); $\nu_{\max}/\text{cm}^{-1}$ 3288 (s, sharp, -C \equiv C-H), 2982 (m, sharp, C-H), 2933 (m, sharp, C-H), 2882 (m, sharp, -O-CH₂-), 2105 (m, sharp, -C \equiv C-), 1576 (s, sharp, Ph), 1503 (s, sharp, Ph), 1306 (s, sharp, C-O), 1287 (s, sharp, C-O); δ_{H} (300 MHz; CDCl₃) 7.00-6.99 (1 H, multiplet, Ph), 6.98-6.95 (1 H, multiplet, Ph), 6.78 (1 H, d, Ph), 4.23-4.19 (4 H, multiplet, -O-CH₂-CH₂-O-), 2.97 (1 H, s, \equiv C-H); δ_{C} (75 MHz; CDCl₃) 144.39 (Ph), 143.06 (Ph), 125.55 (Ph), 120.89 (Ph), 117.22 (Ph), 114.66 (Ph), 83.26 (Ph-C \equiv), 75.63 (\equiv C-H), 64.29 (-O-CH₂-), 64.05 (-O-CH₂-); m/z 161 (MH^+ , 100%).

2-Ethynylnaphthalene (PB032)

PB032 was synthesised from 2-bromonaphthalene and was obtained as a white crystalline solid (78%); mp 39-40°C (from EtOH); $\nu_{\max}/\text{cm}^{-1}$ 3278 (s, sharp, $-\text{C}\equiv\text{C}-\text{H}$), 3051 (w, sharp, naphth), 1593 (m, sharp, naphth), 1497 (m, sharp, naphth); δ_{H} (300 MHz; CDCl_3) 8.07 (1 H, s, naphth), 7.85-7.79 (3 H, multiplet, naphth), 7.59-7.50 (3 H, multiplet, naphth), 3.20 (1 H, s, $\equiv\text{C}-\text{H}$); δ_{C} (75 MHz; CDCl_3) 132.96 (naphth), 132.75 (naphth), 132.25 (naphth), 128.49 (naphth), 127.98 (naphth), 127.72 (naphth), 126.84 (naphth), 126.55 (naphth), 83.99 (Ph- $\text{C}\equiv$), 77.45 ($\equiv\text{C}-\text{H}$); m/z (APCI) 185 (methanol adduct of M^+).

1-(4-ethynylphenyl)pyrrole (PB055)

PB055 was synthesised from 1-(4-iodophenyl)pyrrole and was isolated as fine white needles (77%); mp 104-105°C (from EtOH); $\nu_{\max}/\text{cm}^{-1}$ 3254 (s, sharp, $-\text{C}\equiv\text{C}-\text{H}$), 1604 (s, sharp, Ph), 1515 (s, sharp, Ph); δ_{H} (300 MHz; CDCl_3) 7.56 (2 H, d, Ph), 7.36 (2 H, d, Ph), 7.11 (2 H, t, pyrrole), 6.39 (2 H, t, pyrrole), 3.13 (1 H, s, $\equiv\text{C}-\text{H}$); δ_{C} (75 MHz; CDCl_3) 140.56 (Ph), 133.38 (), 119.79 (), 118.95 (), 110.97 (), 82.89 (Ph- $\text{C}\equiv$), 77.62 ($\equiv\text{C}-\text{H}$); m/z (APCI) 168 (MH^+).

CHARACTERISATION OF HOMOPOLYMERS

Poly 2-(3-ethynylbenzyloxy)tetrahydro-2H-pyran (PB059)

PB059 was synthesised from PB054 and was isolated as a yellow / orange solid 43% yield; $\nu_{\max}/\text{cm}^{-1}$ 2938 (m, sharp, C-H), 2862 (w, sharp, -O-CH₂-), 1636 (m, broad, Ph), 1261 (w, sharp, C-O); SEC (Mw = 202,000 ; Mn = 33,800 ; Pd = 6.0); soluble in DCM, and THF.

Poly 1-(4-ethynylphenyl)pyrrole (PB057)

PB057 was synthesised from PB055 and was isolated as a yellow / orange solid 86% yield; $\nu_{\max}/\text{cm}^{-1}$ 1605 (m, sharp, Ph), 1510 (s, sharp, Ph), 1476 (m, sharp, Ph), 1327 (s, sharp, unassigned); (Found: C, 85.62; H, 5.34; N, 8.37. C₁₂H₉N requires C, 86.20; H, 5.42; N, 8.30).

Poly (4-fluoro)phenylacetylene (PB049)

PB049 was synthesised from 4-fluorophenylacetylene and was isolated as a yellow solid 95% yield; $\lambda_{\max}(\text{DCM})/\text{nm}$ 440; $\nu_{\max}/\text{cm}^{-1}$ 3050 (w, sharp, Ph), 1600 (m, sharp, Ph), 1502 (s, sharp, Ph), 1226 (s, sharp, C-F); $\delta_{\text{H}}(300 \text{ MHz; CDCl}_3)$ 6.34 (broad, Ph), 5.36 (broad, =CH-); $\delta_{\text{C}}(75 \text{ MHz; CDCl}_3 \text{ and DMSO-}d_6)$ 162.79 (), 159.52 (), 137.80 (), 130.18 (), 127.97 (), 114.10 (), 103.92 (); SEC (Mw = 201,000 ; Mn = 17,600 ; Pd = 11); soluble in warm DCM, and warm THF.

Poly (2-ethynynaphthalene) (PB044)

PB044 was synthesised from PB032 and was isolated as a yellow/orange powder 68% yield; (Found: C, 93.45; H, 5.23. C₁₂H₈ requires C, 94.70; H, 5.30); $\nu_{\max}/\text{cm}^{-1}$ 3050 (m, sharp, unassigned), 1595 (m, sharp, Ph), 1500 (m, sharp, Ph); insoluble in all solvents tested.

Poly (4-nitro)phenylacetylene (PB036)

PB036 was synthesised from 4NPA and was isolated as a brown powder 76% yield; (Found: C, 63.87; H, 3.30; N, 9.18. $C_8H_5NO_2$ requires C, 65.31; H, 3.43; N, 9.52); ν_{max}/cm^{-1} 1700 (w, sharp, C=C), 1590 (s, sharp, Ph), 1506 (s, broad, Ph), 1340 (s, broad, NO_2), 1103 (m, sharp, Ar-N), 851 (s, sharp, NO_2); insoluble in all solvents tested.

Poly (3-methoxyphenylacetylene) (PB035)

The yield of polymer was inaccurate because precipitation of the reaction mixture gave a very fine yellow suspension that was difficult to filter.

PB035 was synthesised from 3MeOPA and was isolated as a yellow powder 70% yield; ν_{max}/cm^{-1} 2994 (w, sharp, C-H), 2935 (m, sharp, C-H), 2831 (m, sharp, OCH_3), 1700 (C=C), 1595 (s, sharp, Ph), 1576 (s, sharp, unassigned), 1482 (s, sharp, Ph), 1285 (s, sharp, C-O); δ_H (300 MHz; $CDCl_3$) 6.85-6.80 (1 H, t, Ph), 6.54-6.51 (1 H, d, Ph), 6.29-6.26 (2 H, multiplet, Ph), 5.85 (1 H, s, =CH-), 3.54 (3 H, s, $-OCH_3$); δ_C (75 MHz; $CDCl_3$) 159.25 (Ph), 144.17 (), 139.13 (), 131.62 (C=CH-), 128.60 (Ph), 120.48 (Ph), 112.53 (Ph), 55.02 ($-OCH_3$); SEC (M_w = 213,000 ; M_n = 67,050 ; Pd = 3.15); soluble in DCM, and THF.

Poly (3,4-ethylenedioxyphenylacetylene) (PB031)

PB031 was synthesised from PB029 and was isolated as a yellow/orange powder 40% yield; (Found: C, 72.79; H, 4.98. $C_{10}H_8O_2$ requires C, 74.99; H, 5.03); ν_{max}/cm^{-1} 2971 (w, sharp, C-H), 2927 (w, sharp, C-H), 2871 (w, sharp, unassigned), 1700 (w, sharp, C=C), 1581 (m, sharp, Ph), 1500 (s, sharp, Ph), 1306 (s, sharp, C-O), 1283 (s, sharp, C-O); insoluble in all solvents tested.

Poly 2-(3-ethynylphenoxy)tetrahydro-2H-pyran (PB038)

PB038 was synthesised from PB018 and was isolated as an orange powder 92% yield; λ_{max} (DCM)/nm 420; ν_{max} /cm⁻¹ 2940 (s, sharp, C-H), 2870 (w, sharp, O-CH(R)-O), 1109 (s, sharp, THP), 1075 (m, sharp, THP), 977 (s, sharp, THP); δ_{H} (300 MHz; CDCl₃) 6.70-6.34 (4 H, multiplet, Ph), 5.81 (1 H, s, C=C-H), 5.17 (0.5 H, s, THP), 3.98-3.40 (1 H, multiplet, THP), 1.99-1.53 (6 H, multiplet, THP); δ_{C} (75 MHz; CDCl₃) 156.66 (Ph), 156.01 (broad, Ph), 144.17 (broad, Ph), 138.25 (broad, unassigned), 128.99 (broad, unassigned), 114.16 (broad, unassigned), 63.38 (THP), 30.93 (THP), 25.43 (THP), 19.75 (THP); SEC (Mw = 232,500 ; Mn = 65,650 ; Pd = 3.5); soluble in DCM, and THF.

Poly 2-(4-ethynylphenoxy)tetrahydro-2H-pyran (PB013)

PB013 was synthesised from PEB943 and was isolated as an orange powder 87% yield; λ_{max} (CHCl₃)/nm 410; ν_{max} /cm⁻¹ 2940 (s, sharp, C-H), 2867 (w, sharp, O-CH(R)-O), 1700 (w, sharp, C=C), 1604 (m, sharp, Ph), 1506 (s, sharp, Ph), 1109 (s, sharp, THP) 1075 (m, sharp, THP), 977 (s, sharp, THP); δ_{H} (300 MHz; CDCl₃) 6.67 (3 H, br s, Ph), 5.74 (0.5 H, br s, C=CH), 5.17 (0.5 H, br s, THP), 3.98-3.46 (1 H, multiplet, THP), 1.86-1.51 (6 H, br multiplet, THP); δ_{C} (75 MHz; CDCl₃) 156.04 (Ph), 136.75 (Ph), 128.44 (Ph), 115.62 (C=C), 96.19 (THP), 61.58 (THP), 30.34 (THP), 25.21 (THP), 18.77 (THP); SEC (Mw = 255,500 ; Mn = 21,200 ; Pd = 12); soluble in warm DCM, and warm THF.

Poly (4-methylphenylactylene) (PB008)

PB008 was synthesised from *p*-ethynyltoluene and was isolated as an orange powder 94% yield; ν_{max} /cm⁻¹ 3009 (w, sharp, C-H), 1700 (w, sharp, C=C); slightly soluble in THF.

Poly (4-phenylphenylacetylene) (PEB985)

PEB985 was synthesised from *p*-ethynylbiphenyl and was isolated as an orange powder 92% yield; $\nu_{\max}/\text{cm}^{-1}$ 1700 (w, sharp, C=C), 1482 (m, sharp, Ph); (Found: C, 93.08; H, 5.56. $\text{C}_{14}\text{H}_{10}$ requires C, 94.35; H, 5.65); insoluble in all solvents tested.

Poly (3,5-dichlorophenylacetylene) (PEB992)

PEB992 was synthesised from DCPA and was isolated as a yellow/orange powder 94% yield; $\lambda_{\max}(\text{CHCl}_3)/\text{nm}$ 420; $\nu_{\max}/\text{cm}^{-1}$ 1557 (s, sharp, Ph), 1412 (m, sharp, unassigned), 855 (m, sharp, Ph); SEC (Mw = 453,000 ; Mn = 20,470 ; Pd = 22); NMR data was unavailable owing to problems with solubility in CDCl_3 ; partially soluble in DCM, and THF.

Poly (4-methylester phenylacetylene) (PEB988)

PEB988 was synthesised from 4MEPA and was isolated as a yellow/orange powder 98% yield; $\lambda_{\max}(\text{CHCl}_3)/\text{nm}$ 440; $\nu_{\max}/\text{cm}^{-1}$ 2950 (w, sharp, C-H), 1722 (s, sharp, $-\text{CO}_2-$), 1604 (m, sharp, Ph), 1275 (s, sharp, C-O), 1104 (s, sharp, C-O); $\delta_{\text{H}}(300 \text{ MHz}; \text{CDCl}_3)$ 7.59-7.56 (2 H, d, Ph), 6.67-6.64 (2 H, d, Ph), 5.77 (1 H, s, $-\text{C}=\text{CH}-$), 3.81 (3 H, s, $-\text{CH}_3$); $\delta_{\text{C}}(75 \text{ MHz}; \text{CDCl}_3)$ 166.25 (C=O), 145.97 (), 139.01 (), 132.36 (), 129.35 (), 129.02 (), 127.07 (), 52.06 (); SEC (Mw = 248,000 ; Mn = 26,650 ; Pd = 9.4); soluble in DCM, and THF.

Poly (4-cyanophenylacetylene) (PEB956)

PEB956 was synthesised from 4CPA and was isolated as a brown powder 25% yield; $\nu_{\max}/\text{cm}^{-1}$ 2227 (s, sharp, $\text{Ar}-\text{C}\equiv\text{N}$), 1603 (m, sharp, Ph), 1498 (m, sharp, Ph); soluble in warm DMF.

Poly (4-bromophenylacetylene) (PB017)

PB017 was synthesised from 4BrPA and was isolated as an orange powder 91% yield; $\nu_{\max}/\text{cm}^{-1}$ 1700 (w, sharp, C=C), 1480 (s, sharp, Ph), 1008 (s, sharp, unassigned); (Found: C, 53.08; H, 2.78. $\text{C}_8\text{H}_5\text{Br}$ requires C, 53.08; H, 2.83); insoluble in all solvents tested.

Poly cyclopropyl-4-ethynylphenyl ketone (PB024)

PB024 was synthesised from PB014 and was isolated as a yellow/orange powder 97% yield; λ_{max} (DCM)/nm 450; ν_{max} /cm⁻¹ 2924 (w, sharp, C-H), 1663 (m, sharp, Ar-CO-), 1599 (m, sharp, Ph), 1407 (m, sharp, cyclopropane), 1379 (s, sharp, cyclopropane); δ_{H} (300 MHz; CDCl₃) 7.57-7.55 (2 H, split singlet, Ph), 6.71-6.89 (2 H, split singlet, Ph), 5.86 (1 H, s, C=C-H), 2.36 (1 H, s, -CH-), 1.09-0.94 (2 H, two overlapping singlets, -CH₂-); δ_{C} (75 MHz; CDCl₃) 199.47 (C=O), 145.95 (Ph), 139.02 (Ph), 16.98 (-CH-), 11.85 (-CH₂-); soluble in DCM; insoluble in THF.

Poly (1-(4-ethynyl-2-fluorophenyl)but-1-en-3-one) (PB026)

PB026 was synthesised from PEB923B and was isolated as a dark red solid 98% yield. When first made, this polymer was a yellow orange solid. Washing with methanol and drying the resultant slurry in a vacuum oven, at 50°C, for 6 hours gave a dark red solid; (Found: C, 74.32; H, 4.80. C₁₂H₉FO requires C, 76.58; H, 4.82); ν_{max} /cm⁻¹ 1668 (s, sharp, C=C-CO-), 1602 (s, broad, Ph), 1495 Chapter 6 : Co-polyradicals

CHARACTERISATION OF CO-POLYRADICALS

Co-polyradical 4EPNN co 4CPA (1 :1) (PEB963)

PEB963 isolated as a green solid (91%); $\nu_{\max}/\text{cm}^{-1}$ 2985 (w, sharp, C-H), 2225 (m, sharp, $\text{C}\equiv\text{N}$), 1601 (s, sharp, Ph), 1358 (s, sharp, nitronyl nitroxide), 1215 (m, nitronyl nitroxide), 1165 (m, sharp, nitronyl nitroxide), 1132 (m, sharp, nitronyl nitroxide); 98% spins per $\text{C}_{24}\text{H}_{22}\text{N}_3\text{O}_2$ formula unit.

Co-polyradical 3EPNN co 3CPA (1 :1) (PEB967)

PEB967 isolated as a green solid (67%); $\nu_{\max}/\text{cm}^{-1}$ 2227 (w, sharp, $\text{C}\equiv\text{N}$), 1636 (w, broad, Ph), 1214 (w, sharp, nitronyl nitroxide), 1165 (w, sharp, nitronyl nitroxide), 1132 (w, sharp, nitronyl nitroxide); 109% spin per $\text{C}_{24}\text{H}_{22}\text{N}_3\text{O}_2$ formula unit.

Co-polyradical 4EPNN co 4NPA (1 :2) (PB020)

PB020 isolated as a green solid (72%); $\nu_{\max}/\text{cm}^{-1}$ 1700 (w, sharp, $\text{C}=\text{C}$), 1592 (m, sharp, Ph), 1509 (s, sharp, Ph), 1340 (s, broad, NO_2 and overlap with nitronyl nitroxide), 1217 (w, sharp, nitronyl nitroxide), 1165 (w, sharp, nitronyl nitroxide), 1104 (w, sharp, Ar-N); 86% spin per $\text{C}_{31}\text{H}_{27}\text{N}_4\text{O}_6$ formula unit.

Co-polyradical 3EPNN co 3NPA (1 :1) (PB028)

PB028 isolated as a green solid (57%); $\nu_{\max}/\text{cm}^{-1}$ 1528 (s, sharp, NO_2), 1349 (a, sharp, NO_2), 1498 (m, sharp, Ph), 1394 (w, sharp, nitronyl nitroxide), 1217 (w, sharp, nitronyl nitroxide), 1166 (w, sharp, nitronyl nitroxide), 1134 (w, sharp, nitronyl nitroxide).

Co-polyradical 4EPNN co 4CPA (1 :2) (PB034)

PB034 isolated as a green solid (64%); $\nu_{\max}/\text{cm}^{-1}$ 2226 (s, sharp, $\text{C}\equiv\text{N}$), 1602 (m, sharp, Ph), 1498 (m, sharp, Ph), 1387 (m, sharp, nitronyl nitroxide), 1362 (s, sharp, nitronyl nitroxide), 1302 (m, sharp, nitronyl nitroxide), 1217 (w, sharp, nitronyl nitroxide), 1166 (w, sharp, nitronyl nitroxide), 1133 (w, sharp, nitronyl nitroxide).

Co-polyradical 4EPNN co 4FPA (1 : 1) (PB065)

PB065 isolated as a green solid (58%) – all the polyradical could not be isolated owing to the very fine precipitate; $\nu_{\text{max}}/\text{cm}^{-1}$ 2986 (w, sharp, C-H), 1601 (m, sharp, Ph), 1503 (m, sharp, Ph), 1360 (s, sharp, nitronyl nitroxide), 1220 (m, sharp, nitronyl nitroxide overlapped with F), 1162 (w, sharp, nitronyl nitroxide), 1133 (w, sharp, nitronyl nitroxide); soluble in warm THF and warm DCM, to give a green solution.